Ollscoil na hÉireann, Corcaigh

National University of Ireland, Cork

The Design of Cyclodextrins for Delivery of siRNA - a Structure-Activity Relationship

Thesis presented by

Ayse Kont

https://orcid.org/0000-0002-9341-5453

for the degree of

Doctor of Philosophy

University College Cork

Head of School/Department: Prof. Brendan Griffin, B. Sc. (Pharm), Ph.D., M.P.S.I.

Supervisor: Prof. Caitriona O'Driscoll, B. Sc. (Pharm), Ph.D., M.P.S.I.

January 2024

Contents

Declaration

"This is to certify that the work I am submitting is my own and has not been submitted for another degree, either at University College Cork or elsewhere. All external references and sources are clearly acknowledged and identified within the contents. I have read and understood the regulations of University College Cork concerning plagiarism and intellectual property."

All work was performed independently by the author, with the following exceptions:

Chapter 2:

Dr. Michael Cronin carried out the synthesis of the CDs used.

Chapter 3:

CDs were provided by Cyclolab, CarboHyde and Dr. Michael Cronin. Dr. Andrew Lindsay carried out the confocal imaging.

Chapter 4:

CD polymers were provided by CarboHyde. Dr. Andrew Lindsay carried out the confocal imaging.

Signed:  Date: 02.01.2024

This thesis has emanated from research supported in part by Science Foundation Ireland and the European Regional Development Fund, Grant 17/RC-PhD/3477 and 12/RC/2278_P2 (Advanced Materials and BioEngineering Research, AMBER) and in part by Jazz Pharmaceuticals.

Acknowledgments

This Ph.D. was surely not an easy journey, but thankfully difficult times do not last forever. What I wish to last is the connections I made with all the lovely people I have met during these long five years.

Firstly, I want to thank my supervisor, *Prof. Caitriona O'Driscoll*, for giving me the opportunity to do this Ph.D and supervising me. It helped me to learn a lot for my career and life. A special thanks goes to *Dr. Monique Mendonça* who acted as my second supervisor and played a big part in finishing my Ph.D. It would have not been possible without your help and guidance! I will forever be grateful for your contributions to my research journey and as a big sister who always had an open ear for me.

To all the staff who helped to have a smoothly running lab; to *Dr. Michael Cronin* and *Dr. Ken Devine* who never turned down a call for help, and *Aisha* and *Kathleen* for their endless supply of paper and help in any way possible and beautiful smiles. Also special thanks to *Prof. Abina Crean, Aisha, Dr. Ken Devine, Noreen and Dr. Sonja Vucen* for asking and listening to my problems and genuinely caring about my well-being. And of course, a big thank you to my lab mates! As an international student, you were as important as family! All of you hold very special places in my heart. In alphabetic order:

Annachiara: You are a very loyal friend and always have my back! Thank you for offering me your shoulder to cry on and for never getting upset with me when I got crazy in stressful situations in the lab (there were many!). *Ayat*: I have never met someone who is as hardworking as you are. You are truly a role model and inspiration for every woman who wants to be successful. Your beautiful smile and positive energy

spreads to everyone around you. You are a blessing! *Brian*: You are a lovely person and so understanding! Your absence is felt! *Callum*: You are such a great listener and so kind. Conversations with you were just the best. Thanks for always being there when I needed to vent and for your understanding! *Claudia*: You were a stranger, then a colleague, became my housemate, and then my friend! *Dominic*: I am glad, we could break the shyness and we could become friends. I will miss the exchanges in the lab (You are a great scientist! Extremely impressive!) and the nice conversations about literally any topic. Sorry for crying in front of you so many times hahah :(*Jack*: My Irish friend with the big head (and brain!). UCC societies and the Ceutics lab became just nicer with you! *Khaled*: Asking for help was never so easy! No matter the circumstances, your help was consistent. The day you're awarded the Nobel Prize, I hope you will remember that I was the first one to genuinly believe and tell you that you would. *Laura*: Your aura is unmatched. Being around you makes me feel so calm and I love having conversations with you. *Lianne*: I will never forget the hug that made me cry. *Lotte*: You are a special person and I am glad we were able to accept each other into our small circle. You are loved and appreciated. *Marzia*: One of my first friends in Ireland and always there to cheer for me! Thank you for motivating me and reminding me that I can do anything! I know one day you will become a famous scientist! *Michael*: Thank you so much for the nice talks about "Gott und die Welt". Always a pleasure talking to you. *Miguel*: My little brother and housemate! Such an understanding friend! I appreciate you. *Rehab*: We had a weird start (I do not regret anything!) but better days are ahead :D *Theo*: Thanks for the basketball sessions! If I would be male and taller, you would have no chance against me! I know you agree.

I would also like to give a very special thanks to my former supervisor, *Prof. Jennifer Dressman*, who was a big supporter and helped me to start my research

journey. I am forever grateful for the kindness you have shown me. A kind human, strong scientist and strong woman, who used her superpower to support other women.

And a big thanks to my former demonstrator, *Dr. Moritz Neupärtl*, who convinced me that I am "the" candidate for a Ph.D, and to my former colleague *Dr. Rafael Paraiso*, who encouraged me to move to Ireland. One can never know the impact of our words on younger minds! THANK YOU!

I also want to thank my dear friend, *Rabia*, who lost the battle against cancer but should always be a reminder why cancer research is so important. She was the most genuine, smart, kind, and best friend I could have asked for. She was a ray of sunshine that illuminated my life during my darkest times. She was my motivation to continue, and I am sure she would have been very proud of me. God bless her family to have raised a beautiful woman like her.

A special thanks to *Aasem* who was always there for me no matter the distance.

And *Samya*, literally my very first friend in Cork. The way I appreciate you... thank you for your patience with me. Your kindness is out of this world!

Last but not least, a special and huge thanks go to my wonderful family! My brothers *Murat*, *Necat*, and *Ümüt* for their endless support; and my beautiful sister *Arife*, and my twin *Ayla* who always believed in me and supported me. Seeing what you were thinking I could achieve made me also believe that I could. There is no way to express my gratitude towards you in a few sentences. And of course to my niece, *Gökçe*, who tried to understand and motivate me when I explained to her that I was sad even though she was just a kindergardener trying to understand life. And my nephews, *Hamza, Davud* and *Yaşar*; they do not know but their kisses and hugs were

like therapy. I would also like to thank my aunt *Şahsine*. It is truly a blessing to have been surrounded by strong women. You were great example.

And my **parents**! You are the reason I am who I am today. The confidence and resilience I got from you helped me to endure and finish this Ph.D. I thank God endlessly for having a perfect mother and such a great father. Both of you presented us opportunities you could not even dream of. You are the most unselfish people I know who left their lives, families and everything behind to give us a better life. Your sacrifices are not unnoticed. We know that we can never pay you back, but we will not stop trying. You supported me throughout my whole life to achieve my goals and I hope to always make you proud. May God bless you and give you a long and healthy life. I love you!

Son olarak fakat bir o kadar da önemli olan, harika aileme en içten ve büyük teşekkürlerimi sunmak istiyorum! Sonsuz desteklerinden dolayı Murat, Necat ve Ümüt abilerime; ve bana her zaman inanan ve destek olan güzel ablam Arife ve ikizim Ayla'ya. Neler başarabileceğimi düşündüğünüzü görmek benide başarabileceğime inandırdı. Size olan minnettarlığımı birkaç cümleyle anlatmak imkânsız. Ve tabii ki anaokulu öğrencisi olmasına ve hayatı daha kendisi yeni öğrenmesine rağmen, ona üzüldüğümü anlattığımda beni anlamaya ve motive etmeye çalışan yeğenim Gökçe'ye de. Ve yeğenlerim Hamza, Davud ve Yaşar'a; farkında olmasalarda öpücükleri ve sarılmaları terapi gibiydi. Ayrıca Şahsine teyzeme de teşekkür etmek istiyorum. Iyi ki benim tezyemsin. Kan bağının nekadar önemsiz olduğunun canlı örneğisin. Etrafımın güçlü kadınlarla çevrili olması gerçekten büyük bi nimetiş. Harika bir örneksin.

Ve ebeveynlerim! Bugün olduğum kişi olmamın sebebi sizsiniz. Sizden aldığım güven ve dayanıklılık, bu doktora dönemine dayanmamı ve bitirebilmemi sağladı. Bir

kadın olarak senin gibi bir örnek bir anneye sahip olduğum için Rabbime binlerce kez şükürler olsun. Ve tabii ki adam gibi adam olan bir babaya sahip olmak ayrıca bir gurur. İkiniz de bizlere kendinizin hayal dahi edemeyeceği fırsatlar sundunuz. Sizler bize daha iyi bir yaşam sağlamak için her şeyini veren ve arkada bırakan, tanıdığım en fedakar insanlarsınız. Fedakarlıklarınızı görmemezden gelmek imkansız. Size borcumuzu asla ödeyemeyeceğimizi bildiğimiz halde denemekten vazgeçmeyeceğiz. Tüm hayatım boyunca hedeflerime ulaşmamda bana destek oldunuz, umarım sizi her zaman gururlandırırım. Allah sizden razı olsun ve sizi başımızdan eksik etmesin. Sizi çok ama çok seviyorum!

Tough times do not last, tough people do!

وَمَا تَوْفِيقِيٓ إِلَّا بِٱللَّهِۚ عَلَيْهِ تَوَكَّلْتُ وَإِلَيْهِ أُنِيبُ

My success comes only through Allah. In Him I trust and to Him I turn.

[**Hud 88**]

Author Publications

a. Peer-reviewed publications associated with this thesis.

1. **Chapter 2:** Co-Formulation of Amphiphilic Cationic and Anionic Cyclodextrins Forming Nanoparticles for siRNA Delivery in the Treatment of Acute Myeloid Leukaemia

   Ayse Kont, Monique C.P. Mendonca, Michael F. Cronin, Mary R. Cahill and Caitriona M. O'Driscoll

   International Journal of Molecular Sciences, 2022, 23, 9791

2. **Appendices:**

a) Design of lipid-based nanoparticles for delivery of therapeutic nucleic acids

   Monique C.P. Mendonça[1], **Ayse Kont[1]**, Piotr S. Kowalski, Caitriona M. O'Driscoll

   [1] These authors contributed equally to this work.

   Drug Discovery Today, Volume 28, Number 3, March 2023

b) Advances in the Design of (Nano)Formulations for Delivery of Antisense Oligonucleotides and Small Interfering RNA: Focus on the Central Nervous System

   Monique C. P. Mendonça, **Ayse Kont**, Maria Rodriguez Aburto, John F. Cryan, and Caitriona M. O'Driscoll

   Molecular Pharmaceutics 2021, 18, 1491−1506

b. Conference presentations

1. **Ayse Kont**, Michael F. Cronin, Raphael Darcy, Caitriona M. O'Driscoll. *Characterisation of anionic and cationic amphiphilic cyclodextrins as novel materials for siRNA delivery.* **Poster** presented at 12th World Meeting on Pharmaceutics, Biopharmaceutics and Pharmaceutical Technology, May 2021.
2. **Ayse Kont**, Monique C. P. Mendonça, Michael F. Cronin, Mary R. Cahill, Caitriona M. O'Driscoll. *Co-formulation of amphiphilic cyclodextrins forming nanoparticles for siRNA delivery in acute myeloid leukaemia.* **Poster and Oral Presentation** presented at 20th International Cyclodextrin Symposium, June 2022 - **Best Poster Award.**

Abstract

Previously non-viral delivery of therapeutic nucleic acids (NAs) has been achieved for the treatment of liver disease and in the case of the COVID-19 vaccine. The delivery vector in both applications was a lipid-base nanoparticle (LNP). To expand the therapeutic application of NAs to treat more complex chronic diseases, such as cancer, delivery systems with wider biodistribution capable of going beyond the vaccine and the liver are required. This thesis aims to investigate the potential of modified cyclodextrins (CDs) as alternative biomaterials for siRNA delivery and to identify the optimum functional groups to maximise safety and efficacy.

To help reduce the overall cationic charge and the potential for *in vivo* toxicity a co-formulation approach using a blend of an anionic and cationic amphiphilic CDs was investigated. The co-formulation was characterised and a reduction in the positive charge was achieved. The NPs were evaluated *in vitro* in HL-60, a leukaemia cell line, and results indicate that endosomal escape was a limiting factor to gene silencing with the siRNA.

Structural modification of amphiphilic cationic CDs was investigated as a second approach to enhance the efficacy of CD NPs. The structural changes included varying the terminal amine, the linker, and the CD type, β versus γ.

Primary amine proved to be more successful compared to tertiary amine in β- and γ-CDs. However, neither CD type was superior to the other, containing the primary amines. The exhaustive derivatisation of the secondary side of γ-CDs increased charge density and led to better transfection efficiency compared to *O*2-modified γ-CDs. Finally, the exchange of the linker group from triazole to thiopropyl increased the efficiency further in primary amine *O*2- and *O*3-substituted γ-CD. The

optimum cellular uptake and gene silencing, in a lung cancer cell line (A549), was achieved with an *O*2- and *O*3-substituted γ-CD with a thiopropyl-linked primary amine.

Finally, the potential ability of CD polymers to deliver siRNA was studied. Two cationic β-CD-polymers one functionalised with a primary amine and the other with a quaternary ammonium were used to formulate NPs containing siRNA. Both polymers formed NPs with sizes in the range of 150 to 200 nm. The primary amine functionalised polymer was taken up into the cells (A549) and produced 40% gene silencing. In contrast, the quaternary ammonium polymer failed to show any cellular uptake. The superior delivery effect achieved with the primary amine functional group agreed with the previous results from the monomer CD.

In conclusion, modulation of the physicochemical characteristics of siRNA-NPs was achieved by changing the chemistry of the incorporated CD. The chemical structure significantly influenced the degree of gene knockdown. The primary amine showed superior efficiency in both monomeric amphiphilic cationic CDs and polymeric cationic CDs. Results indicate that further functionalisation of the CD is possible, and the potential exists to fine-tune the structure to achieve more specific biodistribution.

Abbreviations

AMD	age-related macular degeneration
AML	acute myeloid leukaemia
ApoE	apolipoprotein E
ASGPr	asialoglycoprotein receptor
ASO	antisense oligonucleotide
bPEI	branched PEI
BRD4	bromodomain containing protein 4
CCK-8	cell counting kit -8
CD	cyclodextrin
CD-B1	β-CD, ‘click’ triazole attached *O*2-primary amine
CD-B2	β-CD, ester attached *O*2-tertiary amine
CD-G1	γ-CD, ‘click’ triazole attached *O*2-primary amine
CD-G2	γ-CD, ‘click’ triazole attached *O*2, *O*3-primary amine
CD-G3	γ-CD, non-amphiphilic
CD-G4	γ-CD, ‘click’ thiopropyl attached *O*2, *O*3-primary amine
CD-G5	γ-CD, ‘click’ thiopropyl attached *O*2, *O*3-tertiary amine
cDNA	complementary DNA
CSF-1	colony-stimulating factor-1
DOPE	1,2-dioleoyl-sn-glycero-3-phosphoethanolamine
DLS	dynamic light scattering
DMAEMA	2-dimethyl aminoethyl methacrylate
DMEDA	dimethyl ethylene diamine
DSS	Dextran Sodium Sulphate
EE	encapsulation efficiency
EGFP	enhanced green fluorescent protein
EPRE	enhanced permeability and retention effect
FA	folic acid
Fab	fragment antibody

FBS	fetal bovine serum
FDA	U.S. Food and Drug Administration
FT-IR	Fourier-transform infrared spectroscopy
GFP	green fluorescent protein
GGT	γ-glutamyl transpeptidase
hATTR	hereditary transthyretin-mediated
HD	Huntington's Disease
HRMS	high-resolution mass spectrometry
HTT	Huntingtin
IL-2	Interleukin-2
IV	intravenously
LSC	leukaemia stem cell
LNP	lipid nanoparticle
mPEG	methoxypoly(ethylene oxide)
MR	mass ratio
mRNA	messenger RNA
MW	molecular weight
NA	nucleic acid
NF-κB	nuclear factor kappa B
NMR	Nuclear Magnetic Resonance
NP	nanoparticle
N/P	ratio of amines in delivery vector/phosphates in NA
OEI	oligo ethyleneimine
OVA	oval-albumin
PAMAM	poly(amidoamine)
PA-polymer	primary amine β-CD-polymer
PBS	phosphate-buffered saline
PC	polycarbonate
PCL	polycaprolactone
PDI	polydispersity index

pDNA	plasmid DNA
PDMAEMA	poly(2-dimethyl aminoethyl methacrylate)
PEG	polyethylene glycol
PEI	polyethyleneimine
PHEMA	poly(2-hydroxyethyl methacrylate)
PLK1	polo-like kinase 1
PR	polyrotaxane
QA-monomer	quaternary ammonium β-CD-monomer
QA-dimer	quaternary ammonium β-CD-dimer
QA-polymer	quaternary ammonium β-CD-polymer
R8	octa arginine
RES	reticulo endothelial system
RISC	RNA-induced Silencing Complex
RNAi	RNA interference
RVG	rabies virus glycoprotein
SAR	structure-activity-relationship
SAXS	small-angle X-ray scattering
siRNA	short interfering RNA
TAM	tumour-associated macrophages
TEM	Transmission electron microscopy
TNS	2-(p-toluidino) naphthalene-6-sulfonic acid
TNBS	2,4,6-Trinitrobenzene sulfonic acid
Trf	transferrin
TTR	transthyretin
VEGF	vascular endothelial growth factor
5-FU	5-Fluorouracil
7-KC	7-ketocholesterol
γ-PGA	polyglutamic acid

1. Chapter: Introduction

1.1. General introduction

1.1.1. RNA interference – an ancient mechanism

RNA interference (RNAi) is a new therapeutic approach in the field of medicine. However, RNAi discovery dates back 25 years when Fire et al. uncovered the ability of double-stranded RNA to interfere with the activity of certain genes in plants and C. *elegans* (Fire et al. 1998). Later, the knockdown of endogenous messenger RNA (mRNA) was confirmed *in vitro* and *in vivo* with double-stranded short interfering RNA (siRNA) consisting of 20-25 base pairs (bp). Externally introduced siRNA must be fully complementary to the indigenous mRNA of the protein of interest (Friedrich and Aigner 2022). siRNA that interacts with the RNA-induced Silencing Complex (RISC) leads to activation of the complex. Subsequently, the siRNA-RISC associates with the mRNA, resulting in mRNA degradation and preventing translation into protein (Rehman et al. 2022).

The therapeutic potential of siRNA in mammalian cells was first discovered by Elbashir et al. The optimal length of siRNA was determined to be 21 bp, which created the basis for companies to create algorithms in siRNA design. These innovations opened the door for the development of siRNA therapeutics. Nevertheless, considering the complexity of the human body and diseases, the successful and sufficient delivery of siRNAs continues to be challenging (Elbashir et al. 2001; Friedrich and Aigner 2022).

Several obstacles must be overcome to elicit a desired therapeutic effect with nucleic acids (NAs). NAs include siRNA (RNAi), mRNA (increases the production of a dysfunctional or missing protein), and plasmid DNA (pDNA) (introduction of a

gene to produce a specific protein). Natural barriers for NAs include extracellular and intracellular barriers. The harsh extracellular environment can result in the loss of therapeutic NAs by enzymatic degradation, immune recognition, or renal and hepatic clearance. At the cell surface of the tissue of interest, the NA may fail to cross the cell membrane due to challenging physicochemical properties including high molecular weight, negative charge, and the hydrophilic nature of NAs. Even NAs that enter the cell may fail to rapidly escape the endo-lysosomes and release into the cytoplasm (Hu et al. 2020) (Figure 1-1). Chemical modifications of the NA cargo and/or delivery vectors are necessary to facilitate and enhance RNAi activity by overcoming the natural barriers.

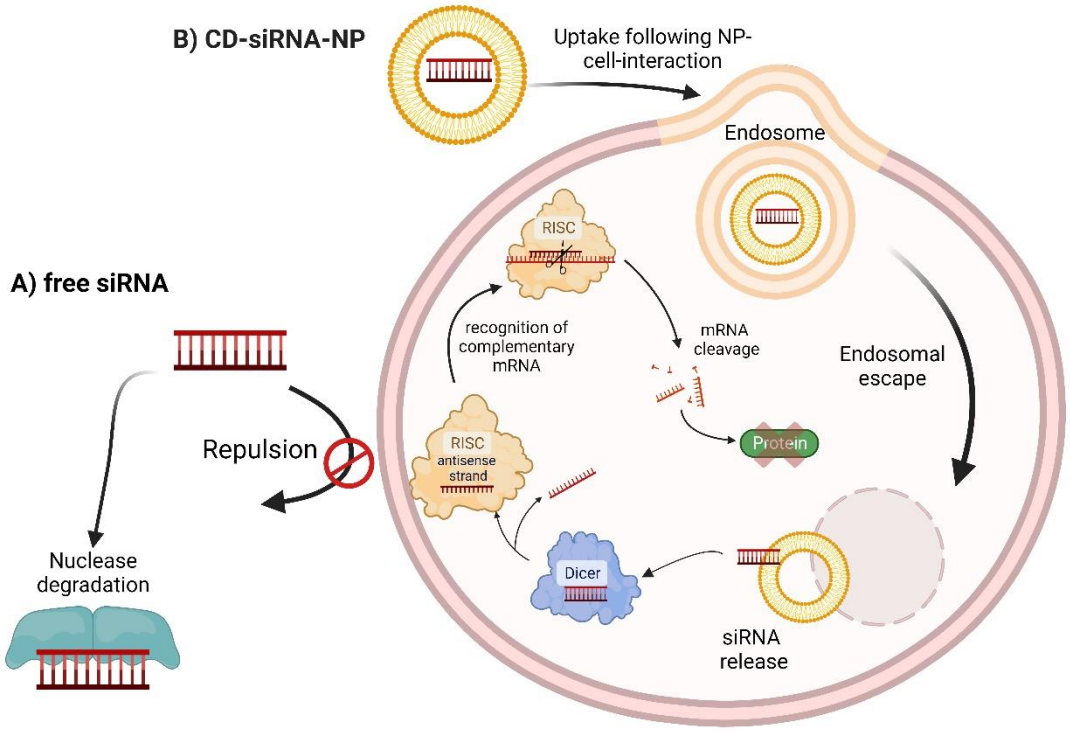

Figure 1-1 Intracellular fate of (A) free siRNA versus (B) siRNA encapsulated in CD delivery vector. mRNA degradation upon successful NP cargo release.

1.1.2. RNAi application in cancer

Cancer is the uncontrolled growth of abnormal cells in any organ which then can evolve and metastasise. It is a major cause of death globally with 10 million cases in 2020 (Sung et al. 2021). There are many small-molecule drugs available for the treatment of cancer. Other therapy options, such as surgery and radiotherapy, can be applied separately or in combination with anticarcinogenic drugs. The treatment plan is developed based on the type and stage of cancer. Notwithstanding, many cancer patients suffer severe side effects due to the action of treatments on healthy tissues. Further, patients may relapse following treatment due to the inability of current approaches to eliminate all diseased cells from the body (Debela et al., 2021).

The treatment with siRNA in cancer therapy offers many advantages over traditional therapeutic modalities. Conventional therapies are very efficient, especially in the early stage of the disease. However, because of the lack of target-specificity, it is impossible to prevent damage to healthy tissue which impacts patients' quality of life. Another problem associated with traditional therapies is drug resistance (low uptake, high efflux) (Debela et al. 2021). RNAi enables the specific elimination of disease-causing factors at the gene level rather than treating at the protein level. Due to its mechanism of action at the post-transcriptional level that cleaves the mRNA preventing protein expression, it provides a promise of treatment for what might previously be seen as 'undruggable' diseases. Despite the potential benefits, challenges associated with the use of siRNA as a medicine include delivery difficulties because of the large size and polyanionic charge, susceptibility to nuclease degradation, faulty recognition of the exogenous siRNA by the innate immune system, and off-target effects due to unspecific binding of activated RISC with mRNA (Friedrich and Aigner 2022; Hu et al. 2020). Yet, it is important to mention that the

RISC machinery is a catalytic system that ‘recycles’ the incorporated siRNA. Thus, relatively low siRNA release into the cytoplasm is necessary to achieve efficient gene knockdown (Friedrich and Aigner 2022; Haley et al. 2020).

Cancer diseases can be divided into two groups: solid cancers and blood cancers. Solid cancers have locally growing tumours with high vascularity and, therefore, high permeability, to provide the tumour with sufficient oxygen and nutrients. From a blood supply perspective, the blood vessels produced by the dysregulated angiogenesis around the tumour have less frequent but larger fenestrae when compared to surrounding healthy tissue. This facilitates drug entry into the tumour. On the clearance side, the lymphatic system may be less well developed around the tumour and therefore drugs are less likely to be transported away. This passive targeting of drugs is called the enhanced permeability and retention effect (EPRE) and is a fundamental concept for the development of anticancerogenic drugs in solid cancers (Hu et al. 2020; Wu 2021). However, this concept is currently under debate as some groups reported that there is rather an active transport involved than a passive transport of NPs into tumour tissue (Sindhwani et al. 2020). Blood cancers cannot benefit from EPRE because the diseased cells are in motion in the blood circulation and are consequently more difficult to reach. A second barrier to the eradication of blood cancer is diseased stem cells. Stem cells are in a quiescent condition and remain in the circulation or bone marrow. As conventional therapies only target dividing cells, stem cells can cause the deadly relapse of blood cancers (Guo et al. 2017; Whiteley et al. 2021).

Due to the overall unsatisfactory outlook of small molecule anticancerogenic drugs, RNAi presents a very promising alternative to treat previously ‘undruggable’ cancers. In particular, the chemical modifications of delivery vectors with targeting

ligands or functional groups providing cell and/or tissue specificity equip RNAi therapeutics to drug difficult-to-access sites. It is envisaged that the combination of both treatments (small molecule drug and RNAi) will be synergistic. RNAi might allow the dose of toxic small-molecule chemotherapy drugs to be reduced while maintaining therapeutic success. The application of multiple therapy options simultaneously can prevent chemo-resistance (Haley et al. 2020).

1.1.3. Modulation of nanoparticle properties for successful RNAi

Safe and effective non-viral delivery of NAs is the key to the success of gene therapy. Approaches to improve the effectiveness of NA delivery involve chemical modification of the NA and/or the tuning of the delivery vectors. Changes in siRNA structure encompass phosphonate, ribose, and base modifications to evade activation of the immune system (sugar modifications, e.g. 2'-O-methyl, 2'-fluor, and/or nucleobase modifications, e.g. 5'-methylcytosine), improve specificity (sugar modifications and/or nucleobase modifications), reduce off-target effects (nucleobase modifications), reduce enzymatic degradation (backbone modification, e.g. phosphorothioate and/or sugar modifications) and consequently increase both potency and efficiency (Hu et al. 2020; Mendonça et al. 2021) (Figure 1-2A).

The negative nature and big size of NAs necessitate a delivery vector to further protect and compact the NA, and to facilitate crossing the negatively charged bilayer cell membrane. Delivery vectors should contain lipophilic components to engage with the bilayer membrane and promote cellular uptake. Functional groups on the delivery vector should ideally encourage interaction with endosomal membrane proteins and consequently release the NA cargo into the cytosol (Mendonça, Kont, et al.,2021).

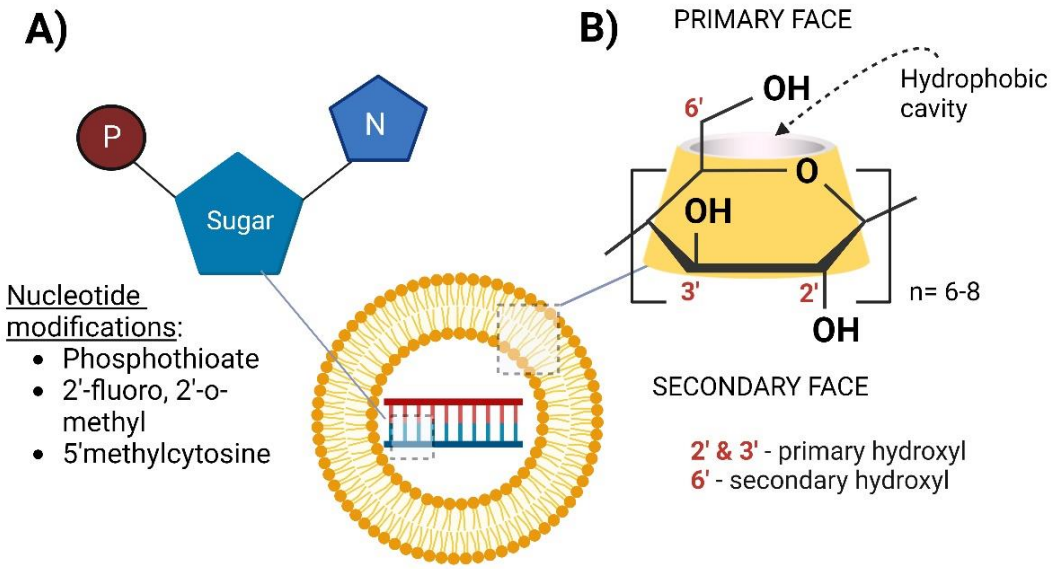

Figure 1-2 Schematic representation of a CD-NP carrying siRNA. Highlighting modification sites on (A) nucleotide and (B) CD-ring.

While chemical modifications on NAs can overcome some delivery challenges, such as protecting against nuclease degradation or increasing circulation half-life; delivery vectors remain necessary to facilitate intracellular uptake and endo-lysosomal escape. The combination of chemical alteration of the NA and utilising a delivery system led to the first U.S. Food and Drug Administration (FDA)-approved lipid nanoparticle (LNP)-system for siRNA delivery, ONPATTRO®, on the market (Hu et al. 2020). This product consists of **i**) siRNA against mutated transthyretin (TTR) gene that causes polyneuropathies as a result of hereditary transthyretin-mediated (hATTR) amyloidosis; **ii**) DLinMC3-DMA, an ionizable cationic lipid with pKa ~6.4 which is mostly neutral in circulation (low toxicity and immunogenicity) and mostly positively charged at low pH during preparation for successful RNA encapsulation; **iii**) DMG-c-PEG that maintains stability during storage but is exchanged in circulation with serum protein ApolipoproteinE (ApoE); **iv**) cholesterol which promotes structural integrity and interaction with ApoE and consequently accumulation in liver; **v**) and DSPC,

helper lipid, facilitating membrane fusion and hence, endosomal release of lipid NP cargo (Akinc et al. 2019; Mendonça, Kont, et al. 2023; Setten, Rossi, and Han 2019).

In the early 2000s the first in-human phase I clinical trial with a cyclodextrin (CD)-based nanoparticle (NP) containing siRNA against ribonucleotide reductase M2, an accepted anti-cancer target, was conducted (Davis et al. 2010). Cysteamine-β-CDs were crosslinked in a condensation reaction with another amine-containing comonomer, dimethyl superimidate, resulting in a short linear polymer. This polymer was incubated with adamantane-polyethylene glycol (PEG) and adamantane-PEG-transferrin to formulate the NP. PEG is a stabilising and protective compound, while transferrin (Trf) is a targeting ligand (Trf receptors are overexpressed on malignant cells compared to healthy cells). Due to dose-limiting toxic events, the trial has terminated (Zuckerman et al. 2014), however, the overall potential of this study intensified investigations of NA delivery and CDs as delivery vectors.

1.2. Cyclodextrins: scaffold for functionalisation

CDs are cyclic oligosaccharides derived from the enzymatic degradation of starch. The CD-ring consists of different numbers of glucose units attached via α-1,4 glycosidic bonds (α-CD = 6 units, β-CD = 7 units, γ-CD = 8 units). The lining up of α-glucoses in a closed ring results in the outwards orientation of the hydroxyl groups creating a hydrophilic surface and a relatively hydrophobic cavity (Figure 1-2B). The primary alcohols are located on the primary site, whereas the secondary alcohols at positions 2 and 3 are on the wider secondary side. Increasing the number of glucose units leads to increased cavity size, which determines the size of the molecules that can be accommodated, and additionally provides greater space for chemical

functionalisation (Liu et al. 2021; O'Mahony, O'Neill, et al. 2012; Sandilya, Natarajan, and Priya 2020).

CDs are traditionally used in pharmaceutical formulations as excipients to improve the stability, bioavailability, and solubility of small-molecule drugs. In particular, poorly water-soluble drugs can be accommodated within the hydrophobic cavity of the CD. This property, of inclusion complex formation, allowed β-CD-dimers to be used as an active ingredient in atherosclerosis and age-related macular degeneration (AMD) where 7-ketocholesterol (7-KC) accumulates in cells and can selectively be removed by the CD (Anderson et al. 2021).

Over the years, the hydroxyl groups on both faces of the CD were utilised for chemical modifications, where each position possesses a different degree of accessibility for functionalisation. The 6'-position OH-group is the most reactive followed by the 2'-OH and finally 3'-OH. The understanding of this reactivity is important to direct the reaction to the desired product with specific characteristics for NA delivery (O'Mahony, Ogier, et al. 2012). The flexibility of the CD ring and the ease of functionalisation have provided opportunities to use the material for NP formulation and delivery of therapeutic NA.

1.2.1. Solubility of cyclodextrins

α- and γ-CDs show preferable solubility in water, while β-CD is ten times less soluble. It is hypothesised that the highly stable intramolecular bonds of β-CDs produce rigidity and consequently low water solubility (Păduraru et al. 2022; Sandilya et al. 2020). β-CD is the most commonly used CD, despite its low aqueous solubility, because of its high availability and low cost (Mavridis and Yannakopoulou 2015). To

overcome this solubility issue, methylation, or hydroxy-alkylation of the β-CD in 2'-OH or 6'-OH position was performed. 2-Hydroxypropyl-β-CD is a widely used pharmaceutical excipient to improve the water solubility of poorly water-soluble drugs (Sandilya et al. 2020; Uekama, Hirayama, and Irie 1998) and is "generally recognised as safe" (GRAS). Other GRAS-listed CDs are the sulfobutylether of β-CD and randomly methylated β-CD.

1.2.2. Cationic cyclodextrins for therapeutic nucleic acid delivery

The chemical structure of CDs presents a platform for many possible modifications. Primarily, the 6'-OH position of a β-CD has been investigated to create cationic and amphiphilic cationic CDs. Given the sterically easy access and high reactivity of this hydroxyl group, various polycationic groups were tested, such as pyridylamino, alkyl imidazole, methoxyethyl amino, or primary amine groups. The fundamental need of cationic groups for NA complexation (and hence gene delivery) was demonstrated by comparing cationic CDs with their neutral counterparts. It was found that neutral CDs were unable to form stable NP with pDNA and therefore showed poor *in vitro* activity (Cryan et al. 2004).

The copper(I)-catalysed 'click' chemistry approach expands the possibilities for secondary side modifications at the lesser reactive 2'-OH rather than the 6'-OH on the primary face, with relative ease and high yield. Firstly, the primary hydroxyl group at the 6'-position was protected with *tert*-butyldimethylsilyl chloride. The 2'-OH was alkylated with propargyl bromide. Subsequently, the 6'-position was deprotected and brominated. The obtained bifunctional CD was ready for copper-catalysed 'click' reaction. The alkynylated 2'-position was reacted with tert-butyl 3-

azidopropylcarbamate to form the intermediate for ‘click’ propylamine; a triazole with boc-protected terminal propylamine. The brominated 6’-position was reacted with a thioalkyl ($SC_{12}H_{25}$) to attach lipophilic chains on the primary site. The deprotection of the primary amine was conducted to obtain ‘click’ propylamine β-CD (O’Mahony, Ogier, et al. 2012) (Figure 1-3A). The resulting ‘click’ propylamine β-CD is amphiphilic due to the coexistence of cationic and lipophilic groups and has been widely used for therapeutic NA delivery.

This ‘click’ propylamine β-CD has been used to formulate NP with siRNA and produced a 68% decrease of luciferase signal in immortalized hypothalamic neurons, and 40% GAPDH knockdown was observed in mHypoE N41 and primary rat (E18) hippocampal cells. The NPs demonstrated stability upon incubation with serum which is an indication that the NA is protected against nuclease degradation (O’Mahony, Godinho, et al. 2012). *In vivo* proof of gene silencing activity has been reported, with this CD in a mouse model (R6/2 mice) of Huntington’s Disease (HD), where delivery of siRNA against mutated Huntingtin (HTT) protein reduced HTT expression by approximately 85% after local injection into the brain (Godinho et al. 2012). The ‘click’ propylamine β-CD also showed *in vivo* potential as a treatment for inflammatory bowel diseases. After rectal administration to a Dextran Sodium Sulphate (DSS) mouse model reduced mRNA expression of Tumour necrosis factor-α by 73% and 58% for Interleukin-6, relative to controls was reported (McCarthy et al. 2013). This CD has also shown great promise for the pulmonary delivery of NAs via nebulised formulations (Hibbitts et al. 2014).

Polycationic β-CDs with the cationic charge facing the primary face and acyl lipid chains on the secondary face have also been explored as delivery vectors. Attached was thiourea resulting a polycationic head. This study proved the power of

thiourea over simple cysteamine because it bio-mimics histone-DNA-complexation. Increasing the charge density by modifying thiourea with the attachment of a further amine (increasing number of cationic functional groups from seven to fourteen) improved transfection further. The polycationic/polyamine face might be able to promote endosomal escape via proton sponge effect (Díaz-Moscoso et al. 2008) (Figure 1-3B). A subsequent study investigated the functionalisation of the secondary site with alkylthiourea and underlined once again the importance of the thiourea group (Ortega-Caballero et al. 2008). One key difference between these two studies is that cysteamine directly attached to the primary site of the CD was able to promote transfection while the same amine directly attached to the secondary site did not show any transfection unless the secondary side was modified with a thiourea linking group (Ortega-Caballero et al. 2008) (Figure 1-3C).

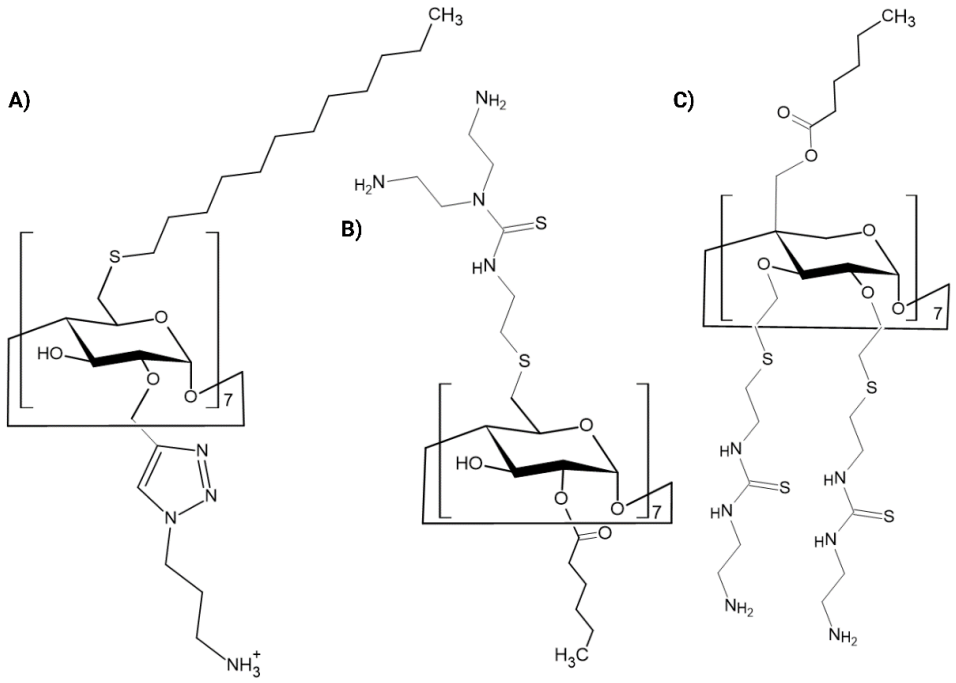

Figure 1-3 Chemical structures of amphiphilic cationic β-CDs. (A) 'click' propyl amine β-CDs (O'Mahony, Ogier, et al., 2012), (B) tetradecaaminothiourea β-CD (Díaz-Moscoso et al., 2008), (C) β-CD with secondary site alkylthiourea (Ortega-Caballero et al., 2008).

Similarly, Díaz-Moscoso et al. conducted a structure-activity-relationship (SAR)-study confirming the suitability of polycationic β-CDs with finely tunable chemistries as optimised vectors for pDNA delivery (Díaz-Moscoso et al. 2009). They showed that the charge density of cationic functionalities reaches a plateau in terms of transfection efficiency. The presence of protonatable amine groups was increased from 7 to 14 and to 21. The polycationic CD with 14 protonatable amines showed superiority over the other two polycationic CDs. It was implied that the arrangement of the cationic heads played also an important role in the complexation of the pDNA. Similarly, as the spacer between the cationic groups and the CD core increased the transfection efficiency *in vitro* decreased. The carbonyl chain varied from C_2 to C_6, expanding the distance between thiourea and terminal amine (Díaz-Moscoso et al. 2009). The biomimetic behaviour of thiourea groups interacting with the phosphate groups of the NA has repeatedly been shown to be of significant importance (Fernández, Benito, and Mellet 2013). Having ascertained the effect of this functional group, another study investigated the 'click' chemistry route to attach a thiourea group to the primary hydroxyl rather than the isocyanate intermediate which impedes higher yields. This study aimed to find a more cost-effective way to establish a library of vectors. However, the introduction of a triazole led to a more rigid structure and reduced transfection efficiency. A way to compensate for this loss was to introduce a nitrogen on the 4'-C of the triazole which enabled the attachment of two thiourea groups extended with terminal amines. This hyperbranched structure was superior to all reported vectors for the delivery of pDNA in this study, resulting in a 10-fold increase compared to a well-performing commercial polymer control (JetPEI). Remarkably, this structure also showed reduced toxicity relative to its competitors (Méndez-Ardoy, Guilloteau, et al. 2011) (Figure 1-4A).

In the following study, amino thiourea was repeatedly demonstrated to be the preferred cationic head group (Gallego-Yerga, Lomazzi, et al. 2014). The SAR study revealed that the presence of primary amine groups at the tail end is necessary for *in vitro* transfection, possibly due to the proton-sponge effect enabling endosomal escape. 'Click' chemistry utilising triazole is a relatively easy and affordable approach to create a library of cationic group modifications on CDs. However, these CDs performed less effectively compared to CDs with amides as cationic group connectors. It is speculated that the rigidity and the possible direct electrostatic interaction of the triazole with the NA may have an impact on the transfection behaviour (Gallego-Yerga, Lomazzi, et al. 2014). The influence of triazole and thiourea was further tested using a charged linear tail such as oligo ethyleneimine (OEI). The thiourea showed superior delivery of pDNA; however, the amphiphilic OEI-β-CD triazole cluster showed lower toxicity (ratio of amines in delivery vector/phosphates in NA (N/P) 10, >95% compared to 75% for its thiourea counterpart) (Martínez et al. 2013) (Figure 1-4B, C).

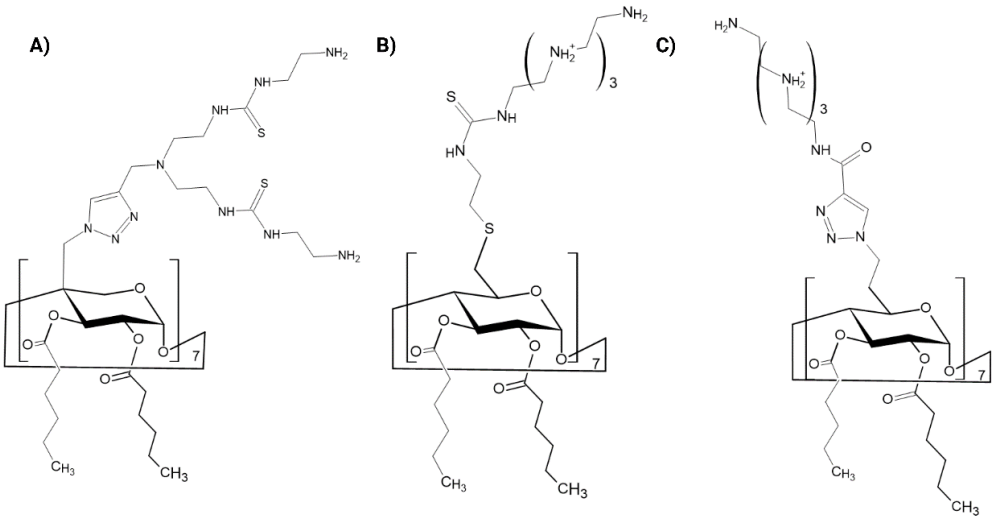

Figure 1-4 (A) 'click'-attached thiourea β-CD (Méndez-Ardoy et al., 2011), (B) Thiourea-attached OEI β-CD (Martínez et al., 2013), (C) 'click'-attached OEI (Martínez et al., 2013).

Later, amphiphilic β-CDs with lipid chains on the secondary site and triazole-attached polyethyleneimine (PEI) with terminal amines on the primary site were investigated. The effect of the extension of the PEI from four to five protonatable amines was tested for the delivery of siRNA to glioblastoma and prostate cancer cell lines. It was seen that increasing the charge density eliminated the activity of the NP because of the strong binding between the vector and siRNA (Manzanares et al. 2017). By synthesising a thiourea analogue of the shorter PEI-β-CD, the levels of two oncogene proteins were reduced by up to 75% in human prostate cancer, human glioblastoma, and rat glioblastoma cell lines. Additionally, a 65% reduction of these proteins was achieved in rat astrocytes, a primary cell culture that is extremely difficult to transfect. This β-CD also increased the therapeutic effect of docetaxel in these cell lines following a co-delivery approach with two siRNAs (Rheb and p42-MAPK) that are involved in the signalling pathway for the survival and proliferation of cancer cells (Torre et al. 2022).

1.2.3. Amphiphilicity bestowing supramolecular self-assembly

Natural CDs form transient assemblies in aqueous solutions (Ryzhakov et al. 2016). Introducing lipophilic tails onto one of the faces leads to more stable self-assembled structures. The coexistence of polar and non-polar features in a CD-molecule confers amphiphilicity. Depending on the nature of the attachment, monolayers, bilayers or micelles can be formed in aqueous media (Donohue et al. 2002; Villari et al. 2013). β-CDs modified with cationic functionalities on the secondary phase and lipophilic tails on the primary face form bilayers if the lipophilic chain contains C_{16} but rearranges in multilayers when in the presence of NAs. CDs with C_{12}, however, form micelles in solution and following the addition of NA form clusters (Villari et al. 2013). These alterations of structures, when examined using

small-angle X-ray scattering (SAXS), showed that the interaction with amphiphilic cationic CDs preserved the A-form of the secondary structure of the siRNA which is essential for gene silencing (Singh et al. 2019; Villari et al. 2013).

Earlier research established that the conjugation of a lipid tail to the primary face influenced the transfection efficacy of polycationic CDs, extending the lipidic attachment from C_6 to C_{16} leading to increased transfection efficiency (Cryan et al. 2004; McMahon et al. 2008). A series of 'inverted' amphiphilic cationic CDs have also been synthesised, where the 6'-OH-position contains the cationic groups, whereas the 2'-OH-position entails the lipophilic moiety (Figure 1-5).

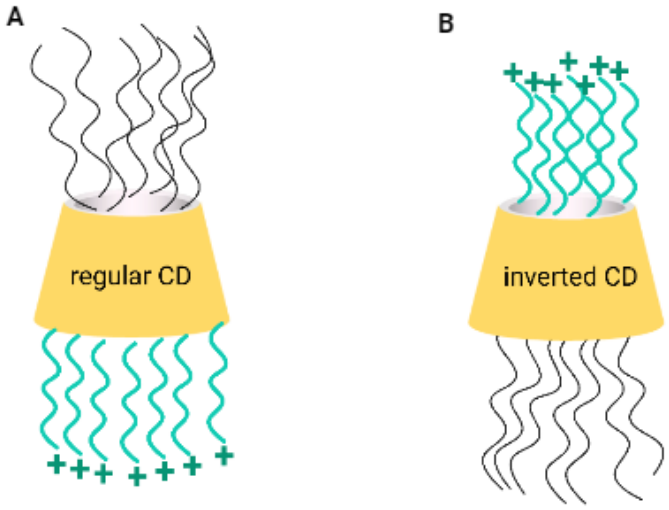

Figure 1-5 Amphiphilic cationic CDs with switched face modifications. (A) regular CD: lipophilic groups face the face while charged groups are attached to the secondary face. (B) Applying a different chemistry will result in an inverted CD where the functional groups (cationic and lipophilic) are switched in comparison to the regular CD.

The chemistry implemented (photochemical addition of thiols of lipids) allowed a controlled substitution of the secondary face with lipophilic tails on the 2'-OH rather than simultaneous substitution of 2'- and 3'-OH positions (seven tails rather than fourteen) that endows water solubility while maintaining self-assembly in

aqueous media (Byrne et al. 2009). A second chemical alteration to the inverted CD structure was the introduction of biologically labile functional groups before the attachment of the cationic functional group. Biologically labile groups include esters, which hydrolyse in acidic environments (endosomal pH 5.5), or disulfides that can be reduced in the cytoplasm upon cellular uptake (Byrne et al. 2009). An inverted CD was synthesised with a primary face containing cysteamine as cationic functions and octyloxycarbonyl on the secondary site. NP formed at mass ratio (MR) 10:1 (cationic CD:siRNA), demonstrated no difference in physicochemical characteristics nor *in vitro* transfection ability in caco-2 cells compared to a previously reported CD with the opposite orientation (O'Neill et al. 2011). In contrast, when the inverted structure was investigated in murine neuronal cells a higher level of gene silencing was reported (O'Mahony, Doyle, et al. 2012). A possible explanation for this might be the minor differences in the structure (Figure 1-6): where the C-chain connecting the primary amine with the CD core in the inverted CD is shorter compared to the other CD. This difference alters the hydrophilic-hydrophobic balance and again emphasises that changes in the chemistry can have an impact on *in vitro* performance (O'Mahony, Doyle, et al. 2012). Pflueger et al. further corroborated that the hydrophilic-hydrophobic balance is of immense importance for transfection ability of CD-NPs by creating a library of CDs with varying numbers of ionizable amino groups (7 and 21) on the primary face and different lengths of lipid chains on the secondary face. It appears that this balance strongly depends on the chemistries applied and hence presents the possibility of making conclusions on SAR (Pflueger et al. 2016).

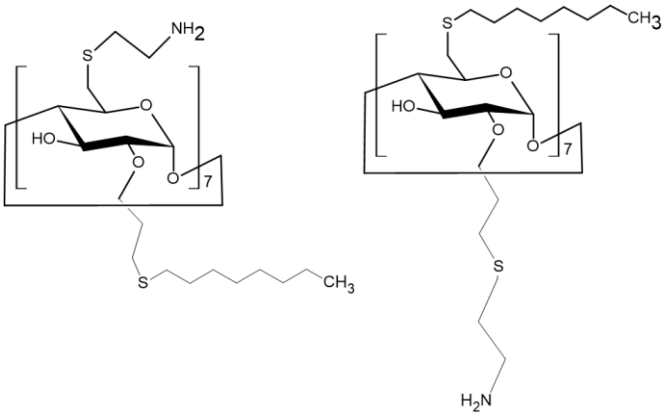

Figure 1-6 (A) inverted CD, (B) regular CD reported in O'Mahony, Doyle, et al., 2012.

Dìaz-Moscoso et al. have also investigated inverted CDs and have reported that lipid chain length can be a limiting factor in gene knockdown efficiency. The attachment of fourteen hexanoyl chains on the secondary face was superior in pDNA condensation compared to myristoyl groups, which irreversibly self-assemble into CD-aggregates in aqueous media, preventing the formation of NPs (Díaz-Moscoso et al. 2009). However, the attachment of myristoyl carbon chains on the primary face did result in pDNA condensation and increased transfection efficiency (Ortega-Caballero et al. 2008).

1.2.4. Blending CDs: tuning physicochemical characteristics

Another method to alter CD-NP characteristics is the co-formulation of two or more CDs with each other. In this case, each CD is synthesised separately, and each can serve a different purpose: cationic CD for NA complexation, neutral CD for charge shielding, and charge reduction.

Charge modulation: decreasing toxicity, increasing stability

The negative charge of NAs requires positively charged delivery vectors for successful complexation. In many cases, an excess of the cationic CD is used, and such NPs display a positive surface charge. While this cationic charge may be preferred in terms of enhancing cellular uptake through the negatively charged cell membrane, *in vivo* toxicity is likely. In circulation, the positive charge can attract negatively charged proteins and lead to aggregation, and/or can be recognised and eliminated by the immune system. Therefore, the reduction of NP charge while maintaining its transfection ability is crucial.

One method for charge alteration is the introduction of PEGylated CDs. NPs covered with PEG chains are called 'stealth' particles (Zalba et al. 2022). A 'click' chemistry approach has been employed as an easy and efficient method to attach cationic moieties to the secondary face of amphiphilic CDs. This approach can also be applied to PEG chains, obtaining amphiphilic neutral PEGylated CDs. A PEGylated CD (CD-PEG500) was mixed with an amphiphilic cationic CD and siRNA to achieve reduced surface charge. While shielding against salt-containing media was observed, full protection in serum was not achieved. The same NPs showed reduced transfection efficiency in caco-2 and neuronal cells due to the hydrophilic charge-shielding through PEG groups and consequently reduced cell interaction (O'Mahony, Ogier, et al. 2012, 2013). This unintended consequence can be rectified with the potential for the addition of a targeting ligand at the end of the PEG chain (Guo, Ogier, et al. 2012; Symens et al. 2012). In another study, Guo et al. was able to synthesise a pH-sensitive reversible PEG attachment that is cleaved in the extracellular tumour environment and consequently releases PEG. This example could present a another possible method to overcome the negative effects of PEG-shielding (Guo, Cheng, et al. 2012). In a further

approach, neutral PEGylated CDs with extended lengths were synthesised (PEG500, PEG 1000, and PEG2000) to further stabilise CD-NP *in vitro* and ultimately *in vivo*. Co-formulated NP showed extended circulation time of siRNA compared to free siRNA, however, the difference was statistically nonsignificant compared to NP with only the amphiphilic cationic CD. Higher molecular weight (MW) PEG attachment might increase stability and protection but can lead to immunogenicity which can cause problems for re-administration. Generally, a precise balance of stability, protection and immunogenicity needs to be achieved (Godinho et al. 2014).

1.2.5. Cell-specific targeting

Most NPs are administered intravenously (IV) to bypass the many barriers of the gastrointestinal tract, such as pH changes and mucous. The first contact in the circulation is with different proteins, depending on the surface characteristics of the NP. These interactions affect the biodistribution. A positive charge will lead to electrostatic contact with negatively charged proteins or immune recognition by macrophages. Lipophilic NPs may interact with lipid trafficking molecules, for example, ApoE that can serve as an endogenous targeting ligand for liver cells (Mendonça, Kont, et al. 2023; Rizvi and Saleh 2018).

There are two key reasons for the use of targeting groups in NP development. Firstly, certain NPs including LNPs accumulate primarily in the liver upon IV administration. Suitable targeting of NPs may achieve wider biodistribution to specific disease sites beyond the liver. Furthermore, targeting ligands bestow the ability to reduce dose, and consequently side effects (Evans, Malhotra, Guo, et al. 2016; Gallego-Yerga et al. 2018; Mendonça, Kont, et al. 2023). Employing CDs as NA

delivery vectors gives multiple formulation opportunities for cell-specific targeting as described below:

1.2.5.1. Covalently attached targeting ligand - targeted CDs

One study employed a co-formulation approach of an amphiphilic cationic and an amphiphilic targeted CD. The cationic and targeted moieties are connected at the 6'-OH of the β-CDs. This co-formulation targets asialoglycoprotein receptor-bearing HepG2 cells utilising the galactosyl group as a targeting ligand. Chemical fine-tuning of the linker lengths proved to be of high importance: transfection levels increased with an increase in linker length from 7 atoms to 15. The increase in pDNA delivery, with targeted CDs was further improved with the inclusion of the fusogenic lipid 1,2-dioleoyl-sn-glycero-3-phosphoethanolamine (DOPE), known to enhance endosomal escape (McMahon et al. 2012).

Gooding et al. studied a similar approach of co-formulation with CDs containing C_{12} lipid chains on its primary site and 'click'-attached functionalisation on its secondary site. Three CDs were co-formulated: CD modified with a primary amine (to complex siRNA), CD with PEG500 chains (to convey stability), and a CD containing PEG500-amine occasionally modified with a targeting ligand (rabies virus glycoprotein (RVG)). The co-formulation diminished the negative impact of PEG-shielding on cellular uptake. After co-formulation of aminated and targeted CD (Figure 1-7A, B), cellular uptake and gene knockdown were tested in neuronal cells. Although enhanced cellular uptake of targeted formulation versus untargeted was observed, gene knockdown was only 27% (half of 'only' amphiphilic cationic CD-siRNA formulation). This does not conclude that this approach has failed but that

mechanisms after cellular uptake, such as NA cargo release into cytoplasm, might have an impact (Gooding et al. 2015). The high positive charge of the unmodified formulation boosts endosomal escape but NPs with positive surface charge have proven to be toxic *in vivo* (Knudsen et al. 2015). Therefore, the improved uptake (because of RVG-targeting) and reduced charge (because of PEG) demonstrated by this formulation, while maintaining its ability to complex siRNA, presents potential for *in vivo* studies (Gooding et al. 2015). Guo et al. used the same approach on the secondary side with anisamide (Figure 1-7C), a ligand against sigma-receptors that are associated with most cancers, especially prostate cancer. The primary face contains the positive charge to complex the NA. This targeted CD-NP showed excellent gene knockdown ability *in vitro* (~80% reduced mRNA levels of reporter gene luciferase). Following IV administration to an *in vivo* tumour mouse model, a 5-fold reduction of vascular endothelial growth factor compared to the control group was reported, highlighting the potential of such formulations (Guo, Ogier, et al. 2012).

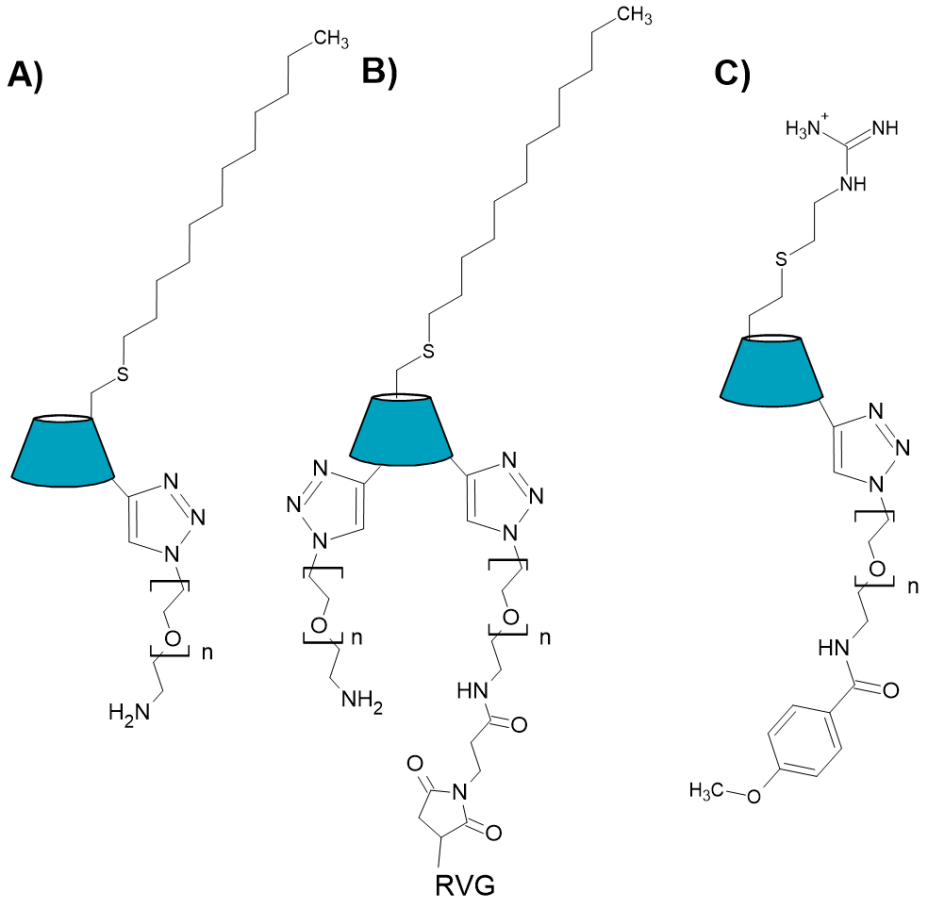

Figure 1-7 (A) Amphiphilic, PEGylated, cationic CD, (B) amphiphilic, PEGylated, cationic, RVG-targeted CD. (A) and (B) were co-formulated in Gooding et al., 2015., (C) an anisamide-targeted cationic CD (Guo, Ogier, et al., 2012).

The use of sugar monomers as targeting ligands (Figure 1-8) is a common approach to direct NPs to macrophages and non-parenchymal liver cells. An amphiphilic polycationic CD was decorated with mannopyranose to deliver pDNA to cells that overexpress fucose-mannose receptors. The sugar monomer was conjugated to the multi-cationic head on the primary face. This has the additional benefit of reducing the number of cationic amine groups, thereby diminishing toxicity while maintaining transfection efficiency in RAW 264.7 (expressing mannose receptors). It was also proven that the uptake depends on ligand-receptor recognition (Díaz-Moscoso et al. 2011). Mendez-Ardoy et al. further elaborated on this technique to

assess the effect of the saccharidic antennae on physicochemical characteristics and the variation of glycotope density on gene delivery capabilities. While preserving the electrostatic interaction of the CD with pDNA, it was evident that the compaction was impeded. The size increase of NPs with increased mannose-conjugation was very subtle, however, charge decrease was detectable even at low mannose occupancy. A stability study confirmed that the mannose coating has a protective role against saline stress. In terms of pDNA delivery, mannose-CD-NPs showed cell selectivity towards the mannose-recognising cell line RAW 264., incorporating 15% mannose (Méndez-Ardoy et al. 2015). In another study, tri-antennary galactose was chosen to decorate the primary face of β-CD for the delivery of mRNA to asialoglycoprotein receptor (ASGPr) in HepG2 cells. 31% of green fluorescent protein (GFP)-positive cells were detected, outperforming jetPEI-Hepatocyte complexes (positive control) (Symens et al. 2012).

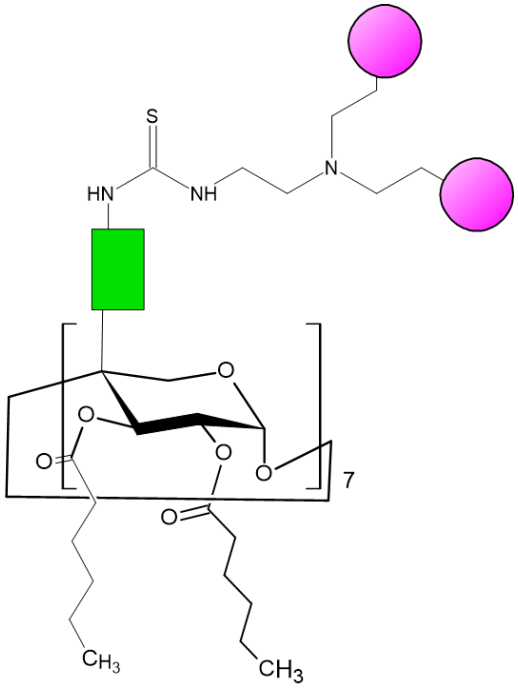

Figure 1-8 Amphiphilic β-CD with cationic and targeting ligands on primary face (purple circles). Green box: linker groups such as triazole or thiourea.

1.2.5.2. Adamantane inclusion complex

Adamantane is a lipophilic molecule that fits effectively into the hydrophobic β-CD cavity. It is commonly conjugated with a targeting moiety via a PEG chain. When this adamantane-PEG-ligand construct is incubated with the CD, an inclusion complex is formed. Fitzgerald et al. reported targeted CD-NP with divalent anisamide ligands (Figure 1-9) aimed at the sigma-1 receptor, which is overexpressed in prostate cancer. The inclusion complex was tested in three prostate cancer cell lines (DU145, PC3, VCaP), achieving 30% gene knockdown of Polo-like kinase 1 (PLK1) relative to the untargeted formulation (Fitzgerald, Malhotra, et al. 2016). Similarly, Mendonca et al. utilised adamantane to include RVG into an amphiphilic cationic CD for the delivery of siRNA against HTT in a novel HD model co-culturing hCMEC/D3 BBB cells and ST14A striatal cells, reducing HTT-mRNA levels by 65% (Mendonça et al. 2021).

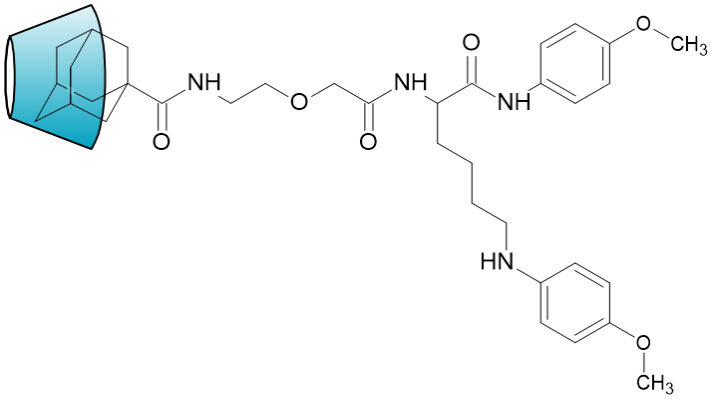

Figure 1-9 Illustration of adamantane-inclusion complex with a CDs (Fitzgerald et al., 2016).

1.2.5.3. Post-insertion utilising DSPE-PEG

Another approach to decorate CD-NPs with targeting ligands involves attaching the targeting ligand via a PEG chain to a lipid, for example, DSPE. This

targeting construct is then incorporated into pre-formed NPs using the 'post-insertion' technique.

O'Mahony et al. targeted neuronal cells with CD-siRNA-complexes post-modified with octa arginine (R8)-PEG2000-DSPE. This formulation decreased the cationic charge, increased the salt stability and the level of cellular uptake, and consequently reduced the mRNA levels of two target proteins (O'Mahony, Desgranges, et al. 2013). A folate-targeted amphiphilic cysteamine-CD-NP was screened in different prostate cancer cell lines expressing the Prostate-Specific Membrane Antigen. The targeting ligand was conjugated to DSPE-PEG5000. Increased uptake was detected compared to the untargeted formulation. RelA (transcription factor p65) was reduced in VCap cells (44%) and LNCaP cells (22%). Additionally, siRNA protection was assessed *in vivo* in mice after IV bolus injection, expressing an 8-fold increase of siRNA half-life upon incorporation of PEG (Evans, Malhotra, Guo, et al. 2016). Similarly, a folate-targeted formulation was tested in a 3D Matrigel^{TM} system. Knockdown of tumour-associated genes, ZEB1 and NRP1, at gene and protein levels were confirmed, and reduced infiltration through the Matrigel was imaged. This study highlighted the efficiency of targeted formulations in siRNA delivery in different models (Evans et al. 2017). A novel 3D model was developed to imitate bone metastasis in prostate cancer and used to test CD-siRNA-NP post-modified with DSPE-PEG5000-anisamide. This formulation showed enhanced uptake and endosomal release in PC3 and DU145, and successful gene knockdown for PLK1 was reported (Evans, Malhotra, Fitzgerald, et al. 2016).

The post-insertion technique was further advanced by conjugating DSPE-PEG with a fragment antibody (Fab) recognising IL-3Rα/CD123, a therapeutic target in acute myeloid leukaemia (AML). CD123 is an overexpressed surface antigen in AML

stem cells, which are responsible for disease relapse with high mortality rates. Fab was conjugated with DSPE-PEG-maleimide, where maleimide served as an active conjugation site. The formulation was tested both *in vitro* and *ex vivo* in AML patient blood samples. The targeted NP significantly reduced the expression of mRNA and protein levels of Bromodomain-containing protein 4. Furthermore, it was possible to detect myeloid differentiation, apoptosis, and reduced blast proliferation. This Fab-targeted NP produced a synergistic effect when combined with the clinically used chemotherapeutic agent, cytarabine (Guo et al. 2017). A similar synergistic effect in colorectal cancer was reported by Zou et al. DPSE-PEG-folate-targeted NPs were prepared with siRNA against nuclear factor kappa B (NF-κB). The knockdown of NF-κB sensitizes the cells to docetaxel and consequently increases the therapeutic effect of the small molecule drug. *In vitro* studies showed an 85% reduction in mRNA levels of NF-κB and a 75% reduction at the protein level. The inhibition of tumour growth was observed for the targeted combination therapy *in vivo* (Zou et al. 2021). The post-insertion method can also be expanded to antisense oligonucleotide (ASO)-cell-specific delivery. The targeting ligand was synthesised by utilising DSPE-PEG-maleimide for the conjugation of RVG, a central nervous system-targeting (and cell-penetrating) peptide. The post-modified CD-ASO-complex accomplished 37% downregulation of possess single-nucleotide polymorphism1 mRNA in co-culture of hCMEC/D3cells (HD related cell lines) (Mendonça, Sun, et al. 2023).

This approach has also been used in immunotherapy directed at tumour-associated macrophages (TAM). M2 macrophages are a type of TAM that depend on colony-stimulating factor-1 (CSF-1) downregulation to reprogram into M1 macrophages which are responsible for stimulating the immune system. Therefore, CSF-1 is an attractive therapeutic target for RNAi. Siglec-1/CD169 is overexpressed

on M2 macrophages and serves as a target for ligand-modified CD-NP. Sialic acid was conjugated to stearic acid-PEG-carboxyl and incubated with pre-formed CD-siRNA complexes. *In vitro* human and mouse-derived prostate cancer cell lines were used to investigate the efficacy of this formulation. The significant reduction of CSF-1 with the targeted formulation led to the reprogramming of M2 to M1 macrophages in both cell lines. The reprogramming with targeted formulations resulted in an increase in apoptosis, measured with flow cytometry, in a prostate cancer cell Trans well model consisting of PC3 and TRAMP C1 prostate cancer cells (apoptosis: 49% and 69% respectively) (Sun et al. 2023).

A summary of the post-inserion approach in CDs for cell specific targeting is summarised below (Table 1-1).

Table 1-1 Summary of cell specific targeting using a post-insertion approach.

Lipid-PEG$_X$- ligand	**Cell type**	**Reference**
DSPE-PEG$_{2000}$-R8	Neuronal cells	(O'Mahony, Desgranges, et al. 2013)
DSPE-PEG$_{5000}$-folate DSPE-PEG$_{5000}$-anisamide DSPE-PEG$_{2000}$-folate	Prostate cancer cells	(Evans et al. 2017; Evans, Malhotra, Guo, et al. 2016) (Evans, Malhotra, Fitzgerald, et al. 2016; Fitzgerald, Malhotra, et al. 2016) (Zou et al. 2021)

DPSE-PEG_{2000}-mal-Fab	Leukaemic cells	(Guo et al. 2017)
DPSE-PEG_{2000}-mal-RVG	Neuronal cells	(Mendonça, Sun, et al. 2023)
Stearic acid-PEG-COO-Sialic acid	Prostate cancer cells	(Sun et al. 2023)

R8= Octa arginine, RVG= rabies virus glycoprotein

1.3. CD-based dimers

CD-dimers consist of two identical molecules linked together and present an alternative delivery system for NAs. Generally, they can be divided into two groups: non-covalent and covalent dimers. Dimerisation can occur through interaction of the lipophilic attachments on CD monomers (aromatic structures (Figure 1-10): π-stacking, inclusion complexes of monomers with for example bis-adamantane (Figure 1-11)), or direct covalent conjugation of CD monomers.

Gallego-Yerga et al. attached a xylene moiety to a single glucose unit at 2'- and 3'- positions on the secondary face (Figure 1-10, **'previous work'**). This chemical modification enabled self-assembly and is thus a suitable alternative to substitution with lipid chains. The self-assembling mechanism depends on the non-covalent dimerization of two CDs in which the xylene acts as a guest molecule in the CD cavity. The pre-organised structure leads to a controlled snake-like NP in the presence of pDNA (confirmed with transmission electron microscopy). Interestingly, these dimer structures are labile in acidic environments. This is an indication that the NP cargo will be released at endosomal pH, which has been corroborated with *in vitro* data in COS-7 cells where CD-NPs were as competent as PEI, a polyplex positive control (Gallego-Yerga, González-Álvarez, et al. 2014).

The possibility of linking one xylene molecule to two neighbouring glucose units in a β-CD (2'-OH and 3'-OH, one position at a separate glucose unit, Figure 1-10, **'current work'**) has been explored to optimise the inclusion and self-assembly properties of the CD. Two kinds of xylene were utilised: o- and m-xylene. While o-xylene was able to maintain the conformation of β-CD (circular topology), the attachment of m-xylene initiated a conformational change (ellipsoidal topology). These changes impact the assembly of the CDs in aqueous solution and also the selective inclusion of guest molecules due to changes in cavity shape as a result of the attachment of aromatic groups on the secondary face (Neva et al. 2018). It is known that NP shape impacts biodistribution. The attachment of aromatic moieties that impose restrictions at a molecular level was further tested *in vitro* to evaluate shape-dependent transfection ability. In this study two factors were changed: the CD core and the aromatic clip. The CD type dictates the size of the cavity, while the aromatic moiety defines the conformational change. Both impact the NP morphology. (Figure 1-10). The library of CDs generated in this study was tested in COS-7 and HepG2 cell lines. Results showed that certain shapes of the NPs (rod, worm, and toroidal) are cell-selective. Bilayer CD complexes, however, were successful in both cell lines regardless of charge density and CD type, highlighting the importance of NP morphology. These results suggest that the design and chemistry of CDs can be tuned to target specific sites (Neva et al. 2020).

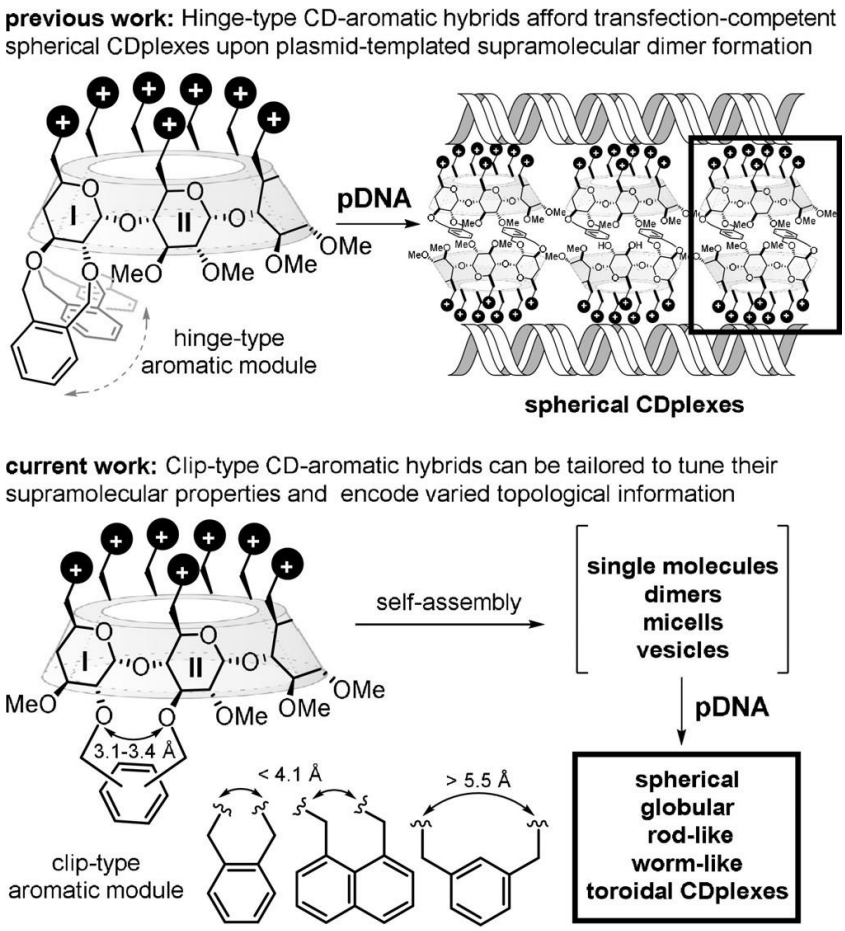

Figure 1-10 Adapted from Neva et al., 2020. Aromatic-modified CDs. 'previous' work presented in Gallego-Yerga, González-Álvarez, et al., 2014 describes β-CDs modified with aromatic functions on secondary site attached to one single glucose in CD-ring. 'current' work describes work from Neva et al., 2018 and Neva et al., 2020 where aromatic structures are attached to adjacent glucose molecules in one ring.

Another strategy to obtain self-assembling cationic CDs (primary face cysteamine-modified) was conducted by taking advantage of the adamantane-CD-inclusion complex approach. Bis-adamantanes (Figure 1-11) with different lengths of amide and thiourea-linker were synthesised and tested both *in vitro* and *in vivo*. Results showed that the distance between the two adamantanes should be at least the length of three carbons for successful pDNA condensation. Formulations with these guest molecules also showed better stability in serum. Bis-adamantanes with six or more atoms did not show any major improvement (Gallego-Yerga et al. 2015).

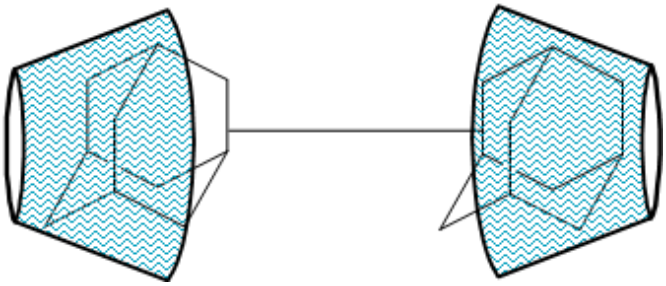

Figure 1-11 Schematic of bis-adamantane employed to bestow self-assembling characteristics to cationic CDs via inclusion complex without the covalent attachment of lipid chains.

The chemistry can be further advanced by covalently conjugating two β-CDs with each other either at their primary (6-6-dimer) or secondary face (2-2-dimer) (Figure 1-12). This also enables control of the shape of formulated NPs and creates NPs that can target organs selectively. The transfection properties *in vitro* were shape-dependent and differed depending on the cell line, which was confirmed through tissue-selective pDNA delivery of ellipsoid NP to the spleen *in vivo* in a mice model (Gallego-Yerga et al. 2018).

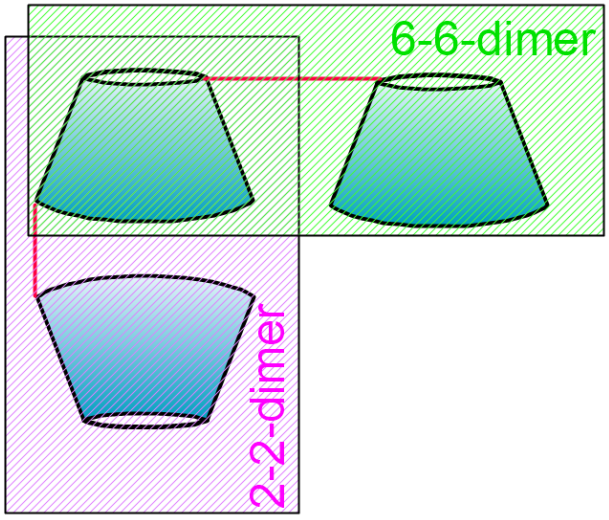

Figure 1-12 Schematic representation of covalently attached CDs either on primary (6-6-dimer) or secondary (2-2-dimer) face. The CD-dimers are modified with a polycationic head on primary face and lipophilic chains on secondary face, thus being amphiphilic. The dimerisation is independent of attached functionalities.

Non-amphiphilic covalently attached dimers were investigated as active ingredients for the selective extraction of 7-KC. Investigations revealed that the linker characteristics and modifications of remaining hydroxyl groups on CD-scaffold can define the selectivity of the inclusion complex (Anderson et al. 2021).

In summary, these finding confirm the importance of applied chemistry at molecular level and its biological functions.

1.4. CD Polymer-based nanoparticles

A second approach to utilise CDs for gene delivery is to synthesise polymeric systems, either as monomers of the polymer or as building blocks for other polymers. CDs can bestow distinct design features when incorporated into pre-formed polymers such as acting as a host for the active ingredient, or the targeting ligand, or as a second polymer to moderate the toxicity of the other polymers. CD-polymer networks in this chapter can be classified into five main types (Escobar et al. 2023; Liu et al. 2021) (Figure 1-13): A) Linear CD-Polymers, B) Polyrotaxane, C) CD grafted polymers, D) star-shaped polymers containing CDs, and E) CD-cross-linked polymers.

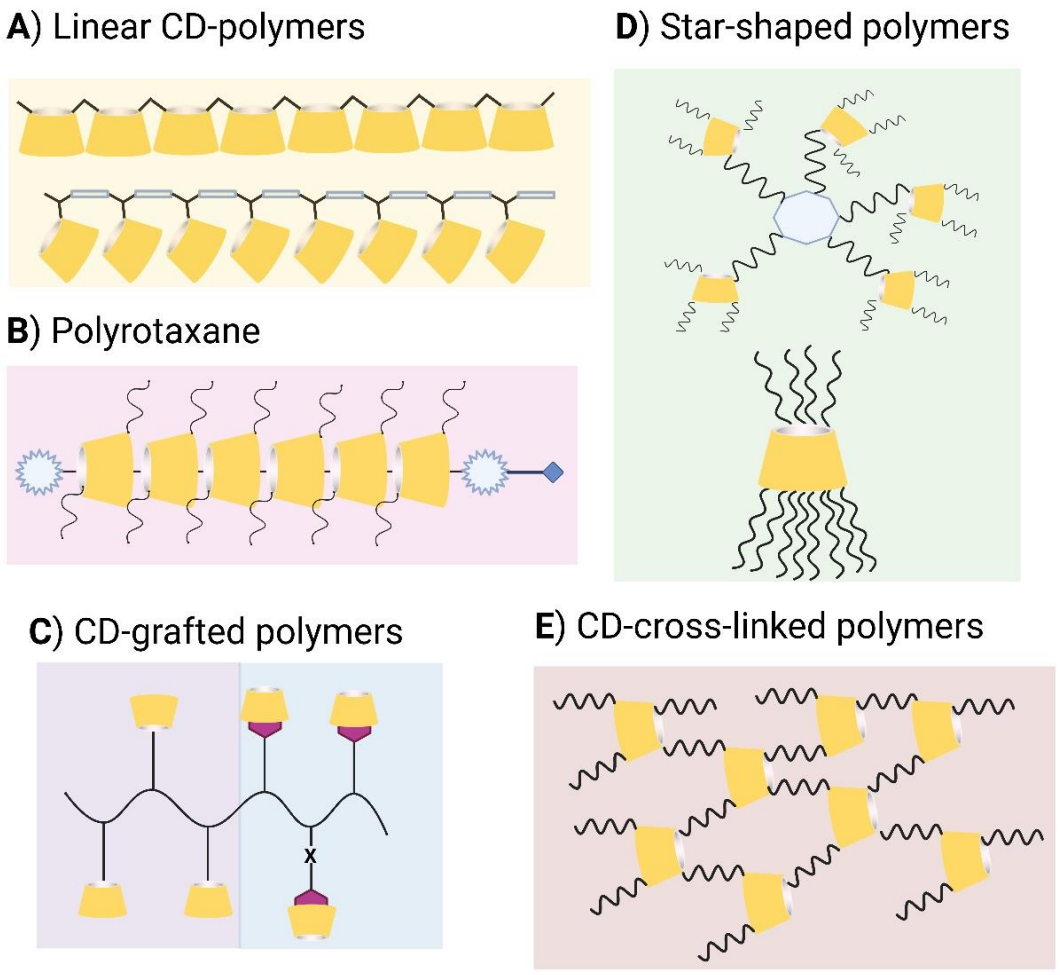

Figure 1-13 (A) Linear CD-polymers., (B) Polyrotaxane: CDs threaded along a linear polymer that are end-capped with different molecules., (C) CD grafted polymers: CD can confer reduced toxicity and solubility to linear polymers., (D) Star-shaped polymers where CDs are either part of the 'arms' or build the 'body' of the polymer., (E) CD-cross-linked polymers. CDs are used to build the main structure of the polymer.

CD-based polymers have potential as drug delivery vectors. Site-specific tumour release can be achieved by in-built stimuli-responsive systems. They can be biodegradable and may be decorated with organ-targeting ligands. Modulation of size can allow the delivery vector to exploit the EPRE in solid tumours, and evade clearance by the mononuclear phagocytic system, thus prolonging half-life. In

addition, depending on the chemistry many polymers self-assemble into micelles, vesicles, nano-sponges, or NPs (Liu et al. 2021).

1.4.1. Linear CD-polymers

The first CD based delivery system for siRNA to reach the clinic was CALAA-01 (Figure 1-14), a linear-linked β-CD-based polymer (Zuckerman et al. 2014). Firstly, the primary face of the CD was modified with cysteamines as building blocks for water-soluble polycations. A condensation reaction with the cross-linking agent, dimethyl suberimidate (homobifunctional amine-reactive imidoester (Hermanson 2013)), resulted in a linear polymer (Davis et al. 2004). Adamantane-PEG with and without targeting ligand transferrin are used to form inclusion complexes with the hydrophobic cavity of the CDs. PEG was employed to increase circulation time and transferrin served as a targeting ligand to compensate for loss of uptake due to the shielding effect of PEG (Bellocq et al. 2003). The ends of the polymer were capped with imidazole to increase delivery efficiency (Davis 2009; Mishra et al. 2006). After successful preclinical studies (Bartlett and Davis 2007) (Hu-Lieskovan et al. 2005), the formulation was evaluated in non-human primates. The formulation achieved siRNA delivery in monkeys and was well tolerated following multiple systemic dosing (Heidel et al. 2007). Based on this data, the formulation proceeded to first-in-human phase I clinical trial. NPs were prepared at the bedside (one vial containing the siRNA, the second vial with the delivery compounds) and administered intravenously to 24 patients with stubborn solid cancers. The siRNA was designed to knockdown the anti-tumour target, Ribonucleotide reductase subunit M2. Tissue samples showed that NPs were localized in the tumour, showing a reduction in the expression of the targeted gene at mRNA and protein levels (Davis et al. 2010; Zuckerman et al. 2014).

Disappointingly, the study needed to be terminated early because trial participants experienced dose-limiting toxicity in the form of fatigue and fever (Barata, Sood, and Hong 2016)), even after changing the dosing regimen (Zuckerman et al. 2014).

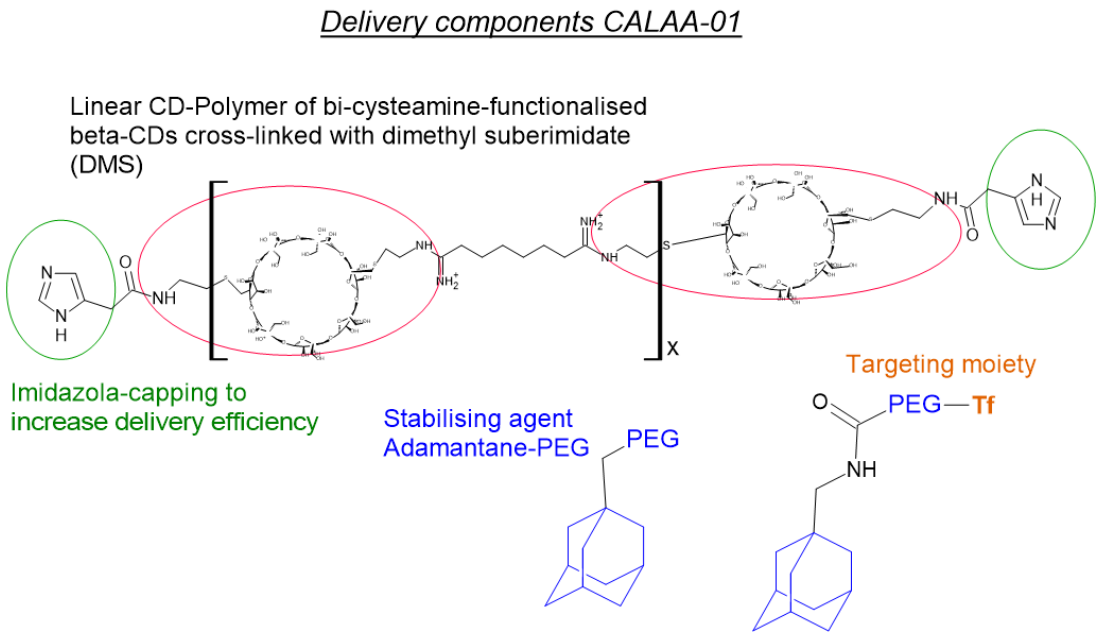

Figure 1-14 Components of CALAA-01.water-soluble, cationic, linear CD-polymer (red cicle) to complex the siRNA, Imidazole-capping (green circle) to increase the delivery efficiency, Adamantane-PEG as stabilsiing agent in blue, Adamantane-PEG-transferring (orange) to target human trasnferrin. All delivery components come in one vial and are mixed with a second vial containing the siRNA on the bed side.

In another study, β-CDs were activated with 1,1'-carbonyldiimidazole to be reacted with PEI2k. This simple conjugation resulted in CD-linked PEI (CP 2k). Li et al. investigated this CD-cross-linked polymer for intranasal delivery of mRNA as a vaccine against HIV-1 gp120. CP 2k successfully delivered mRNA in three different cell lines and was significantly better than PEI25k. *In vivo*, intranasal administration of the formulation in mice showed extended adhesion in the nasal mucosa, while simultaneously infiltrating the epithelial barrier causing systemic and mucosal immunity which was confirmed by antibody and cytokine titres (Li et al. 2016).

1.4.2. CD-based polyrotaxanes

Polyrotaxanes (PR) are linear polymers that are decorated with CDs threaded along the polymer string where the hydrophobic cavity of the CD builds an inclusion complex with the linear polymer. The hydroxyl groups of the CDs can be chemically modified with cationic functional groups. These modifications enable the use of PRs in non-viral delivery of NAs. The interaction between PR and NA chemically mimics histones, and morphologically imitates the nucleosome when complexed with double-stranded DNA (Shibaguchi et al. 2019). Yokoyama et al. investigated the relevance of the number of threaded CDs and concluded that increasing the number bestows a more rigid structure and improved cellular uptake (Yokoyama et al. 2014). PRs are polymers that have more than five CDs threaded along its axis. If less than five CDs are involved, the structure is termed rotaxanes. Both ends of the linear polymer can be capped with various functionalities that allow the CDs to move freely without de-threading and facilitates optimised interaction with the NA cargo. The absence or presence of certain structures determines the nomenclature of PRs. In the absence of end-caps, PRs are called pseudo-PRs (Ooya et al. 2006; Poggetto et al. 2020). The blocking caps can contain cleavable bonds which facilitate the breakdown of the polyplex, and hence, the release of the cargo and clearance of the polymeric material out of the body (Shibaguchi et al. 2019; Yamada et al. 2012). PRs possess low water solubility due to the strong intramolecular hydrogen bonding of the threaded CDs. Chemical modifications of the hydroxyl groups on either side of the threaded CD or the introduction of functional groups at the ends of the linear polymer can increase water solubility and additionally enhance the self-assembling character based on the hydrophilic-lipophilic balance in the PR. The introduction of cationic groups on the

CD additionally enables the complexation of NAs and also enables endosomal escape (Li, Liu, and Qiu 2023).

In the early 2000s, PRs with Poly[(ethylene oxide)-ran-(propylene oxide)], a linear system threaded with OEI-modified-α-CD, was utilised to deliver pDNA encoding renilla luciferase. The cationic nitrogen of the ethylenimine groups on the CD allowed for complexation with the polyanionic NA. The linear axis was capped with bulky 2,4,6-Trinitrobenzene sulfonic acid (TNBS) groups. High transfection efficiency was observed in various kidney cell lines (HEK293, COS7, BHK-21), and cancer cell lines (ovary tissue SKOV-3; uterus MES-SA) (Yang et al. 2007).

A commercial non-ionic A-B-A-triblock copolymer, Pluronic, was employed at different A/B ratios, where A represents the hydrophilic component, poly oxyethylene, and B stands for the lipophilic component, the poly oxypropylene. 2-hydroxypropyl-β-CD was threaded on the Pluronic chain and further modified with dimethyl ethylene diamine (DMEDA) to enable siRNA complexation. The PR ends were capped with cholesterol. Nanocomplexes delivered siRNA to HeLa and NIH 3T3 cells causing >80% gene knockdown with favourable cell viability (>90%) (Badwaik et al. 2016).

PEGylated CD-based PRs combinations are widely used due to low toxicity (Li et al. 2023). Kulkarni et al. synthesised PRs of different MW and showed that higher MW PEG-based PRs show better transfection (PEG10 000 > 3500 > 2000). α-CDs were threaded along a PEG-chain end capped with TNBS (Figure 1-15). The CD-hydroxyls were modified with DMEDA to promote NA complexation. CHO-GFP and NIH3T3-GFP cells were used to test the gene knockdown by the polymer NP. Gene silencing was comparable to commercial controls (Lipofectamine 2000 and branched

PEI (bPEI)). RNAi maximum was achieved at N/P 10. Toxicity profiles were >100-fold lower than bPEI (Kulkarni, Defrees, et al. 2013).

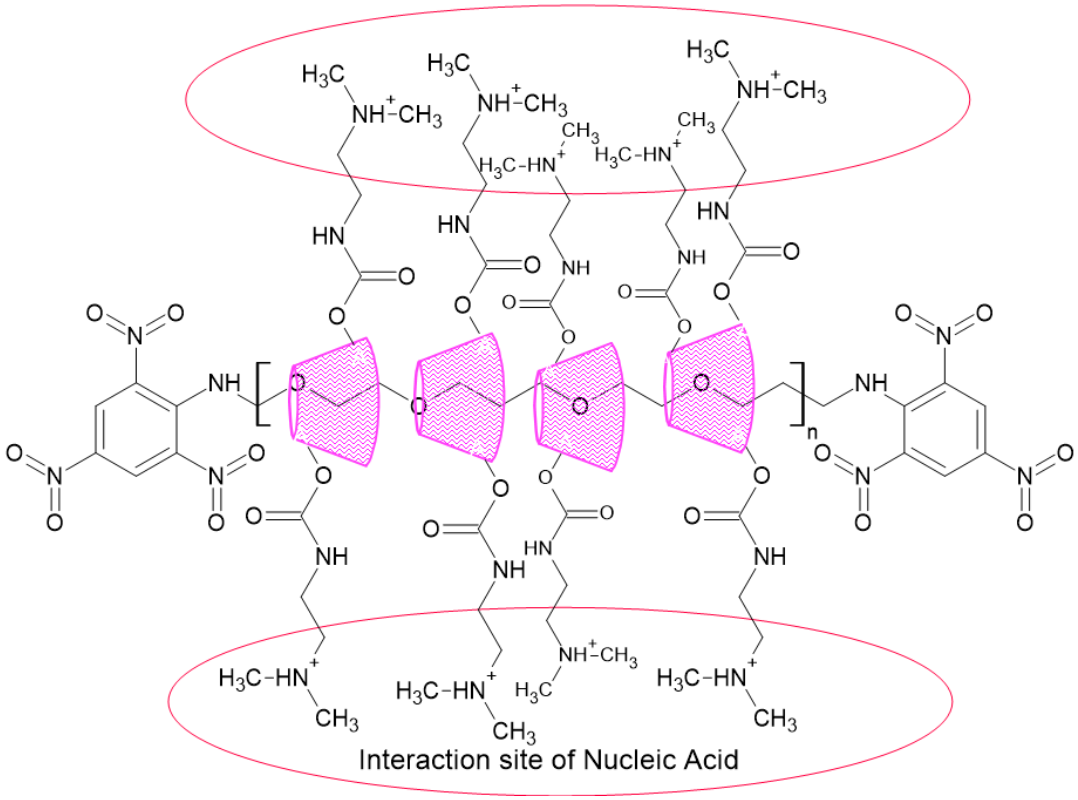

Figure 1-15 Poly rotaxane with linear PEG chain that carries α-CDs, modified with N,N'-dimethylethylenediamine, and end capped with 2,4,6-Trinitrobenzene sulfonic acid. As modified from (Kulkarni, Defrees, Schuldt, Hyun, et al. 2013).

Song et al. synthesised a PEG backbone decorated with an α-CD modified with ethanolamine groups to complex pDNA, and a degradable polypeptide (poly(aspartic acid)) conjugated to each end of the PEG. The breakdown of the polypeptide mobilises the CDs and facilitates the release of the NA. *In vitro* experiments using C6 cells, a rat glioma cell line, indicated that cell migration was prevented, apoptosis was boosted, and cell proliferation was inhibited. This result was reflected *in vivo*, where successful repression of tumour growth in mice was observed (Song et al. 2018).

Similar to other nanomaterial systems, PRs can be modified with targeting ligands such as folic acid (FA), commonly expressed on the surface of cancer cells. PEG4000 was threaded with PEI600-modified α-CDs and end-capped with FA for the delivery of p53 pDNA. These complexes showed superior antitumour effects in nude mice compared to PEI-25k (Zhou et al. 2012). Researchers used a new approach where the two terminal hydroxyls of PEG were modified with different functionalities. To achieve a bifunctional PR, each site was attached to either polycaprolactone (PCL) or folate, both in a one-step reaction. This PR was complexed with Nile red dye and showed the ability to enter cells and the potential to deliver therapeutic NAs (Poggetto et al. 2020).

PRs can also be used to generate hydrogels. This concept is based on the development of a triblock polymer with a cationic end (PEI), a hydrophobic PCL connector, and a PEG end (Figure 1-16). This linear triblock polymer can form micelles due to its amphiphilic character and can condense pDNA into polyplexes. These complexes outperformed PEI in terms of toxicity and transfection efficiency. When added to the polyplexes, α-CDs act as a cross-linking agent. It threads along the PEG-fragment creating a pseudo-PR, while the NA remains complexed to the PEI-fragment. Hydrogel formation could also be achieved *in situ* at tumour site. An advantage of this copolymer is its biodegradability. This strategy proved successful in nude mice, where the hydrogel showed sustained release of the NA cargo and inhibited tumour growth *in vivo* in chemotherapy-resistant cancer (Liu et al. 2017).

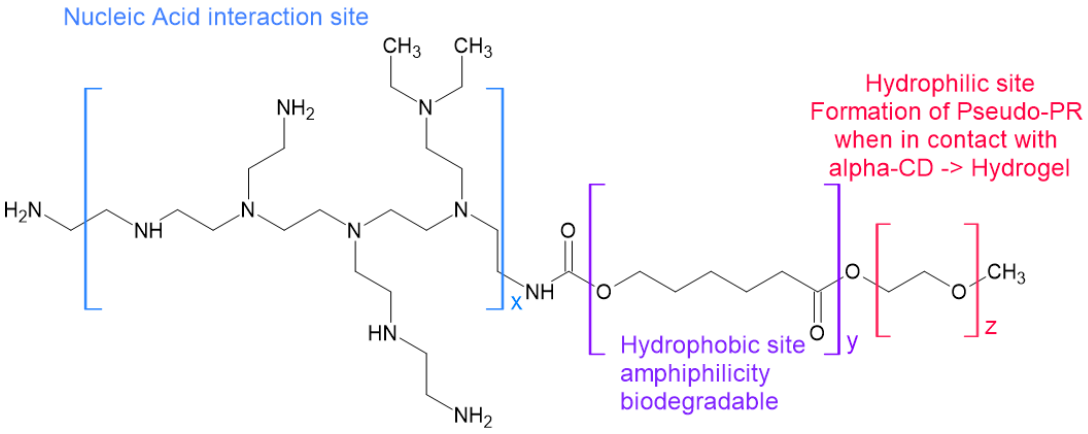

Figure 1-16 Triblock polymer with a cationic end (PEI), a hydrophobic PCL-connector, and a PEG end which builds a hydrogel when in contact with α-CD. The CDs thread along the PEG axis. Modified from (X. Liu et al., 2017).

1.4.3. Grafted CD polymers

Grafted CD polymers are linear polymers that are decorated with pendant CDs along its axis. The CDs can either be directly conjugated to the polymer or can form an inclusion complex with a lipophilic compound previously attached to the polymer. The incorporation of CDs modified with cationic groups allows the complexation and delivery of NA (Li et al. 2023).

PEI is often used for nonviral delivery of NAs; however, its use is limited by its toxicity. CDs mediate PEI tolerability which increases proportionally with the percentage of CD-grafting. While CD grafted PEI condenses pDNA, CD cavities allow inclusion complexes with adamantane-PEG, which significantly increases stability in high salt media due to the shielding effect of PEG. The uptake of the resultant NPs improved relative to unmodified PEI. The reduced toxicity with the introduction of CDs was observed *in vitro* and *in vivo*. Pure PEI-containing particles mainly accumulated in the lung, while CD-modified PEI localised in the liver (Pun et al. 2004). In another study, PEG-bearing poly(vinyl alcohol) (PVA) chains that were

grafted with lipophilic groups (e.g. adamantane (Kulkarni, Deng, et al. 2012) or cholesterol (Kulkarni, Defrees, et al. 2012)) via an acid-sensitive linker, to facilitate a host-guest interaction with amine-modified β-CDs. This construct was finally complexed with pDNA or siRNA. The acid-sensitive linker was designed to be cleaved in the endosome, triggering the release of the NA cargo. The grafted PVA had lower toxicity *in vitro* with similar efficacy compared to commercial transfection reagents such as bPEI and Lipofectamine 2000 (Kulkarni, Defrees, et al. 2012; Kulkarni, Deng, et al. 2012). Finally, the effect of the lipophilic pendant group was tested for the delivery of pDNA. Results showed that the binding affinity of the pendant group to the CD influences the physicochemical properties and the release profile *in vitro*. Stronger affinity led to more dense particles and stronger protection against serum and heparin. While the release within the cell was slower, the highly stable particles may result in advantageous longer circulation times *in vivo* (Kulkarni, Badwaik, et al. 2013).

Early generations of grafted CD polymers were associated with issues such as reproducibility and non-biodegradability. A new generation of polymers was developed to tackle these issues. Ring-opening polymerisation resulted in well-defined polymers. A library of diblock copolymers (methoxypoly(ethylene oxide) (mPEG) and polycarbonate (PC)) with various pendant groups (cholesteryl-, adamantanyl-, benzyl-, ethyl- esters) that have different affinities to the CD cavity were synthesised. PC was chosen due to its favourable degradation products and time-controlled degradation. Another major change was the modification of β-CD with PEI instead of simple amines. To form complexes, β-CD-PEI was pre-complexed with pDNA and subsequently added to the diblock polymer (mPEG-PC modified with pendant groups), where a host-guest-interaction takes place between the β-CD and the

lipophilic pendant of the copolymer. Sizes reported were below 250 nm and zeta potential were in the range of 5-10 mV. All pendant groups (adamantane, cholesterol, benzol) and different MWs of PC had a similar effect *in vitro* in HeLa cells (comparable to Lipofectamine 2000). However, following previous studies from this group, the pendant group with lower affinity to the CD cavity (benzyl) showed moderately better *in vitro* performance. It was suggested that hydrolysis in the endosome (pH 5.5) of ester-bound pendants is the main driver for transfection efficiency (Wright et al. 2018).

Wong et al. constructed a multifunctional NP system that is stimuli-responsive and cell-specific. This ensemble consists of three components: a β-CD-grafted PEI, an adamantane-end-capped 4-arm Tetronic-PR, and a ligand-functionalised CD to target $\alpha_v\beta_3$ receptors of U87 cells. The grafted PEI condensed the NA cargo and contributed to the proton-sponge effect. Tetronic-PR releases its α-CDs in the endosomal environment because of the decomposition of the adamantane-end-capping, leading to endosomal disruption due to cholesterol extraction from the membrane by the released CDs. Successful delivery of pDNA and microRNA *in vitro* was reported. Toxicity data showed improved viability compared to PEI polyplexes with enhanced transfection efficiencies for both NAs. Experiments confirmed that stability in destructive environments (high heparin and serum) did not alter the particle integrity, except for low pH which led to the desired release of the NA because of the acid-sensitive adamantane-PR. Cell-specific uptake was confirmed by competitive binding assays (Wong et al. 2018).

1.4.4. Star-shaped polymers containing CDs

This section includes systems that consist of multiple components, including CDs, to build a construct that is shaped like a star (dendrimers), and some include CDs as cores with polymeric arms (Figure 1-13D). Some polymers such as PEI, are very efficient transfection agents, particularly at high MW. However, they are also associated with high toxicity. Decreasing the MW can reduce the toxicity but usually is accommodated with reduced transfection efficiency. The utilisation of CDs or other core molecules enables the attachment of cationic polymer arms which results in delocalisation of the positive charge, creating a star-construct and a way of improving the transfection efficiency with reduced toxicity. Additionally, 'stealth' polymers can be incorporated to further reduce toxicity and protect the NP from harsh environments (Loh and Wu 2015).

A simple example is β-CD decorated with short OEI on its primary face. The OEI was utilised to conjugate FA as a targeting ligand. This polymer was employed in dual delivery of a small molecule chemotherapeutic and a pDNA to drug-resistant tumours. A superior therapeutic efficacy with the dual approach was compared to the monotherapy of each agent (Chen et al. 2016). Similarly, Loh et al. used β-CD as the core to create a star-polymer with poly(2-dimethyl aminoethyl methacrylate) (PDMAEMA)-arms to condense pDNA and poly(2-hydroxyethyl methacrylate) (PHEMA) to endow stability. In this work, mouse embryonic cells were transfected, as they represent an attractive target, especially to study the inhibition of vascularization and tissue reorganisation. The PDMAEMA/ PHEMA ratio was varied, with the ~50:50 ratio found to be comparable to or moderately better than Lipofectamine *in vitro* delivery (Loh and Wu 2015). Another β-CD core star-shaped delivery platform was synthesised in a three-step procedure. Caprolactone ring-

opening was initiated by CDs. The CD was decorated with biodegradable and stable PCL, presenting hydroxyl groups that are converted into macroinitiators by bromination. Further decoration was conducted with PDMAEMA attachment. The presence of hydrophobic (PCL) and cationic (PDMAEMA) components resulted in an amphiphilic structure that self-assembled into micelles. This polymer condensed pDNA more efficiently than PEI25k, with lower cytotoxicity. Transfection was achieved in both HEK293T and HepG2, cell lines. The introduction of PCL proved to be significant in terms of cytotoxicity, possibly because of the ability to form micelles. The slow degradability of PCL also favours its use for prolonged delivery (Fan et al. 2018).

CD-based nano-delivery systems are often used for the co-delivery of small molecules and NA. CDs have both a core that can accommodate small lipophilic chemotherapeutic agents and hydroxyl groups that can be decorated with cationic moieties to complex polyanionic NAs. One such NA delivery system has a "hairbrush" structure. It is a dipolymer, consisting of PEG attached to poly-β-CD. This construct was then further modified with 2-dimethyl aminoethyl methacrylate (DMAEMA) at the CD-hydroxyls. This structure provides a high charge-to-surface area ratio, which helps to reduce the amount of material needed and as a result can mitigate cytotoxicity. This was confirmed by transfecting kidney-derived cells, COS-7 and 293T, with pDNA coding for luciferase. Even at low N/P ratios, such as 4, the formulations showed strong transfection efficacy (Zhang et al. 2014). Chen et al. investigated the co-delivery of doxorubicin and p53-encoding pDNA to MCF-7 cancer cells using the same concept. The synergistic effect of both drugs enhanced the level of apoptosis and suppressed cell proliferation (W. Chen et al. 2019).

Another study investigated the dual delivery of doxorubicin and a short hairpin RNA (shRNA) plasmid (Zhou et al. 2018). A hyperbranched polyglycerol was initially modified with PCL and afterwards with benzimidazole. This construct was mixed with PEI600-modified β-CD (Figure 1-17). The terminal benzimidazole was hosted by the CD cavity to build the star-shaped polymer. The rationale behind this system was to exploit the favourable low toxicity of PEI600 and improve its transfection efficiency by introducing a multifunctional core. The host-guest-interaction is pH-dependent and disassembles at low pH such as in the endosome, allowing the escape of the NA cargo. Doxorubicin was loaded onto the hydrophobic core; PEI600 in the termini of the star-polymer complexed the NA. This polymer was compatible with blood and serum; moreover, it showed better transfection efficiency *in vitro* in the presence of serum. The authors propose three reasons for this: **i**) hyperbranched polyglycerol and its abundant hydroxyl groups on the polymer surface prevent recognition by macromolecules and serum, **ii**) low molecular weight of PEI600 which is composed of less charged amines, **iii**) pH-dependent release of NA cargo which increases the chance of successful transfection. The co-delivery of both drugs was tested in MCF-7 tumour cells (breast adenocarcinoma) and resulted in superior inhibition of cell proliferation and migration *in vitro* and *in vivo* compared to monotherapy of each drug. The low toxicity (<20%) and high stability in blood were also remarkable (Zhou et al. 2018). A very similar approach was successfully conducted by Mohammed et al. with folate-PEG-appended dendrimers conjugated to glucuronylglucosyl-β-CD as a co-delivery vector for siRNA and doxorubicin *in vitro* (KB-cells) and in *vivo* (in mice) (Mohammed et al. 2019).

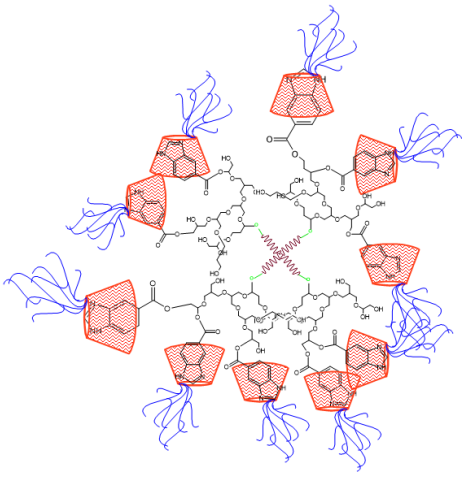

Figure 1-17 Star-shaped polymer end-modified with OEI-CDs that built an inclusion complex with the benzimidazole in the termini of the hyperbranched polyglycerol. As modified from (X. Zhou et al., 2018).

In another study, a poly(amidoamine) (PAMAM) dendrimer modified with α-CDs, PEG, and lactose as targeting ligands against hepatocytes (ASGP-receptors) was investigated. This dendrimer was complexed with siRNA against the TTR gene (a similar therapeutic target to ONPATTRO®). These polyplexes showed high cellular uptake, serum resistance, successful endosomal escape due to the proton-sponge effect of PAMAM, no cytotoxicity, and as a result the potent gene silencing effect *in vitro*. Gene silencing was also observed *in vivo* after IV administration into mice with no side effects (Hayashi et al. 2019).

1.4.5. CD-crosslinked polymers

Another category of CD-based polymers are polymers that are cross-linked with CDs as cross-linking agents. Chemical modifications of the CD-scaffold and the ability to build inclusion complexes opens possibilities for the co-delivery of chemicals and biologicals where necessary.

The co-delivery of a small molecule chemotherapeutic (monensin) and pDNA using a low-MW PEI and sulfhydryl-β-CD was investigated, in which the CD served as a cross-linking agent, and as a host for the poorly water-soluble drug. PEI complexed the pDNA, which was released in the tumour environment through the redox-cleavable disulphide (S-S) bond within the crosslinked copolymer. A dual-targeting approach using polyglutamic acid (γ-PGA) and a tumour-homing RGD-modified γ-PGA were used as ligands to target the tumour-associated γ-glutamyl transpeptidase (GGT) and integrin receptors respectively. The polyanionic nature of the γ-PGA was thought to reduce toxicity in blood circulation. The interaction between the polymer (PEI- sulfhydryl-β-CD) and γ-PGA was pH-mediated to enable targeting ligand disassembly in the tumour microenvironment, allowing PEI to pursue its proton-sponge-effect. Drug-loaded complexes were tested in human colon HCT8/ADR cells (overexpressing GGT). The mono-targeted (γ-PGA only) formulation showed superior behaviour compared to non-targeted counterparts and PEI25k. The inclusion of a second targeting ligand was tested *in vivo* and efficiently inhibited chemo-resistant tumour growth (Xu et al. 2018).

Ping et al. also reported a redox-sensitive gene vector using a β-CD cross-linked low-MW PEI. This construct was subsequently conjugated with a MC11 peptide, targeting fibroblast growth factor receptors, that are expressed on proliferating cancer cells, for the delivery of pDNA. A stealth component was introduced via S-S conjugation of adamantane and PEG, where adamantane forms an inclusion complex with the CD. This redox-sensitive connection reduces the risk of PEG-impeded transfection while still successfully protecting against salt or bovine serum albumin-induced aggregation. After PEG release, the PEI is exposed and can act as a proton-sponge effect initiator for endosomal escape. Targeted formulations

showed higher transfection efficiency compared to non-targeted formulations *in vitro* and *in vivo* (Ping et al. 2013). A similar formulation for the delivery of siRNA where low-MW PEI cross-linked using 2-hydroxypopyl-β-CD, decorated with FA was used to silence vascular endothelial growth factor (VEGF). The targeted siRNA formulation showed more than 90% gene knockdown *in vitro* in HeLa cells. *In vivo* studies confirmed the selective inhibition of VEGF, as evidenced by the markedly reduced tumour size in mice (Li et al. 2013).

In a recent study cross-linked aminated-β-CD polymer (primary amine, quaternary ammonium and guanidino) were utilised to deliver 5-Fluorouracil (5-FU) and Interleukin-2 (IL-2) to Caco-2 cells, as an immunotherapy approach in colon cancer. While all three polymers were able to complex both drugs (electrostatic interaction), it was observed that only the CD-polymer modified with primary amines showed permeability through the mucosal membrane of Caco-2 cells, presenting a suitable platform for the oral co-delivery of 5-FU and IL-2 (Akkın et al. 2022).

Another approach to immunotherapy in cancer was taken with hyperbranched-β-CD modified with choline chloride (quaternary ammonium). It was utilised for the delivery of oval-albumin (OVA)-mRNA. OVA serves as an antigen to activate an immune response after local injection in melanoma cancer. The melanoma cancer cell line (B16-F10) was used to assess toxicity and uptake of polymer-NP in 2D and 3D spheroids: no toxicity and strong fluorescence was detectable (using enhanced green fluorescent protein (EGFP)). Subsequently, an *in vivo* melanoma mouse model was treated with the EGFP-polymer-NP. After proving successful accumulation in tumoral tissue, the OVA-polymer-NP was tested. The tumour suppression in mice treated with OVA-polymer-NP was three times higher compared to the control group with no treatment. For a longer-lasting anti-tumoral effect, it is critical that the adaptive

immunes system is activated. To confirm this, the tumour and spleen cells from the mouse model were harvested and stained with cell-surface markers of immune cells that are increased during an immune response. The experiments proved that OVA-polymer-NPs can induce an immune response (Monfared et al. 2023). The different approaches using CD polymers shows how versatile the use of these polymers can be and how easily they can be modified and adjusted to specific circumstances in future applications.

1.5. Aims and Objectives

To build on the success of CDs as RNA delivery vectors, described above, the effects of a range of functional groups, on CD monomers and polymers, on siRNA delivery was investigated with the objective of establishing a structure-activity-relationship. The specific aims of the thesis include:

Aim 1: To investigate an approach to reduce the charge density of cationic CD.siRNA-NPs in order to moderate their potential toxicity *in vivo* (Chapter 2).

Aim 2: To study the influence of varying the functional groups on amphiphilic cationic CDs on NP formation and siRNA delivery (Chapter 3).

Aim 3: To assess the ability of CD polymers, modified with a primary amine or quaternary ammonium, to deliver siRNA *in vitro* (Chapter 4).

A detailed description of results is outlined in the following chapters, completed with a general discussion, setting the results of the chapters in perspective with the literature and suggestions for future directions.

2. Chapter: Co-Formulation of Amphiphilic Cationic and Anionic Cyclodextrins Forming Nanoparticles for siRNA Delivery in the Treatment of Acute Myeloid Leukaemia

Ayse Kont [1], Monique C. P. Mendonça [1], Michael F. Cronin [1], Mary R. Cahill [2] and Caitriona M. O'Driscoll [1]

[1] Pharmacodelivery Group, School of Pharmacy, University College Cork, T12 YN60 Cork, Ireland,

[2] Department of Haematology and CancerResearch@UCC, Cork University Hospital,

University College Cork, T12 XF62 Cork, Ireland.

Published in: International Journal of Molecular Sciences, 2022, 23, 9791

DOI: https://doi.org/10.3390/ijms23179791

Abstract:

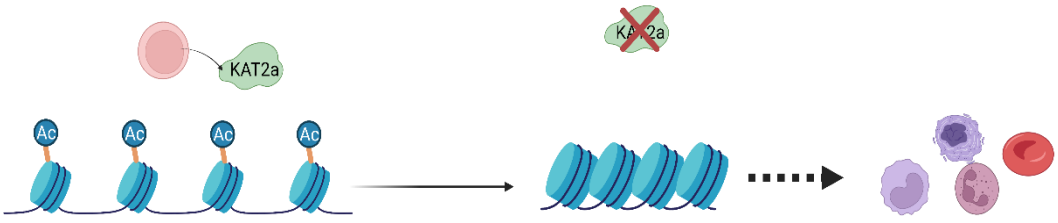

Non-viral delivery of therapeutic nucleic acids (NAs), including siRNA, has potential in the treatment of diseases with high unmet clinical needs such as acute myeloid leukaemia (AML). While cationic biomaterials are frequently used to complex the

NAs into nanoparticles (NPs), attenuation of charge density is desirable to decrease *in vivo* toxicity. Here, an anionic amphiphilic cyclodextrin (CD) was synthesised and the structure was confirmed by Fourier-transform infrared spectroscopy (FT-IR), Nuclear Magnetic Resonance (NMR), and high-resolution mass spectrometry (HRMS). A cationic amphiphilic CD was initially used to complex the siRNA and then co-formulated with the anionic amphiphilic CD. Characterisation of the co-formulated NPs indicated a significant reduction in charge from 34 ± 7 mV to 24 ± 6 mV ($p < 0.05$) and polydispersity index (PDI) 0.46 ± 0.1 to 0.16 ± 0.04 ($p < 0.05$), compared to the cationic CD NPs. Size was similar, 161–164 nm, for both formulations. Flow cytometry and confocal microscopy experiments, using AML cells (HL-60), indicated a similar level of cellular uptake (60% after 6 h) followed by endosomal escape. The nano co-formulation significantly reduced the charge while maintaining gene silencing (21%). Results indicate that blending of anionic and cationic amphiphilic CDs can produce bespoke NPs with optimised physicochemical properties and potential for enhanced *in vivo* performance in cancer treatment.

Keywords: modified cyclodextrins, nanomaterials, nucleic acids, non-viral gene delivery, acute myeloid leukaemia

2.1. Introduction

Acute myeloid leukaemia (AML) is a malignant blood cancer with an increased incidence and poor prognosis in adults. Myeloid progenitor cells, leukaemic blasts, stop differentiating and start to proliferate uncontrollably in the bone marrow, peripheral blood, and spleen. Leukaemic myeloblasts replace functioning bone marrow (Kouchkovsky and Abdul-Hay 2016). Conventional therapies, which target

only dividing cells, are capable of reducing the number of leukaemic cells and may be unable to eliminate the non-dividing leukaemia stem cells (LSCs). Therefore, LSCs resistant to conventional therapies, may remain in the bone marrow, and at a later stage begin to divide again causing relapse with a high mortality rate (Guo et al. 2017; Whiteley et al. 2021).

As an alternative approach, gene therapy targeting AML fusion transcripts has been considered promising (Khamidullina et al. 2021). AML has a complex genomic landscape and numerous clones are defined by or associated with mutations in key genes. Some of the best-known mutations include alterations in the PML-RARA and FLT3 genes which have led to targeted therapies and improved prognosis (Tyner et al. 2018). Mutations and changes in expression are also noted in the KMT2a and KAT2a genes in AML. Pre-clinical results showed that KAT2a knockdown exhibited transcriptional instability in AML stem cells rather than hematopoietic stem cells, making this gene a potential target for AML cells and leukaemic stem cells directed therapy (Arede et al. 2022). KAT2a, an epigenetic modulator is a lysine acetyltransferase overexpressed in all AML types, participating in the maintenance of leukaemia via acetylating histone H3 lysine 9. For this reason, silencing of KAT2a leads to deacetylation at transcription sites and consequently to impaired transcription of the gene responsible for maintaining stemness in the AML clone (Kahl et al. 2019). The knockdown interrupts self-renewal and moves the cell cycle into the differentiation state (Domingues et al. 2020).

Despite early promising data, the delivery of NAs into cells faces multiple challenges, including delivery across lipid bilayers and degradation of NAs by endonucleases, therefore, a delivery system is required to overcome these barriers and to achieve the required duration of activity at the diseased site (Dowdy 2017).

Additionally, blood cells have proven to be difficult to transfect compared to other cell types (Landry et al. 2012; Uebbing et al. 2020). The non-viral delivery of NAs utilising the NP approach is a promising tool to overcome physiological barriers (Durymanov and Reineke 2018). A range of materials have been investigated as non-viral delivery vectors for therapeutic NAs (Li and Kataoka 2021; O'Mahony, O'Neill, et al. 2012).

Previously, to overcome the obstacles in transfecting blood cells, antibody-targeted CD-based NPs were investigated for siRNA delivery to AML LSCs. The antibody against the IL-3 receptor alpha-chain (IL-3R alpha, also known as CD123) was incorporated into the formulation for selective targeting of KG1 cells, an AML leukaemia stem and progenitor cell line. The authors demonstrated efficient delivery of bromodomain containing protein 4 (BRD4) siRNA to KG1 cells and in *ex vivo* primary AML patient derived samples, which resulted in downregulation at mRNA and protein levels. The silencing of BRD4 induced myeloid differentiation and triggered leukaemia apoptosis (Guo et al. 2017).

While cationic materials are required to complex negatively charged NAs, a reduced cationic charge density at physiological pH is desirable to minimise *in vivo* toxicity (Zhou et al. 2021) and improve the stability of the formulation in salt- and serum-containing media (Abstiens et al. 2019), an important characteristic for clinical translation. Consequently, the aim of the present study was to develop a novel delivery system with reduced charge density by co-formulating amphiphilic cationic CDs with negatively charged amphiphilic CDs. The benefits of incorporating a negatively charged entity to pre-formed cationic NPs were previously illustrated by the work of Ball et al. (Ball et al. 2018). They assessed the co-formulation of mRNA and siRNA aiming to target diseases with concurrent abnormal gene up- and downregulation. The co-delivery of both RNAs increased gene silencing in contrast to siRNA only LNPs.

To expand the potential of this finding to a broader range of diseases and reduce costs related to the additional RNA species, mRNA was substituted with a synthetic negatively charged polymer. LNPs containing the polyanion and siRNA showed the same efficacy as the co-formulation of mRNA and siRNA. It was suggested that the inclusion of the 'helper polymer' could increase the stability and electrostatic interaction within the particle and also improve the efficiency of the delivery system (Ball et al. 2018). In this study, we are aiming to simulate this positive effect with the co-formulation of an anionic amphiphilic CD.

The CDs formulated with siRNA against KAT2a were characterized, and the safety and efficacy of the NPs were evaluated in HL-60 cells, an AML cell line expressing the gene of interest. To our knowledge, this is the first time such a CD co-formulation approach has been investigated for siRNA delivery.

2.2. Materials and Methods

2.2.1. Materials

MISSION® siRNA Universal Negative Control #1 and MISSION® siRNA Fluorescent Universal Negative Control #1 6-FAM were purchased from Sigma Aldrich. Pre-designed KAT2a (or GCN5) (antisense CCUACUUGUCAAUGAGGCCtc) was obtained from ThermoFisher (Dublin, Ireland). All chemicals and materials were of analytical grade and purchased from Sigma-Aldrich (Wicklow, Ireland), unless otherwise specified.

The cationic amphiphilic CD was synthesised as previously described by using a 'click' chemistry approach to attach the amine group on the secondary side, the primary side was modified with lipid chains (C_{12}) (Aoife M. O'Mahony, Ogier, et al.

2012). The anionic amphiphilic CD was synthesised as described below and the structure was confirmed by Fourier transform infrared spectroscopy (FT-IR), Nuclear Magnetic Resonance (NMR), and high-resolution mass spectrometry (HRMS).

2.2.2. Nanoparticle preparation

Both amphiphilic cationic and anionic CDs were dispersed in RNase-free water (0.25 mg/mL) via water bath sonication (Branson 1510) for 1 h at 70 °C and used immediately after sonication. NPs with different mass ratios (MRs) were prepared by adding the required amount of siRNA and cationic CD to RNasefree water, herein referred as the formulation. The formulation was then incubated at room temperature at 450 rpm for 30 min in a thermomixer. Following incubation, the amphiphilic anionic CD was added to the cationic CD.siRNA-complex, forming the co-formulation, which was subsequently incubated at 65 °C, 450 rpm for 30 min. The final siRNA concentration was 500 nM.

2.2.3. Physicochemical characterisation

2.2.3.1. Size, Poly Dispersity and Zeta potential

Particle size and zeta potential were measured by dynamic light scattering (DLS) using the Zetasizer Nano-ZS (Malvern Instruments, Malvern, UK). Particle size (Z-Average) and poly dispersity measurements were conducted using a non-invasive backscatter system (scattered light angle of 170°) in a disposable narrow size cuvette with a volume of 500 µl. Electrophoretic mobility is used to determine the zeta potential (forward scatter angle of 12.8°). Zeta potential was measured with dis-

posable folded capillary cells (DTS1070) with minimum required volume of 750 µl at the monomodal mode with 60 s delay between measurements. The settings were as follows: Protein as material (refractive index 1.450 and absorption 0.001), water as dispersant (viscosity 0.8872cP, refractive index 1.330) at 25 °C.

2.2.3.2. Complexation efficiency

The complexation efficiency was investigated using a 1% Agarose gel in Tris/Borate/EDTA buffer. Both running buffer and gel, contained SafeView (NBS Bio-logicals, Huntingdon, UK), a Nucleic Acid Stain (6 µl/100 ml). Free siRNA (positive control) and samples contained 3 µl BlueJuiceTM Gel Loading Buffer (10X) (Invitrogen, Waltham, MA, USA) and 27 µl sample. The gel was run at 90 V for 60 min (Bio-Rad, PowerPacBasic, Hercules, CA, USA) and imaged under UV with Uvitec Cambridge Mini HD.

2.2.3.3. Encapsulation efficiency

Encapsulation efficiency (EE) was assessed using the modified Quant-iT RiboGreenTM RNA Assay kit (Invitrogen, Invitrogen, Waltham, MA, USA) (Raval et al. 2019). Freely accessible siRNA was determined before the addition of surfactant (F_{free}), encapsulated siRNA was measured upon lysis of the particles with 10% Triton X-100 (F_{total}) (final Triton concentration per well: 1%). After addition of the RiboGreen reagent, Fluorescence intensity was determined using a Tecan Spark® microplate reader at 485 nm excitation wavelength and 535 nm emission wavelength in a black 96-well plate (Gain 55, top reading), siRNA was quantified by means of a calibration curve. The EC was calculated using the equation:

$$EE = [(F_{total} - F_{free})/F_{total}] * 100$$

2.2.3.4. Determination of pKa

Buffers from pH 4–12 in increments of 0.5 (pH 4–6.5 citrate buffer, pH 7–8 phosphate buffer, pH 8.5–12 Tris-HCl buffer), and 2-(p-toluidino)-6-naphthalene sulfonic acid (TNS) solution at 300 µM in DMSO were prepared. In a black 96-well plate, 90 µl of buffer with 10 µl samples were mixed. Finally, 2 µl of TNS solution was added (6 µM TNS/well) and incubated at room temperature in a shaker for 5 min, protected from light. Fluorescence intensity was measured using the Tecan Spark® (Männedorf, Switzerland) microplate reader at an excitation of 340 nm and an emission of 485 nm (top reading). Sigmoidal interpolation was applied to the collected data, where the inflection point (LogIC50) defined the apparent pKa of the formulations (Uebbing et al. 2020).

2.2.3.5. Serum stability

To assess the behaviour of the NPs in the presence of serum, samples were exposed to 10% fetal bovine serum (FBS, heat-inactivated) for different time intervals at 37 °C for up to 24 h. Particle aggregation was monitored by DLS.

To assess the ability of the CD-NPs to protect siRNA from degradation following exposure to serum, a heparin displacement assay was used. Following incubation at 37 °C in 10% FBS for different time intervals, samples were treated with freshly prepared heparin (10 mg/ml, roughly 2000 I.U. in phosphate-buffered saline (PBS)) for 75 min at room temperature (20% heparin in final sample). BlueJuiceTM Gel Loading Buffer (10X) (Invitrogen, Invitrogen, Waltham, MA, USA) was added to the samples and loaded onto the gel, containing SafeView (NBS Biologicals, Huntingdon, UK). The gel was run at 120 V for 30 min (Bio-Rad, PowerPacBasic, Hercules, CA, USA) and imaged under UV. The heparin-treated samples were

measured with NanoDrop One (ThermoScientific, Dublin, Ireland) to quantify the residual siRNA.

2.2.4. Cell culture

HL-60, a human peripheral blood cell line derived from a 36-year-old woman with acute leukaemia, was kindly donated by Cancer Research @UCC and was maintained in Iscove Modified Dulbecco Media with 20% FBS (heat-inactivated) and 1% Penicillin-Streptomycin in a humidified 37 °C incubator with 5% CO2. For all experiments the FBS concentration was decreased to 10%.

2.2.4.1. Cellular uptake

Flow cytometry was used to assess cellular uptake. Cells were seeded at 3.5×10^5 cells per ml in a 24-well plate and transfected with formulations encapsulating FAM-labelled siRNA for 6, 12 and 24 h (100 nM final concentration per well). After incubation, cells were centrifuged at 1500 rpm for 5 min at 4 °C and the supernatant was removed. The pellet of cells was resuspended with 400 µl PBS and transferred into polystyrene round-bottom tubes (Becton Dickinson, Franklin Lakes, NJ, USA). Data were acquired on BD CELESTA Facs Analyser (minimum 40,000 events).

2.2.4.2. Intra-cellular trafficking

The intracellular localization and co-localization of the formulations with lysosomes were evaluated by confocal microscopy. Cells were seeded at 5×10^5 cells per ml onto Poly-D-Lysine coated coverslips in a 24-well plate and treated with FAM-labelled siRNA containing formulations. The incubation periods varied from 6, 12 to 24 h. LysoTrackerTM Red DND-99 (Invitrogen, Invitrogen, Waltham, MA, USA), a

red-fluorescent dye for labelling and tracking acidic organelles, was prepared at 100 nM in serum-free media. The SytoTM Deep Red Nucleic Acid Stain (Invitrogen, Invitrogen, Waltham, MA, USA), which stains the nuclei of cells, was added to the Lysotracker working solution to give a final nucleic acid stain of 1 µM. After incubation, the media was removed carefully, and the dyes were added to each well (500 µl dye solution/well); after 150 min the dye solution was withdrawn. The cells were fixed with 4% paraformaldehyde for 10 min at room temperature followed by wash with PBS. The coverslips were removed and mounted with Fluorescent Mounting Media (Dako, Agilent, Santa Clara, US); the cells were imaged using an OLYMPUS FV1000 Confocal Laser Scanning Biological Microscope.

2.2.4.3. Toxicity assay

The cell counting kit -8 (CCK-8) assay was used to assess cell viability. In a 96-well plate, 100 µl of cell suspension (2.5×10^5/ml) was transfected with 25 µl of sample (siRNA 100 nM/well), followed by incubation for 3 days at 37 °C incubator with 5% CO2. After incubation, 10 µl of CCK-8 solution was added followed by a further 4 h incubation, and absorbance was measured using a plate reader at 450 nm. Freshly prepared growth media was used as a blank.

2.2.4.4. Gene knockdown

Cells (3×10^5 cells/ml) were transfected with siRNA against KAT2a (100 nM/well) in a 24-well plate for 3 days. RNA extraction was conducted using GeneEluteTM Total RNA Purification Kit according to manufacturer's guideline. Complementary DNA (cDNA) was generated using the High-Capacity cDNA Reverse Transcription kit (Ap-plied BiosystemsTM, Waltham, MA, USA). Real-time quantitative PCR (RT-qPCR) was performed using TaqMan Universal PCR Master

Mix (Applied Biosys-temsTM) and BIO-RAD CFX96TM Real-Time System. GAPDH was chosen as the house-keeping gene (4331182) and KAT2a probe with the most coverage was purchased (AM16704, TaqMan assay, Applied BiosystemsTM). Thermal cycling conditions were as follows: 50 °C for 2 min, 95 °C for 5 min, 95 °C for 15 s, 55 °C for 30 s, 72 °C for 1 min, 40 cycles. The last cycle was finalised with a holding step for 7 min at 72 °C.

2.2.5. Statistical analysis

All statistical analysis was performed using GraphPad Prism 7. Unpaired t-test was used for physicochemical characterization measurements to compare the two formulations. 1-way ANOVA with subsequent multiple comparison Dunnett's post hoc test was utilized to compare all groups in cell culture experiments. Statistical significance was considered when $p < 0.05$.

2.3. Results and Discussion

2.3.1. Synthesis of the amphiphilic anionic CD

The amphiphilic cationic CD was synthesised as previously described (Aoife M. O'Mahony, Ogier, et al. 2012). The amphiphilic anionic CD was synthesised as follows (Sukegawa et al. 2002): β-CD was silylated at the 6-OH position (Aoife M. O'Mahony, Ogier, et al. 2012) in order to direct the subsequent esterification of 2-OH and 3-OH positions using dodecylanhydride. Facile desilylation to yield compound 3 was followed by treatment with 23 equivalents sulphurtrioxide-triethylamine complex at 80 °C for 5 days in an inert atmosphere to generate the sulphate (4) as a

trimethylamine salt in quantitative yield. All steps required purification by silica-based chromatography (Figure 2-1).

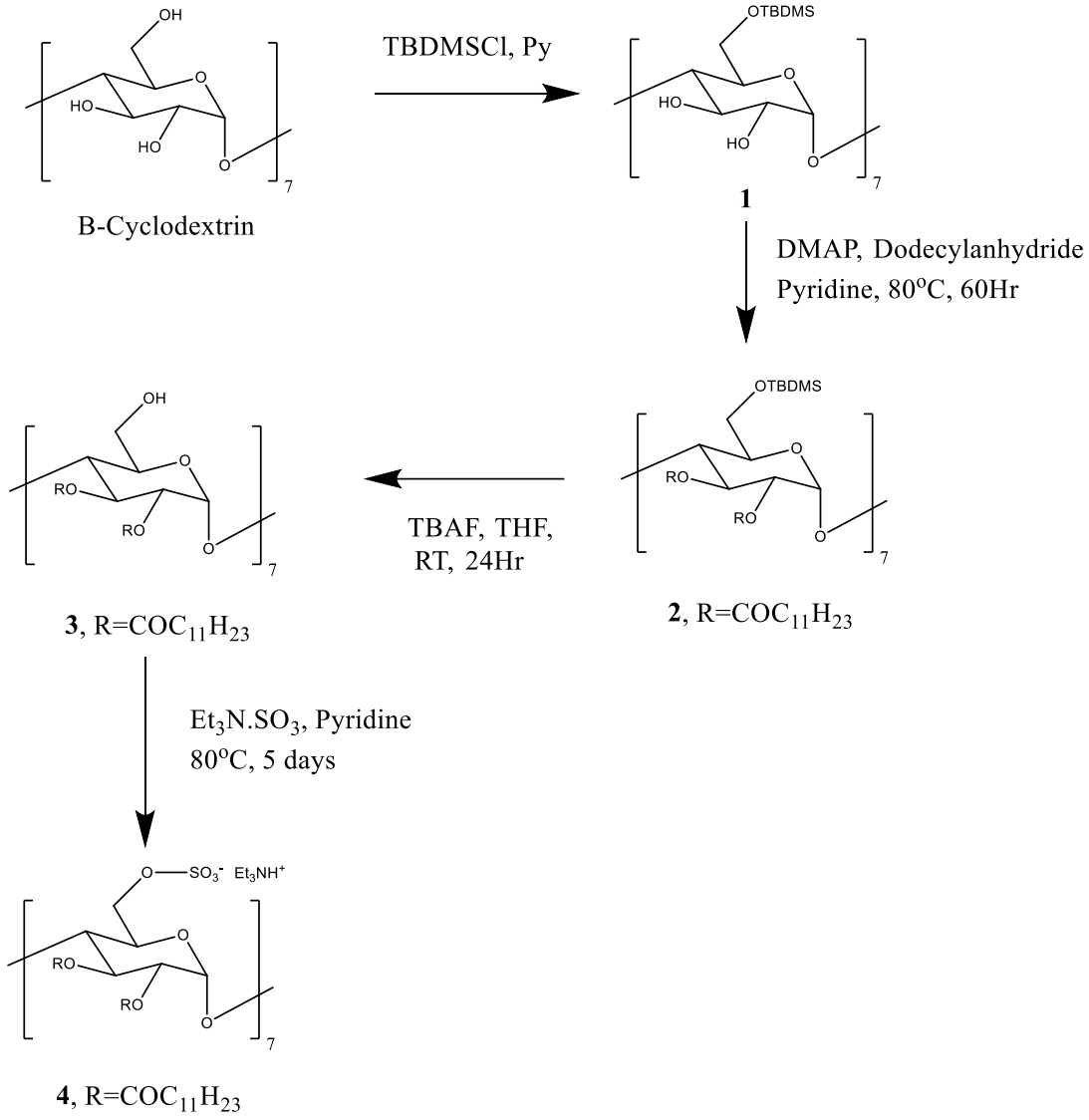

Figure 2-1 Chemical synthesis of anionic amphiphilic cyclodextrin (CD). Silylation at position 6 of the β-CD which enables the direct esterification with dodecylanhydride (C12) at positions 2 and 3. Subsequently, desilylation and sulphation at position 6 produces the trimethylamine salt, resulting in a negatively charged amphiphilic CD.

The molecular structure was confirmed by means of Fourier-transform infrared spectroscopy (FT-IR), Nuclear Magnetic Resonance (NMR), and high-resolution mass spectrometry (HRMS), with following results:

FT-IR, thin film on NaCl (cm^{-1}) 3476, 2956, 2924, 2854, 1748, 1466, 1260, 1203, 1173, 1047, 1006. The spectrum peak at 1748 cm^{-1} is characteristic for carbonyl groups that were created during esterification of 2-OH and 3-OH positions. The peak at 1260 cm^{-1} is an indication for the successful generation of sulphate (Cabassi, Casu, and Perlin 1978).

^{1}H NMR, 300 MHz, $CDCl_3$ ppm: 0.83 (6H, m); 1.20 (32H, m); 1.19 (9H, t, J = 7.2 Hz); 1.45 (2H, m); 2.05 (2H, m); 2.25 (4H, m); 3.15 (6H, m); 3.41 (1H, m), 3.89 (1H, t, J = 9.0 Hz); 4.15 (1H, m); 4.30 (1H, m); 4.70 (1H, dd, J = 10.2, 3 Hz); 5.15 (1H, d, J = 3 Hz); 5.25 (^{1}H, t, J = 9 Hz); 9.15 (^{1}H, s, D_2O exchange) (Figure 7-1 A).

^{13}C NMR, 100 MHz, $CDCl_3$ ppm: 8.75, 9.71, 10.97, 14.07, 14.12, 19.69, 22.72, 23.00, 23.74, 24.65, 24.83, 27.10, 28.93, 29.41, 29.45, 29.50, 29.60, 29.68, 29.72, 29.86, 29.91, 30.36, 31.98, 34.00, 34.13, 37.11, 38.72, 46.45, 68.16, 128.81, 130.90, 132.45, 167.79, 172.52, 172.81 (Figure 7-1B).

The MW of the anionic CD $C_{210}H_{378}O_{70}S_7$ [M^+] was calculated as 4244.4060 g/mol and confirmed to be 4244.3947 g/mol by HRMS with an error of 2.66 ppm.

2.3.2. Physicochemical characterisation

Previously cationic CDs have proven highly effective in silencing gene expression in a range of *in vivo* animal models of disease (Godinho et al. 2012; Guo, Ogier, et al. 2012; McCarthy et al. 2013). A reduction in the cationic charge density is likely to extend the *in vivo* circulation time and minimise potential aggregation and toxicity (Godinho et al. 2014; Qian et al. 2018). To help achieve this charge reduction the co-formulation of cationic with anionic amphiphilic CDs was explored. The concept of co-formulating cationic and anionic entities to enhance the performance of non-viral

delivery of siRNA was reinforced by the work of Ball et al. (Ball et al. 2018). Ball and co-workers initially co-formulated siRNA with mRNA using a blend of lipids and observed an improved gene-silencing effect compared to siRNA-only NPs at the same siRNA concentration. Following this observation, mRNA was substituted with a polyanionic polymer creating LNPs containing only siRNA that provided the same gene silencing efficiency as the formulation with both NAs. The additional negative charge helped to increase the electrostatic interaction within the particles reducing the dose of siRNA and increasing the gene silencing efficacy (Ball et al. 2018).

In this study, an anionic amphiphilic CD was synthesized and co-formulated with an amphiphilic cationic CD (Figure 2) aiming to reduce the overall positive charge, improve the stability and the gene knockdown activity.

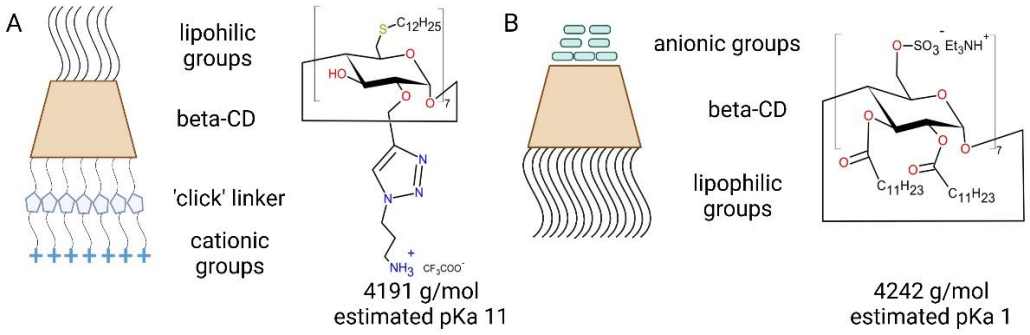

Figure 2-2 Chemical structure (MW and pKa) and schematic of charged amphiphilic CDs. (A) The amphiphilic cationic CD, with lipid chains (SC_{12}) on the primary side and a primary amine function on the secondary side. (B) The amphiphilic anionic CD, with a negative functional group on the primary side and lipid chains (SC_{12}) on the secondary side.

Initially, the capacity of the amphiphilic anionic CD to neutralise the positively charged CD was assessed in the absence of siRNA (Figure 7-2). Neutralisation occurred between mass ratios (MRs) of 0.85:1 to 0.9:1 (amphiphilic cationic:anionic CD), indicating that the charge density of the amphiphilic anionic CD may not be as

high as that of the amphiphilic cationic CD. Therefore, 15% more anionic CD is needed to neutralise the cationic CD.

Using this initial data, preliminary studies were performed to identify the optimum MR of both CDs with the aim of achieving NPs containing 100 nM siRNA, with a charge between −30 mV to 30 mV, size below 200 nm and PDI between 0–0.3. These physicochemical parameters are desirable in NP delivery where: negatively or positively charged particles were proven to show better *in vitro* uptake than neutral NPs (Foroozandeh and Aziz 2018); particles below 200 nm are able to escape the reticulo endothelial system (RES) (Hoshyar et al. 2016; Kulkarni and Feng 2013) and low PDI guarantees uniform particles (Danaei et al. 2018) thus increasing the possibility to reach the site of disease.

Optimisation studies in the presence of the negatively charged siRNA indicated a MR of 8.5:1:5.3 (cationic CD:siRNA:anionic CD) for the co-formulation (Figure 7-3). A higher MR of the anionic CD resulted in displacement of the siRNA (Figure 7-4). A summary of the physicochemical properties for both NP formulations is given in Table 2-1, where the formulation at MR 8.5:1 (cationic CD:siRNA) displayed a surface charge of 34 ± 7 mV, a size of 164 ± 44 nm, and PDI of 0.46 ± 0.1 while the co-formulation MR 8.5:1:5.3 (cationic CD:siRNA:anionic CD) exhibited a surface charge of 24 ± 6 mV, size of 161 ± 14 nm, and PDI 0.16 ± 0.04. Similar size and PDI values have been reported for LNPs (Hajj et al. 2019). The addition of the amphiphilic anionic CD resulted in a significant ($p < 0.05$) reduction in charge and PDI. No increase in size was detected with the co-formulation, which may indicate increased electrostatic and lipophilic interactions, thus, leading to more condensed and monodisperse particles (O'Mahony et al. 2014).

Table 2-1 Summary of physicochemical characterisation of CD:siRNA NPs.

	Size (nm)	PDI	Charge (mV)
Formulation (cationic CD:siRNA)	164 ± 44	0.46 ± 0.1	34 ± 7
Co-formulation (cationic CD:siRNA:anionic CD)	161 ± 14	0.16 ± 0.04	26 ± 4

The encapsulation efficiency (EE) of both formulations was investigated by RiboGreenTM assay. The formulation showed 95% EE and the co-formulation displayed approximately 75% EE (Figure 2-3 A). Comparable entrapment was reported elsewhere (Raval et al. 2019). Binding of siRNA by both formulations was confirmed utilising gel retardation (Figure 7-5). Polyanions are known to displace NAs in NP (Vader et al. 2012), however, results indicate no displacement of the siRNA on addition of the anionic CD at the MR studied.

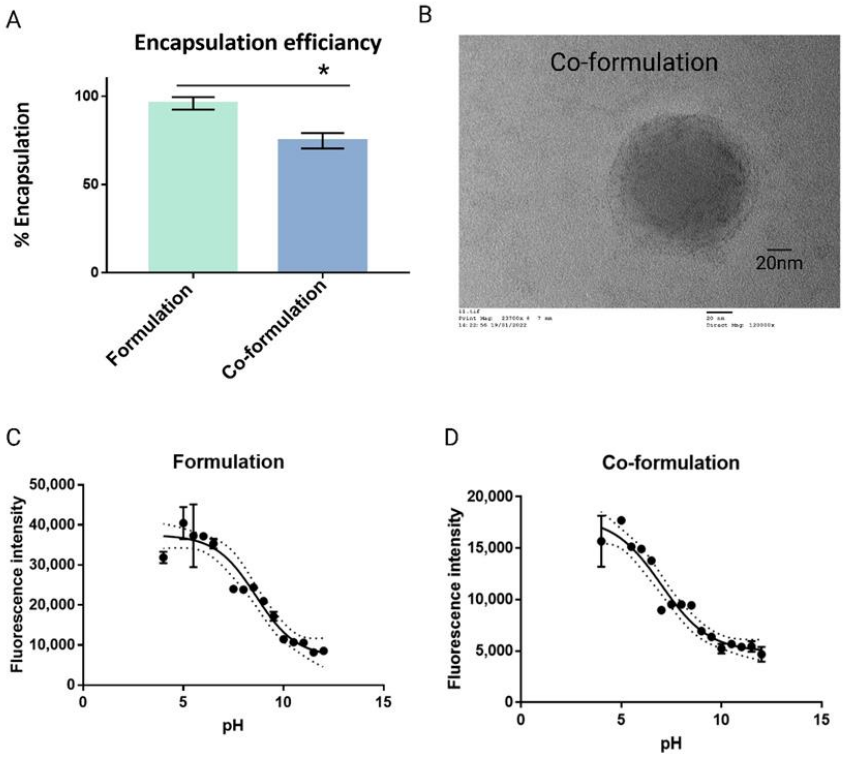

*Figure 2-3 Physicochemical characterisation of cyclodextrin (CD)-based NPs. (A) Encapsulation efficiency using Quant-iT RiboGreenTM RNA Assay. (B) Transmission Electron Microscopy (TEM) of the co-formulation with MR 8.5:1:5.3 (cationic CD:siRNA:anionic CD). Magnification 120,000×; * $p < 0.05$, unpaired t-test. (C, D) Acid dissociation constant (pKa) determination of the NPs by means of 2-(p-toluidino) naphthalene-6-sulfonic acid (TNS) assay.*

In addition to the electrostatic interaction of the CDs, the potential interaction of the lipidic functionality of both CDs may also contribute to the formation and stability of the co-formulation. Transmission electron microscopy (TEM) was used to examine the size and morphology of the co-formulation and indicated the integration of both lipidic functionalities forming a bilayer-like structure (Figure 2-3 B). Earlier publications have reported similar structural arrangement in CD-siRNA NPs (Singh et al. 2019; Villari et al. 2013). Compared to DLS, the smaller particle size of 100 nm is likely due to the sample preparation for TEM which includes drying of the sample, leading to shrinkage of the particles.

It has been reported that materials with pKa values around 6.5 are optimal for non-viral delivery of NAs, since such pKa will ensure a positive charge during formulation at acidic pH and a near neutral charge at physiological pH 7.4 (Akinc et al. 2019; Kulkarni J, Darjuan M 2018). The pKa of both CDs were estimated based on their chemical structure as 11 and 1 for the cationic and anionic CD, respectively (Figure 2-2). Following NP formation, the surface pKa was determined. The formulation displayed a pKa of 8.5 ± 0.1, significantly higher ($p < 0.05$) than that of the co-formulation with a pKa of 7 ± 0.35 (Figure 2-3 C, D). Since these are surface pKa values, the reduction in the number of cationic species on the particle surface is reflected by a reduction in the surface pKa in the same way that surface charge is seen to be reduced by co-formulation.

The ability of CDs to protect the incorporated siRNA in the presence of serum was monitored. This is important considering the exposure of NAs in the blood circulation and the potential for degradation (Whitehead, Langer, and Anderson 2009). Both formulations show similar behaviour in FBS over the time course studied. It is suggested that the FBS covers the surface with non-specific binding (Richtering, Alberg, and Zentel 2020; Wang et al. 2020; Witzigmann et al. 2020) which possibly led to the slight increase of 10 nm observed for both formulations immediately after FBS exposure, however, no further increase in size was detected at longer incubation times up to 24 h (Figure 2-4 A, B), as reported previously for dendrimer nanocomplexes (Raval et al. 2019). The protective role of the CDs was confirmed by heparin-release assay (Fitzgerald, Rahme, et al. 2016), in which heparin, a negatively charged polysaccharide, displaces the incorporated siRNA due to charge competition. As shown in Figure 2-4 C, siRNA release was verified at all time points for both CD-NP formulations. For further confirmation, RNA concentrations were measured (Figure 2-4 D). Free siRNA decreased in concentration by half in less than 3 h, while the siRNA concentration in the NP formulations remained constant, independent of the time exposed to serum. These results conclude that the siRNA released by the heparin was intact and undegraded, indicating that both NP formulations could protect the NA from enzymatic degradation in serum (Raval et al. 2019).

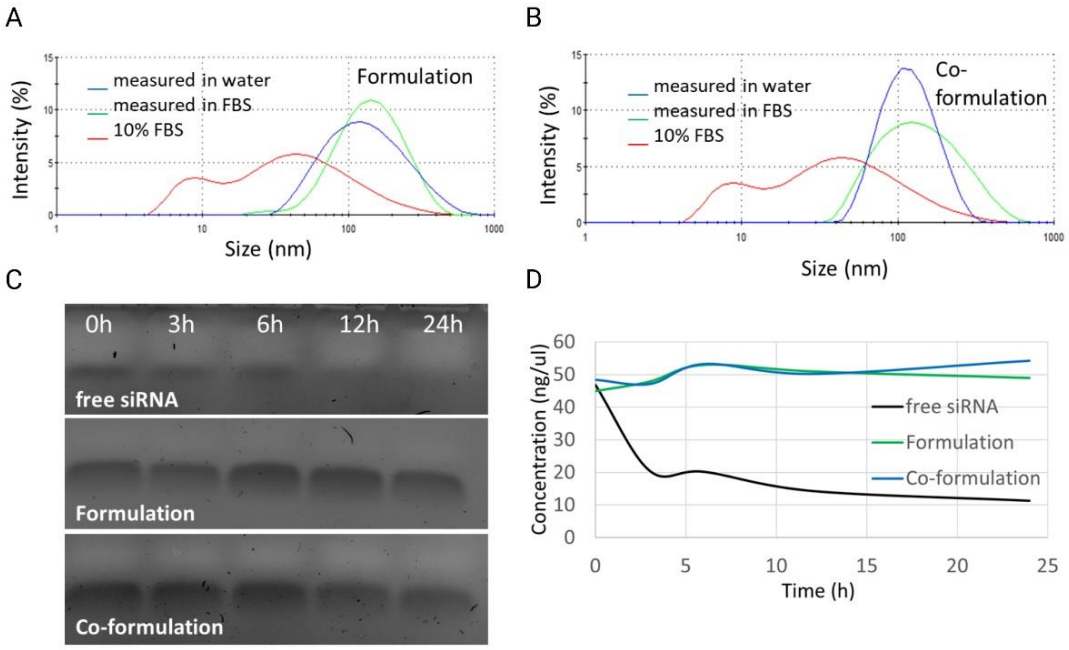

Figure 2-4 CD-NP stability in serum. (A) Particle size measurement after 24 h incubation in 10% serum for formulation MR 8.5:1 (cationic CD:siRNA). (B) Particle size measurement after 24 h incubation in 10% serum for formulation co-formulation MR 8.5:1:5.3 (cationic CD:siRNA:anionic CD). (C) siRNA displacement assay of serum-treated NPs with polyanion Heparin to confirm the ability to protect siRNA in CD-NP. (D) Quantification of siRNA of serum- and heparin-treated NP with NanoDrop One.

2.3.3. In vitro cell culture

Having determined that the addition of the amphiphilic anionic CD to the formulation can significantly impact the surface charge, both formulations were evaluated using HL-60 cells. HL-60 is a human peripheral blood cell line derived from a 36-year-old woman with AML, where the epigenetic modulator KAT2a is overexpressed (Kahl et al. 2019). The cells were incubated with the CD-based formulation carrying FAM-labelled siRNA at a final concentration of 100 nM per well and cellular uptake was monitored by flow cytometry and confocal microscopy.

Confocal microscopy confirmed siRNA internalization in HL-60 cells as demonstrated by the green fluorescence present around the nuclei at all imaged time

points (Figure 2-5 A). The relatively lower surface charge of the co-formulation did not alter the cellular uptake indicating that charge alone is not the sole driver for internalisation (Wang et al. 2020). In contrast, the amphiphilicity of the CDs promoting a lipophilic interaction at cellular level may also be a significant factor (Abumanhal-Masarweh et al. 2019). As shown in Figure 2-5 B, the uptake patterns were similar for both formulations over time (6, 12 and 24 h), reaching approximately 60% after 6 h and decreasing by half after 24 h, consistent with the confocal images that show reduced siRNA signal over time. Similar behaviour has been previously published (Landry et al. 2012).

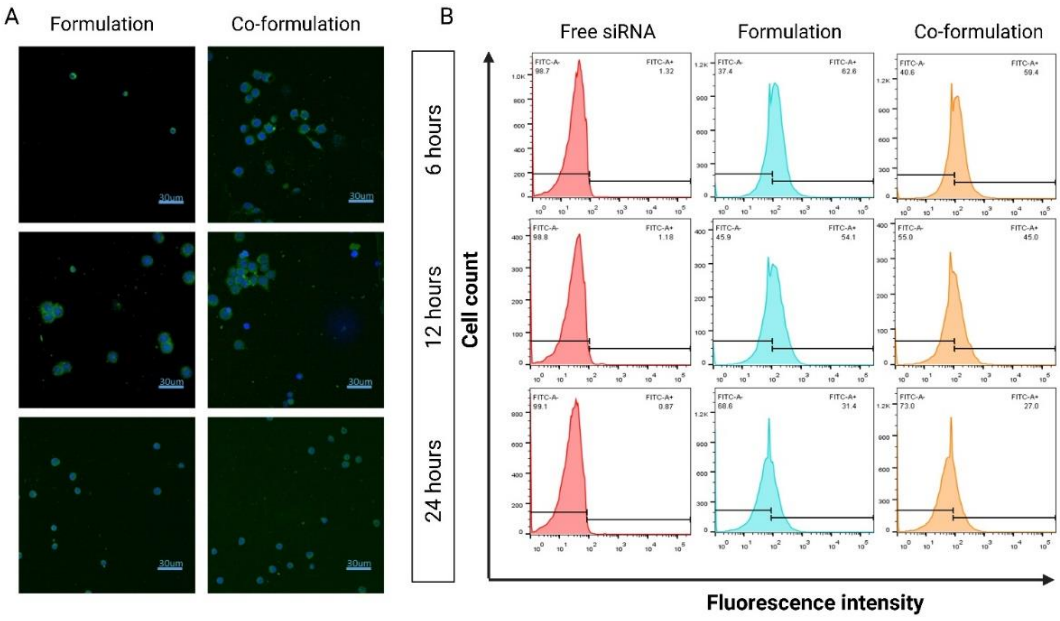

Figure 2-5 Cellular Uptake. (A) Confocal images of uptake into HL-60 cells with NPs incorporating FAM-labelled siRNA (green). Magnification 40×. (B) Flow cytometric analysis of HL-60 cells treated with different CD-based NP formulations at 6, 12 and 24 h. Formulation MR 8.5:1 (cationic CD:siRNA) and co-formulation MR 8.5:1:5.3 (cationic CD:siRNA:anionic CD).

Generally, after entering the cells via endocytosis, NPs containing siRNA if trapped in early endosomes, which mature into late endosomes and ultimately fuse with lysosomes, may be degraded (Deprey, Batistatou, and Kritzer 2020). Therefore, effective escape from late endosomes/lysosomes is a critical step to achieve gene silencing. Herein, Lysotracker Red was used to label later endosomes/lysosomes and the intracellular trafficking was investigated by confocal microscopy. After 6 h, both formulations were located within the late endosome/lysosome, as indicated by the co-localisation of siRNA (green) and LysoTracker (red) (Figure 2-6, indicated by white arrows). The time frame for late endo-lysosomal release differed for the two NP formulations. After 12 h, late endosomal/lysosomal release was seen with the formulation (Figure 2-6 A), but not with the co-formulation which still showed co-localisation (Figure 2-6 B). Endo-lysosomal escape for the co-formulation appeared mainly to occur at the later time of 24 h.

The different endosomal release patterns of the two formulations may be due in part to the difference in overall surface charge and surface pKa. It is well known that positively charged particles more readily escape from the endosome via electrostatic interaction with the endogenous anionic components of the endosomal membrane resulting in endosomal disruption (Degors et al. 2019; Heyes et al. 2005). At endosomal pH of 5.5, the co-formulation NPs with surface pKa of 7 may display less of the cationic species at the NP surface in comparison to the formulation NPs with surface pKa of 8.5. This decrease may lead to weaker NP-endosomal-membrane-interaction thus explaining the slower endosomal escape of the co-formulation detected after 24 h (Figure 2-6 B).

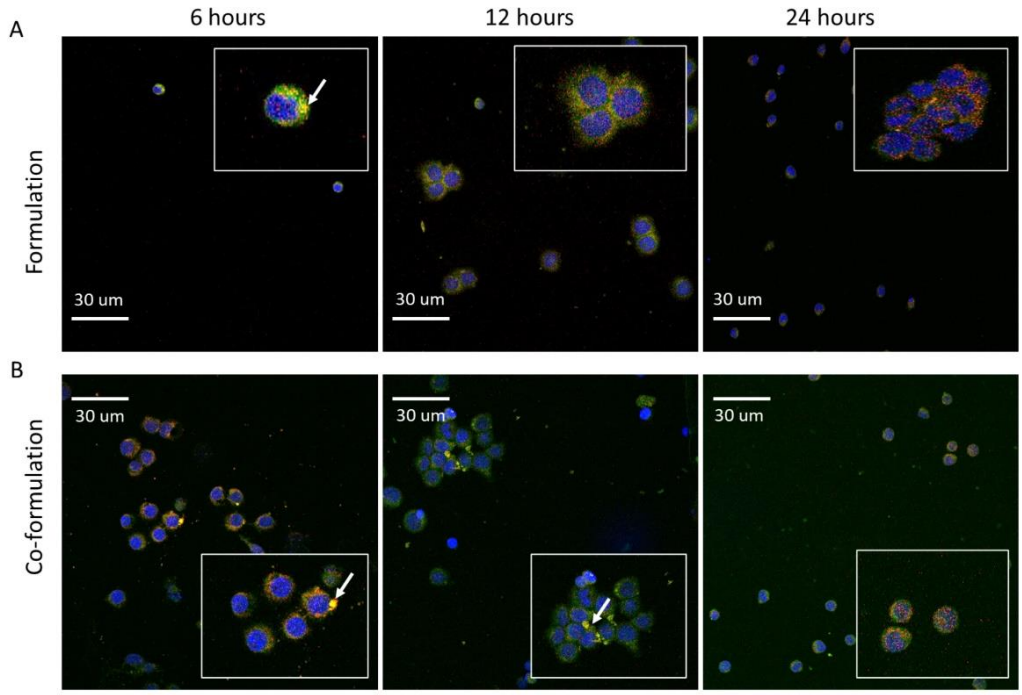

Figure 2-6 Confocal microscopy showing KAT2a siRNA intracellular trafficking. HL-60 cells were treated for 6, 12 and 24 h with CD-based NP formulations containing KAT2a siRNA (100 nM siRNA concentration per well). The fluorescent markers used included: FAM-labelled siRNA (green) positive cells with the lysosomes stained by LysoTrackerTM Red DND-99 (red), and the nuclei (blue) by SytoTM Deep Red Nucleic Acid Stain). (A) Formulation, (B) Co-formulation. Magnification 40×.

To assess the level of gene knockdown, HL-60 cells were transfected with 100 nM KAT2a siRNA per well for 3 days. Although blood cells are difficult to transfect with non-viral vectors (Landry et al. 2012; Uebbing et al. 2020), both CD-NP formulations significantly reduced mRNA levels relative to free KAT2a ($p < 0.05$) by 29 ± 11% for the formulation, and 21 ± 2% for the co-formulation (Figure 2-7), in the absence of toxicity (Figure 7-6). Landry and colleagues reported GFP silencing in THP-1, another leukaemia cell line, of 20–26%, indicating that the levels of gene knockdown achieved in this study are comparable (Landry et al. 2012).

The gene knockdown efficiencies for both formulations are not significantly different, however, the trend for a slightly lower level seen with the co-formulation

may be due to the lower loading capacity, (Figure 2-3 A), and the slower endosomal release potentially resulting in greater endosomal degradation (Figure 2-6). While the co-formulation did not enhance the level of gene silencing in this in vitro study, the reduction in charge density achieved following addition of the anionic CD may be a significant advantage for reducing in vivo toxicity (Zhou et al. 2021).

Work is ongoing to improve the transfection efficiency by further modifying the CD chemistry with the aim of enhancing endosomal escape. In addition, due to the flexibility of the CD basic structure potential exists to incorporate a targeting ligand to help ensure cell specific uptake *in vivo*. Antibody-labelled NPs have shown potential especially in the design of precision medicines for cancer therapy (Lee et al. 2017; Sun et al. 2014). This targeting approach has also been applied to CDs, where Guo et al. (Guo et al. 2017), have shown that antibody-targeted CD-based NPs increased the level of knockdown in KG1 cells, an AML stem and progenitor cell line, and *ex vivo* in patient samples by 35% relative to the untargeted formulation.

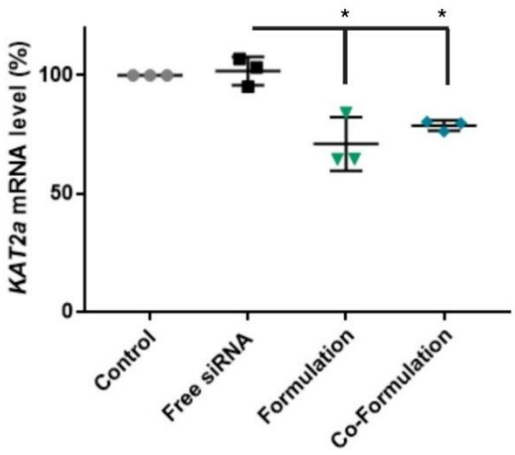

*Figure 2-7 KAT2a mRNA levels after gene knockdown. mRNA levels of KAT2a (as percentage relative to the control (grey dots)) in HL-60 cells measured 72 h post-transfection by TaqMan qPCR and normalized to untreated cells. Mean ± S.E.M of 3 technical replicates per-formed in triplicate (siRNA: black squares; Formulation: green triangles, Co-formulation: blue diamond). One-way ANOVA followed by Dunnett's post hoc test was used. * $p < 0.05$ compared to un-treated group.*

2.4. Conclusions

The chemical versatility of CDs facilitates a range of structural modifications to optimize the physicochemical characteristics and subsequent efficacy of NPs containing therapeutic NAs. By varying the MRs of an amphiphilic cationic CD with an amphiphilic anionic CD in a co-formulation approach it is possible to modulate the size and charge of NPs containing siRNA. The co-formulation of the anionic amphiphilic CD led to a charge reduction of 10 mV and an approximate 3-fold reduction in polydispersity. While the reduction in the cationic charge is likely to be beneficial for *in vivo* delivery, the current *in vitro* studies indicate that endosomal escape maybe the main barrier to enhancing gene silencing above the levels reported (21 ±2%). Structure-activity studies using functionalised CDs, including optimisation of the pKa, to enhance endosomal escape are under investigation. In summary, the data presented illustrates the potential of CDs as a delivery platform for NA therapeutics to treat cancers such as leukaemia with high unmet clinical needs.

3. Chapter: Modified Amphiphilic Cationic Cyclodextrins for siRNA Delivery- a Structure-Activity Study

Ayse Kont[1], Monique C. P. Mendonça[1], Milo Malanga[2], Kristof Felegyi[2], Andrew Lindsay[3], Michael F. Cronin[1], Mary R. Cahill[4], Caitriona M. O'Driscoll[1]

[1]Pharmacodelivery Group, School of Pharmacy, University College Cork, Ireland

[2] CarboHyde Zrt., Berlini str., 47-49. Budapest,1045, Hungary

[3] School of Biochemistry and Cell Biology, Biosciences Institute, University College Cork, Ireland

[4] Department of Haematology and CancerResearch@UCC, Cork University Hospital,

University College Cork, T12 XF62 Cork, Ireland

To be submitted

Abstract

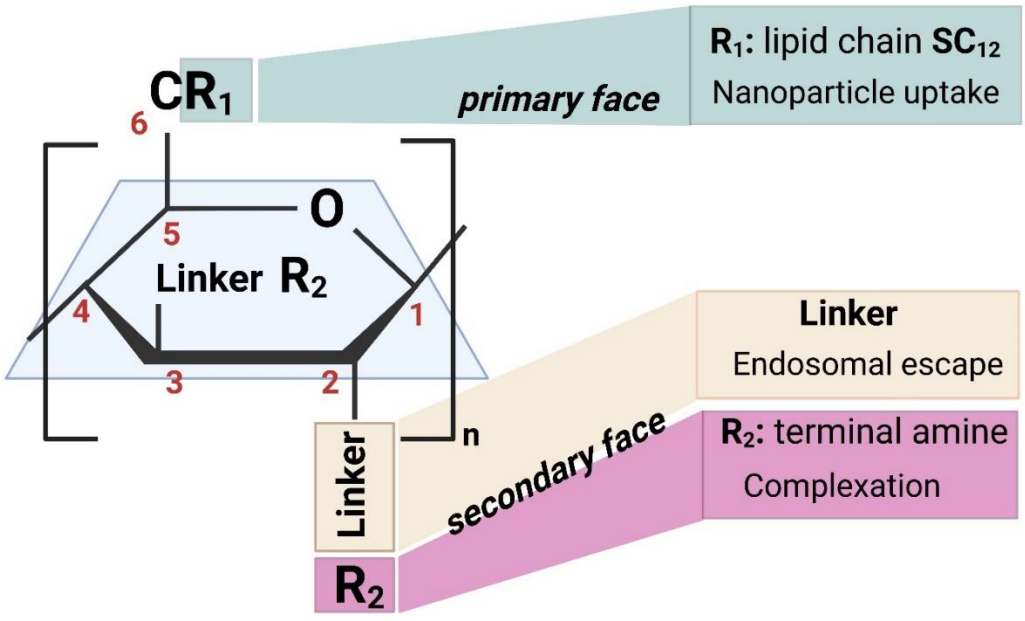

Due to the presence of several hydroxyl groups with different reactivities which enables efficient functionalisation, cyclodextrins (CDs) have proven to be promising vectors for siRNA delivery. In the quest to identify the most effective chemical structure for enhancing activity, a wide array of amphiphilic CDs was meticulously engineered and synthesised. This encompassed a spectrum of chemical and structural properties, such as β-CD versus γ-CD, low pKa versus high pKa, various functionalized chains, terminal primary amine versus tertiary amine, and the choice between triazole-linker and thiopropyl-linker.

Nanoparticles (NPs) with siRNA were formulated at mass ratios (MR) 7.5:1 and 10:1 (CD:siRNA) and characterised. A comparative study assessing the ability of these NPs to silence genes was performed *in vitro* using the reporter gene luciferase in A549-luc cells. Preliminary studies revealed that the introduction of terminal amines at both the C2 and C3 positions of γ-CD (double chain) resulted in more robust gene silencing when compared to the substitution at the C2 position alone (single chain).

An examination of the linker employed for conjugating a terminal primary amine to double-chain γ-CDs revealed enhanced gene knockdown efficacy with a thiopropyl group compared to a triazole group. Remarkably, a double-chain γ-CD appended with a thiopropyl-linked primary amine achieved an 80% gene knockdown, even when the dose was reduced by half. In summary, concerning cationic amphiphilic CDs, the specific nature and strategic location of functional groups play a pivotal role in optimising gene silencing activity.

Keywords: cationic cyclodextrins, chemical modification, nucleic acids, linker chemistry

3.1. Introduction

The development of therapeutic nucleic acid (NA)-delivery strategies has gained a lot of interest in the last decade (Sahu et al. 2023). This was reinforced by the success of the messenger RNA (mRNA) vaccine development against SARS-CoV-2 delivered using lipid nanoparticles (LNPs). The successful approval of mRNA vaccines paves the way for the development of other alternative non-viral NP-based delivery systems targeted at more complex non-infectious disease conditions. Among them, CD-based NPs have demonstrated potential for successful delivery and knockdown of genes in several diseases such as acute myeloid leukaemia (Guo et al. 2017), prostate cancer (Evans et al. 2017), glioblastoma (Gooding et al. 2015; Manzanares et al. 2020), Huntington's disease (Godinho et al. 2012; Mendonça et al. 2021), and lung cancer (Li et al. 2020; Liu and Liu 2022).

CDs have been extensively used as excipients in the pharmaceutical industry to overcome solubility, bioavailability and stability issues (Jambhekar and Breen 2016). CDs as cyclic oligosaccharides differ in the number of glucose units (six (α-CD); seven (β-CD); eight (γ-CD)). All CDs possess a narrow rim with primary hydroxyl groups and a larger face with two types of secondary hydroxyl groups. These hydroxyl groups can be regioselectively modified due to differences in reactivity, thus allowing the production of various CDs bearing neutral, cationic or anionic functional groups (Haley et al. 2020; Xu et al. 2021). These derivatives may display enhanced chemical properties, for instance, modifications of the hydroxyl groups are often performed to increase the aqueous solubility of cyclodextrins (CDs), or the selective introduction of apolar groups, thereby significantly enhancing the lipophilicity of the target derivative. The chemical versatility of these derivatives collectively enhances the utility of CDs as non-viral delivery vectors, for instance, by improving the

membrane permeability. Following this principle, it was possible to synthesise a range of functionalised CDs including amphiphilic cationic, anionic and neutral CDs capable of delivering siRNA and antisense oligonucleotides (ASOs) into neuronal cells (Mendonça, Sun, et al. 2023; O'Mahony, Ogier, et al. 2012), prostate cancer cells (Sun et al., 2023) and leukaemia cells (Guo et al. 2017). The efficient delivery of siRNA and gene silencing efficacy was further demonstrated *in vivo* (Godinho et al. 2012; Guo, Ogier, et al. 2012; McCarthy et al. 2013; Mohammed et al. 2019; Zou et al. 2021).

It is well known that specific functionalisation of biomaterials, including CDs, can impact the physiochemical properties and the subsequent delivery efficiency and biodistribution (Buck et al. 2019; Eygeris et al. 2022; Haley et al. 2020). In this work, NPs containing siRNA were formulated with a range of structurally modified amphiphilic cationic CDs, and evaluated as non-viral delivery vectors. The study included a comparison of the type of CD (β versus γ), functional modifications to the secondary face such as primary versus tertiary amines and the level of substitution per glucose unit in a CD-ring (single versus double chain). Additionally, the effect of linker groups, (triazole and thiopropyl), used to attach these amines, was investigated. The aim of the current work is to expand the library of amphiphilic cationic CDs and to identify the optimum structure to overcome barriers to siRNA delivery, including stability, cellular uptake across bilayer membrane and endosomal escape and consequently enhance gene silencing efficacy.

3.2. Materials and Methods

3.2.1. Materials

siRNA against fluorescent luciferase (FLuc) was purchased from Dharmacon (Lafayette, Colorado, United States) with the target sequence (Sense Strand) 5' CGACAAGCCUGGCGCAGUA 3'. MISSION® siRNA Universal Negative Control #1 and MISSION® siRNA Fluorescent Universal Negative Control #1 6-FAM (Fluorescein amidites) were purchased from Sigma Aldrich (Wicklow, Ireland). All other materials were purchased from Sigma Aldrich at analytical grade, unless mentioned otherwise.

3.2.2. CD synthesis and nanoparticle preparation

Amphiphilic cationic CDs were modified using a range of functional groups as listed in Table 3-1.

Table 3-1 Structurally modified cationic CDs.

CD name	CD type	Number of cationic functional groups on secondary side	Linker group	Terminal amine on secondary face	Reference
CD-B1	β	1	Triazole	Primary	(O'Mahony, Ogier, et al. 2012)
CD-B2	β	1	Ester	Tertiary	(Mendonça et al. 2021)
CD-G1	γ	1	Triazole	Primary	
CD-G2	γ	2	Triazole	Primary	(Mendonça, Sun, et al. 2023)
CD-G3	γ	1	Thiol	Primary (on primary face)	
CD-G4	γ	2	Thiopropyl	Primary	
CD-G5	γ	2	Thiopropyl	Tertiary	

SAR comparison		
CD-chemistry	**CD representative**	**Rationale**
CD type	β- versus γ-CD	Water solubility, industrial scale up
Terminal amine (chain number, pKa)	CD-B1 versus CD-B2 CD-B1 versus CD-G1 CD-G1 versus CD-G2 CD-G4 versus CD-G5	Complexation, endosomal escape
Linker	CD-G1 versus CD-G4	Endosomal escape, industrial scale-up

SAR = structure-activity-relationship

The synthesis of β-CDs, CD-B1 and CD-B2, and γ-CD, CD-G2, have previously been reported (Mendonça et al. 2021; Monique C. P. Mendonça, Sun, et al. 2023; Aoife M. O'Mahony, Ogier, et al. 2012). The structures of the newly synthetized CDs (CD-G1, CD-G3-5) were confirmed using Fourier-transform infrared spectroscopy (FT-IR), nuclear magnetic resonance (NMR), and high-resolution mass spectrometry (HRMS) (7.2.1 Synthesis Details).

After dispersion of the CD in RNase-free water (0.25 mg/ml) using a probe sonicator (Branson Sonifier 250) for 10 mins; NPs were prepared by incubating with siRNA at 450 rpm for 30 mins at 25 ℃ in a thermomixer. The final siRNA concentration was 500 or 1000 nM.

3.2.3. Physicochemical characterisation

3.2.3.1. Size, Poly dispersity index and Zeta potential

Particle properties were assessed by dynamic light scattering (DLS) (Zetasizer Nano-ZS, Malvern Instruments, Malvern, UK). Particle size (Z-Average) and poly dispersity index (PDIs) were measured with non-invasive backscatter system

(scattered light angle of 170°) in a narrow size cuvette (REF 67.742). Zeta potential was determined with folded capillary cells (DTS1070) by means of electrophoretic mobility (forward scatter angle of 12.8°) in monomodal mode. Chosen settings were protein as material (refractive index 1.450 and absorption 0.001), and water as dispersant (viscosity 0.8872cP, refractive index 1.330) at 25 °C.

3.2.3.2. Complexation efficiency

The complexation efficiency was assessed with 1%-Agarose gel (1%) which was run in Tris/Borate/EDTA buffer containing SafeView (NBS Biologicals, Huntingdon, UK), a Nucleic Acid Stain (6 µ/100ml). BlueJuice^{TM} Gel Loading Buffer (10X) (Invitrogen, Waltham, MA, USA) was added to samples. The gel was run at 90 V for 45 min (Bio-Rad, PowerPacBasic, Hercules, CA, USA) and imaged under UV with Uvitec CambridgeMini HD.

3.2.3.3. Encapsulation efficiency

Encapsulation efficiency was assessed with the Quant-iT RiboGreen^{TM} RNA Assay kit (Invitrogen, Invitrogen, Waltham, MA, USA). The fluorescent intensity of the interaction between free RNA and RNA-dye was measured after NP incubation (Jiang et al. 2020) with a Tecan Spark® (Männedorf, Switzerland) microplate reader at 485 nm excitation wavelength and 535 nm emission wavelength in a black 96-well plate (Gain 55, top reading). siRNA quantification was determined by means of a calibration curve ($R^2 > 0.995$, x-axis: siRNA concentration, y-axis: dye signal).

3.2.3.4. Determination of pKa

2-(*p*-toluidino)-6-naphthalene sulfonic acid solution (TNS) in DMSO was prepared (300 µM) to measure the fluorescence intensity of CD-NPs at different pH (0.1 M buffers from pH 4–12 in increments of 0.5; pH 4–6.5 citrate buffer, pH 7–11.5

Trizma® buffer). The fluorescence signal was determined in a black 96-well plate. using Tecan Spark® (Männedorf, Switzerland) using a microplate reader at an excitation of 340 nm and an emission of 485 nm (top reading). 90 µl buffer was combined with 10 µl sample and 2 µl TNS (6 µM TNS/well). The inflection point (LogIC50) on the resultant sigmoidal plot defined the apparent pKa of the formulation and/or the CD (Uebbing et al. 2020).

3.2.3.5. Transmission electron microscopy (TEM)

TEM samples were dried on a 400-mesh copper coated carbon film, as previously described (Monique C. P. Mendonça, Sun, et al. 2023) and analysed with a JEOL JEM 2000FXII (Jeol Ltd., Tokyo, Japan), at 200 kV.

3.2.3.6. Heparin release

NPs were incubated at 37 ℃ with heparin (10 mg/ml) at a final heparin concentration of 20% (w/v) for different time points. Displaced siRNA was visualised by UV on a 1% Agarose gel after 30 mins at 90 V.

3.2.3.7. Serum stability

Samples were incubated at 37 ℃ with 50% fetal bovine serum (FBS, heat-inactivated) (Aylward 2019) for different time intervals. Subsequently, samples were treated with heparin (10 mg/ml) for 75 min at room temperature (20% (w/v) heparin in final sample). Samples were loaded onto 1% Agarose gel after addition of BlueJuice^{TM} Gel Loading Buffer (10X) (Invitrogen, Invitrogen, Waltham, MA, USA). The gel and buffer contain SafeView (NBS Biologicals, Huntingdon, UK), a Nucleic Acid Stain (6 µ/100 ml). The gel was run at 90 V for 30 min (bio-Rad, PowerPacBasic Hercules, CA, USA) and imaged under UV.

3.2.4. Cell culture

A549-luc2 were purchased from ATCC (American Type Culture Collection) and donated by Dr. Piotr Kowalski (University College Cork). A549 are epithelial cells derived from lung cancer in a white, 58-year-old male patient. The cells were maintained in Dulbecco's Modified Eagle Medium (DMEM) with 10% (v/v) FBS (heat-inactivated), 1% (v/v) Penicillin-Streptomycin and 8 µg/ml Blasticidin at 37 ℃ and 5% CO_2. Cell lines with luciferase as reporter gene are useful and practical tools to screen a variety of NA delivery vectors (Neefjes et al. 2021).

3.2.4.1. Cellular uptake

1.5 x 10^5 cells/ well were seeded in a 24-well plate in complete media (10% (v/v) FBS and 1% (v/v) Penicillin/Streptomycin). After 24 hours, the media was changed to low-serum media (2% (v/v) FBS and 1% (v/v) P/S) (400 µl). Transfection was performed with FAM-labelled siRNA for 6 hours (100 µl of NP; equals 20 pmol siRNA/well). After incubation, cells were trypsinised and collected in tubes, subsequently centrifuged at 1500 rpm for 5 min at 4 °C. Cells were washed with PBS and finally resuspended in PBS and transferred into polystyrene round bottom tubes (Becton Dickinson). BD CELESTA Facs Analyser was utilised to assess cellular uptake (10 000 events). Data was analysed with FlowJo 10 (Franklin Lakes, New Jersey, United States).

3.2.4.2. Intracellular trafficking

Intracellular uptake was also confirmed by confocal microscopy. Cells (1.5 x 10^5/well) were grown in complete media on glass coverslips in a 24-well plate 24 hours prior to transfection. For transfection purposes FBS was reduced to 2% (v/v) in

the media and 20 pmol/well FAM-siRNA-NPs were added per well and incubated for 0 h, 6 h, 24 h and 48 h. Subsequently, slides were incubated with DAPI in PBS for 30 mins and mounted with Mowiol Mounting Media. Zeiss LSM510 META confocal microscope (Carl Zeiss, Jena, Germany) using a 63× objective was used to acquire confocal images.

3.2.4.3. Toxicity assay and Gene knockdown

Cells were seeded at 1 x 10^4 cells/well in a white 96-well plate 24 hours before transfection. After replacing the complete media with low serum complete media, transfection for 6 hours was conducted at 10 or 20 pmol FLuc siRNA per well (final volume per well: 100 µl/well). The media was changed to high FBS complete media and incubated for further 18 hours, CellTiter-Fluor™ Cell Viability Assay was used to assess the potential cytotoxicity of the treatments. The substrate was prepared at 5X and 20 µl was added to each well. After 35 mins incubation (5% CO_2, 37 °C), the luminescence was measured in a Tecan Spark® (Männedorf, Switzerland) microplate reader at an excitation of 380 nm and an emission of 535 nm (top reading). Subsequently, levels of knockdown were evaluated using ONE-Glo™ EX Luciferase Assay (Promega, Madison, Wisconsin, United States) according to manufacturer's guidelines in the same plate, using the luminescence mode in the Tecan Spark® microplate reader. Luciferin signals were normalized against the average of the cell viability of the control group, as follows:

$$\frac{\text{luciferin signal}}{\text{viability signal} \Big/ \text{average of viability signal of control group}}.$$

3.2.5. Statistical analysis

Data was statistically analysed using GraphPad Prism 8. The One-way ANOVA was used and Tukey's multi comparison post hoc test was applied to compare all formulations. Statistical significance was considered at different levels, **** $p < 0.0001$, *** $p < 0.001$, ** $p < 0.01$, * $p < 0.05$.

3.3. Results and Discussion

3.3.1. CD structure and chemistry

All of the amphiphilic CDs studied contained a C_{12} lipid chain, shown previously to enhance gene silencing activity (A. M. O'Mahony, Godinho, et al. 2012). The lipophilic groups facilitate self-assembling into NP and promote membrane permeability (Singh et al. 2019), while the positively charged groups on the secondary side are necessary to form electrostatic complexes with the negatively charged NAs.

Seven modified CDs were analysed in this study (Figure 3-1): six amphiphilic cationic CDs (two β- and four γ-CDs), all with C_{12} lipid chains on the primary side at the 6-OH position and one non-amphiphilic cationic CD (CD-G3). The first amphiphilic β-CD (CD-B1) was prepared using 'click' chemistry to attach the cationic functional group selective on the *O*2 of the glucopyranose units. CD-B1 contains a primary amine attached *via* a triazole to the β-CD. The second amphiphilic cationic β-CD (CD-B2) incorporates a tertiary amine, with the aim of reducing the apparent acid dissociation constant (pKa) and assessing the influence of pKa on NP performance.

To assess the effect of the cavity size on the complexation, γ-CD was selectively modified by click chemistry on the *O*2 position with primary amine (CD-G1). Additionally, the γ-CD analogue with secondary-side *O*2 and *O*3 exhaustively

substituted (CD-G2) was used to evaluate the effect of the number of cationic groups (charge density of the CDs).

To investigate the structure-activity-relationship (SAR) further for the γ-CDs, three additional derivatives were synthesised, and their performances were established. Firstly, a cationic and non-amphiphilic γ-CD derivative with primary amine located on the narrow rim of the CD unit (CD-G3) was synthesised with the aim to confirm the importance of amphiphilicity. Subsequently, γ-CD modified on the primary side with dodecylthio apolar chains (C_{12} lipid chains) was completely substituted on the secondary side (both *O*2 and *O*3 substitutions) with primary amine (CD-G4) or tertiary amine (CD-G5) to assess the importance of the nature of the terminal amine in gene knockdown potential. Ultimately, the triazole linker was compared to the thiopropyl linker, by examining CD-B1 versus CD-G4.

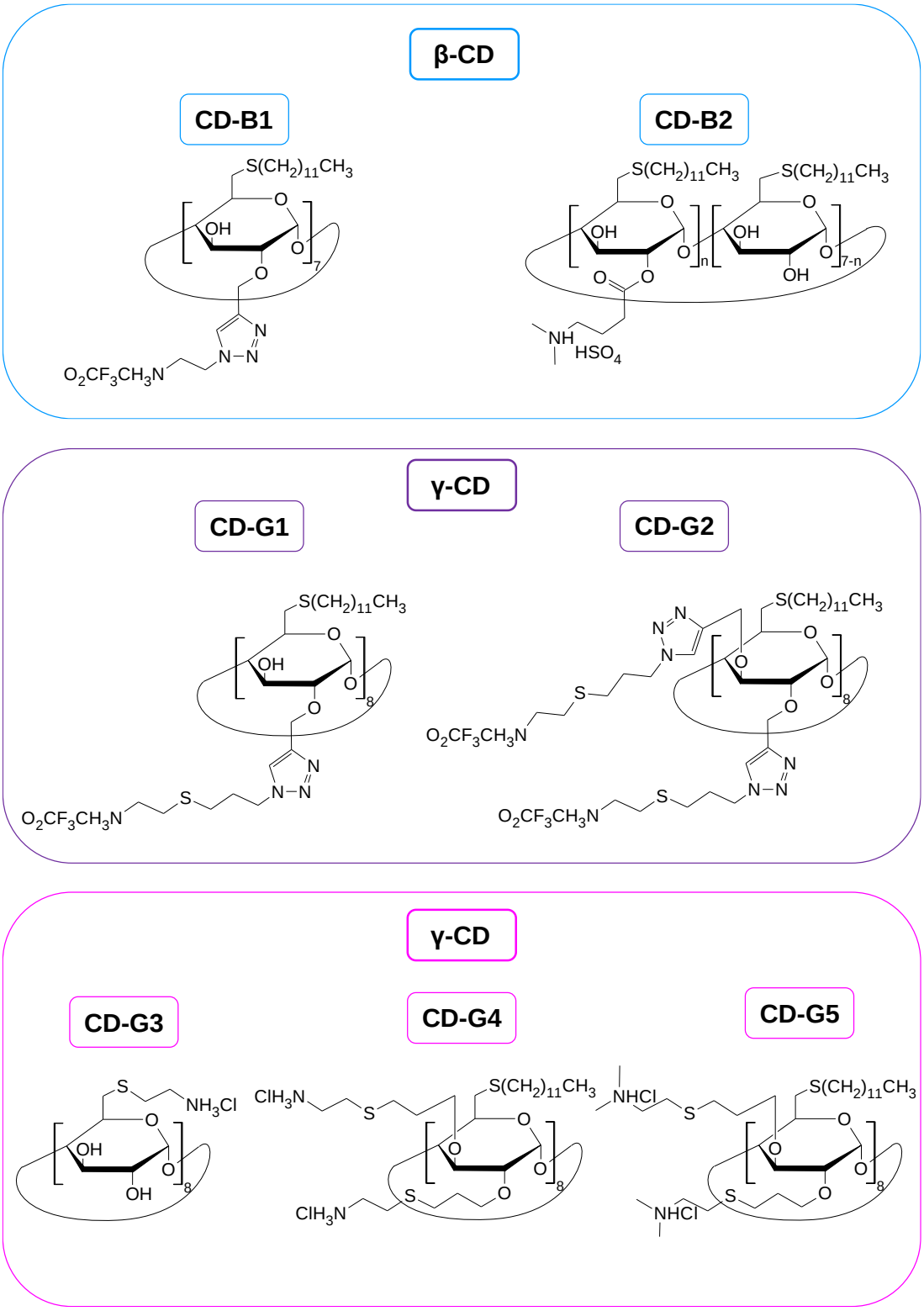

Figure 3-1 Chemical structures of the amphiphilic cationic β- and γ-CDs used in this study.

3.3.2. Physicochemical characterisation

To explore the effects of structural modification on the physicochemical properties, changes in size, PDI, charge, and pKa were monitored for all CD derivatives.

Nanoparticle Size and PDI

All NPs measured with DLS showed average sizes from 110 - 220 nm regardless of the molar ratio (MR) and CD type used in the formulation (Figure 3-2 A). The increase in MR from 7.5:1 to 10:1 (cationic CD:siRNA) did not significantly impact the size. Poly dispersity index (PDI) ranged from 0.3-0.5. The TEM analysis revealed spherical particles with sizes ~100 nm (Figure 3-2 C). The lower particle size by TEM is due to sample preparation which includes a drying process that tends to shrink the particle. Similar results for size and PDI were observed previously (Mendonça et al. 2021; Sun et al. 2023).

Nanoparticle Charge

A significant decrease in charge associated with MR reduction from 10:1 to 7.5:1 was observed for γ-CDs CD-G1 (***p <0.001) and CD-G2 (*p < 0.05) which decreased from 32 mV to 22 mV and 37 to 30 mV, respectively. β-CD showed a similar trend, however, these changes in charge were not statistically significant (Figure 3-2B).

Comparison of the CD type: β-CD versus γ-CD

The CD-B1 and CD-G1 have similar functional groups, incorporating a SC12 lipid chain on the primary side and a triazole-attached primary amine regioselectively located on the *O*2 of the secondary side, the most prominent difference is the number of glucose units in the ring structure. This allows a reasonable comparison of the effects of changing the cavity size from β- to γ-CDs. At MR7.5:1 a significant charge

difference was detected from 35 to 22 mV (**** $p < 0.0001$, CD-B1 and CD-G1 respectively). The same trend of charge reduction occurred at MR 10:1 from 38 to 32 mV (* $p < 0.05$).

Effect of the number of amines on the secondary side

The γ-CD derivative, CD-G1, containing one primary amine per glucopyranose unit (*O*2-substitution) was compared to CD-G2 analogue, bearing identical structural motifs on both *O*2 and *O*3 positions. As expected, an increase in the positive charge was detected when γ-CDs were compared within the same MR. The increase was more prominent at MR7.5:1 (G1 at 22 mV versus G2 at 30 mV, (**$p < 0.01$) but not significantly higher at MR10:1 (G1: 32 mV versus G2: 37 mV). The higher zeta potential might occur as a consequence of a higher charge density per γ-CD glucose unit.

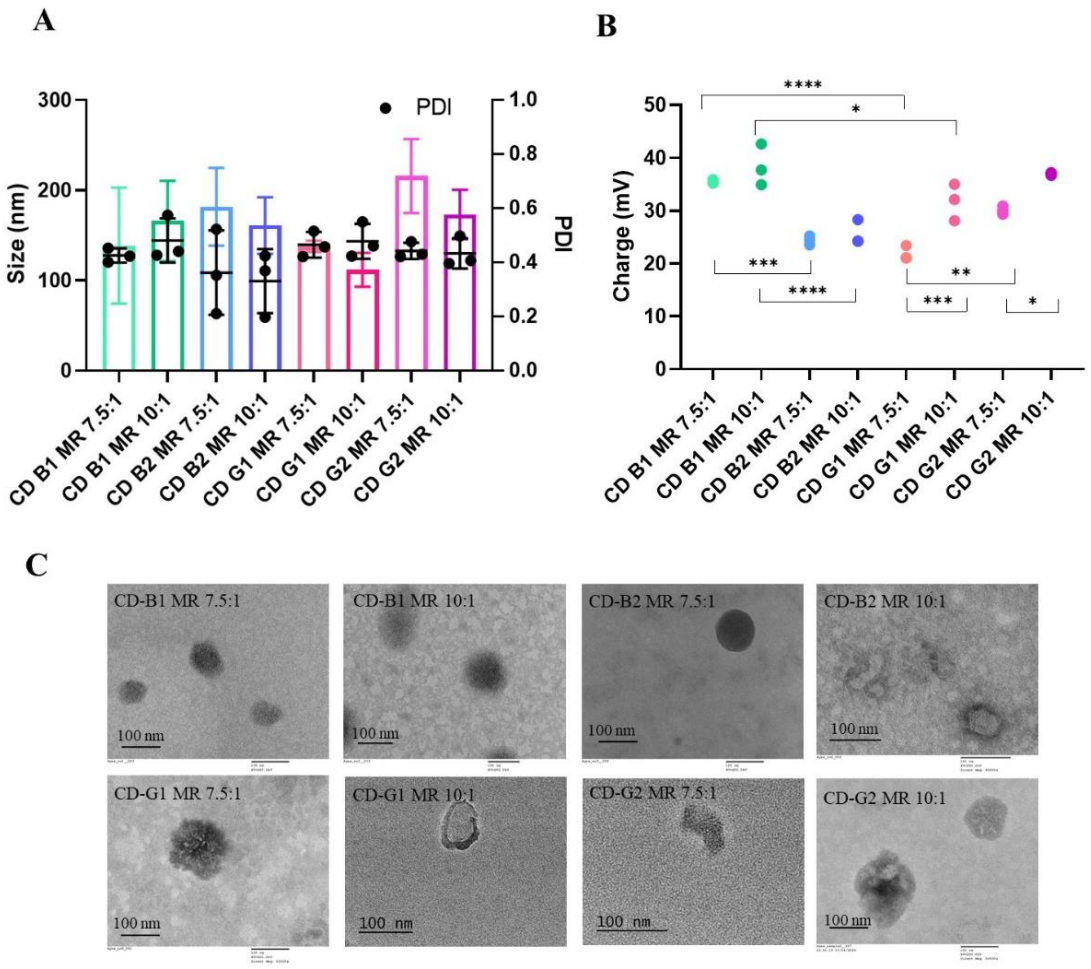

*Figure 3-2 Physicochemical characterisation of CDs. (A) Size ± SD (Bar chart) and Polydispersity index ± SD (PDI) (black symbols •)(N=3); (B) Charge ± SD of the NPs (N=3). (C) Representative TEM images of CD-NPs at different mass ratios. Scale bar= 100 nm. One-way ANOVA followed by Tukey's multi comparison test, **** p < 0.0001, *** p < 0.001, ** p < 0.01, * p <0.05.*

Binding of the siRNA by the CDs

In all CD:siRNA formulations, no free siRNA was detectable (based on gel electrophoresis investigation) indicating full binding of the siRNA by the cationic CDs (Figure 7-7 A). This result was corroborated by an encapsulation efficiency of >90% (Table 7-1). The strong binding is essentially driven by the electrostatic interactions between the cationic CDs and the oppositely charged NA, however, it is also influenced by the MR of CD to siRNA used (Aydinlioglu et al. 2023; Jiang et al. 2020).

Effect of the terminal amine on pKa

Table 3-2 Description and physicochemical characteristics of CDs used in this study. Estimated (CD-B1) or experimental (CD-B2, CD-G1-5) pKa of pure CD determined by TNS assay. MW= molecular weight.

	CD-B1	**CD-B2**	**CD-G1**	**CD-G2**	**CD-G3**	**CD-G4**	**CD-G5**
Linker	'click' triazole	ester	'click' triazole	'click' triazole	thiol	thiopropyl	thiopropyl
Amine	primary	tertiary	primary	primary	primary	primary	tertiary
MW (g/mol)	4192	3479	4367	7796	1952	5198	5679
pKa (pure CD)	11	6.2	10	10	10	8.2	7.8
Lipid chain	SC_{12}	SC_{12}	SC_{12}	SC_{12}	N/A	SC_{12}	SC_{12}

In the case of cationic lipids, it has been reported that a pKa of approximately 6.5 is ideal for the delivery of NA, facilitating maximum ionisation and subsequent siRNA binding at low pH, while being near neutral at physiological pH. The apparent pKa of the CD-based formulations was evaluated because pKa is suggested to be an important factor driving the efficiency of NPs *in vivo* (Hajj et al. 2019). The amine function on the β-CD (CD-B1 versus CD-B2) was changed from primary to tertiary. To evaluate the effect of the change in pKa and charge density after NP formulation, pKa values were determined in nuclease-free water (pH 6.5). Whilst γ-CD-NP containing triazole-attached primary amines (CD-G1 and CD-G2 presented pKa values of 10 across both MRs) NPs formed with β-CDs showed a significant drop from pKa 9 (CD-B1, triazole-attached primary amine) to ~6 once the amine was switched to tertiary amine attached *via* an ester (CD-B2) (Figure 3-3 A). This was anticipated in the light of previously measured pKa of pure CD-B1 and CD-B2 (Table 3-2). Also, CD-B2 has a lower amine substitution level due to the synthetic challenges encountered during the acylation step.

The apparent surface pKa of NPs is a result of surface composition (Hajj et al. 2019; Patel, Ibrahim, and Cheng 2021). It is reasonable to expect a correlation between pKa and surface charge. Changing the functional groups on the secondary site (e.g., 'triazole' primary amine (B1) to 'ester' tertiary amine (B2)) has an impact on surface charge and apparent pKa of NPs. CD-B2-NP, displaying the lowest pKa values, ranging from 6 to 7, also exhibited lower charge measurements, as illustrated in Figure 3-3 B. Conversely, CD-B1, with a pKa of 9, demonstrated higher surface charges, as seen in Figure 3-3 C. On the other hand, the γ-CDs displayed fluctuations in charge measurements depending on the degree of substitution on the secondary face and the

MR. However, it is noteworthy that the presented pKa values remained consistent around 10 throughout, as shown in Figure 3-3 D.

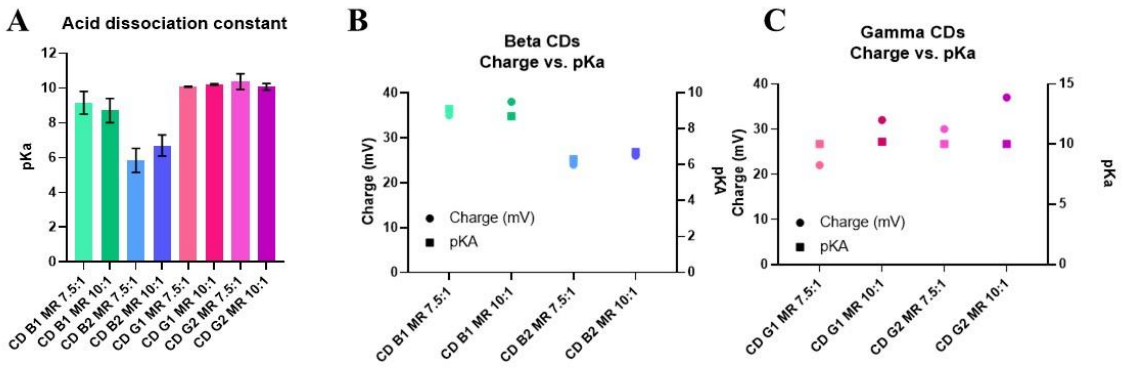

Figure 3-3 Measurement of surface pKa with TNS assay of amphiphilic cationic CD-siRNA-NPs. (A) pKa ± SD s for the NPs (N=3).; (B) Correlation between charge measurements in the DLS and pKa values measured with the TNS assay.; (C) Correlation relationship for β-CDs.; Correlation relationship for γ-CDs.

Physiological barriers to transfection

A good delivery system should be able to provide protection against destructive biological environments (nucleases, acidic environment in endosome and endosomal escape) and exhibit an efficient release of the siRNA into the target cell/tissue. CD-B2 (β-CD substituted with tertiary amine through ester bond) did not show any increase in RNA release over time (24 hours) (Figure 7-8). This was also observed when antisense oligonucleotides (ASO) was used (Mendonça, Sun, et al. 2023). Tertiary amines have been shown to improve the interaction between delivery vector and NA in a previous study where chitosan (containing primary amines) was substituted with diethylaminoethyl moieties (Martins et al. 2019). This strong interaction could be disadvantageous *in vitro*. The remaining NPs (CD-B1, CD-G1, CD-G2) showed constant RNA release.

To test the stability in biological fluids, CD-NPs were incubated with 50% FBS over 24 hours and the samples were collected at multiple timepoints (Figure 7-9). CD-B1 showed protective behaviour until 6 hours at MR7.5:1 and until 24 hours at MR10:1, after which weakening of siRNA band is evident. In contrast, CD-B2 showed strong protection / binding as the released siRNA bands does not change intensity over time although NA release is low as discussed above (Figure 7-8). This observation highlights the importance of CD structural design to influence the optimal balance of NA protection and release (Raja, Katas, and Wen 2015). The *O*2-substituted γ-CDs (CD-G1) behaved similar to CD-B1, in which MR 10:1 was the preferred formulation. CD-G2 represents a good example of a delivery system that can protect and release the siRNA as indicated by the constant strong bands for both MRs across this experiment.

3.3.3. Uptake and gene knockdown of β- and γ-CD

Biological membranes remain one of the main barriers for NA activity *in vitro* and *in vivo.* Amphiphilic CDs facilitate crossing the lipid bilayer. The bilayer membrane has an overall negative charge, therefore, impede the uptake of negatively charged siRNA (Donahue, Acar, and Wilhelm 2019). FAM-labelled siRNA (fluorescence label) was used to monitor NP uptake and trafficking. All NP studied exhibited an uptake >30% (Figure 3-4), measured by flow cytometry. The highest level of uptake was detected with the β-CDs, reaching 60% with CD-B1 at MR 10:1 and >70% with CD-B2. γ-CDs achieved lower levels of uptake between 30-50%. This was further corroborated by confocal microscopy of γ-CD, CD-G2 (*O*2- and *O*3-substitution with triazole linker and primary amine), showing successful intracellular uptake at 6 hours (Figure 3-4 B) and diffusion of siRNA at subsequent time points.

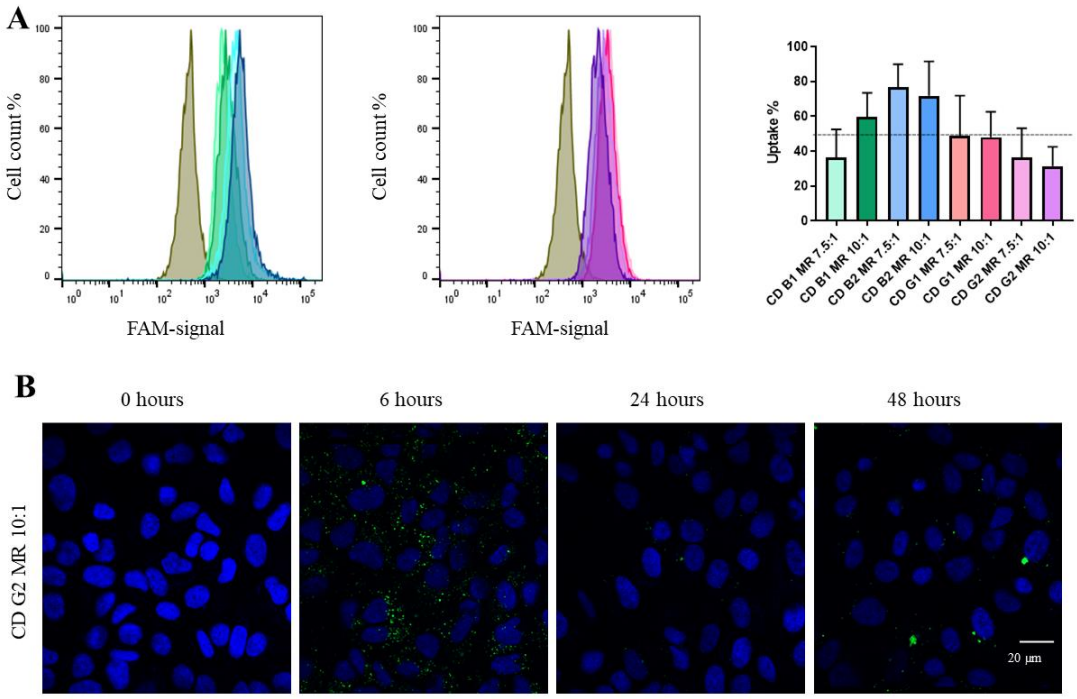

Figure 3-4 (A) Cellular uptake of amphiphilic cationic CD-siRNA-complexes at different MRs in comparison to siRNA-only treatment group using FAM-labelled siRNA (brown) analysed with flow cytometer. Uptake profiles of amphiphilic cationic β-CDs (blue-green) and amphiphilic cationic γ-CDs (pink-purple) after 6 hours; Summary of percentual uptake profiles of amphiphilic cationic CDs (N=3) after 6 hours. No significance was detected applying One-way ANOVA followed by Tukey's multi comparison test. 1.5 x 10^5 cells were treated with 20 pmol siRNA/well. Green: CD-B1, blue: CD-B2, orange-red: CD-G1, pink-purple: CD-G2, (B) Intracellular uptake of CD-G2-N PMR10:1 encapsulating FAM-labelled siRNA imaged and monitored with confocal microscopy over 48 hours.

To evaluate gene silencing and cell viability, luciferase siRNA formulated in CD-NPs were screened using A549-luc, lung cancer cells, with the luciferase reporter gene (Neefjes et al. 2021). Cells were treated with 20 pmol/well siRNA for 48 hours and luciferase activity was measured in a microplate reader by quantifying the luminescence signal after cell lysis (Figure 3-5 A). The maximum gene knockdown was achieved with CD-G2 (*O*2- and *O*3-substitution with triazole linker and -primary amine) at MR10:1 (41 ±12%). When this CD was used to deliver ASO in ST14A (rat striatal neuronal cells), a similar level of knockdown of Huntingtin mRNA (>50%) was reported (Monique C. P. Mendonça, Sun, et al. 2023). A direct comparison of the

influence of the number of amine groups showed that the charge density might have an enhancing effect on gene silencing effect. While CD-G1 showed only gene silencing effect of 20 ±8% at MR10:1, CD-G2 presented gene knockdown of 23±5% at MR7.5:1. The enhancing effect provided by the higher number of amine moieties could be explained by improved endosomal escape, as previously reported (Monique C. P. Mendonça, Sun, et al. 2023). In the case of the β-CDs, significant gene knockdown (20 ±15%) was detected only with CD-B1 at the higher MR10:1 statistically different to the result with CD-G2 MR10:1 (* p <0.05). This result was in contrast to previously published data (A. M. O'Mahony, Godinho, et al. 2012; Aoife M. O'Mahony, Ogier, et al. 2012). The gene knockdown ability for CD-B1 might be cell line dependent. The formulations did not affect the cell viability, demonstrating the safe use of these CDs (Figure 3-5 B).

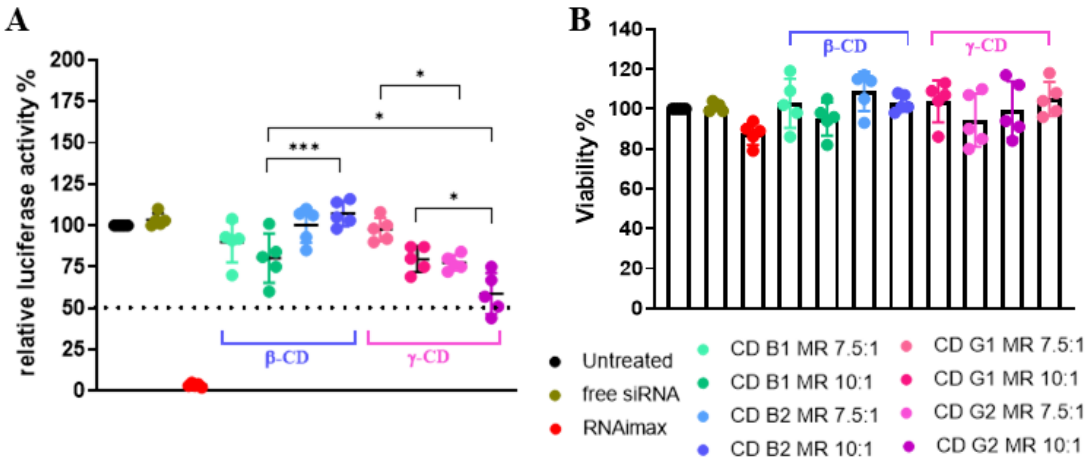

*Figure 3-5 (A) Gene knockdown ±SD of amphiphilic cationic CD-siRNA-complexes at different mass ratios relative to untreated cells. siLuc. 10^5 cells/well were treated with 20 pmol/well siRNA for 48 hours and the luciferase signal were measured by reading the plate in the microplate reader (N=5).; (B) Cell viability ±SD profiles of amphiphilic cationic CDs (N=5). One-way ANOVA followed by Tukey's multi comparison test, *** $p < 0.001$, * $p < 0.05$.*

3.3.4. Further optimisation of the design of double chained γ-CDs

After initial assessment of β- and γ-CDs, it can be concluded that CD-G2 is the best performing CD with preferrable siRNA release, stability properties and gene knockdown ability. These findings initiated the investigation of other *O*2/*O*3-substituted γ-CDs. Questions that remain are whether the type of amine or the linker may influence this behaviour. As mentioned before, CD-G4 and CD-G5 were *ad-hoc* designed to properly answer these questions. Additionally, a cationic, non-amphiphilic γ-CD derivative (CD-G3) was also included in the following experiments to assess the importance of amphiphilicity. MR10:1 has been used throughout the study.

The mean size of NPs prepared from CD-G3 was 267 nm while CD-G4 (primary amine) and CD-G5 (tertiary amine) showed similar size (180-200 nm) (Figure 3-6 A) compared to the amphiphilic CDs reported above. Size and PDI were not significantly different between the three γ-CDs, however, charge measurements showed a significant difference between non-amphiphilic CD-G3 and amphiphilic CDs-G4 and -G5 (22 mV vs. 28 mV, respectively) (Figure 3-6 B). Both complexation (Figure 7-7 B) and encapsulation (>90%) (Table 7-1) were successfully accomplished. The apparent pKa values were obtained for NPs from TNS measurements. 9.8 for CD-G3 and 8 for both amphiphilic CDs-G4 and -G5 (Figure 3-6 C). This finding is unexpected taking into account that different type of amines are involved (primary versus tertiary). In contrast, when the same structural modifications were applied to the β-CD, (CD-B1 (primary) and CD-B2 (tertiary)) a drop in pKa was observed.

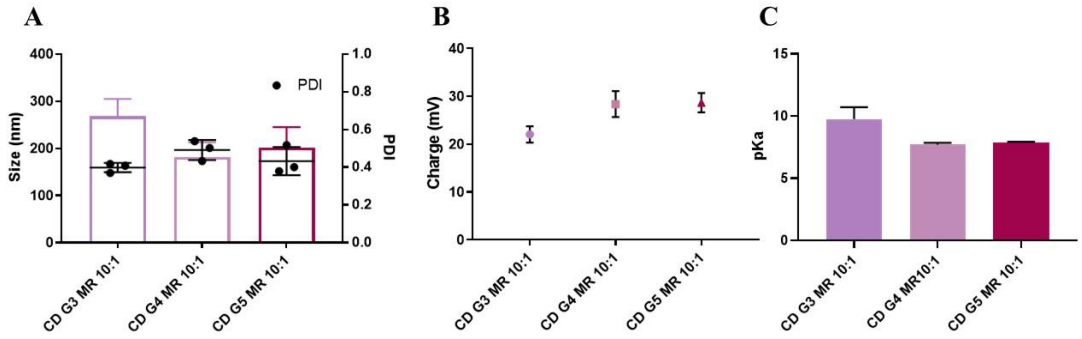

*Figure 3-6 Physicochemical characterisation. A Size ±SD and PDI ±SD (black symbol •) of NPs measured with DLS (N=3). B Charge ±SD measurements of formed NPs determined with electrophoretic mobility in DLS (N=3). C Acid dissociation constants ±SD (pKa) of γ-CD-NPs investigated by means of TNS assay (N=3). One-way ANOVA followed by Tukey's multi comparison test, ** p < 0.01, * p <0.05.*

Even though double chained, triazole-attached, primary amine γ-CD (CD-G2) showed the lowest uptake, a gene knockdown of ~40% was recorded. It was intriguing to examine whether the replacement of triazole ring with a thiopropyl linker would allow for a more regionally flexible terminal amine, and hence, improve gene knockdown ability. A similar objective was investigated by the group of J. M. García Fernández earlier, where the replacement of triazole moiety with a thiourea in β-CDs showed improved performance *in vivo* (Méndez-Ardoy, Guilloteau, et al. 2011; Méndez-Ardoy, Urbiola, et al. 2011).

γ-CDs were tested in A549-luc cells (Figure 3-7). The uptake studies clarified that the amphiphilicity of the CDs is an important factor for successful uptake. The absence of lipophilic functional groups prevented uptake into cells and consequently resulted in no gene knockdown for CD-G3 (Figure 3-7 B, C). It was reported that hydrophilic siRNA can only cross biological membranes if its hydrophobicity is increased by direct chemical modification or through formulation into NPs with lipophilic compounds (Zheng and Tai 2020).

Figure 3-7 A presents the intracellular trafficking of FAM-labelled siRNA entrapped in the amphiphilic *O*2/*O*3-substituted γ-CDs, indicating successful uptake at 6 hours and successful diffusion/release into the cytoplasm which is supported by the reduced labelling around the nuclei at 24 hours. It appears that maximum uptake happens at 6 hours, therefore, flow cytometry studies were conducted at this time point. As shown in Figure 3-7 B, CD-G3 did not show uptake while the two amphiphilic CDs showed similar uptake around 80%. Despite this, CD-G4 showed gene knockdown of 80% (similar to commercial control RNAimax), whereas CD-G5 showed 40% gene silencing (****$p < 0.0001$) (Figure 3-7 C). A similar trend between primary and tertiary amine was observed for CD-B1 MR10:1 (primary amine) and CD-B2 (tertiary amine) MR10:1, however, the effect was not very pronounced. All three γ-CDs showed no toxicity (Figure 3-7 D). Comparing CD-G4 MR10:1 (thiopropyl linker) with CD-G2 MR10:1 (triazole linker), the superior knockdown ability of CD-G4 is evident. This indicates that the thiopropyl linker group may be favourable over the triazole linker.

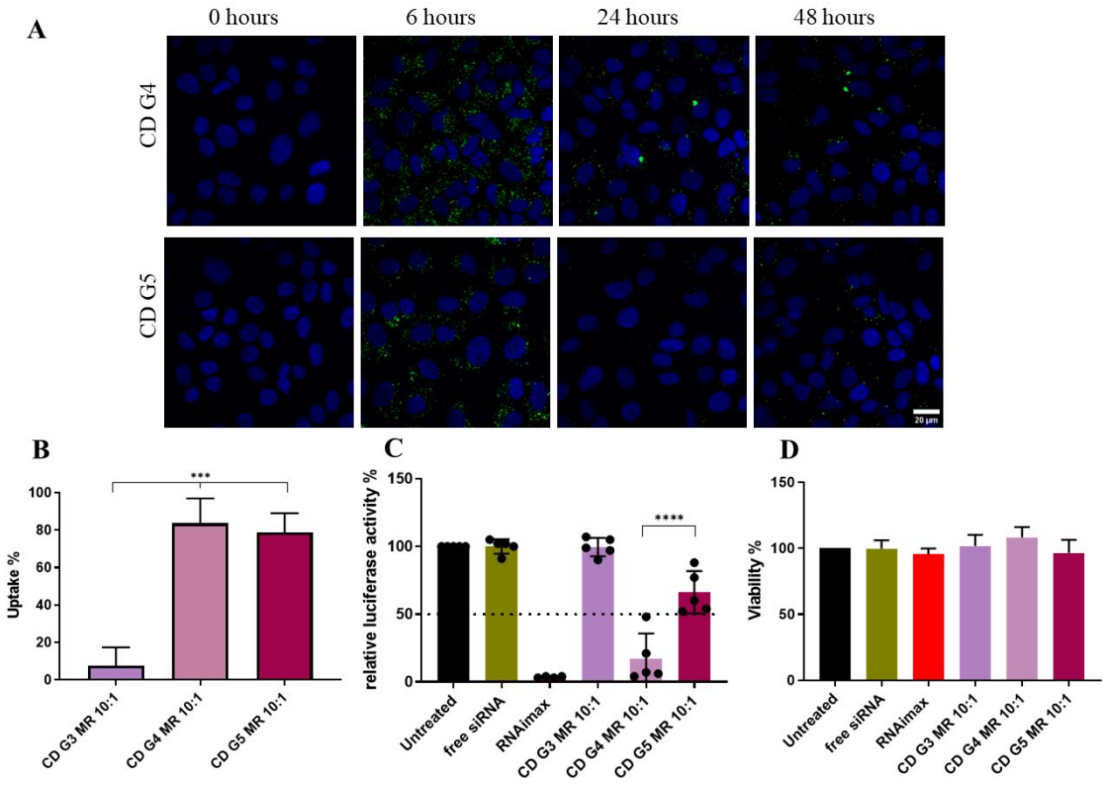

*Figure 3-7 γ-CD NPs in A549-luc cells. (A) Intracellular trafficking of FAM-labelled siRNA incorporated into CD-NP. 1.5 x 10^5 cells were treated with 20 pmol siRNA/well for different time points and imaged with a confocal microscope. (B) Flow cytometry ±SD analysis of cellular uptake of amphiphilic cationic γ-CD-siRNA-complexes at MR10:1 using FAM-labelled siRNA. 1.5 x 10^5 cells were treated with 20 pmol siRNA/well for 6 hours and analysed. (N=3); (C) Analysis of gene knockdown ±SD of γ-CD-siRNA-complexes relative to an untreated group using siLuc. 10^5 cells/well were treated with 20 pmol/well siRNA for 2 days and the luciferase signal was measured (N=5).; (D) Cell viability profiles ±SD of γ-CDs (N=5). One-way ANOVA followed by Tukey's multi comparison test, **** $p < 0.0001$, *** $p < 0.001$.*

The effect of dosage

Having studied the different structures of amphiphilic γ-CDs and their potency, it was logical to try lowering the concentration of siLuc using the most successful formulation CD-G4 MR10:1. It was attempted to reduce the concentration of siRNA per well by half. It could be seen that concentration was not a significant factor with 82% for 500 nM and 91% gene knockdown for 1000 nM (Figure 3-8 A). These results validated CD-G4 as a potent and very promising RNA delivery vector.

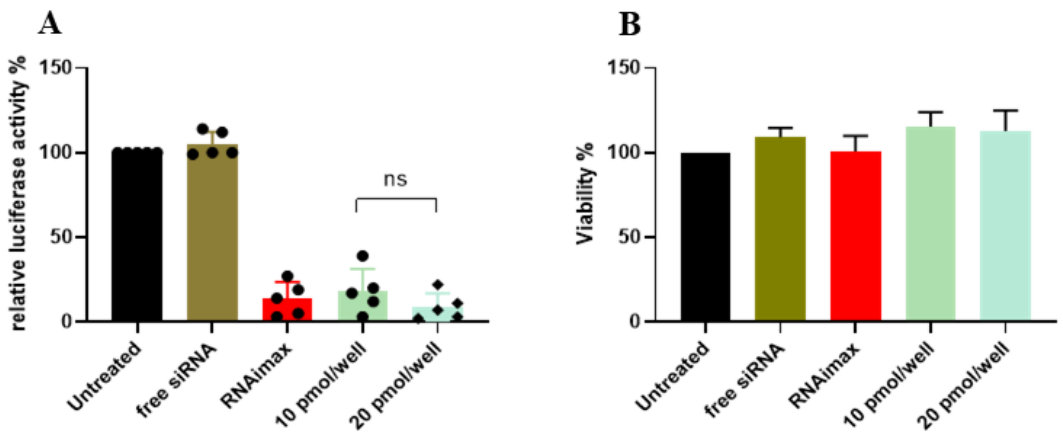

*Figure 3-8 (A) Analysis of gene knockdown ±SD of CD-G4 MR 10:1 relative to untreated group using siLuc. 10^5 cells/well were treated with 10 and 20 pmol/well siRNA for 2 days and the luciferase signal was measured (N=3).; (B) Cell viability ±SD profiles of CD G4 (N=5). One-way ANOVA followed by Tukey's multi comparison test, **** p < 0.0001, ns non-significant.*

In this study, a non-amphiphilic cationic and a variety of amphiphilic cationic CDs were obtained by modification of both native β- and/or γ-CDs. Sub-variations were the number of chains attached to the secondary face of a single glucose unit of the CD scaffold, changes in the linker and the type of terminal amines. The physicochemical characteristics of the engineered compounds and the *in vitro* efficiency were assessed. The first study indicated that *O*2/*O*3-substitution on γ-CD generated better performing candidates with respect to *O*2-substituted β-and γ-CDs. In a second phase of the study, a larger variety of *O*2/*O*3 substituted γ-CDs were tested to further improve the properties of the γ-CD library. CD-G4, a γ-CD derivative functionalized with primary amines through a thiopropyl linker, resulted in gene knockdown up to 80%, even after reducing the dose by half. By comparing the two *O*2/*O*3-substituted γ-CD derivatives the importance of the linker groups on gene knockdown efficiency was revealed. Thiopropyl linker increased gene knockdown ability up to ~40% compared to its triazole counterpart. For further investigation, there

is potential to look at lower dosage levels. This will enable a reduction in the amount of CD needed. Lower dosages are also preferable to reduce possible *in vivo* toxicity.

3.4. Conclusion

Primary amines proved to be successful in this study. A possible explanation might be the proton-influx caused by primary amines into the endosome and the consequent osmotic swelling and disruption, the exchange of triazole with thiopropyl (CD-G4) may support an osmotic effect. The protonation of the amines at the end of the linker can lead to an increase in the distance between the amines because of electrostatic repulsion which may consequently lead to swelling within the endosomal compartment and disruption. The exhaustive derivatization of the secondary side in some γ-CDs increases the charge density and further supports the swelling theory. Similarly, Gallego-Yerga published earlier that primary amines and more flexible linker (triazole versus thiourea) led to improved transfection efficiency in the delivery of pDNA (Gallego-Yerga, Lomazzi, et al. 2014).

Given that cells can exhibit variations in endosome size, which, in turn, can influence the rate and extent of swelling and disruption, as observed in the study by Vermeulen et al. in 2018, it is reasonable to assert that the efficiency of NP delivery may be contingent upon the specific characteristics of the individual cell. In other words, the manner in which NPs are delivered and their effectiveness in cellular uptake could be subject to variability depending on the particular cell type and its endosomal dynamics (Vermeulen et al. 2018).

Further research is underway to assess the ideal formulation across various cell lines, with the goal of determining whether these favourable effects are transferable to

different cell types. This investigation aims to provide deeper insights into the application of CD chemistry concerning cell specificity, potentially paving the way for CD-NP developments tailored to specific diseases, all without the need for costly and labour-intensive targeting ligands.

To improve the stability and reduce the potential for toxicity of CD-NPs *in vivo*, we are exploring co-formulations with PEG-CDs. This strategy holds the promise of enhancing the practicality and safety of CD-NPs in clinical applications. Moreover, for the purposes of commercialisation, γ-CDs present a significant advantage due to their water solubility, which facilitates industrial-scale production and processing. This characteristic simplifies the scaling up of production for practical and cost-effective mass manufacturing.

4. Chapter: Cyclodextrin Dimers and Polymers for siRNA Delivery

Ayse Kont[1], Monique C. P. Mendonça[1], Milo Malanga[2], Kristof Felegyi[2], Andrew Lindsay[3], Michael F. Cronin[1], Mary R. Cahill[4], Caitriona M. O'Driscoll[1]

1 Pharmacodelivery Group, School of Pharmacy, University College Cork, Ireland

2 CarboHyde Zrt., Berlini str., 47-49. Budapest,1045, Hungary

3 School of Biochemistry and Cell Biology, Biosciences Institute, University College Cork, Ireland

4 Department of Haematology and CancerResearch@UCC, Cork University Hospital, University College Cork, T12 XF62 Cork, Ireland

To be submitted

Abstract

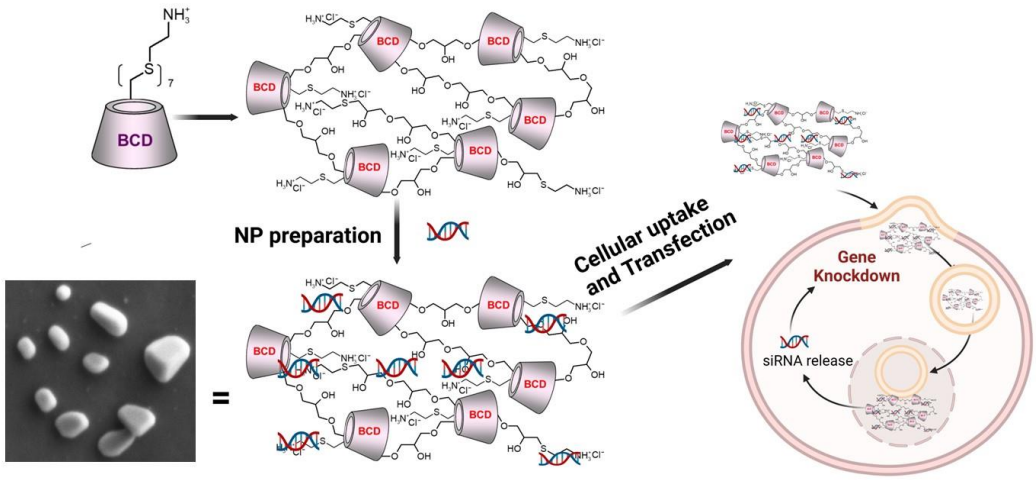

Cyclodextrins (CDs) are cyclic oligosaccharides representing a versatile platform for chemical modifications due to the presence of hydroxyl groups on both the primary and secondary sides of the toroidal (doughnut-shaped) molecular structure. In light of their distinctive properties and readily adaptable structure, CDs have been extensively investigated as non-viral vectors, aiming to achieve efficient delivery of antisense oligonucleotides (ASO) and small interfering RNA (siRNA) (Kont et al., 2022; Mendonça, Sun, et al., 2023). This study evaluates and compares the ability of a quaternary ammonium-appended β-CD-polymer (QA-polymer) and a primary amine-substituted β-CD-polymer (PA-polymer) to complex and deliver siRNA *in vitro*. Both polymers successfully complexed siRNA and formed nanoparticles (NPs) within the size range of 150 to 200 nm at mass ratios (MRs) (cationic polymer:siRNA) of 5:1, 7.5:1, and 10:1. Long-term stability studies demonstrated that the PA-polymer-NP was superior to the QA-polymer-NP at 4 °C, even after cycles of freeze-drying and resuspension. When tested *in vitro* using a reporter gene cell line, A549luc, no cellular uptake was detected with the QA-polymer. In contrast, the PA-polymer demonstrated significant cellular uptake, reaching up to 40% uptake, with 40% gene knockdown while maintaining adequate cell viability (≥80%). In summary, these results indicate that the chemical structure of the β-CD-polymer influences interactions at the cellular level, suggesting that polymers incorporating primary amines hold promise for future development as biomaterials for siRNA delivery.

Keywords: Cationic cyclodextrin polymers, functional amines, nucleic acid delivery, siRNA

4.1. Introduction

Polymers, a versatile class of advanced materials, have been extensively applied in several areas, including textile, nutrition, transportation, buildings, energy, and biomedical fields (Namazi 2017). Due to their versatility and multifunctionality, polymeric biomaterials have emerged as promising vectors for gene therapy. These macromolecules can be systematically categorised into two groups: linear and branched. Various linear polymers, including polyethyleneimine, amino polyesters, and their branched counterparts, such as poly(amidoamine), polylysine, and polypropylene imine have been extensively investigated as gene delivery systems (Khan et al. 2018; Kowalski et al. 2018; Kumar et al. 2021). Polymer synthesis is a sophisticated process wherein large molecules with repeating structural units are created through chemical bonding. There are several polymerisation methods, each with its applications. One of them is condensation polymerisation, which involves the formation of small molecules as byproducts during the polymerisation process, resulting in the creation of macromolecules (Crini et al. 1998). The properties of the polymer can be altered by incorporating selected functional groups before the polymerisation (pre-branching modification) or through the modification of the polymerised structure (post-branching modification).

Cyclodextrins (CDs), cyclic oligosaccharides with several hydroxyl groups available for modification, are naturally occurring monomers largely used in the preparation of dimers or polymers.

The dimerisation process typically involves the formation of a covalent bond between CD units, resulting in a molecule with distinct physical or chemical properties compared to the initial building block; these differences may manifest in terms of structure, function, or stability. In the specific case of CDs, the outcome of the

dimerisation process can give rise to a CD dimer, where the CD units are interconnected through the primary face, the secondary face, or a structure in which the primary side of one CD unit is linked to the secondary side of the other (or vice versa). The relative orientation of the CD units concerning the connecting linker becomes crucial, particularly in the design of asymmetric dimers (Lebedinskiy, Lobaz, and Jindřich 2022).

Synthetically CD dimers are formed by connecting the CD units with a bifunctional linker or, for example, *via* click reaction using copper-catalysed azide-alkyne cycloaddition. (Lebedinskiy et al. 2022). A study showed the benefit of secondary-face dimerised CDs in the selective extraction of 7-ketocholesterol in the presence of cholesterol (Anderson et al. 2021). CD dimers offer enhanced properties compared to the corresponding CD monomers, such as increased binding affinity, improved stability, or tunable cavity sizes so they easily found applications in drug delivery, materials science, and supramolecular chemistry.

Within the majority of polymeric systems, CDs function as supplementary components to enhance drug delivery systems through the mitigation of immunotoxicity, the formation of inclusion complexes with guest molecules, and by serving as linker components in the primary polymer structure. (Haley et al. 2020). Among the multitude of different types of CD-based polymers we can mention: cross-linker initiated polymers, star-shaped polymers, and grafted CD in which the CDs are either covalently attached to a polymer chain or build inclusion complexes with lipophilic functionalities along the polymer (Liu et al. 2021). CD polymer synthesis includes three main strategies: CD-attachment to pre-synthesised polymers, polymerisation reaction with acrylic groups resulting in linear polymers, and finally, cross-linking reaction using bi- or multifunctional agents such as biepoxides,

diisocyanate or epichlorohydrin. Utilising cross-linking in polymerisation reactions leads to the formation of three-dimensional structures, making them advantageous for applications in gene delivery therapies (Escobar et al. 2023).

CD-containing polymeric systems have been used as drug delivery systems for chemotherapeutics in various cancers, including brain (Y. F. Chen et al. 2019), bone (Ahmadi et al. 2020; Plesselova et al. 2021), and breast cancer (Jia et al. 2021). In addition, polymers formed using only CDs have also shown promising results as drug delivery systems *in vitro* in lung and liver cancer cells (Bognanni et al. 2021), and colorectal cancer cells (Akkın et al. 2022). A recently published paper by the Trotta group showed the successful delivery of mRNA in local cancer immunotherapy *in vitro* and *in vivo* (Monfared et al. 2023).

In this study, we synthesized both a β–CD monomer (QA-monomer) and a secondary-faced β-CD dimer-core (QA-Dimer), appended with quaternary ammonium groups. Additionally, two β-CD-based polymers were decorated with primary amines (PA-polymer) or with permanently charged quaternary ammonium groups (QA-polymer). A comparative study assessing the ability of the monomer, dimer, and polymers to complex siRNA and deliver to A549luc, a lung cancer cell line with a reporter gene, was undertaken.

4.2. Materials and Methods

4.2.1. Materials

Fluorescent luciferase-siRNA (Sense Strand 5’ CGACAAGCCUGGCGCAGUA 3’) was purchased from Dharmacon. MISSION® siRNA Fluorescent Universal Negative Control #1 6-FAM (Fluorescein amidite) was

bought from Sigma Aldrich (Wicklow, Ireland). All other materials are from Sigma Aldrich (analytical grade), if not mentioned otherwise. Sodium hydroxide (reagent grade, ≥98%, pellets (anhydrous)), glycidyltrimethylammonium chloride (technical, ≥90% (calc. based on dry substance, AT)), cysteamine hydrochloride (≥97.0% (RT)), and triethylamine (≥99.5%).

4.2.2. CD synthesis and nanoparticle preparation

4.2.2.1. Preparation of CD derivatives

QA-Monomer

β-CD (11.35 g, 10 mmol) was suspended in 80 ml of water, and the addition of NaOH (40 mmol, 1.6 g) under vigorous stirring resulted in prompt solubilization. The colourless solution was then cooled to 5 °C, and glycidyltrimethylammonium chloride (60 mmol, 8 ml) was added dropwise. The reaction mixture was stirred at room temperature overnight. The next day, the reaction mixture was heated at 50 °C for 4 hours, then cooled, neutralized with HCl, concentrated under reduced pressure using a rotavapor, and finally extensively dialyzed for 24 hours (cut-off membrane: 100-500 Dalton). The concentrated solution was evaporated to dryness (yielding 15 g). The average degree of substitution for the quaternary ammonium moiety with respect to the CD unit was estimated to be between 3-4 based on the integration of the ^{1}H-NMR spectrum.

QA-Dimer

The quaternary ammonium appended β-CD dimer was kindly donated by Cyclarity Therapeutics and prepared according to the procedure reported in WO2020142716A1.

QA polymer

The QA-polymer was prepared in two steps through post-branching modification. Water-soluble β-CD polymer was synthesized following established procedures, wherein β-CD was initially solubilized with an excess of NaOH, and subsequently cross-linked with epichlorohydrin (Agnes et al. 2022). The QA-polymer was derived from the previously prepared macromolecule by reacting it with glycidyltrimethylammonium chloride in the presence of NAOH in water, resulting in a product with an average degree of substitution of 3.5 (Thomsen et al. 2017).

PA-polymer

The PA-polymer was prepared through iodination of the neutral CD polymer according to Vilsmeyer-halogenation (Malanga et al. 2014) followed by nucleophilic substitution with cysteamine hydrochloride in DMF with triethylamine. The desired product was obtained in good yield with an approximative degree of substitution of 7.

4.2.2.2. Analysis of the CD derivatives

NMR spectra were recorded in deuterated chloroform-d, methanol-d4, or water-d2 on Varian VXR-600 at 400 or 600 MHz instrument at 295 K. MALDI-TOF mass spectra were recorded on a Bruker Microflex LRF system. The microflex LRF operated in positive ion mode using the linear detector. Ion generation was achieved using a 60 Hz N_2 -Cartridge-Laser including variable power attenuator and UV optics. The laser operated at 337 nm, and 2,5-dihydroxybenzoic acid (DHB) was used as the matrix.

4.2.2.3. Nanoparticle preparation

CD-polymer was resuspended in RNase-free water at 0.25 mg/ml using a probe sonicator (Branson Sonifier 250) for 15 mins. NPs were prepared by incubating with

siRNA at 450 rpm for 30 mins at 25 ℃ in a thermomixer. The final siRNA concentration was 1000 nM.

4.2.3. Physicochemical characterisation

4.2.3.1. Size, Poly dispersity index and Zeta potential

Particles were characterised by dynamic light scattering (DLS) (Zetasizer Nano-ZS, Malvern Instruments, Malvern, UK). Particle size (Z-Average) and poly dispersity indices were determined with a non-invasive backscatter system (scattered light angle of 170°, narrow size cuvette). Zeta potential was assessed with folded capillary cells (DTS1070) with electrophoretic mobility (forward scatter angle of 12.8°, monomodal mode). DLS settings were protein as material (refractive index 1.450 and absorption 0.001), and water as dispersant (viscosity 0.8872 cP, refractive index 1.330) at 25 ℃.

4.2.3.2. Complexation efficiency

1%-Agarose gel was prepared, containing SafeView (NBS Biologicals, Huntingdon, UK), a Nucleic Acid Stain (0.06 µl/ml). BlueJuice™ Gel Loading Buffer (10X) (Invitrogen, Waltham, MA, USA) was added to the samples. Running conditions were 90 V for 45 mins with Bio-Rad, PowerPacBasic (Hercules, CA, USA) in Tris/Borate/EDTA buffer. The gel was imaged under UV with Uvitec CambridgeMini HD.

4.2.3.3. Encapsulation efficiency

Encapsulation efficiency was investigated with Quant-iT RiboGreen™ RNA Assay kit (Invitrogen, Invitrogen, Waltham, MA, USA). The interaction between unbound siRNA and fluorescent RNA dye is quantified after NP incubation (Jiang et

al. 2020) and measured in a black 96-well microplate with a Tecan Spark® (Männedorf, Switzerland) microplate reader at 485 nm excitation wavelength and 535 nm emission wavelength (Gain 55, top reading). A calibration curve with $R^2 > 0.995$ was used to quantify free siRNA (x-axis: siRNA concentration, y-axix: fluorescence signal).

4.2.3.4. Determination of pKa

Buffer at different pH (0.1 M buffers from pH 4–12 in increments of 0.5; pH 4–6.5 citrate buffer, pH 7–11.5 Trizma® buffer), NPs and 2-(p-toluidino)-6-naphthalene sulfonic acid (TNS) (6 µM TNS/well) were combined in a black 96-well plate. The final concentration of NP per well was 10% (v/v). TNS signals were measured using a Tecan Spark® (Männedorf, Switzerland) microplate reader at an excitation of 340 nm and an emission of 485 nm (top reading). After sigmoidal interpolation, the inflection point (LogIC50) defined the apparent pKa of the siRNA-CD-polymer-complex (Uebbing et al. 2020).

4.2.3.5. Focused ion beam scanning electron microscopy

50 µl sample was dried onto a polished Silicon wafer overnight at room temperature and subsequently analysed with TESCAN AMBER X - FIB-SEM at 2 keV using an Everhart–Thornley detector.

4.2.3.6. Heparin release

Heparin (10 mg/ml) was added to NPs (final Heparin concentration 20%) and incubated at 37 °C. Sample collection was performed at several time points, and frozen until ready to be run on Agarose. Samples were combined with BlueJuice™ Gel Loading Buffer (10X) (Invitrogen, Invitrogen, Waltham, MA, USA) and loaded onto

the1%-Agarose gel. The gel was run at 90 V for 30 min. siRNA release was detected with UV.

4.2.3.7. Serum stability

NPs were incubated with 50% fetal bovine serum (FBS, heat-inactivated) (Aylward 2019) at 37 ℃ for 24 hours. Samples at different time intervals and stored in the freezer until ready to be imaged. After thawing, samples were treated with heparin (10 mg/ml, 20% heparin in final sample) for 75 min at room temperature. BlueJuice^{TM} Gel Loading Buffer (10X) (Invitrogen, Invitrogen, Waltham, MA, USA) was combined with samples and subsequently loaded onto 1% Agarose gel, that contained SafeView (NBS Biologicals, Huntingdon, UK). Running conditions were 90 V for 30 min (Bio-Rad, PowerPacBasic Hercules, CA, USA).

4.2.4. Cell culture

Cell culture experiments were performed in A549-luc cells, epithelial cells from a 58-year-old male patient with lung cancer (ATCC (American Type Culture Collection)); donated by Dr. Piotr Kowalski. Upon thawing, cells were cultured in Dulbecco's Modified Eagle Medium (DMEM) with 10% FBS (heat-inactivated), 1% Penicillin-Streptomycin, and 8 µg/ml Blasticidin at 37 ℃ and 5% CO_2. Before the experiments, the FBS concentration was decreased to 2% while other excipients were kept the same.

4.2.4.1. Cellular uptake

Before the day of transfection, cells were seeded in a 24-well plate (1.5 x 10^5 cells/ well, DMEM supplemented with 10%FBS and 1%Penicillin/Streptomycin). The media was changed to low-FBS media (2%FBS and 1%P/S). Transfection was

conducted with FAM-siRNA for 6 hours (20 pmol siRNA/well). Following incubation, trypsinised cells were collected and centrifuged at 1500 rpm for 5 min at 4 ℃. Subsequently, cells were washed with PBS, resuspended in PBS and finally transferred into polystyrene round bottom tubes (Becton Dickinson). Cellular uptake was determined with BD CELESTA Facs Analyser (10,000 events). Data was analysed using FlowJo 10.

4.2.4.2. Toxicity assay and Gene knockdown

1 x 10^4 cells/well were plated in a white 96-well plate 24 hours prior to the day of transfection. Full growth media was replaced with low-FBS media and treated with NP at 20 pmol FLuc siRNA per well (final volume per well: 100 µl/well) for 6 hours. After 6 hours of incubation, the media was replaced with full growth media and incubated for a further 18 hours. Firstly, cell viability was evaluated with CellTiter-Fluor™ Cell Viability Assay. After 35 mins incubation with cell viability dye in the incubator (5% CO_2, 37°C), the plate was measured in Tecan Spark® (Männedorf, Switzerland) microplate reader at an excitation of 380 nm and an emission of 535 nm (top reading). Gene knockdown was determined with ONE-Glo™ EX Luciferase Assay (Promega, Madison, Wisconsin, United States) according to the manufacturer's guidelines. The plate reader (Tecan Spark®) setting was set in luminescence mode. The luciferin signals were normalized against the average of the cell viability of the control group, as follows: [luciferin signal / (viability signal/average of viability signal of control group)].

4.2.4.3. Intracellular trafficking

To confirm intracellular uptake, confocal images were undertaken. Twenty-four hours in advance of transfection, 1.5 x 10^5 cells/ well were seeded in complete media on glass coverslips in a 24-well plate. After replacing high-FBS media with 2%-

FBS media, cells were treated with 20 pmol/well FAM-siRNA-NP, and incubated for 0 h, 6 h, 24 h, and 48 h. Coverslips were incubated with DAPI for 30 mins and mounted with Mowiol Mounting Media on slides. Confocal images were obtained with Zeiss LSM510 META confocal microscope (Carl Zeiss, Jena, Germany) using a 63× objective.

4.2.5. Stability testing

4.2.5.1. Storage stability

Following storage at 4-8℃ for two months the stability of the NPs was evaluated by monitoring changes in size and polydispersity (PDI) using DLS.

4.2.5.2. Lyophilisation – effect on NP integrity

NPs were lyophilised at 400-450 torr for 24 hrs, and the condenser temperature was set at -80℃. The lyophilised NPs were resuspended in RNase-free water and analysed for comparative measurements by DLS.

4.2.6. Statistical analysis

GraphPad Prism 8 was used for statistical analysis. One-way ANOVA followed by either Tukey's multi-comparison or Sidak's multi-comparison post hoc tests were used. Statistical significance was considered when **** $p < 0.0001$, *** $p < 0.001$, ** $p < 0.01$, and * $p < 0.05$.

4.3. Results and Discussion

4.3.1. CD-derivative and nanoparticles

Initially, the QA-CD-monomer and the QA-CD-dimer (Figure 4-1 A, B) compounds were examined for their capacity to form NPs using mass ratios (MRs) of 5:1, 7.5:1 and 10:1 (QA-dimer:siRNA). In both cases, incomplete complexation of siRNA was observed (Figure 7-10). Large particle sizes > 3500 nm with high PDI values (~ 1) were observed, indicating high polydispersity. In an attempt to successfully form NPs, the MR was increased to 100:1 and 200:1. At MR100:1, charge measurements indicated an almost neutral charge for the QA-monomer NPs while a slightly higher value, 3mV, was observed for the QA-dimer NPs. Increasing the MR to 200:1, led to a marginal increase, up to 5 mV for the QA-dimer (Figure 4-1 B) with no change detected in the case of the monomer. The QA-monomer failed to bind the siRNA, and while partial binding was achieved with the dimer it was considered inadequate and consequently was not investigated further (Figure 4-1 C).

Two β-CD-polymers were synthesised from β-CD monomer using epichlorohydrin as cross-linker and post-modified with either primary or quaternary amines, resulting in a QA-β-CD-polymer (Figure 4-2 A) and a PA-β-CD-polymer (Figure 4-2 B). Due to their nature, CD-polymers can self-assemble, similarly observed in other polymeric systems (Foster et al. 2020). Amine groups play an important role in the complexing of siRNA into NPs and contribute to the apparent surface pKa (Mendonça, Kont, et al. 2023). This comparative approach allows investigation of the influence of the different amine groups on the performance of the β-CD-polymers as a non-viral vector.

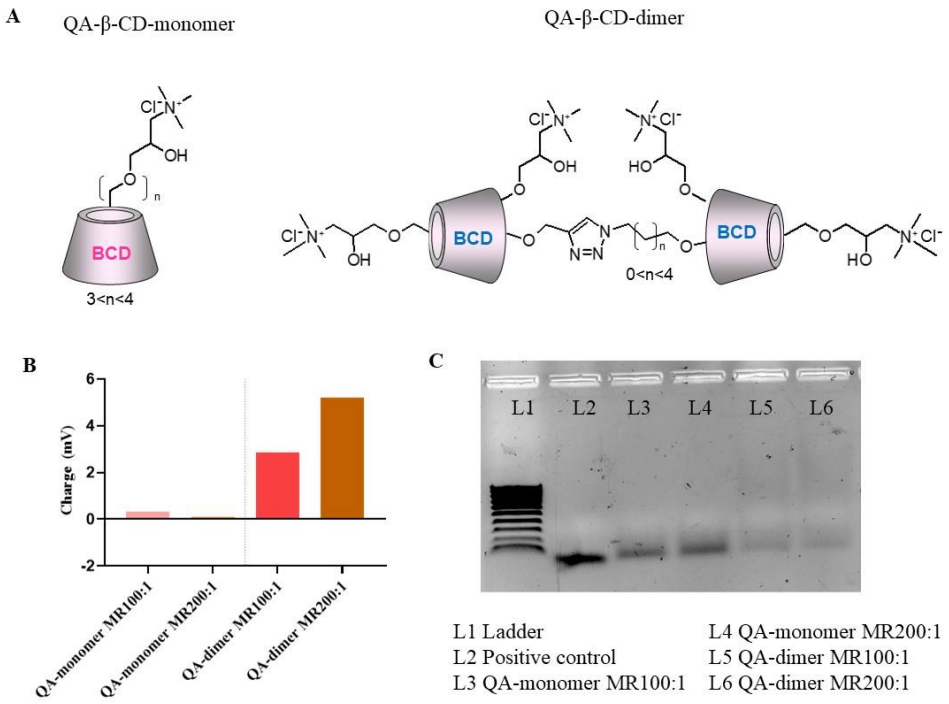

Figure 4-1 (A) Chemical structure of the QA-modified β-CD-monomer and dimer.; (B) NP charge measurement (DLS), 1000 nM siRNA; (C) 1%-Agarose complexation for NP with monomer and dimer at 1000 nM siRNA, positive control is unencapsulated siRNA.

4.3.2. Physicochemical characterisation of β-CD-polymer-nanoparticle

	β-CD-Monomer	β-CD-Polymer Cross-linked with epichlorohydrin	Physicochemical properties
QA-polymer	Quaternary ammonium 3<n<4		- Solubility: soluble in water - Working solution (0.25g/l) pH: 6.8 - Working solution (0.25g/l) charge: 33.2 mV
PA-polymer	Primary amine	Cysteamine=CYS	- Solubility: soluble in water - Working solution (0.25g/l) pH: 6.6 - Working solution (0.25g/l) charge: 50.2 mV

Figure 4-2 β-CD-polymer structure and physicochemical properties.

NPs were formulated with siRNA for both polymers at the three MRs. The particle sizes ranged between 150 nm and 200 nm, with higher PDI (0.4) for the PA-polymer NPs compared to the QA-polymer NPs (0.2) (Figure 4-3 A). With an increase in MR from 5:1 to 10:1 a slight but statistically insignificant increase in charge was detected with the PA-polymer NPs (34 to 37 mV) versus the QA-polymer NPs (26 to 33 mV) (Figure 4-3 B). The higher charge in the PA-polymer is due to the higher substitution level (seven positive charges per ring) compared to the QA-polymer (three positive charges per ring). SEM images for both QA- and PA-polymer-NPs at MR10:1 show a similar non-spherical, cuboid shape (Figure 4-3 C, D) which can be advantageous, for example in avoiding immune recognition or improve uptake (Kapate, Clegg, and Mitragotri 2021).

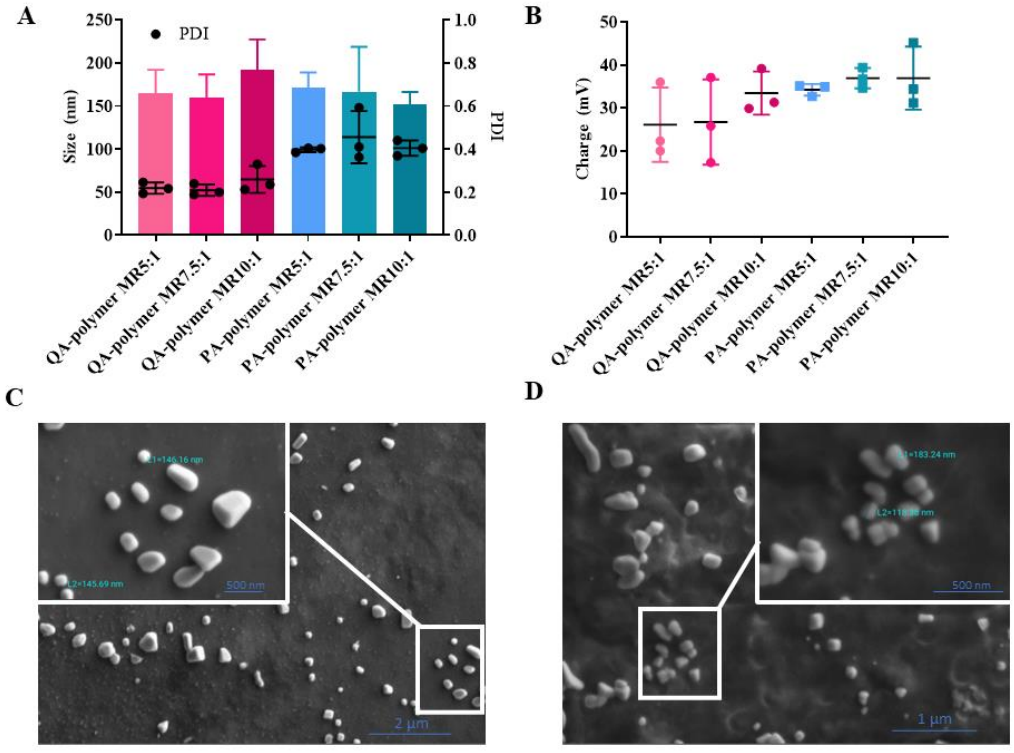

Figure 4-3 Physicochemical characterisation of polymeric NPs (A)Size ±SD and PDI ±SD by means of DLS. (N=3).; (B) Charge ±SD results measured with DLS. (N=3). One-way ANOVA followed by Tukey's multi-comparison test; (C) SEM-image of QA-polymer-NP MR10:1, magnification 39.9 kx, zoom-in magnification 138 kx; (D) SEM-image of PA-polymer-NP MR10:1, magnification 75 kx, zoom-in magnification 266 kx.

Agarose-gel electrophoresis indicated that full binding of siRNA was achieved with the PA-polymer at all MRs. In the case of the QA-polymer-NP binding was incomplete at the lower MRs and showed improvement at the higher MR10:1 (Figure 4-4 A). Quantification of the encapsulation efficiency confirmed the observed binding behaviour (Figure 4-4 B). While PA-polymer encapsulates ≥96% of the NA, the QA-polymer showed only 47% for MR5:1, 69% for MR7.5:1 and 75% for MR10:1, presenting a significant increase (**** $p < 0.0001$) from MR 5:1 to MR7.5:1. In an attempt to increase the encapsulation efficacy for the QA-polymer, the MR was further increased to MR15:1 and MR20:1, however, no significant improvement was detected (80%) (Figure 4-4 C). An analogous pattern was noted in a separate study involving a CD-polymer featuring quaternary ammonium groups, introduced through choline chloride. This polymer exhibited 85% encapsulation efficiency with pDNA at MR25:1 (Monfared et al. 2022).

The acid dissociation constants (pKa) of both the PA-polymer stock and the resulting NPs were similar, pKa ~9 (Figure 4-4 D). These results suggest that the PA-polymer will be predominantly ionised in the endosome (pH 5.5-6), the cytosol (pH 7.2), and the blood circulation (pH 7.4). While for the uptake and endosomal release, positively charged NPs are favourable, toxicity in the blood circulation *in vivo* is likely to be a concern. To help address this, the number of positive charges can be selectively reduced as needed, due to the high versatility of the synthetic approach. Ultimately, the incorporation of a predetermined number of anionic moieties into the polymer (e.g., sulfobutyl groups) could be utilized to systematically decrease the overall positive net charge, thereby modulating Coulombic forces and enhancing the toxicity profile of the construct (Godinho et al. 2014; Martins et al. 2019). A pKa for the QA-polymer was not evaluated, as the quaternary ammonium is permanently charged, and

hence, not a candidate for the TNS assay that measures changes in the amount of freely available positive charges with a change in pH (Uebbing et al. 2020).

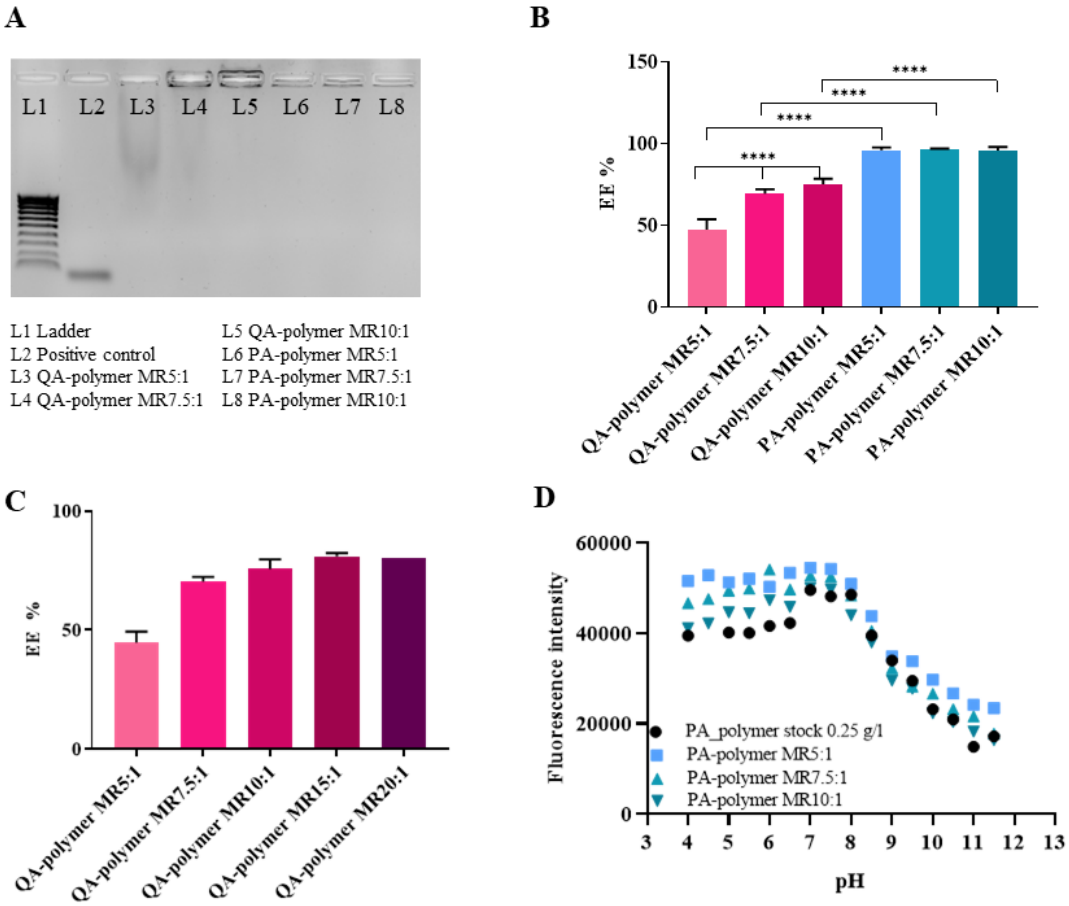

*Figure 4-4 Physicochemical characterisation (A) complexation efficiency in 1% Agarose gel.; (B) Encapsulation efficiency ±SD of NPs was quantified with Quant-iT RiboGreenTM RNA Assay kit, N=3.; (C) Encapsulation efficiency ±SD assessed at higher MR of QA-polymer. (N=3).; (D) TNS assay to determine pKa of PA-polymer stock and NPs at MR 5:1, 7.5:1, 10:1.; EE= Encapsulation efficiency. One-way ANOVA followed by Tukey's multi-comparison test **** $p < 0.0001$.*

In the development of NPs containing NAs, it is important to assess the stability of the siRNA under physiological conditions. Most NP for cancer therapy are administered intravenously (Ferrari et al. 2018), and are exposed to high protein concentrations (Aylward 2019), that could inactivate the NA through degradation or aggregation. After the successful formulation of the NP, 50% FBS was added to the NP (imitating blood protein concentration (Aylward 2019)), and the stability was

evaluated following incubation for 24 hours at 37°C. The PA-polymer NPs were stable over 24 hours (siRNA bands constant), indicating the ability of the complex to protect the siRNA (Figure 7-11). In contrast, the QA-polymer NP was only stable at the higher MR10:1; lower MRs showed weakened siRNA bonds at 24 hours (Figure 7-11).

Although successful complexation and stability are crucial requirements to achieve effective delivery by overcoming the biological barriers (nucleases in blood circulation, clearance, cellular membrane), the release of the siRNA into the cytoplasm at the target site is necessary to achieve successful gene knockdown (Gujrati et al. 2014; Itakura et al. 2016). Conducting a heparin release study revealed that both polymers promptly released their siRNA cargo upon contact with heparin (Figure 7-12).

4.3.3. Uptake and Gene knockdown

The effects of the polymer functional groups, quaternary ammonium versus the primary amine, on the cellular uptake, gene silencing, and cytotoxicity of the β-CD-polymers NPs were investigated *in vitro* using A549luc cells, an epithelial lung cancer cell line expressing the luciferase reporter gene.

Cellular uptake was determined using FAM-labelled siRNA and measured by flow cytometry and confocal microscopy. The uptake of the PA-polymer ranged between 24-40% relative to untreated control; MR5:1 displaying 24 ±23%, MR7.5:1 33 ±19% and MR10:1 40 ±14%. The increase was statistically nonsignificant (Figure 4-5 A). In contrast, no uptake was detected with the QA-polymer. Similar behaviour was reported by Akkın et al. where a QA-polymer failed to increase the membrane permeability of interleukin-2 and 5-Fluorouracil loaded in nanoplexes across Caco2-cells (Akkın et al. 2022).

The uptake of the PA-polymer NPs was further investigated using confocal microscopy. Cellular uptake and dispersed cytosolic siRNA distribution occurred as early as 6 h post-transfection (Figure 4-5 B), in accordance with the flow cytometry results. The fluorescence signal from FAM-siRNA remained detectable at 24 hours across all MRs. However, after 48 hours, a decrease in fluorescence was observed particularly at the lower MR5:1 and 7.5:1.

The gene silencing efficiency of the PA-NPs was investigated using luciferase siRNA (Figure 4-5 C). Increasing the MR from 5:1 to 10:1 significantly decreased the expression of luciferase from 97 ±24% to 59 ±7% (*** $p < 0.001$), consistent with the higher cellular uptake previously detected at the higher MR10:1. Cell viability following incubation with all MRs of the PA-NPs was above 80% (Figure 7-13).

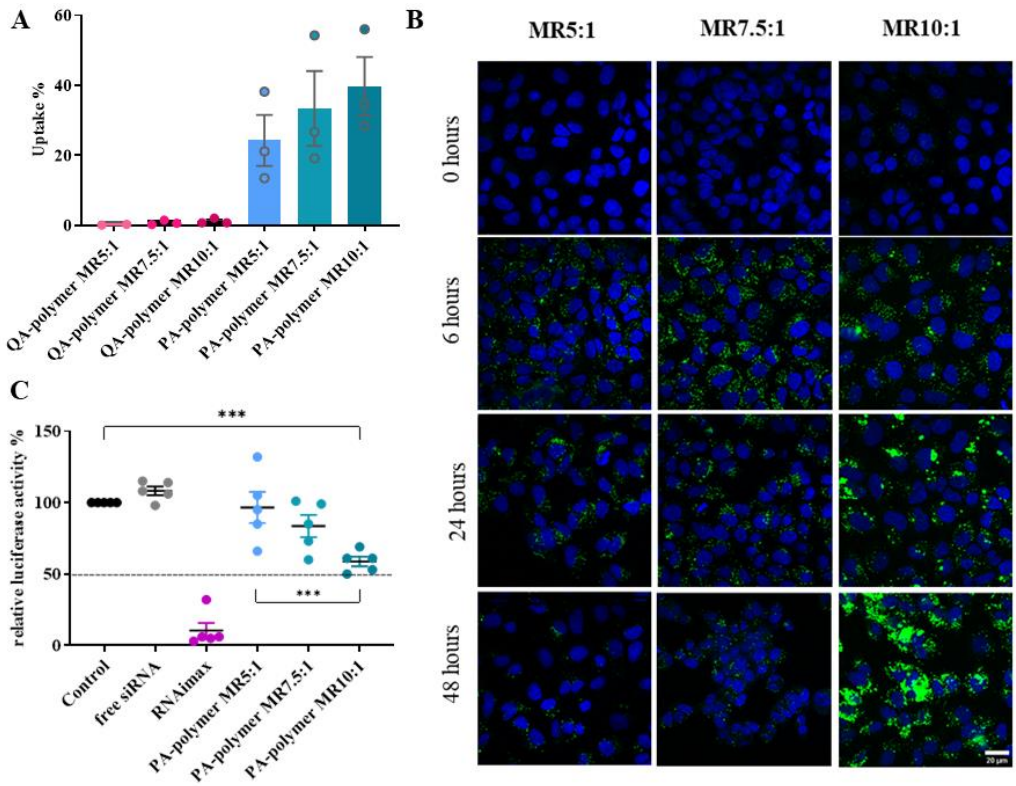

*Figure 4-5 In vitro cell culture studies of the polymer NPs. (A) Flow cytometry for all MR of QA- and PA-polymers at 6 hours uptake of free FAM-siRNA and FAM-siRNA-NP relative to untreated control % ±SD, N=3.; B) Confocal microscopy of the PA-polymer at all three MRs using green FAM-labelled siRNA and blue nuclei staining. Scale bar= 20 μM.; (C) Gene knockdown ±SD of all three MRs of PA-polymer. One-way ANOVA followed by Tukey's multi-comparison test *** $p < 0.001$. N=5.*

In summary, results show that the NPs formulated using the polymer modified with primary amines were superior in terms of stability, uptake, and gene knockdown. This is in agreement with previous work in our group (3. Chapter), where an amphiphilic γ-CD monomer modified with a primary amine on the secondary side obtained up to 80% gene knockdown in A549luc cell line (10 pmol/well). However, in the design of polymeric CDs, additional factors can be considered, including the choice of the crosslinking agent which may influence both the number of hydrophobic sites, and which in turn can affect the self-assembling behaviour, the ability to cross bilayer membranes, and the exposure of hydrophilic sites necessary to interact with the NA.

4.3.4. Shelf-life stability

The stability of the NPs will influence the shelf-life and the distribution conditions of the product. Thus, the long-term stability of NPs formulated in water using both the QA- and PA- polymers was evaluated by monitoring the size and PDI over time at 4 ^{o}C. As shown in Figure 4-6, the size of the PA-polymer NPs remained unchanged over two months (size <200 nm, PDI 0.4-0.6). The statistically non-significant increase in PDI from 0.4 to 0.6 was observed for PA-NP MR7.5:1. On the contrary, the QA-polymer NPs increased two- to three-fold in size from <200 nm to 400-600 nm (MR5:1 and MR 7.5:1, * p <0.05) and PDI from ~0.2 to 0.4-0.7 (MR5:1 and MR 7.5:1, *** p < 0.001) indicating particle aggregation which is an unwanted effect in pharmaceutical formulations and is associated with colloidal instability (Phan and Haes 2019). NP characteristic changes over time have been associated with alterations in *in vitro* and *in vivo* performance. Albanese et al. demonstrated that aggregated NPs show unpredictable cellular uptake profiles *in vitro*, specifically a

decrease in uptake was seen in HeLa (cervical cancer cells) and A549 cells (non-small cell lung cancer cells), whereas an increase was detected in breast cancer MDA-MB 435 cell (melanoma cells) (Albanese and Chan 2011). *In vivo* monitoring suggests that smaller-sized particles survive longer in circulation (Wei et al. 2018). Overall, aggregation can alter in *vitro* and *in vivo* behaviour affecting dose, uptake, cytotoxicity, pharmacokinetics, and biodistribution (Moore et al. 2015).

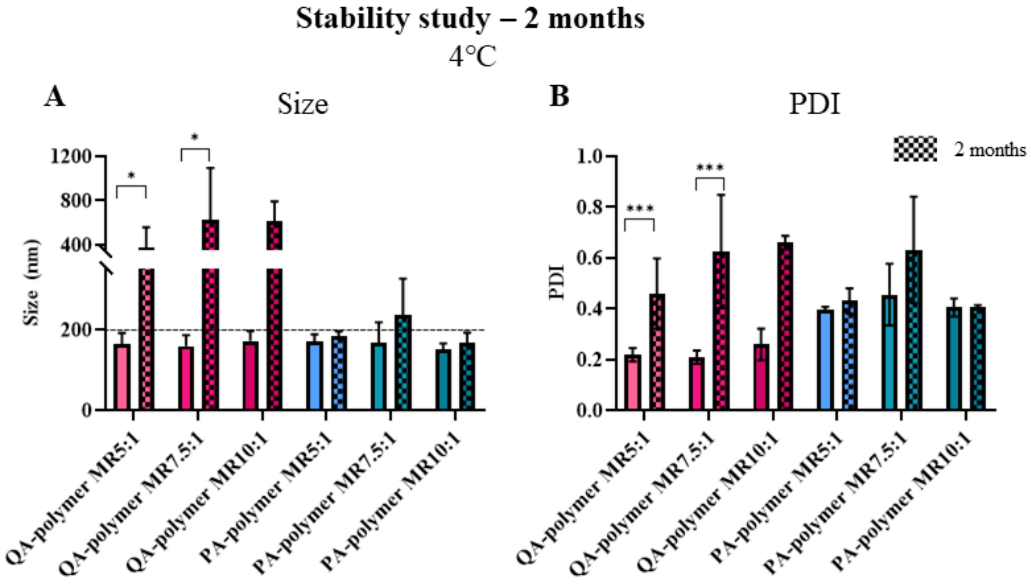

*Figure 4-6 Stability following storage for 2 months at 4°C versus freshly prepared controls. Changes in particle characteristics ±SD was monitored with DLS. (A) Size.; (B) PDI. One-way ANOVA followed by Sidak multi-comparison test. *** $p < 0.001$, and * $p < 0.05$.*

In the final dosage form, opting for lyophilised state may be beneficial as it can prevent microbial growth, and decrease chemical and physical degradation thereby substantially enhancing long-term storage stability (shelf-life). The NPs formulated using both QA- and PA- polymers were lyophilised (Figure 7-14) and following resuspension the stability of the resulting product was assessed by monitoring size changes by DLS. Similar to the storage stability results above (Figure

4-6), the QA-polymer-NPs, following redispersion, showed an increase in PDI which indicates a heterogeneous population of NPs (Figure 4-7 A, Figure 7-15 A, B). In contrast, the PA-polymer-based NPs demonstrated a stable profile with similar size and PDI values pre and post lyophilisation (Figure 4-7 B, Figure 7-15 C, D). Before translating this freeze-dried product to the clinic, it will be essential to ensure the bioactivity is retained.

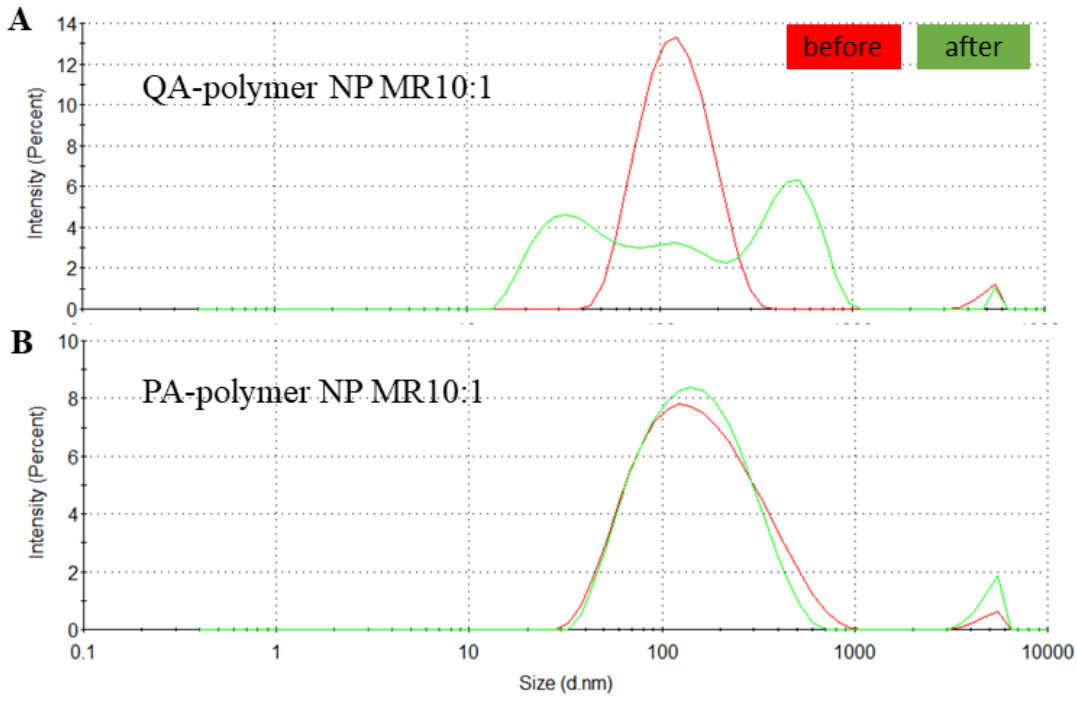

Figure 4-7 DLS measurements of QA- and PA-polymer-based NPs MR10:1 pre and post lyophilisation and reconstitution. NP were prepared at 1000 nm siRNA concentration.

4.4. Conclusion

The beneficial structure of CDs with hydroxyl groups available for chemical modifications was used to synthesise β-CD monomer, dimer, and polymers for the delivery of siRNA *in vitro*. Non-amphiphilic monomer and dimer that contained a quaternary ammonium were synthesised, however, due to insufficient encapsulation

of siRNA no further investigation of monomer and dimer was performed. Subsequently, two polymers functionalised with primary amine (PA-polymer) versus quaternary ammonium groups (QA-polymer) were synthesised and formulated with siRNA. The resulting NPs were compared in terms of physicochemical characteristics, *in vitro* cellular delivery, and gene silencing efficiency. The PA-polymer-NPs displayed superior stability, cellular uptake, and gene knockdown. The positive charge of the PA-NP (~35 mV) presents potential for toxicity *in vivo*, this can be attenuated by reducing the number of positive charges selectively or incorporation of anionic moieties into polymer and thereby reduce immune recognition, early elimination, and toxicity (Shi et al. 2021). In addition, to enable the uptake of QA-NP or further improve PA-NP uptake, the attachment of lipid groups to form amphiphilic polymers, or the incorporation of targeting ligands is possible and could be explored (Almeida et al. 2021).

In summary, this data indicates that CD-based polymers modified with primary amines are promising biomaterials for siRNA delivery and the benefits of this functional group corroborate previously published data for CD monomers.

5. Chapter: General Discussion

5.1. Introduction

In 2018 the first non-viral siRNA drug product was approved by the FDA (Patisiran). Later RNAi emerged as a life-saving therapeutic alternative to viral vaccines during the COVID-19 pandemic. These incidences boosted the trust of scientific and non-scientific audience to accept non-viral delivery of NAs as a successful therapy approach. The prompt adaptability of LNPs as a delivery system to this acute crisis paved the way for intensification of research in this field. While Patisiran is administered intravenously (IV), COVID-19 vaccines are injected intramuscularly (IM). LNPs end up in the liver after IV administration due to their lipophilic character, which is desirable in disease related to the liver. However, more complex diseases such as cancer require the delivery to other sites in the body. This increased research interest in developing other delivery biomaterials such as CDs. CDs are generally recognised as safe and have low immunogenicity and biocompatibility. The chemical versatility of CDs allows the synthesis of modified CDs with the potential to develop a range of CD-based excipients performing similar functions like the components in LNP formulations, such as ionisable cationic lipids to complex the NA during formulation of NP, PEG-lipid to ensure storage stability, and helper lipids that induces membrane fusion and endosomal release of NP cargo.

Due to the structure of the CD scaffold, functional modifications can be made on both the primary face and secondary face (Figure 5-1). In this work, a library of CDs derivatives was studied. An amphiphilic anionic CD was synthesised with SC_{12} chains at the 2'- and 3'-positions (=R_2) and a sulfite (SO_3-) at 6'-O (=R_1). For the amphiphilic cationic CD series in this thesis the 6'-position was kept constant with SC_{12} chains

(=R_1), and the 2'- and 3'-positions were modified extensively (=R_2); the number of attached cationic groups per glucose unit in the ring varied from one to two. Additionally, β-CD and γ-CDs were compared. Finally, linker groups and linked terminal amines were altered.

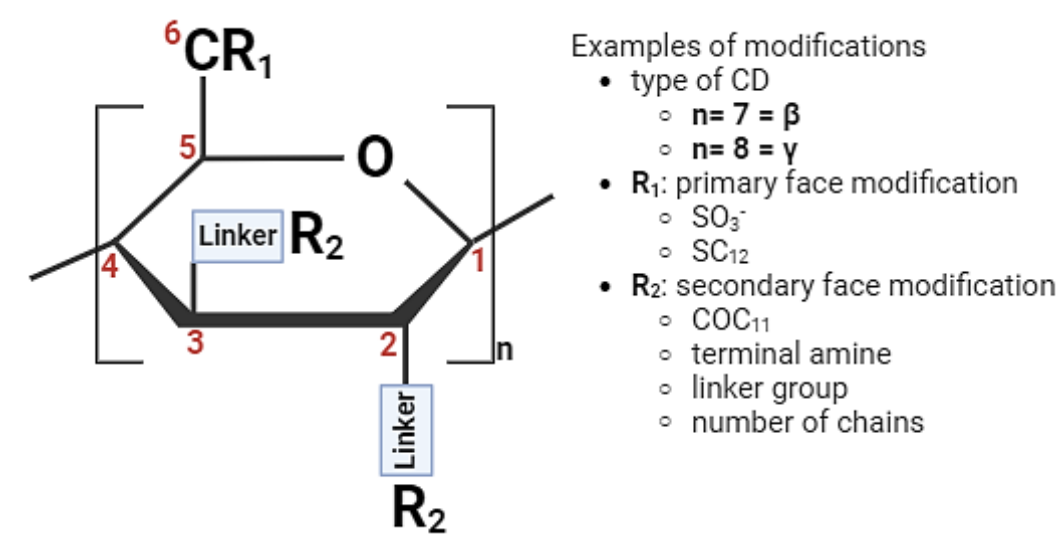

Figure 5-1 The CD scaffold highlighting the locations of the various functional groups in the modified amphiphilic cationic and anionic CDs.

The overall aim of this thesis was to develop safe and efficient CD delivery vectors for siRNA delivery, and to understand the relationship between molecular structure and *in vitro* activity.

5.2. The ideal delivery system – requirements

To translate the concept of RNAi into a medicine, NP need to overcome many challenges extra- and intracellular *in vivo* (Figure 5-2).

In extracellular environment loss of therapeutic NAs can occur by enzymatic degradation, plasma protein aggregation, RES recognition, or renal and hepatic

clearance. In addition, due to high molecular weight, hydrophilic nature and negative charge, NA may fail to cross the cell membrane. Once inside the cell, escape from the endo-lysosomal pathway into the cytoplasm is essential for activity (Hu et al. 2020).

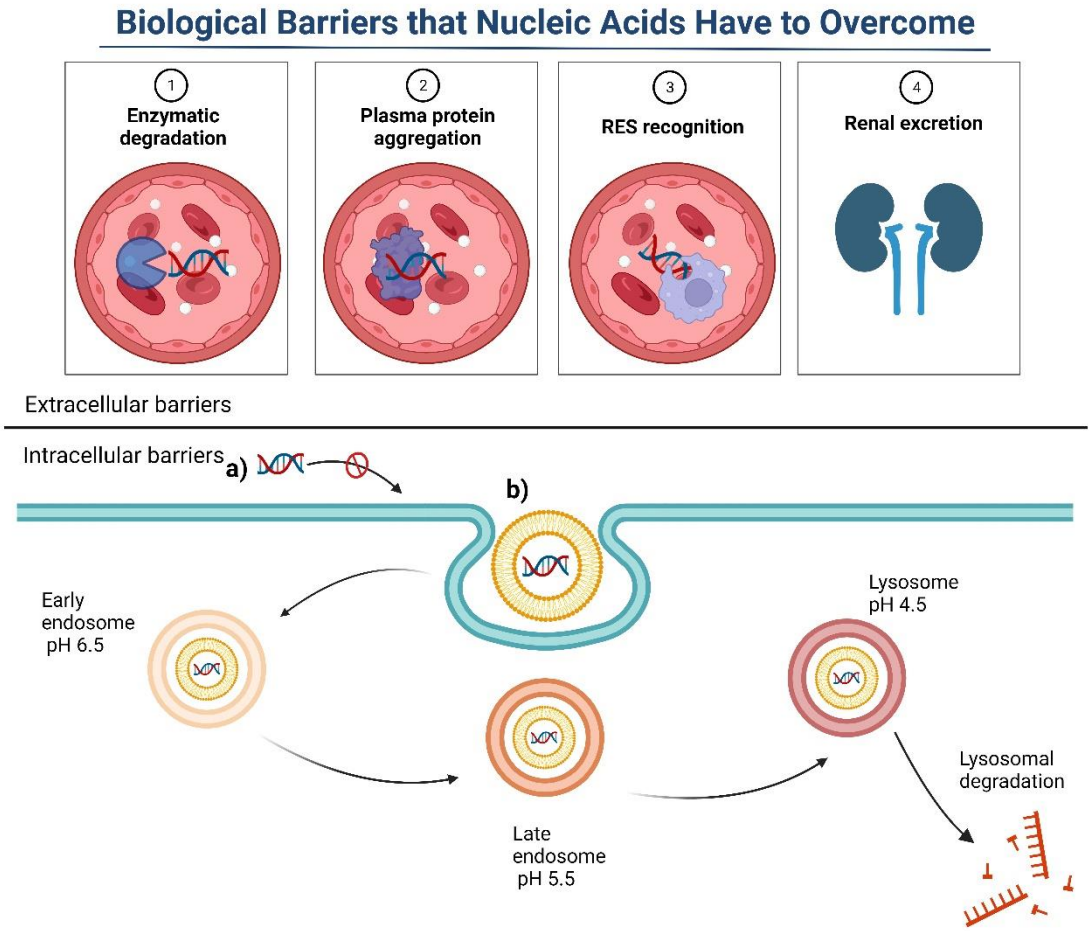

Figure 5-2 Biological barriers to delivery of NA and the intracellular fate of NPs, a) free siRNA does not cross cellular membrane, b) NP uptake and its fate through pH changes while experiencing the endocytic pathway.

In order to overcome the barriers to delivery, the design of the biomaterial and the subsequent NP needs to be optimised. Size and PDI are the first critical parameters to be controlled during NP formation. The most common technique to measure size and PDI is DLS or alternatively TEM. Sizes below 200 nm are preferable to avoid recognition by the complement system (Hoshyar et al. 2016). To prevent rapid

clearance, NP need to be above 10 nm. A PDI below 0.2 is considered necessary to guarantee the production of uniform particles. Surface charge can also influence NP fate. It will influence NP stability; high positive or high negative charges prevent aggregation of particle due to electrostatic repulsion (Honary and Zahir 2013). Positive charge is also preferable for uptake through negatively charged cell membranes, however, toxic *in vivo* (Knudsen et al. 2015). Therefore, for parenteral drug delivery 0-10 mV is desired. Near-neutral charge is also necessary to prevent immune recognition, aggregation with blood components, and early clearance out of body (Xu et al. 2022). Researchers have also found that the chemistry of the delivery material, the ratio of NP components, and the incorporated NA can have an impact on NP shape, which in return can impact on distribution and organ-selectivity (Gallego-Yerga et al. 2018; Kulkarni et al. 2017; Kulkarni J, Darjuan M 2018).

Ideally, in the formation process of the NP the drug delivery vector should complex the full amount of NA. However, although complexation, encapsulation and protection of NA against degradation and agglomeration is necessary, so is release of the NA from the delivery system. A balance between these releases and protective features of the delivery system is crucial.

After assessing physicochemical characteristics, NP are tested in *in vitro* cell culture models. Firstly, cell viability is investigated. The delivery vectors should not be toxic to the cells. The aim for RNAi therapeutics is to either knockdown a gene that is relevant in the maintaining or progressing of the disease.

For successful gene knockdown, the NP needs to enter the cell, however, successful uptake does not always correlate with gene knockdown efficiency, which

indicates that other factors such as endosomal escape and NA recycling plays an important role (Ahmad, Khan, and Haque 2019).

5.3. Design strategy of the CD-based biomaterial – Results and Discussion

The design strategy used in the amphiphilic charged CDs aimed to overcome challenges to delivery of siRNA by NPs. It was hypothesised that the design of the biomaterials used to formulate NPs will influence the efficiency (Figure 5-3).

To complex the NA and to enhance endosomal escape, a variety of amines were conjugated to the secondary site of the amphiphilic CDs.

The nature of the linker group between the amine and the CD was also investigated as it has been reported previously that this can affect endosomal escape and transfection. The amphiphilicity of the CDs was conveyed by the conjugation of lipid chains which is important to enhance cellular uptake. In this work the lipid chain was maintained constant (C_{12}).

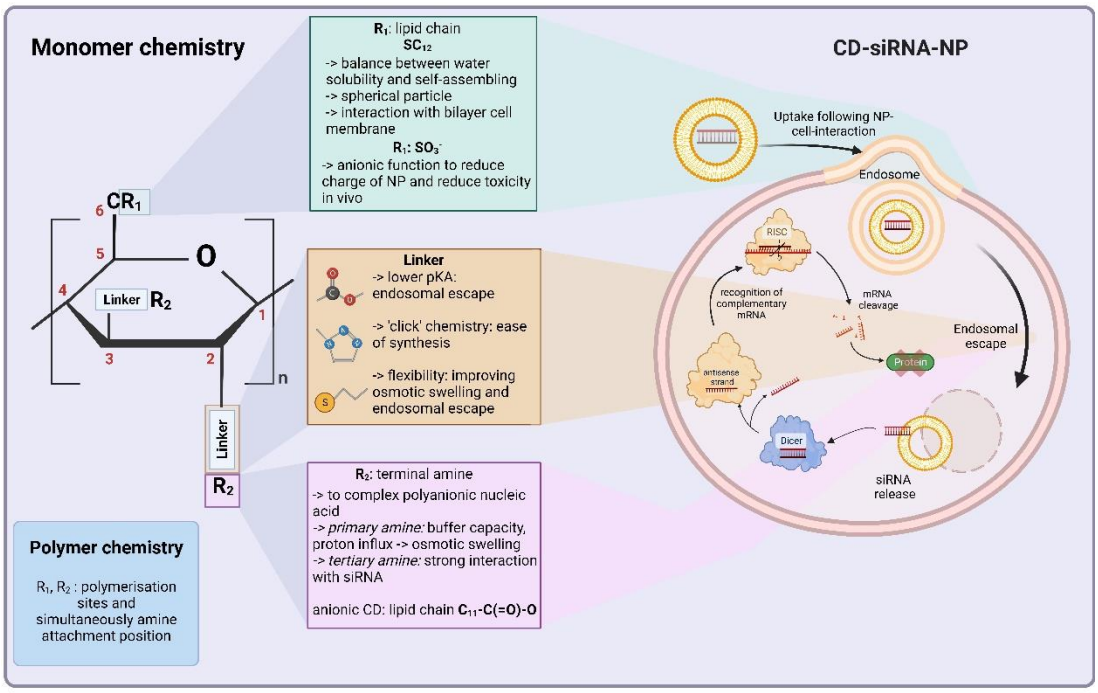

Figure 5-3. Summary of the structural variations of the CDs investigated and the implications for efficacy at the cellular level.

The coexistence of lipophilic groups and charged groups in one molecule is defined as amphiphilicity. All CDs designed within the scope of the thesis include lipid chains attached to either the primary face (cationic CDs) or secondary face (anionic CD). The introduction of lipid chains has been shown to improve transfection efficiency (Cryan et al. 2004). Additionally, the length of the carbon chain has shown that efficacy increases up to C_{16} (McMahon et al. 2008), however, with longer lipid chains solubility may be a challenge. Consequently in this work, C_{12} was selected in order to optimise aqueous solubility and self-assembling of the CD (O'Mahony, Ogier, et al. 2012).

It is essential to use positively charged functional groups in the synthesis of amphiphilic cationic CDs to facilitate electrostatic complexation of anionic NAs (S.-A. Cryan et al. 2004). Complete complexation is important to protect the siRNA from degradation. Amine-containing functional groups are ideal for this purpose because of

their positive charge during formulation process. Additionally amines enable endosomal escape through osmotic swelling or membrane disruption (Vermeulen et al. 2018).

The most commonly used amphiphilic cationic CD in our group is 'click-propylamine', in which the primary face is functionalised with C_{12}-lipid chains and the secondary face with a primary amine using the 'click' chemistry approach (O'Mahony, Ogier, et al. 2012). NPs formulated with this CD result in high surface charge due to the excess of CD needed. Positive charge is associated with potential toxicity *in vivo* (Knudsen et al. 2015). A technique to reduce *in vivo* toxicity is by co-formulation with an amphiphilic anionic CD (2. Chapter). NPs incorporating the cationic and anionic CD including siRNA presented no change in size (<170 nm), a reduction in PDI from 0.46 to 0.16, and a drop in charge from 34 ±7 mV to 26 ±4 mV compared to NPs with the cationic CDs and siRNA only. Cellular uptake, as measured by flow cytometry, did not show any difference (~60%). However, a decline in transfection (from 29 ±11% to 21 ±2%) was observed which may be related to impeded endosomal escape following incorporation of the anionic CD, confirmed with confocal imaging. Although, siRNA delivery efficiency was impeded *in vitro* following the addition of the anionic CD, the charge reduction with the co-formulation might be beneficial *in vivo*.

This incorporation of a negative compound was also investigated by Ball et al. where the co-delivery of mRNA with siRNA as a second negatively charged compound resulted in improved efficiency. To further investigate the effect of the additional negative charge, the mRNA was replaced by a negatively charged polymer (poly(sodium 4-sytrenesulfonate)). The presence of the additional negatively charged material increased the efficacy and consequently enabled reduction of the siRNA dose,

compared to siRNA-only lipid NP (Ball et al. 2018). More recent work by the Whitehead group showed that the co-formulation of cationic or anionic lipids shifted the biodistribution of the widely used ‘four-component’-lipid NPs to extra-hepatic organs (LoPresti et al. 2022). The replacement of a helper lipid with a negative lipid caused a shift to the lungs, and the substitution of a cationic lipid shifted the particle specificity to the spleen. It was demonstrated that the shift is directly related to the chemical structure of the added excipient and its effect on NP formation and characteristics.

In summary, these findings highlight the importance of further investigation of the chemistry of CD delivery vectors. Hence, a SAR study was conducted with amphiphilic cationic CDs (3. Chapter). NPs containing siRNA formulated with six amphiphilic cationic CDs and one non-amphiphilic CD showed sizes below 220 nm. The electrostatic interaction between negatively charged siRNA and the cationic vector was the driving force to facilitate complexation; the amphiphilicity helped to form circular shaped particles and enhanced membrane permeability. PDIs were reported to be below 0.5. Amphiphilic cationic CDs formulated with siRNA usually result in high positive surface charges (~40 mV). A second approach to reduce NP charge was to modify the chemistry of cationic CD (‘click’ propylamine) to achieve a cationic CD with lower pKa and consequently lower surface charge (Hajj et al. 2019) (3. Chapter). The reduction in surface charge (down to ~26 mV) was possible by replacing the triazole linker with an ester and the primary amine with a tertiary amine. While a charge reduction was achieved, no gene knockdown was detected for the lower pKa cationic CD. By way of comparison, the ‘click-propylamine’ NP at MR10:1 (cationic CD:siRNA) showed an average knockdown of 20 ±15%. However, cellular uptake was similar for both CDs (40-70%). These results indicate that, particularly for

the lower pKa CD, endosomal escape remains as a potential barrier for successful gene knockdown.

A small-scale library of amphiphilic cationic CDs was then developed to examine more closely the SAR. These were characterised and tested *in vitro* (3. Chapter). CD-type (β versus γ), charge density, linker chemistry, and terminal amines were varied and compared (Figure 5-4).

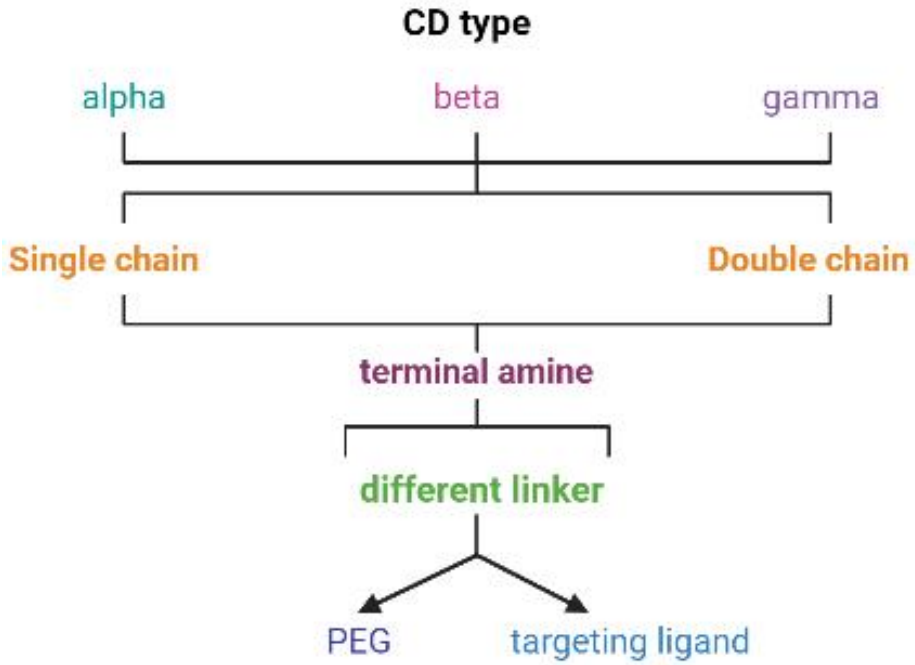

Figure 5-4. Design approach to optimise the transfection activity of amphiphilic cationic CDs.

The series of *O*2-substituted β- and γ-CDs (single chained CDs) did not show adequate gene knockdown. Therefore, *O*2 and *O*3 positions were substituted simultaneously in a γ-CD (double chained γ-CD). The resulting CD contained primary amines attached via a triazole linker. The increase in charge density per CD molecule resulted in transfection efficiency up to 40%. A similar behaviour was observed

previously in a Spanish group where the increase of protonatable amines resulted in a significant improvement of transfection (Díaz-Moscoso et al. 2008).

Due to the promising initial results with double chain γ-CD, it was decided to investigate further structural modifications. The use of γ-CD has the advantage of easier scale-up for industrial purposes due to its better water-solubility compared to other natural CDs. The type of amine and the linker may also have an influence on transfection efficiency. Linker groups between the core CD scaffold and the cationic groups are important in terms of the synthetic route required, the complexity of the synthesis and therefore the yield and the cost of scale-up. While 'click' chemistry utilising triazole is a relatively easy method to link amines, the chemistry route with thiopropyl presents a greener synthesis due to eliminating the use of copper-catalyst. The replacement of the triazole linker with a thiopropyl linker allows more flexibility for the attached amine. A second modification employed was the synthesis of thiopropyl attached primary and tertiary amine, thus allowing the comparison for the effects of amine groups.

The overall finding was that primary amines are the superior terminal amines, particularly when applied as double chain γ-CD. The introduction of a more flexible linker group such as thiopropyl improved the transfection efficiency by 2-fold (~80% compared to triazole attached primary amine: ~40%). A similar approach was conducted earlier where the replacement of triazole moiety with a thiourea in β-CDs boosted pDNA performance *in vivo* (Méndez-Ardoy, Guilloteau, et al. 2011; Méndez-Ardoy, Urbiola, et al. 2011). Since both NPs with different linker groups displayed similar size (~200 nm) and surface charge (30-40 mV), the enhanced transfection was related to differences in the chemical structure.

The chemical versatility of CDs is not restricted to monomer CDs, they are also available for polymer synthesis (4. Chapter). Advantages of polymers are controlled drug release, stable yet biocompatible systems that can be adjusted to meet physicochemical requirements and the ease of preparation (Charelli et al. 2022).Two β-CD polymers were synthesised that differed from each other in the amines incorporated: primary amine (PA-polymer) was compared to quaternary ammonium (QA-polymer). For both polymers, it was possible to formulate NPs with sizes below 175 nm, with PDIs below 0.4 and surface charge ranging from 26-37 mV. With respect to the amine functionalities, as reported above for the monomer CD, a similar trend was observed in the polymer chemistry where the primary amine also showed better transfection. While the QA-polymer did not show any cellular uptake, the PA-polymer uptake increased with an increase in MR (polymer:siRNA). At PA-polymer MR10:1 40 ±14% uptake and 41 ±7% gene knockdown was detected. Similar results were reported by Akkin et al where the PA-polymer was compared to a QA-polymer and a Guanidino-polymer. In a permeability study, the PA-polymer was the only compound to enhance permeability (Akkın et al. 2022). In contrast, in another more recent study, a QA-β-CD-polymer was successfully employed to deliver mRNA to 2D and 3D melanoma cell lines. This QA-polymer links a quaternary ammonium to the hydroxyl of the CD via a carboxyl group and C_2-chain (Monfared et al. 2022, 2023). However, the quaternary ammonium in this thesis and in the study by Akkin et al is attached as a (2-hydroxy-3-*N,N,N*-trimetyhlamino)propyl (C_3-chain) which might be more rigid compared to aforementioned carboxyl group. The linker group depends on the type of initiator used in the polymer reaction. These results confirm the importance of the type of linker and its flexibility, a similar finding was observed in monomer chemistry (3. Chapter). It is interesting to note that in Monfared et al. the linker contains the oxygen

analogue of thiourea which was previously shown to be highly successful (Méndez-Ardoy, Guilloteau, et al. 2011; Méndez-Ardoy, Urbiola, et al. 2011).

While in the case of the polymer CDs only the amine functional groups were investigated, a similar design strategy like in Figure 5-4 can be developed for CD-polymers, such as trying out other CD-types, or varying linker groups to further improve their activity as delivery vectors. To increase stability and cell specificity, PEG a targeting ligand can be utilised.

5.4. Main findings

A library of CDs was synthesised to improve characteristics and enhance the transfection efficiency of CD-based NPs.

This thesis shows that co-formulation of modified amphiphilic CDs, anionic and cationic, is possible to modulate the physicochemical properties of NPs. This has potential for *in vivo* applications as it reduces the potential *in vivo* toxicity of positively charged NPs.

The degree and type of functionalisation on CDs influence their physicochemical characteristics and consequently *in vitro* performance. It was possible to identify chemical modifications, such as primary amine and flexible thiorpropyl linker, in monomeric CDs that enhanced *in vitro* siRNA transfection efficiency.

Cationic β-CD polymers were synthesised and able to complex siRNA. The delivery of siRNA with β-CD-polymer was successful when modified with primary amines. This is to our knowledge the first time to deliver siRNA with CD-polymers.

5.5. Future directions

To further progress the use of monomeric and polymeric CDs as delivery vectors, the vector design could be modified to include PEG. In addition, cell-specific uptake could be enhanced by attaching a targeting ligand to the PEG-chain (Gooding et al. 2015). Previous work in our group showed that CDs allow the incorporation of targeting ligands with 'post-insertion' and improve *in vitro* and *ex vivo* efficiency (Guo et al. 2017).

Further alteration to the lipid chains, such as increasing the carbon length, or the introduction of branched lipid chains on amphiphilic monomeric CDs may increase efficiency (Hajj et al. 2019; McMahon et al. 2008). Similarly, in the case of polymers, transfection efficiency could be increased by the introduction of lipid chains.

Microfluidics could produce large batches of NPs (scale-up) while simultaneously reducing the size and poly dispersity (Belliveau et al. 2012; Mendonça, Kont, et al. 2023). This technique can also be used to either co-formulate different CDs or to blend CDs with lipid excipients.

While a reporter gene was utilised for *in vitro* screening purposes, for future experiments, disease-related siRNA should be used.

The ability of CD-NPs to deliver other NAs such as mRNA could also be investigated.

The NP described in this thesis could be tested *in vivo* and the results compared to the *in vitro* presented. This will illustrate any differences between *in vitro* and *in vivo* data.

6. References

Abstiens, Kathrin, Sara Maslanka Figueroa, Manuel Gregoritza, and Achim M. Goepferich. 2019. “Interaction of Functionalized Nanoparticles with Serum Proteins and Its Impact on Colloidal Stability and Cargo Leaching.” *Soft Matter* 15(4):709–20. doi: 10.1039/C8SM02189A.

Abumanhal-Masarweh, Hanan, Dana da Silva, Maria Poley, Assaf Zinger, Evgenya Goldman, Nitzan Krinsky, Ron Kleiner, Gal Shenbach, Josh E. Schroeder, Jeny Shklover, Janna Shainsky-Roitman, and Avi Schroeder. 2019. “Tailoring the Lipid Composition of Nanoparticles Modulates Their Cellular Uptake and Affects the Viability of Triple Negative Breast Cancer Cells.” *Journal of Controlled Release* 307:331–41. doi: 10.1016/j.jconrel.2019.06.025.

Agnes, Marco, Elisabetta Pancani, Milo Malanga, Eva Fenyvesi, and Ilse Manet. 2022. “Implementation of Water-Soluble Cyclodextrin-Based Polymers in Biomedical Applications: How Far Are We?” *Macromolecular Bioscience* 22(8). doi: 10.1002/mabi.202200090.

Ahmad, Aqeel, Javed Masood Khan, and Shafiul Haque. 2019. “Strategies in the Design of Endosomolytic Agents for Facilitating Endosomal Escape in Nanoparticles.” *Biochimie* 160:61–75. doi: 10.1016/j.biochi.2019.02.012.

Ahmadi, Delshad, Mojtaba Zarei, Mahdi Rahimi, Marzieh Khazaie, Zatollah Asemi, Seyed Mostafa Mir, Alireza Sadeghpour, Ansar Karimian, Fourogh Alemi, Mohammad Rahmati-Yamchi, Roya Salehi, Farhad Jadidi-Niaragh, Mehdi Yousefi, Nafiseh Khelgati, Maryam Majidinia, Amin Safa, and Bahman Yousefi. 2020. “Preparation and In-Vitro Evaluation of PH-Responsive Cationic Cyclodextrin Coated Magnetic Nanoparticles for Delivery of Methotrexate to the Saos-2 Bone Cancer Cells.” *Journal of Drug Delivery Science and Technology* 57(February). doi: 10.1016/j.jddst.2020.101584.

Akinc, Akin, Martin A. Maier, Muthiah Manoharan, Kevin Fitzgerald, Muthusamy Jayaraman, Scott Barros, Steven Ansell, Xinyao Du, Michael J. Hope, Thomas D. Madden, Barbara L. Mui, Sean C. Semple, Ying K. Tam, Marco Ciufolini, Dominik Witzigmann, Jayesh A. Kulkarni, Roy van der Meel, and Pieter R. Cullis. 2019. “The Onpattro Story and the Clinical Translation of Nanomedicines Containing Nucleic Acid-Based Drugs.” *Nature Nanotechnology* 14(12):1084–87. doi: 10.1038/s41565-019-0591-y.

Akkın, Safiye, Gamze Varan, Davut Aksüt, Milo Malanga, Ayşe Ercan, Murat Şen, and Erem Bilensoy. 2022. “A Different Approach to Immunochemotherapy for Colon Cancer: Development of Nanoplexes of Cyclodextrins and Interleukin-2 Loaded with 5-FU.” *International Journal of Pharmaceutics* 623(June). doi: 10.1016/j.ijpharm.2022.121940.

Albanese, Alexandre, and Warren C. W. Chan. 2011. “Effect of Gold Nanoparticle Aggregation on Cell Uptake and Toxicity.” *ACS Nano* 5(7):5478–89. doi: 10.1021/nn2007496.

Almeida, Mauro Sousa de, Eva Susnik, Barbara Drasler, Patricia Taladriz-Blanco, Alke Petri-Fink, and Barbara Rothen-Rutishauser. 2021. “Understanding

Nanoparticle Endocytosis to Improve Targeting Strategies in Nanomedicine." *Chemical Society Reviews* 50(9):5397–5434. doi: 10.1039/d0cs01127d.

Anderson, Amelia M., Tamari Kirtadze, Milo Malanga, Darren Dinh, Carolyn Barnes, Angielyn Campo, Daniel M. Clemens, Rebeca Garcia-Fandiño, Ángel Piñeiro, and Matthew S. O'Connor. 2021. "Cyclodextrin Dimers: A Versatile Approach to Optimizing Encapsulation and Their Application to Therapeutic Extraction of Toxic Oxysterols." *International Journal of Pharmaceutics* 606. doi: 10.1016/j.ijpharm.2021.120522.

Arede, Liliana, Elena Foerner, Selinde Wind, Rashmi Kulkarni, Ana Filipa Domingues, George Giotopoulos, Svenja Kleinwaechter, Maximilian Mollenhauer-Starkl, Holly Davison, Aditya Chandru, Ryan Asby, Ralph Samarista, Shikha Gupta, Dorian Forte, Antonio Curti, Elisabeth Scheer, Brian J. P. Huntly, Laszlo Tora, and Cristina Pina. 2022. "KAT2A Complexes ATAC and SAGA Play Unique Roles in Cell Maintenance and Identity in Hematopoiesis and Leukemia." *Blood Advances* 6(1):165–80. doi: 10.1182/bloodadvances.2020002842.

Aydinlioglu, Esra, Mona Abdelghani, Gaëlle Le Fer, Jan C. M. van Hest, Olivier Sandre, and Sébastien Lecommandoux. 2023. "Robust Polyion Complex Vesicles (PICsomes) Based on PEO-b-Poly(Amino Acid) Copolymers Combining Electrostatic and Hydrophobic Interactions: Formation, SiRNA Loading and Intracellular Delivery." *Macromolecular Chemistry and Physics* 224(1):1–11. doi: 10.1002/macp.202200306.

Aylward, Lesa L. 2019. *Biomarkers of Environmental Exposures in Blood*. 2nd ed. Elsevier Inc.

Badwaik, Vivek D., Emilio Aicart, Yawo A. Mondjinou, Merrell A. Johnson, Valorie D. Bowman, and David H. Thompson. 2016. "Structure-Property Relationship for in Vitro SiRNA Delivery Performance of Cationic 2-Hydroxypropyl-β-Cyclodextrin: PEG-PPG-PEG Polyrotaxane Vectors." *Biomaterials* 84:86–98. doi: 10.1016/j.biomaterials.2015.11.032.

Ball, Rebecca L., Khalid A. Hajj, Jamie Vizelman, Palak Bajaj, and Kathryn A. Whitehead. 2018. "Lipid Nanoparticle Formulations for Enhanced Co-Delivery of SiRNA and MRNA." *Nano Letters* 18(6):3814–22. doi: 10.1021/acs.nanolett.8b01101.

Barata, Pedro, Anil K. Sood, and David S. Hong. 2016. "RNA-Targeted Therapeutics in Cancer Clinical Trials: Current Status and Future Directions." *Cancer Treatment Reviews* 50:35–47. doi: 10.1016/j.ctrv.2016.08.004.

Bartlett, Derek W., and Mark E. Davis. 2007. "Physicochemical and Biological Characterization of Targeted, Nucleic Acid-Containing Nanoparticles." *Bioconjugate Chemistry* 18(2):456–68. doi: 10.1021/bc0603539.

Belliveau, Nathan M., Jens Huft, Paulo J. C. Lin, Sam Chen, Alex K. K. Leung, Timothy J. Leaver, Andre W. Wild, Justin B. Lee, Robert J. Taylor, Ying K. Tam, Carl L. Hansen, and Pieter R. Cullis. 2012. "Microfluidic Synthesis of Highly Potent Limit-Size Lipid Nanoparticles for In Vivo Delivery of SiRNA." *Molecular Therapy*. doi: 10.1038/mtna.2012.28.

Bellocq, Nathalie C., Suzie H. Pun, Gregory S. Jensen, and Mark E. Davis. 2003. "Transferrin-Containing, Cyclodextrin Polymer-Based Particles for Tumor-Targeted Gene Delivery." *Bioconjugate Chemistry* 14(6):1122–32. doi: 10.1021/bc034125f.

Bognanni, Noemi, Maurizio Viale, Alessia Distefano, Rita Tosto, Nadia Bertola, Fabrizio Loiacono, Marco Ponassi, Domenico Spinelli, Giuseppe Pappalardo, and Graziella Vecchio. 2021. "Cyclodextrin Polymers as Delivery Systems for Targeted Anti-Cancer Chemotherapy." *Molecules* 26(19):1–12. doi: 10.3390/molecules26196046.

Buck, Jonas, Philip Grossen, Pieter R. Cullis, Jo Huwyler, and Dominik Witzigmann. 2019. "Lipid-Based DNA Therapeutics : Hallmarks of Non-Viral Gene Delivery." *ACS Nano* 13(4):3754–82. doi: 10.1021/acsnano.8b07858.

Byrne, Colin, Florence Sallas, Dilip K. Rai, Julien Ogier, and Raphael Darcy. 2009. "Poly-6-Cationic Amphiphilic Cyclodextrins Designed for Gene Delivery." *Organic and Biomolecular Chemistry* 7(18):3763–71. doi: 10.1039/b907232b.

Cabassi, Franco, Benito Casu, and Arthur S. Perlin. 1978. "Infrared Absorption and Raman Scattering of Sulfate Groups of Heparin and Related Glycosaminoglycans in Aqueous Solution." *Carbohydrate Research* 63(C):1–11. doi: 10.1016/S0008-6215(00)80924-6.

Charelli, Letícia Emiliano, Gabriela Calidone de Mattos, Ariane de Jesus Sousa-Batista, José Carlos Pinto, and Tiago Albertini Balbino. 2022. "Polymeric Nanoparticles as Therapeutic Agents against Coronavirus Disease." *Journal of Nanoparticle Research* 24(1). doi: 10.1007/s11051-022-05396-5.

Chen, Wenjuan, Mingming Zhang, Wei Shen, Bo Du, Jing Yang, and Qiqing Zhang. 2019. "A Polycationic Brush Mediated Co-Delivery of Doxorubicin and Gene for Combination Therapy." *Polymers* 11(1):1–9. doi: 10.3390/polym11010060.

Chen, Xiaohong, Ying Kun Qiu, Cally Owh, Xian Jun Loh, and Yun Long Wu. 2016. "Supramolecular Cyclodextrin Nanocarriers for Chemo- and Gene Therapy towards the Effective Treatment of Drug Resistant Cancers." *Nanoscale* 8(45):18876–81. doi: 10.1039/c6nr08055c.

Chen, Yi Fan, Yen Hsin Wang, Cing Syuan Lei, Chun A. Changou, Mark E. Davis, and Yun Yen. 2019. "Host Immune Response to Anti-Cancer Camptothecin Conjugated Cyclodextrin-Based Polymers." *Journal of Biomedical Science* 26(1):1–12. doi: 10.1186/s12929-019-0583-0.

Crini, Grégorio, Cesare Cosentino, Sabrina Bertini, Annamaria Naggi, Giangiacomo Torri, Carmen Vecchi, Ludovic Janus, and Michel Morcellet. 1998. "Solid State NMR Spectroscopy Study of Molecular Motion in Cyclomaltoheptaose (β-Cyclodextrin) Crosslinked with Epichlorohydrin." *Carbohydrate Research* 308(1–2):37–45. doi: 10.1016/S0008-6215(98)00077-9.

Cryan, S. A., R. Donohue, B. J. Ravoo, R. Darcy, and C. M. O'Driscoll. 2004. "Cationic Cyclodextrin Amphiphiles as Gene Delivery Vectors." *Journal of Drug Delivery Science and Technology* 14(1):57–62. doi: 10.1016/s1773-2247(04)50006-0.

Cryan, Sally-Ann, Ann Holohan, Ruth Donohue, Raphael Darcy, and Caitriona M.

O'Driscoll. 2004. "Cell Transfection with Polycationic Cyclodextrin Vectors." *European Journal of Pharmaceutical Sciences* 21(5):625–33. doi: 10.1016/j.ejps.2004.01.001.

Danaei, M., M. Dehghankhold, S. Ataei, F. Hasanzadeh Davarani, R. Javanmard, A. Dokhani, S. Khorasani, and M. R. Mozafari. 2018. "Impact of Particle Size and Polydispersity Index on the Clinical Applications of Lipidic Nanocarrier Systems." *Pharmaceutics* 10(2):1–17. doi: 10.3390/pharmaceutics10020057.

Davis, M. E., S. H. Pun, N. C. Bellocq, T. M. Reineke, S. R. Popielarski, S. Mishra, and J. D. Heidel. 2004. "Self-Assembling Nucleic Acid Delivery Vehicles via Linear, Water-Soluble, Cyclodextrin-Containing Polymers." *Current Medicinal Chemistry* 11(2):179–97. doi: 10.2174/0929867043456179.

Davis, Mark E. 2009. "The First Targeted Delivery of SiRNA in Humans via a Self-Assembling, Cyclodextrin Polymer-Based Nanoparticle: From Concept to Clinic." *Molecular Pharmaceutics* 6(3):659–68. doi: 10.1021/mp900015y.

Davis, Mark E., Jonathan E. Zuckerman, Chung Hang J. Choi, David Seligson, Anthony Tolcher, Christopher A. Alabi, Yun Yen, Jeremy D. Heidel, and Antoni Ribas. 2010. "Evidence of RNAi in Humans from Systemically Administered SiRNA via Targeted Nanoparticles." *Nature* 464(7291):1067–70. doi: 10.1038/nature08956.

Debela, Dejene Tolossa, Seke G. Y. Muzazu, Kidist Digamo Heraro, Maureen Tayamika Ndalama, Betelhiem Woldemedhin Mesele, Dagimawi Chilot Haile, Sophia Khalayi Kitui, and Tsegahun Manyazewal. 2021. "New Approaches and Procedures for Cancer Treatment: Current Perspectives." *SAGE Open Medicine* 9. doi: 10.1177/20503121211034366.

Degors, Isabelle M. S., Cuifeng Wang, Zia Ur Rehman, and Inge S. Zuhorn. 2019. "Carriers Break Barriers in Drug Delivery: Endocytosis and Endosomal Escape of Gene Delivery Vectors." *Accounts of Chemical Research* 52(7):1750–60. doi: 10.1021/acs.accounts.9b00177.

Deprey, Kirsten, Nefeli Batistatou, and Joshua A. Kritzer. 2020. "A Critical Analysis of Methods Used to Investigate the Cellular Uptake and Subcellular Localization of RNA Therapeutics." *Nucleic Acids Research* 48(14):7623–39. doi: 10.1093/nar/gkaa576.

Díaz-Moscoso, Alejandro, Patricia Balbuena, Marta Gómez-García, Carmen Ortiz Mellet, Juan M. Benito, Loïc Le Gourriérec, Christophe Di Giorgio, Pierre Vierling, Antonino Mazzaglia, Norberto Micali, Jacques Defaye, and José M. García Fernández. 2008. "Rational Design of Cationic Cyclooligosaccharides as Efficient Gene Delivery Systems." *Chemical Communications* (17):2001–3. doi: 10.1039/b718672j.

Díaz-Moscoso, Alejandro, Löic Le Gourriérec, Marta Gómez-García, Juan M. Benito, Patricia Balbuena, Fernando Ortega-Caballero, Nicolas Guilloteau, Christophe Di Giorgio, Pierre Vierling, Jacques Defaye, Carmen Ortiz Mellet, and José M. Garcí. Fernández. 2009. "Polycationic Amphiphilic Cyclodextrins for Gene Delivery: Synthesis and Effect of Structural Modifications on Plasmid DNA Complex Stability, Cytotoxicity, and Gene Expression." *Chemistry - A European Journal* 15(46):12871–88. doi: 10.1002/chem.200901149.

Díaz-Moscoso, Alejandro, Nicolas Guilloteau, Céline Bienvenu, Alejandro Méndez-Ardoy, José L. Jiménez Blanco, Juan M. Benito, Loïc Le Gourriérec, Christophe Di Giorgio, Pierre Vierling, Jacques Defaye, Carmen Ortiz Mellet, and José M. García Fernández. 2011. "Mannosyl-Coated Nanocomplexes from Amphiphilic Cyclodextrins and PDNA for Site-Specific Gene Delivery." *Biomaterials* 32(29):7263–73. doi: 10.1016/j.biomaterials.2011.06.025.

Domingues, Ana Filipa, Rashmi Kulkarni, George Giotopoulos, Shikha Gupta, Laura Vinnenberg, Liliana Arede, Elena Foerner, Mitra Khalili, Rita Romano Adao, Ayona Johns, Shengjiang Tan, Keti Zeka, Brian J. Huntly, Sudhakaran Prabakaran, and Cristina Pina. 2020. "Loss of KAT2A Enhances Transcriptional Noise and Depletes Acute Myeloid Leukemia Stem-like Cells." *ELife* 9:1–29. doi: 10.7554/eLife.51754.

Donahue, Nathan D., Handan Acar, and Stefan Wilhelm. 2019. "Concepts of Nanoparticle Cellular Uptake, Intracellular Trafficking, and Kinetics in Nanomedicine." *Advanced Drug Delivery Reviews* 143:68–96. doi: 10.1016/j.addr.2019.04.008.

Donohue, Ruth, Antonino Mazzaglia, Bart Jan Ravoo, and Raphael Darcy. 2002. "Cationic β-Cyclodextrin Bilayer Vesicles." *Chemical Communications* 2(23):2864–65. doi: 10.1039/b207238f.

Dowdy, Steven F. 2017. "Overcoming Cellular Barriers for RNA Therapeutics." *Nature Biotechnology* 35(3):222–29. doi: 10.1038/nbt.3802.

Durymanov, Mikhail, and Joshua Reineke. 2018. "Non-Viral Delivery of Nucleic Acids: Insight into Mechanisms of Overcoming Intracellular Barriers." *Frontiers in Pharmacology* 9(AUG):1–15. doi: 10.3389/fphar.2018.00971.

Elbashir, Sayda M., Jens Harborth, Winfried Lendeckel, Abdullah Yalcin, Klaus Weber, and Thomas Tuschl. 2001. "Duplexes of 21-Nucleotide RNAs Mediate RNA Interference in Cultured Mammalian Cells." *Nature* 411(May):494–98.

Escobar, Karen, Karla A. Garrido-Miranda, Ruth Pulido, Nelson Naveas, Miguel Manso-Silván, and Jacobo Hernandez-Montelongo. 2023. "Coatings of Cyclodextrin/Citric-Acid Biopolymer as Drug Delivery Systems: A Review." *Pharmaceutics* 15(1):1–21. doi: 10.3390/pharmaceutics15010296.

Evans, James C., Meenakshi Malhotra, Kathleen A. Fitzgerald, Jianfeng Guo, Michael F. Cronin, Caroline M. Curtin, Fergal J. O'Brien, Raphael Darcy, and Caitriona M. O'Driscoll. 2016. "Formulation and Evaluation of Anisamide-Targeted Amphiphilic Cyclodextrin Nanoparticles to Promote Therapeutic Gene Silencing in a 3D Prostate Cancer Bone Metastases Model." *Molecular Pharmaceutics* 14(1):42–52. doi: 10.1021/acs.molpharmaceut.6b00646.

Evans, James C., Meenakshi Malhotra, Jianfeng Guo, Joseph P. O'Shea, Karen Hanrahan, Amanda O'Neill, William D. Landry, Brendan T. Griffin, Raphael Darcy, R. William Watson, and Caitriona M. O'Driscoll. 2016. "Folate-Targeted Amphiphilic Cyclodextrin.SiRNA Nanoparticles for Prostate Cancer Therapy Exhibit PSMA Mediated Uptake, Therapeutic Gene Silencing in Vitro and Prolonged Circulation in Vivo." *Nanomedicine: Nanotechnology, Biology, and Medicine* 12(8):2341–51. doi: 10.1016/j.nano.2016.06.014.

Evans, James C., Meenakshi Malhotra, Katrina Sweeney, Raphael Darcy, Colleen C. Nelson, Brett G. Hollier, and Caitriona M. O'Driscoll. 2017. "Folate-Targeted Amphiphilic Cyclodextrin Nanoparticles Incorporating a Fusogenic Peptide Deliver Therapeutic SiRNA and Inhibit the Invasive Capacity of 3D Prostate Cancer Tumours." *International Journal of Pharmaceutics* 532(1):511–18. doi: 10.1016/j.ijpharm.2017.09.013.

Eygeris, Yulia, Mohit Gupta, Jeonghwan Kim, and Gaurav Sahay. 2022. "Chemistry of Lipid Nanoparticles for RNA Delivery." *Accounts of Chemical Research* 55(1):2–12. doi: 10.1021/acs.accounts.1c00544.

Fan, Xiaoshan, Hongwei Cheng, Yihong Wu, Xian Jun Loh, Yun Long Wu, and Zibiao Li. 2018. "Incorporation of Polycaprolactone to Cyclodextrin-Based Nanocarrier for Potent Gene Delivery." *Macromolecular Materials and Engineering* 303(9):1–8. doi: 10.1002/mame.201800255.

Fernández, José M. García, Juan M. Benito, and Carmen Ortiz Mellet. 2013. "Cyclodextrin-Scaffolded Glycotransporters for Gene Delivery." *Pure and Applied Chemistry* 85(9):1825–45. doi: 10.1351/PAC-CON-12-10-13.

Ferrari, R., M. Sponchioni, M. Morbidelli, and D. Moscatelli. 2018. "Polymer Nanoparticles for the Intravenous Delivery of Anticancer Drugs: The Checkpoints on the Road from the Synthesis to Clinical Translation." *Nanoscale* 10(48):22701–19. doi: 10.1039/c8nr05933k.

Fire, Andrew, SiQun Xu, Mary K. Montgomery, Steven A. Kostas, Samuel E. Driver, and Craig C. Mello. 1998. "Potent Andspecific Genetic Interferenceby Double-StrandedRNA in Caenorhabditiselegans." *Nature* 391(February):806–11.

Fitzgerald, Kathleen A., Meenakshi Malhotra, Matt Gooding, Florence Sallas, James C. Evans, Raphael Darcy, and Caitriona M. O'Driscoll. 2016. "A Novel, Anisamide-Targeted Cyclodextrin Nanoformulation for SiRNA Delivery to Prostate Cancer Cells Expressing the Sigma-1 Receptor." *International Journal of Pharmaceutics* 499(1–2):131–45. doi: 10.1016/j.ijpharm.2015.12.055.

Fitzgerald, Kathleen A., Kamil Rahme, Jianfeng Guo, Justin D. Holmes, and Caitriona M. O'Driscoll. 2016. "Anisamide-Targeted Gold Nanoparticles for SiRNA Delivery in Prostate Cancer - Synthesis, Physicochemical Characterisation and in Vitro Evaluation." *Journal of Materials Chemistry B* 4(13):2242–52. doi: 10.1039/c6tb00082g.

Foroozandeh, Parisa, and Azlan Abdul Aziz. 2018. "Insight into Cellular Uptake and Intracellular Trafficking of Nanoparticles." *Nanoscale Research Letters* 13. doi: 10.1186/s11671-018-2728-6.

Foster, Jeffrey C., Irem Akar, Marcus C. Grocott, Amanda K. Pearce, Robert T. Mathers, and Rachel K. O'Reilly. 2020. "100th Anniversary of Macromolecular Science Viewpoint: The Role of Hydrophobicity in Polymer Phenomena." *ACS Macro Letters* 9(11):1700–1707. doi: 10.1021/acsmacrolett.0c00645.

Friedrich, Maik, and Achim Aigner. 2022. "Therapeutic SiRNA: State-of-the-Art and Future Perspectives." *BioDrugs* 36(5):549–71. doi: 10.1007/s40259-022-00549-3.

Gallego-Yerga, Laura, Juan M. Benito, Laura Blanco-Fernández, María Martínez-

Negro, Itziar Vélaz, Emilio Aicart, Elena Junquera, Carmen Ortiz Mellet, Conchita Tros de Ilarduya, and Jose M. García Fernández. 2018. "Plasmid-Templated Control of DNA–Cyclodextrin Nanoparticle Morphology through Molecular Vector Design for Effective Gene Delivery." *Chemistry - A European Journal* 24(15):3825–35. doi: 10.1002/chem.201705723.

Gallego-Yerga, Laura, Laura Blanco-Fernández, Koldo Urbiola, Thais Carmona, Gema Marcelo, Juan M. Benito, Francisco Mendicuti, Conchita Tros De Ilarduya, Carmen Ortiz Mellet, and José M. García Fernández. 2015. "Host-Guest-Mediated DNA Templation of Polycationic Supramolecules for Hierarchical Nanocondensation and the Delivery of Gene Material." *Chemistry - A European Journal* 21(34):12093–104. doi: 10.1002/chem.201501678.

Gallego-Yerga, Laura, M. José González-Álvarez, Natalia Mayordomo, Francisco Santoyo-González, Juan M. Benito, Carmen Ortiz Mellet, Francisco Mendicuti, and José M. García Fernández. 2014. "Dynamic Self-Assembly of Polycationic Clusters Based on Cyclodextrins for PH-Sensitive DNA Nanocondensation and Delivery by Component Design." *Chemistry - A European Journal* 20(22):6622–27. doi: 10.1002/chem.201402026.

Gallego-Yerga, Laura, Michela Lomazzi, Valentina Franceschi, Francesco Sansone, Carmen Ortiz Mellet, Gaetano Donofrio, Alessandro Casnati, and José M. García Fernández. 2014. "Cyclodextrin- and Calixarene-Based Polycationic Amphiphiles as Gene Delivery Systems: A Structure-Activity Relationship Study." *Organic and Biomolecular Chemistry* 13(6):1708–23. doi: 10.1039/c4ob02204a.

Godinho, Bruno M. D. C., Julien R. Ogier, Raphael Darcy, Caitriona M. O'Driscoll, and John F. Cryan. 2012. "Self-Assembling Modified β-Cyclodextrin Nanoparticles as Neuronal SiRNA Delivery Vectors: Focus on Huntington's Disease." *Molecular Pharmaceutics* 10(2):640–49. doi: 10.1021/mp3003946.

Godinho, Bruno M. D. C., Julien R. Ogier, Aoife Quinlan, Raphael Darcy, Brendan T. Griffin, John F. Cryan, and Caitriona M. O'Driscoll. 2014. "PEGylated Cyclodextrins as Novel SiRNA Nanosystems: Correlations between Polyethylene Glycol Length and Nanoparticle Stability." *International Journal of Pharmaceutics* 473(1–2):105–12. doi: 10.1016/j.ijpharm.2014.06.054.

Gooding, Matt, Meenakshi Malhotra, David J. Mccarthy, Bruno M. D. C. Godinho, John F. Cryan, Raphael Darcy, and Caitriona M. O'Driscoll. 2015. "Synthesis and Characterization of Rabies Virus Glycoprotein-Tagged Amphiphilic Cyclodextrins for SiRNA Delivery in Human Glioblastoma Cells : In Vitro Analysis." *European Journal of Pharmaceutical Sciences* 71:80–92.

Gujrati, Maneesh, Anthony Malamas, Tesia Shin, Erlei Jin, Yunlu Sun, and Zheng Rong Lu. 2014. "Multifunctional Cationic Lipid-Based Nanoparticles Facilitate Endosomal Escape and Reduction-Triggered Cytosolic SiRNA Release." *Molecular Pharmaceutics* 11(8):2734–44. doi: 10.1021/mp400787s.

Guo, Jianfeng, Woei Ping Cheng, Jingxia Gu, Caixia Ding, Xiaozhong Qu, Zhenzhong Yang, and Caitriona O'Driscoll. 2012. "Systemic Delivery of Therapeutic Small Interfering RNA Using a PH-Triggered Amphiphilic Poly-l-Lysine Nanocarrier to Suppress Prostate Cancer Growth in Mice." *European Journal of*

Pharmaceutical Sciences 45(5):521–32. doi: 10.1016/j.ejps.2011.11.024.

Guo, Jianfeng, Julien R. Ogier, Stephane Desgranges, Raphael Darcy, and Caitriona ODriscoll. 2012. "Anisamide-Targeted Cyclodextrin Nanoparticles for SiRNA Delivery to Prostate Tumours in Mice." *Biomaterials* 33(31):7775–84. doi: 10.1016/j.biomaterials.2012.07.012.

Guo, Jianfeng, Eileen G. Russell, Raphael Darcy, Thomas G. Cotter, Sharon L. McKenna, Mary R. Cahill, and Caitriona M. O'Driscoll. 2017. "Antibody-Targeted Cyclodextrin-Based Nanoparticles for SiRNA Delivery in the Treatment of Acute Myeloid Leukemia: Physicochemical Characteristics, in Vitro Mechanistic Studies, and Ex Vivo Patient Derived Therapeutic Efficacy." *Molecular Pharmaceutics* 14(3):940–52. doi: 10.1021/acs.molpharmaceut.6b01150.

Hajj, Khalid A., Rebecca L. Ball, Sarah B. Deluty, Shridhar R. Singh, Daria Strelkova, Christopher M. Knapp, and Kathryn A. Whitehead. 2019. "Branched-Tail Lipid Nanoparticles Potently Deliver MRNA In Vivo Due to Enhanced Ionization at Endosomal PH." *Small* 15(6):1–7. doi: 10.1002/smll.201805097.

Haley, Rebecca M., Riccardo Gottardi, Robert Langer, and Michael J. Mitchell. 2020. "Cyclodextrins in Drug Delivery: Applications in Gene and Combination Therapy." *Drug Delivery and Translational Research* 10(3):661–77. doi: 10.1007/s13346-020-00724-5.

Hayashi, Yuya, Taishi Higashi, Keiichi Motoyama, Hirofumi Jono, Yukio Ando, Risako Onodera, and Hidetoshi Arima. 2019. "Hepatocyte-Targeted Delivery of SiRNA Polyplex with PEG-Modified Lactosylated Dendrimer/Cyclodextrin Conjugates for Transthyretin-Related Amyloidosis Therapy." *Biological and Pharmaceutical Bulletin* 42(10):1679–88. doi: 10.1248/bpb.b19-00278.

Heidel, Jeremy D., Zhongping Yu, Joanna Yi Ching Liu, Shyam M. Rele, Yongchao Liang, Ryan K. Zeidan, Douglas J. Kornbrust, and Mark E. Davis. 2007. "Administration in Non-Human Primates of Escalating Intravenous Doses of Targeted Nanoparticles Containing Ribonucleotide Reductase Subunit M2 SiRNA." *Proceedings of the National Academy of Sciences of the United States of America* 104(14):5715–21. doi: 10.1073/pnas.0701458104.

Hermanson, Greg T. 2013. "Liposome Conjugates and Derivatives." *Bioconjugate Techniques* 921–49. doi: 10.1016/b978-0-12-382239-0.00021-2.

Heyes, James, Lorne Palmer, Kaz Bremner, and Ian MacLachlan. 2005. "Cationic Lipid Saturation Influences Intracellular Delivery of Encapsulated Nucleic Acids." *Journal of Controlled Release* 107(2):276–87. doi: 10.1016/j.jconrel.2005.06.014.

Hibbitts, A., A. M. O'Mahony, E. Forde, L. Nolan, J. Ogier, S. Desgranges, R. Darcy, R. Macloughlin, C. M. O'driscoll, and S. A. Cryan. 2014. "Early-Stage Development of Novel Cyclodextrin-SiRNA Nanocomplexes Allows for Successful Postnebulization Transfection of Bronchial Epithelial Cells." *Journal of Aerosol Medicine and Pulmonary Drug Delivery* 27(6):466–77. doi: 10.1089/jamp.2013.1045.

Honary, Soheyla, and Foruhe Zahir. 2013. "Effect of Zeta Potential on the Properties

of Nano-Drug Delivery Systems - A Review (Part 2).” *Tropical Journal of Pharmaceutical Research* 12(2):265–73. doi: 10.4314/tjpr.v12i2.20.

Hoshyar, Nazanin, Samantha Gray, Hongbin Han, and Gang Bao. 2016. “The Effect of Nanoparticle Size on in Vivo Pharmacokinetics and Cellular Interaction.” *Nanomedicine* 11(6):673–92.

Hu-Lieskovan, Siwen, Jeremy D. Heidel, Derek W. Bartlett, Mark E. Davis, and Timothy J. Triche. 2005. “Sequence-Specific Knockdown of EWS-FLI1 by Targeted, Nonviral Delivery of Small Interfering RNA Inhibits Tumor Growth in a Murine Model of Metastatic Ewing’s Sarcoma.” *Cancer Research* 65(19):8984–92. doi: 10.1158/0008-5472.CAN-05-0565.

Hu, Bo, Liping Zhong, Yuhua Weng, Ling Peng, Yuanyu Huang, Yongxiang Zhao, and Xing Jie Liang. 2020. “Therapeutic SiRNA: State of the Art.” *Signal Transduction and Targeted Therapy* 5(1). doi: 10.1038/s41392-020-0207-x.

Itakura, Shoko, Susumu Hama, Ryo Matsui, and Kentaro Kogure. 2016. “Effective Cytoplasmic Release of SiRNA from Liposomal Carriers by Controlling the Electrostatic Interaction of SiRNA with a Charge-Invertible Peptide, in Response to Cytoplasmic PH.” *Nanoscale* 8(20):10649–58. doi: 10.1039/c5nr08365f.

Jambhekar, Sunil S., and Philip Breen. 2016. “Cyclodextrins in Pharmaceutical Formulations I: Structure and Physicochemical Properties, Formation of Complexes, and Types of Complex.” *Drug Discovery Today* 21(2):356–62. doi: 10.1016/j.drudis.2015.11.017.

Jia, Die, Xianbin Ma, Yi Lu, Xinyi Li, Shengxin Hou, Yuan Gao, Peng Xue, Yuejun Kang, and Zhigang Xu. 2021. “ROS-Responsive Cyclodextrin Nanoplatform for Combined Photodynamic Therapy and Chemotherapy of Cancer.” *Chinese Chemical Letters* 32(1):162–67. doi: 10.1016/j.cclet.2020.11.052.

Jiang, Yuhang, Qiao Lu, Yongheng Wang, Emily Xu, Alison Ho, Priya Singh, Yifei Wang, Zhaozhong Jiang, Fan Yang, Gregory T. Tietjen, Peter Cresswell, and W. Mark Saltzman. 2020. “Quantitating Endosomal Escape of a Library of Polymers for MRNA Delivery.” *Nano Letters* 20(2):1117–23. doi: 10.1021/acs.nanolett.9b04426.

Kahl, Melanie, Annamaria Brioli, Martin Bens, Florian Perner, Anne Kresinsky, Ulf Schnetzke, Anna Hinze, Yordan Sbirkov, Sven Stengel, Giorgia Simonetti, Giovanni Martinelli, Kevin Petrie, Arthur Zelent, Frank Dietmar Böhmer, Marco Groth, Thomas Ernst, Florian H. Heidel, Sebastian Scholl, Andreas Hochhaus, and Tino Schenk. 2019. “The Acetyltransferase GCN5 Maintains ATRA-Resistance in Non-APL AML.” *Leukemia* 33(11):2628–39. doi: 10.1038/s41375-019-0581-y.

Kapate, Neha, John R. Clegg, and Samir Mitragotri. 2021. “Non-Spherical Micro- and Nanoparticles for Drug Delivery: Progress over 15 Years.” *Advanced Drug Delivery Reviews* 177:113807. doi: 10.1016/j.addr.2021.05.017.

Khamidullina, Alvina I., Ekaterina A. Varlamova, Nour Alhuda Hammoud, Margarita A. Yastrebova, and Alexandra V. Bruter. 2021. “Gene Transcription as a Therapeutic Target in Leukemia.” *International Journal of Molecular Sciences* 22(14):1–33. doi: 10.3390/ijms22147340.

Khan, Omar F., Piotr S. Kowalski, Joshua C. Doloff, Jonathan K. Tsosie, Vasudevan Bakthavatchalu, Caroline Bodi Winn, Jennifer Haupt, Morgan Jamiel, Robert Langer, and Daniel G. Anderson. 2018. "Endothelial SiRNA Delivery in Nonhuman Primates Using Ionizable Low-Molecular Weight Polymeric Nanoparticles." *Sci. Adv* 4(June):8409–36.

Knudsen, Kristina Bram, Helle Northeved, E. K. Pramod Kumar, Anders Permin, Torben Gjetting, Thomas L. Andresen, Steen Larsen, Karen Malene Wegener, Jens Lykkesfeldt, Kim Jantzen, Steffen Loft, Peter Møller, and Martin Roursgaard. 2015. "In Vivo Toxicity of Cationic Micelles and Liposomes." *Nanomedicine: Nanotechnology, Biology, and Medicine* 11(2):467–77. doi: 10.1016/j.nano.2014.08.004.

Kouchkovsky, I. De, and M. Abdul-Hay. 2016. "'Acute Myeloid Leukemia: A Comprehensive Review and 2016 Update.'" *Blood Cancer Journal* 6(7). doi: 10.1038/bcj.2016.50.

Kowalski, Piotr S., Umberto Capasso Palmiero, Yuxuan Huang, Arnab Rudra, Robert Langer, and Daniel G. Anderson. 2018. "Ionizable Amino-Polyesters Synthesized via Ring Opening Polymerization of Tertiary Amino-Alcohols for Tissue Selective MRNA Delivery." *Advanced Materials* 30(34):1–10. doi: 10.1002/adma.201801151.

Kulkarni, Aditya, Vivek Badwaik, Kyle Defrees, Ryan A. Schuldt, Dinara S. Gunasekera, Cory Powers, Alexander Vlahu, Ross Verheul, and David H. Thompson. 2013. "Effect of Pendant Group on PDNA Delivery by Cationic-β-Cyclodextrin: Alkyl-PVA-PEG Pendant Polymer Complexes." *Biomacromolecules* 15(1):12–19. doi: 10.1021/bm401096v.

Kulkarni, Aditya, Kyle Defrees, Seok Hee Hyun, and David H. Thompson. 2012. "Pendant Polymer:Amino-β-Cyclodextrin:SiRNA Guest:Host Nanoparticles as Efficient Vectors for Gene Silencing." *Journal of the American Chemical Society* 134(18):7596–99. doi: 10.1021/ja300690j.

Kulkarni, Aditya, Kyle Defrees, Ryan A. Schuldt, Alexander Vlahu, Ross Verheul, Seok Hee Hyun, Wei Deng, and David H. Thompson. 2013. "Multi-Armed Cationic Cyclodextrin:Poly(Ethylene Glycol) Polyrotaxanes as Efficient Gene Silencing Vectors." *Integrative Biology (United Kingdom)* 5(1):115–21. doi: 10.1039/c2ib20107k.

Kulkarni, Aditya, Wei Deng, Seok Hee Hyun, and David H. Thompson. 2012. "Development of a Low Toxicity, Effective Pdna Vector Based on Noncovalent Assembly of Bioresponsive Amino-β-Cyclodextrin:Adamantane-Poly(Vinyl Alcohol)-Poly(Ethylene Glycol) Transfection Complexes." *Bioconjugate Chemistry* 23(5):933–40. doi: 10.1021/bc2005158.

Kulkarni J, Darjuan M, Mercer J. et al. 2018. "On the Formation and Morphology of Lipid Nanoparticles Containing Ionizable Cationic Lipids and SiRNA." *ACS Nano* 12(5):4787–95. doi: 10.1021/acsnano.8b01516.

Kulkarni, Jayesh A., Johnathan Layne Myhre, Sam Chen, Yuen Yi C. Tam, Adrian Danescu, Joy M. Richman, and Pieter R. Cullis. 2017. "Design of Lipid Nanoparticles for in Vitro and in Vivo Delivery of Plasmid DNA." *Nanomedicine: Nanotechnology, Biology, and Medicine* 13(4):1377–87. doi:

10.1016/j.nano.2016.12.014.

Kulkarni, Sneha A., and Si-Shen Feng. 2013. “Effects of Particle Size and Surface Modification on Cellular Uptake and Biodistribution of Polymeric Nanoparticles for Drug Delivery.” *Pharmaceutical Research* 30(10):2512–22. doi: 10.1007/s11095-012-0958-3.

Kumar, Ramya, Cristiam F. Santa Chalarca, Matthew R. Bockman, Craig Van Bruggen, Christian J. Grimme, Rishad J. Dalal, McKenna G. Hanson, Joseph K. Hexum, and Theresa M. Reineke. 2021. “Polymeric Delivery of Therapeutic Nucleic Acids.” *Chemical Reviews* 121(18):11527–652. doi: 10.1021/acs.chemrev.0c00997.

Landry, Breanne, Hamidreza Montazeri Aliabadi, Anuja Samuel, Hilal Gül-Uludağ, Xiaoyan Jiang, Olaf Kutsch, and Hasan Uludağ. 2012. “Effective Non-Viral Delivery of SiRNA to Acute Myeloid Leukemia Cells with Lipid-Substituted Polyethylenimines.” *PLoS ONE* 7(8). doi: 10.1371/journal.pone.0044197.

Lebedinskiy, Konstantin, Volodymyr Lobaz, and Jindřich Jindřich. 2022. “Preparation of β-Cyclodextrin-Based Dimers with Selectively Methylated Rims and Their Use for Solubilization of Tetracene.” *Beilstein Journal of Organic Chemistry* 18:1596–1606. doi: 10.3762/bjoc.18.170.

Lee, Dian Jang, Eva Kessel, Taavi Lehto, Xueying Liu, Naoto Yoshinaga, Kärt Padari, Ying Chen Chen, Susanne Kempter, Satoshi Uchida, Joachim O. Rädler, Margus Pooga, Ming Thau Sheu, Kazunori Kataoka, and Ernst Wagner. 2017. “Systemic Delivery of Folate-PEG SiRNA Lipopolyplexes with Enhanced Intracellular Stability for in Vivo Gene Silencing in Leukemia.” *Bioconjugate Chemistry* 28(9):2393–2409. doi: 10.1021/acs.bioconjchem.7b00383.

Li, Feng-Qing, Qi-Lin Yu, Yao-Hua Liu, Hua-Jiang Yu, Yong Chen, and Yu Liu. 2020. “Highly Efficient Photocontrolled Targeted Delivery of SiRNA by a Cyclodextrin-Based Supramolecular Nanoassembly.” *Chemical Communications* 56(27):3907–10. doi: 10.1039/d0cc00629g.

Li, Jin-Ming, Yuan-Yuan Wang, Wei Zhang, Hua Su, Liang-Nian Ji, and Zong-Wan Mao. 2013. “Low-Weight Polyethylenimine Cross-Linked 2-Hydroxypopyl-β-Cyclodextrin and Folic Acid as an Efficient and Nontoxic SiRNA Carrier for Gene Silencing and Tumor Inhibition by VEGF SiRNA.” *International Journal of Nanomedicine* 8:2101–17. doi: 10.2147/IJN.S42440.

Li, Junjie, and Kazunori Kataoka. 2021. “Chemo-Physical Strategies to Advance the in Vivo Functionality of Targeted Nanomedicine: The Next Generation.” *Journal of the American Chemical Society* 143(2):538–59. doi: 10.1021/jacs.0c09029.

Li, Man, Mengnan Zhao, Yao Fu, You Li, Tao Gong, Zhirong Zhang, and Xun Sun. 2016. “Enhanced Intranasal Delivery of MRNA Vaccine by Overcoming the Nasal Epithelial Barrier via Intra- A Nd Paracellular Pathways.” *Journal of Controlled Release* 228:9–19. doi: 10.1016/j.jconrel.2016.02.043.

Li, Xuebing, Junda Liu, and Neng Qiu. 2023. “Cyclodextrin-Based Polymeric Drug Delivery Systems for Cancer Therapy.” *Polymers* 15(6):1400. doi: 10.3390/polym15061400.

Liu, Xuan, Xiaohong Chen, Ming Xuan Chua, Zibiao Li, Xian Jun Loh, and Yun Long

Wu. 2017. “Injectable Supramolecular Hydrogels as Delivery Agents of Bcl-2 Conversion Gene for the Effective Shrinkage of Therapeutic Resistance Tumors.” *Advanced Healthcare Materials* 6(11):1–11. doi: 10.1002/adhm.201700159.

Liu, Yao-Hua, and Yu Liu. 2022. “Highly Effective Gene Delivery Based on Cyclodextrin Multivalent Assembly in Target Cancer Cells.” *Journal of Materials Chemistry B* 10(6):958–65. doi: 10.1039/d1tb02585f.

Liu, Zongjian, Lin Ye, Jianing Xi, Jin Wang, and Zeng-guo Feng. 2021. “Cyclodextrin Polymers: Structure, Synthesis, and Use as Drug Carriers.” *Progress in Polymer Science* 118:101408. doi: 10.1016/j.progpolymsci.2021.101408.

Loh, Xian-Jun, and Yun-Long Wu. 2015. “Cationic Star Copolymers Based on β-Cyclodextrins for Efficient Gene Delivery to Mouse Embryonic Stem Cell Colonies.” *Chemical Communications* 51(54):10815–18. doi: 10.1039/c5cc03686k.

LoPresti, Samuel T., Mariah L. Arral, Namit Chaudhary, and Kathryn A. Whitehead. 2022. “The Replacement of Helper Lipids with Charged Alternatives in Lipid Nanoparticles Facilitates Targeted MRNA Delivery to the Spleen and Lungs.” *Journal of Controlled Release* 345:819–31. doi: 10.1016/j.jconrel.2022.03.046.

Malanga, Milo, Mihály Bálint, István Puskás, Kata Tuza, Tamás Sohajda, László Jicsinszky, Lajos Szente, and Éva Fenyvesi. 2014. “Synthetic Strategies for the Fluorescent Labeling of Epichlorohydrin-Branched Cyclodextrin Polymers.” *Beilstein Journal of Organic Chemistry* 10:3007–18. doi: 10.3762/bjoc.10.319.

Manzanares, Darío, Ingrid Araya-Durán, Laura Gallego- Yerga, Pablo Játiva, Valeria Márquez-Miranda, Jonathan Canan, José Luis, Jiménez Blanco, Carmen Ortiz Mellet, Fernando Danilo González-Nilo, José Manuel García Fernández7, and &. Valentín Ceña. 2017. “Molecular Determinants for Cyclo- Mediated Effective SiRNA Transfection.” *Nanomedicine* 12:1607–21.

Manzanares, Darío, María Dolores Pérez-Carrión, José Luis Jiménez Blanco, Carmen Ortiz Mellet, José Manuel García Fernández, and Valentín Ceña. 2020. “Cyclodextrin-Based Nanostructure Efficiently Delivers Sirna to Glioblastoma Cells Preferentially via Macropinocytosis.” *International Journal of Molecular Sciences* 21(23):1–17. doi: 10.3390/ijms21239306.

Martínez, Álvaro, Céline Bienvenu, José L. Jiménez Blanco, Pierre Vierling, Carmen Ortiz Mellet, José M. García Fernández, and Christophe Di Giorgio. 2013. “Amphiphilic Oligoethyleneimine-β-Cyclodextrin ‘Click’ Clusters for Enhanced DNA Delivery.” *Journal of Organic Chemistry* 78(16):8143–48. doi: 10.1021/jo400993y.

Martins, Grazieli Olinda, Maicon Segalla Petrônio, Aline Margarete Furuyama Lima, André Miguel Martinez Junior, Vera Aparecida de Oliveira Tiera, Marília de Freitas Calmon, Patricia Simone Leite Vilamaior, Sang Won Han, and Marcio José Tiera. 2019. “Amphipathic Chitosans Improve the Physicochemical Properties of SiRNA-Chitosan Nanoparticles at Physiological Conditions.” *Carbohydrate Polymers* 216(March):332–42. doi: 10.1016/j.carbpol.2019.03.098.

Mavridis, Irene M., and Konstantina Yannakopoulou. 2015. “Anionic Cyclodextrins as Versatile Hosts for Pharmaceutical Nanotechnology: Synthesis, Drug Delivery, Enantioselectivity, Contrast Agents for MRI.” *International Journal of Pharmaceutics* 492(1–2):275–90. doi: 10.1016/j.ijpharm.2015.06.004.

McCarthy, J., M. J. O’Neill, L. Bourre, D. Walsh, A. Quinlan, G. Hurley, J. Ogier, F. Shanahan, S. Melgar, R. Darcy, and C. M. O’Driscoll. 2013. “Gene Silencing of TNF-Alpha in a Murine Model of Acute Colitis Using a Modified Cyclodextrin Delivery System.” *Journal of Controlled Release* 168(1):28–34. doi: 10.1016/j.jconrel.2013.03.004.

McMahon, A., E. Gomez, R. Donohue, D. Forde, R. Darcy, and Caitriona M. O’Driscoll. 2008. “Cyclodextrin Gene Vectors: Cell Trafficking and the Influence of Lipophilic Chain Length.” *Journal of Drug Delivery Science and Technology* 18(5):303–7. doi: 10.1016/S1773-2247(08)50060-8.

McMahon, Anthony, Martin J. O’Neill, Eva Gomez, Ruth Donohue, Damien Forde, Raphael Darcy, and Caitriona M. O’Driscoll. 2012. “Targeted Gene Delivery to Hepatocytes with Galactosylated Amphiphilic Cyclodextrins.” *Journal of Pharmacy and Pharmacology* 64(8):1063–73. doi: 10.1111/j.2042-7158.2012.01497.x.

Méndez-Ardoy, Alejandro, Alejandro Díaz-Moscoso, Carmen Ortiz Mellet, Christophe Di Giorgio, Pierre Vierling, Juan M. Benito, and José M. García Fernández. 2015. “Harmonized Tuning of Nucleic Acid and Lectin Binding Properties with Multivalent Cyclodextrins for Macrophage-Selective Gene Delivery.” *RSC Advances* 5(93):76464–71. doi: 10.1039/c5ra16087a.

Méndez-Ardoy, Alejandro, Nicolas Guilloteau, Christophe Di Giorgio, Pierre Vierling, Francisco Santoyo-González, Carmen Ortiz Mellet, and José M. García Fernández. 2011. “β-Cyclodextrin-Based Polycationic Amphiphilic ‘Click’ Clusters: Effect of Structural Modifications in Their DNA Complexing and Delivery Properties.” *Journal of Organic Chemistry* 76(15):5882–94. doi: 10.1021/jo2007785.

Méndez-Ardoy, Alejandro, Koldo Urbiola, Cristina Aranda, Carmen Ortiz-Mellet, José Manuel Garca-Fernndez, and Conchita Tros De Ilarduya. 2011. “Polycationic Amphiphilic Cyclodextrin-Based Nanoparticles for Therapeutic Gene Delivery.” *Nanomedicine* 6(10):1697–1707. doi: 10.2217/nnm.11.59.

Mendonça, Monique C. P., Michael F. Cronin, John F. Cryan, and Caitriona M. O’Driscoll. 2021. “Modified Cyclodextrin-Based Nanoparticles Mediated Delivery of SiRNA for Huntingtin Gene Silencing across an in Vitro BBB Model.” *European Journal of Pharmaceutics and Biopharmaceutics* 169(October):309–18. doi: 10.1016/j.ejpb.2021.11.003.

Mendonça, Monique C. P., Ayse Kont, Maria Rodriguez Aburto, John F. Cryan, and Caitriona M. O’Driscoll. 2021. “Advances in the Design of (Nano)Formulations for Delivery of Antisense Oligonucleotides and Small Interfering RNA: Focus on the Central Nervous System.” *Molecular Pharmaceutics* 18(4):1491–1506. doi: 10.1021/acs.molpharmaceut.0c01238.

Mendonça, Monique C.P., Ayse Kont, Piotr S. Kowalski, and Caitriona M. O’Driscoll. 2023. “Design of Lipid-Based Nanoparticles for Delivery of Therapeutic Nucleic

Acids.” *Drug Discovery Today* 28(3). doi: 10.1016/j.drudis.2023.103505.

Mendonça, Monique C. P., Yao Sun, Michael F. Cronin, Andrew J. Lindsay, and Caitriona M. O’Driscoll. 2023. “Cyclodextrin-Based Nanoparticles for Delivery of Antisense Oligonucleotides Targeting Huntingtin.” *Pharmaceutics*.

Mishra, Swaroop, Jeremy D. Heidel, Paul Webster, and Mark E. Davis. 2006. “Imidazole Groups on a Linear, Cyclodextrin-Containing Polycation Produce Enhanced Gene Delivery via Multiple Processes.” *Journal of Controlled Release* 116(2 SPEC. ISS.):179–91. doi: 10.1016/j.jconrel.2006.06.018.

Mohammed, Ahmed Fouad Abdelwahab, Taishi Higashi, Keiichi Motoyama, Ayumu Ohyama, Risako Onodera, Khaled Ali Khaled, Hatem Abdelmonsef Sarhan, Amal Kamal Hussein, and Hidetoshi Arima. 2019. “In Vitro and In Vivo Co-Delivery of SiRNA and Doxorubicin by Folate-PEG-Appended Dendrimer/Glucuronylglucosyl-β-Cyclodextrin Conjugate.” *AAPS Journal* 21(4):1–10. doi: 10.1208/s12248-019-0327-9.

Monfared, Yousef Khazaei, Mohammad Mahmoudian, Claudio Cecone, Fabrizio Caldera, Sanya Haiaty, Hamid Reza Heidari, Reza Rahbarghazi, Adrián Matencio, Parvin Zakeri-Milani, and Francesco Trotta. 2022. “Hyper-Branched Cationic Cyclodextrin Polymers for Improving Plasmid Transfection in 2D and 3D Spheroid Cells.” *Pharmaceutics* 14(12). doi: 10.3390/pharmaceutics14122690.

Monfared, Yousef Khazaei, Mohammad Mahmoudian, Parvin Zakeri-Milani, Claudio Cecone, Tomoya Hayashi, Ken J. Ishii, João Conde, Adrián Matencio, and Francesco Trotta. 2023. “Intratumoural Delivery of MRNA Loaded on a Cationic Hyper-Branched Cyclodextrin-Based Polymer Induced an Anti-Tumour Immunological Response in Melanoma.” *Cancers* 15(14). doi: 10.3390/cancers15143748.

Moore, Thomas L., Laura Rodriguez-Lorenzo, Vera Hirsch, Sandor Balog, Dominic Urban, Corinne Jud, Barbara Rothen-Rutishauser, Marco Lattuada, and Alke Petri-Fink. 2015. “Nanoparticle Colloidal Stability in Cell Culture Media and Impact on Cellular Interactions.” *Chemical Society Reviews* 44(17):6287–6305. doi: 10.1039/c4cs00487f.

Namazi, Hasan. 2017. “Polymers in Our Daily Life.” *BioImpacts* 7(2):73–74. doi: 10.15171/bi.2017.09.

Neefjes, M., B. A. C. Housmans, G. G. H. van den Akker, L. W. van Rhijn, T. J. M. Welting, and P. M. van der Kraan. 2021. “Reporter Gene Comparison Demonstrates Interference of Complex Body Fluids with Secreted Luciferase Activity.” *Scientific Reports* 11(1):1–13. doi: 10.1038/s41598-020-80451-6.

Neva, Tania, Ana I. Carbajo-Gordillo, Juan M. Benito, Hugo Lana, Gema Marcelo, Carmen Ortiz Mellet, Conchita Tros de Ilarduya, Francisco Mendicuti, and José M. García Fernández. 2020. “Tuning the Topological Landscape of DNA–Cyclodextrin Nanocomplexes by Molecular Design.” *Chemistry - A European Journal* 26(66):15259–69. doi: 10.1002/chem.202002951.

Neva, Tania, Thais Carmona, Juan M. Benito, Cédric Przybylski, Carmen Ortiz Mellet, Francisco Mendicuti, and José M. García Fernández. 2018. “Xylylene

Clips for the Topology-Guided Control of the Inclusion and Self-Assembling Properties of Cyclodextrins." *Journal of Organic Chemistry* 83(10):5588–97. doi: 10.1021/acs.joc.8b00602.

O'Mahony, A.M., D. Doyle, R. Darcy, J. F. Cryan, and C. M. O'Driscoll. 2012. "Characterisation of Cationic Amphiphilic Cyclodextrins for Neuronal Delivery of SiRNA: Effect of Reversing Primary and Secondary Face Modifications." *European Journal of Pharmaceutical Sciences* 47(5):896–903. doi: 10.1016/j.ejps.2012.08.020.

O'Mahony, A. M., B. M. D. C. Godinho, J. Ogier, M. Devocelle, R. Darcy, J. F. Cryan, and C. M. O'Driscoll. 2012. "Click-Modified Cyclodextrins as Nonviral Vectors for Neuronal SiRNA Delivery." *ACS Chemical Neuroscience* 3(10):744–52. doi: 10.1021/cn3000372.

O'Mahony, Aoife M., Michael F. Cronin, Anthony McMahon, James C. Evans, Kathleen Daly, Raphael Darcy, and Caitriona M. O'Driscoll. 2014. "Biophysical and Structural Characterisation of Nucleic Acid Complexes with Modified Cyclodextrins Using Circular Dichroism." *Journal of Pharmaceutical Sciences* 103(5):1346–55. doi: 10.1002/jps.23922.

O'Mahony, Aoife M., Stephane Desgranges, Julien Ogier, Aoife Quinlan, Marc Devocelle, Raphael Darcy, John F. Cryan, and Caitriona M. O'Driscoll. 2013. "In Vitro Investigations of the Efficacy of Cyclodextrin-SiRNA Complexes Modified with Lipid-PEG-Octaarginine: Towards a Formulation Strategz for Non-Viral Neuronal SiRNA Delivery." *Pharmaceutical Research* 30(4):1086–98.

O'Mahony, Aoife M., Martin J. O'Neill, Bruno M. D. C. Godinho, Raphael Darcy, John F. Cryan, and Caitriona M. O'Driscoll. 2012. "Cyclodextrins for Non-Viral Gene and SiRNA Delivery." *Pharmaceutical Nanotechnology* 1(1):6–14. doi: 10.2174/22117385130105.

O'Mahony, Aoife M., Julien Ogier, Raphael Darcy, John F. Cryan, and Caitriona M. O'Driscoll. 2013. "Cationic and PEGylated Amphiphilic Cyclodextrins: Co-Formulation Opportunities for Neuronal Sirna Delivery." *PLoS ONE* 8(6). doi: 10.1371/journal.pone.0066413.

O'Mahony, Aoife M., Julien Ogier, Stephane Desgranges, John F. Cryan, Raphael Darcy, and Caitriona M. O'Driscoll. 2012. "A Click Chemistry Route to 2-Functionalised PEGylated and Cationic β-Cyclodextrins: Co-Formulation Opportunities for SiRNA Delivery." *Organic and Biomolecular Chemistry* 10(25):4954–60. doi: 10.1039/c2ob25490e.

O'Neill, Martin J., Jianfeng Guo, Colin Byrne, Raphael Darcy, and Caitriona M. O' Driscoll. 2011. "Mechanistic Studies on the Uptake and Intracellular Trafficking of Novel Cyclodextrin Transfection Complexes by Intestinal Epithelial Cells." *International Journal of Pharmaceutics* 413(1–2):174–83. doi: 10.1016/j.ijpharm.2011.04.021.

Ooya, Tooru, Hak Soo Choi, Atsushi Yamashita, Nobuhiko Yui, Yuko Sugaya, Arihiro Kano, Atsushi Maruyama, Hidetaka Akita, Rie Ito, Kentaro Kogure, and Hideyoshi Harashima. 2006. "Biocleavable Polyrotaxane-Plasmid DNA Polyplex for Enhanced Gene Delivery." *Journal of the American Chemical*

Society 128(12):3852–53. doi: 10.1021/ja055868+.

Ortega-Caballero, Fernando, Carmen Ortiz Mellet, Loïc Le Gourriérec, Nicolas Guilloteau, Christophe Di Giorgio, Pierre Vierling, Jacques Defaye, and José M. García Fernéndez. 2008. "Tailoring β-Cyclodextrin for DNA Complexation and Delivery by Homogeneous Functionalization at the Secondary Face." *Organic Letters* 10(22):5143–46. doi: 10.1021/ol802081z.

Păduraru, Dan Nicolae, Adelina Gabriela Niculescu, Alexandra Bolocan, Octavian Andronic, Alexandru Mihai Grumezescu, and Rodica Bîrlă. 2022. "An Updated Overview of Cyclodextrin-Based Drug Delivery Systems for Cancer Therapy." *Pharmaceutics* 14(8). doi: 10.3390/pharmaceutics14081748.

Patel, Pratikkumar, Nurudeen Mohammed Ibrahim, and Kun Cheng. 2021. "The Importance of Apparent PKa in the Development of Nanoparticles Encapsulating SiRNA and MRNA." *Trends in Pharmacological Sciences* 42(6):448–60. doi: 10.1016/j.tips.2021.03.002.

Pflueger, Iris, Coralie Charrat, Carmen Ortiz Mellet, José M. García Fernández, Christophe Di Giorgio, and Juan M. Benito. 2016. "Cyclodextrin-Based Facial Amphiphiles: Assessing the Impact of the Hydrophilic-Lipophilic Balance in the Self-Assembly, DNA Complexation and Gene Delivery Capabilities." *Organic and Biomolecular Chemistry* 14(42):10037–49. doi: 10.1039/c6ob01882c.

Phan, Hoa T., and Amanda J. Haes. 2019. "What Does Nanoparticle Stability Mean? HHS Public Access." *J Phys Chem C Nanomater Interfaces* 123(27):16495–507. doi: 10.1021/acs.jpcc.9b00913.What.

Ping, Yuan, Qida Hu, Guping Tang, and Jun Li. 2013. "FGFR-Targeted Gene Delivery Mediated by Supramolecular Assembly between β-Cyclodextrin-Crosslinked PEI and Redox-Sensitive PEG." *Biomaterials* 34(27):6482–94. doi: 10.1016/j.biomaterials.2013.03.071.

Plesselova, Simona, Pablo Garcia-Cerezo, Victor Blanco, Francisco J. Reche-Perez, Fernando Hernandez-Mateo, Francisco Santoyo-Gonzalez, María Dolores Giron-Gonzalez, and Rafael Salto-Gonzalez. 2021. "Polyethylenimine-Bisphosphonate-Cyclodextrin Ternary Conjugates: Supramolecular Systems for the Delivery of Antineoplastic Drugs." *Journal of Medicinal Chemistry* 64(16):12245–60. doi: 10.1021/acs.jmedchem.1c00887.

Poggetto, Giovanni Dal, Salvatore Simone Troise, Salvatore Simone Troise, Claudia Conte, Roberta Marchetti, Francesca Moret, Alfonso Iadonisi, Alba Silipo, Rosa Lanzetta, Mario Malinconico, Fabiana Quaglia, and Paola Laurienzo. 2020. "Nanoparticles Decorated with Folate Based on a Site-Selective AcD-Rotaxanated PEG-: B -PCL Copolymer for Targeted Cancer Therapy." *Polymer Chemistry* 11(23):3892–3903. doi: 10.1039/d0py00158a.

Pun, Suzie H., Nathalie C. Bellocq, Aijie Liu, Greg Jensen, Todd Machemer, Erlinda Quijano, Thomas Schluep, Shufen Wen, Heidrun Engler, Jeremy Heidel, and Mark E. Davis. 2004. "Cyclodextrin-Modified Polyethylenimine Polymers for Gene Delivery." *Bioconjugate Chemistry* 15(4):831–40. doi: 10.1021/bc049891g.

Qian, Yanping, Xiao Liang, Jingyun Yang, Chengjian Zhao, Wen Nie, Li Liu, Tao Yi,

Yu Jiang, Jia Geng, Xia Zhao, and Xiawei Wei. 2018. “Hyaluronan Reduces Cationic Liposome-Induced Toxicity and Enhances the Antitumor Effect of Targeted Gene Delivery in Mice.” *ACS Applied Materials and Interfaces* 10(38):32006–16. doi: 10.1021/acsami.8b12393.

Raja, Maria Abdul Ghafoor, Haliza Katas, and Thum Jing Wen. 2015. “Stability, Intracellular Delivery, and Release of SiRNA from Chitosan Nanoparticles Using Different Cross-Linkers.” *PLoS ONE* 10(6):1–19. doi: 10.1371/journal.pone.0128963.

Raval, Nidhi, Hardi Jogi, Piyush Gondaliya, Kiran Kalia, and Rakesh K. Tekade. 2019. “Method and Its Composition for Encapsulation, Stabilization, and Delivery of SiRNA in Anionic Polymeric Nanoplex: An In Vitro- In Vivo Assessment.” *Scientific Reports* 9(1):1–18. doi: 10.1038/s41598-019-52390-4.

Rehman, Urushi, Neha Parveen, Afsana Sheikh, Mohammed A. S. Abourehab, Amirhossein Sahebkar, and Prashant Kesharwani. 2022. “Polymeric Nanoparticles-SiRNA as an Emerging Nano-Polyplexes against Ovarian Cancer.” *Colloids and Surfaces B: Biointerfaces* 218(June):112766. doi: 10.1016/j.colsurfb.2022.112766.

Richtering, Walter, Irina Alberg, and Rudolf Zentel. 2020. “Nanoparticles in the Biological Context:Surface Morphology and Protein Corona Formation.” *Small* 16(39):1–8. doi: 10.1002/smll.202002162.

Rizvi, Syed A. A., and Ayman M. Saleh. 2018. “Applications of Nanoparticle Systems in Drug Delivery Technology.” *Saudi Pharmaceutical Journal* 26(1):64–70. doi: 10.1016/j.jsps.2017.10.012.

Ryzhakov, Alexey, Thao Do Thi, Jef Stappaerts, Laura Bertoletti, Kristof Kimpe, André Rodrigues Sá Couto, Phennapha Saokham, Guy Van den Mooter, Patrick Augustijns, Govert W. Somsen, Sergey Kurkov, Sabine Inghelbrecht, Albertina Arien, M. Ilias Jimidar, Koen Schrijnemakers, and Thorsteinn Loftsson. 2016. “Self-Assembly of Cyclodextrins and Their Complexes in Aqueous Solutions.” *Journal of Pharmaceutical Sciences* 105(9):2556–69. doi: 10.1016/j.xphs.2016.01.019.

Sahu, Kantrol Kumar, Madhulika Pradhan, Deependra Singh, Manju Rawat Singh, and Krishna Yadav. 2023. “Non-Viral Nucleic Acid Delivery Approach: A Boon for State-of-the-Art Gene Delivery.” *Journal of Drug Delivery Science and Technology* 80(December 2022):104152. doi: 10.1016/j.jddst.2023.104152.

Sandilya, Avilasha A., Upendra Natarajan, and M. Hamsa Priya. 2020. “Molecular View into the Cyclodextrin Cavity: Structure and Hydration.” *ACS Omega* 5(40):25655–67. doi: 10.1021/acsomega.0c02760.

Setten, Ryan L., John J. Rossi, and Si-ping Han. 2019. “The Current State and Future Directions of RNAi-Based Therapeutics.” *Nature Reviews Drug Discovery* 18(June):421–46. doi: 10.1038/s41573-019-0017-4.

Shi, Liwang, Jinqiu Zhang, Man Zhao, Shukun Tang, Xu Cheng, Wenyuan Zhang, Wenhua Li, Xiaoying Liu, Haisheng Peng, and Qun Wang. 2021. “Effects of Polyethylene Glycol on the Surface of Nanoparticles for Targeted Drug Delivery.” *Nanoscale* 13(24):10748–64. doi: 10.1039/d1nr02065j.

Shibaguchi, Kai, Atsushi Tamura, Masahiko Terauchi, Mitsuaki Matsumura, Hiroyuki Miura, and Nobuhiko Yui. 2019. "Mannosylated Polyrotaxanes for Increasing Cellular Uptake Efficiency in Macrophages through Receptor-Mediated Endocytosis." *Molecules* 24(3). doi: 10.3390/molecules24030439.

Sindhwani, Shrey, Abdullah Muhammad Syed, Jessica Ngai, Benjamin R. Kingston, Laura Maiorino, Jeremy Rothschild, Presley MacMillan, Yuwei Zhang, Netra Unni Rajesh, Tran Hoang, Jamie L. Y. Wu, Stefan Wilhelm, Anton Zilman, Suresh Gadde, Andrew Sulaiman, Ben Ouyang, Zachary Lin, Lisheng Wang, Mikala Egeblad, and Warren C. W. Chan. 2020. "The Entry of Nanoparticles into Solid Tumours." *Nature Materials* 19(5):566–75. doi: 10.1038/s41563-019-0566-2.

Singh, Raghvendra Pratap, Tania Hidalgo, Pierre Andre Cazade, Raphael Darcy, Michael F. Cronin, Irina Dorin, Caitríona M. O'Driscoll, and Damien Thompson. 2019. "Self-Assembled Cationic β-Cyclodextrin Nanostructures for SiRNA Delivery." *Molecular Pharmaceutics* 16(3):1358–66. doi: 10.1021/acs.molpharmaceut.8b01307.

Song, Hai Qing, Yu Qi, Rui Quan Li, Gang Cheng, Nana Zhao, and Fu Jian Xu. 2018. "High-Performance Cationic Polyrotaxanes Terminated with Polypeptides as Promising Nucleic Acid Delivery Systems." *Polymer Chemistry* 9(17):2281–89. doi: 10.1039/c8py00333e.

Sukegawa, Takeshi, Tetsuya Furuike, Kenichi Niikura, Akihiko Yamagishi, Kenji Monde, and Shin Ichiro Nishimura. 2002. "Erythrocyte-like Liposomes Prepared by Means of Amphiphilic Cyclodextrin Sulfates." *Chemical Communications* 2(5):430–31. doi: 10.1039/b110673b.

Sun, Tianmeng, Yu Shrike Zhang, Bo Pang, Dong Choon Hyun, Miaoxin Yang, and Younan Xia. 2014. "Engineered Nanoparticles for Drug Delivery in Cancer Therapy." *Angewandte Chemie - International Edition* 53(46):12320–64. doi: 10.1002/anie.201403036.

Sun, Yao, Michael F. Cronin, Monique C. P. Mendonça, Jianfeng Guo, and Caitriona M. O'Driscoll. 2023. "Sialic Acid-Targeted Cyclodextrin-Based Nanoparticles Deliver CSF-1R SiRNA and Reprogram Tumour-Associated Macrophages for Immunotherapy of Prostate Cancer." *European Journal of Pharmaceutical Sciences* 185(January):106427. doi: 10.1016/j.ejps.2023.106427.

Sung, Hyuna, Jacques Ferlay, Rebecca L. Siegel, Mathieu Laversanne, Isabelle Soerjomataram, Ahmedin Jemal, and Freddie Bray. 2021. "Global Cancer Statistics 2020: GLOBOCAN Estimates of Incidence and Mortality Worldwide for 36 Cancers in 185 Countries." *CA: A Cancer Journal for Clinicians* 71(3):209–49. doi: 10.3322/caac.21660.

Symens, Nathalie, Alejandro Méndez-Ardoy, Alejandro Díaz-Moscoso, Elena Sánchez-Fernández, Katrien Remaut, Joseph Demeester, José M. Garcí. Fernández, Stefaan C. De Smedt, and Joanna Rejman. 2012. "Efficient Transfection of Hepatocytes Mediated by MRNA Complexed to Galactosylated Cyclodextrins." *Bioconjugate Chemistry* 23(6):1276–89. doi: 10.1021/bc3001003.

Thomsen, Hanna, Gábor Benkovics, Éva Fenyvesi, Anne Farewell, Milo Malanga,

and Marica B. Ericson. 2017. “Delivery of Cyclodextrin Polymers to Bacterial Biofilms — An Exploratory Study Using Rhodamine Labelled Cyclodextrins and Multiphoton Microscopy.” *International Journal of Pharmaceutics* 531(2):650–57. doi: 10.1016/j.ijpharm.2017.06.011.

Torre, Cristina de la, Pablo Játiva, Inmaculada Posadas, Darío Manzanares, José L. Jiménez Blanco, Carmen Ortiz Mellet, José Manuel García Fernández, and Valentín Ceña. 2022. “A β-Cyclodextrin-Based Nanoparticle with Very High Transfection Efficiency Unveils SiRNA-Activated TLR3 Responses in Human Prostate Cancer Cells.” *Pharmaceutics* 14(11). doi: 10.3390/pharmaceutics14112424.

Tyner, Jeffrey W., Cristina E. Tognon, Daniel Bottomly, Beth Wilmot, Stephen E. Kurtz, Samantha L. Savage, Nicola Long, Anna Reister Schultz, Elie Traer, Melissa Abel, Anupriya Agarwal, Aurora Blucher, Uma Borate, Jade Bryant, Russell Burke, Amy Carlos, Richie Carpenter, Joseph Carroll, Bill H. Chang, Cody Coblentz, Amanda d’Almeida, Rachel Cook, Alexey Danilov, Kim Hien T. Dao, Michie Degnin, Deirdre Devine, James Dibb, David K. Edwards, Christopher A. Eide, Isabel English, Jason Glover, Rachel Henson, Hibery Ho, Abdusebur Jemal, Kara Johnson, Ryan Johnson, Brian Junio, Andy Kaempf, Jessica Leonard, Chenwei Lin, Selina Qiuying Liu, Pierrette Lo, Marc M. Loriaux, Samuel Luty, Tara Macey, Jason MacManiman, Jacqueline Martinez, Motomi Mori, Dylan Nelson, Ceilidh Nichols, Jill Peters, Justin Ramsdill, Angela Rofelty, Robert Schuff, Robert Searles, Erik Segerdell, Rebecca L. Smith, Stephen E. Spurgeon, Tyler Sweeney, Aashis Thapa, Corinne Visser, Jake Wagner, Kevin Watanabe-Smith, Kristen Werth, Joelle Wolf, Libbey White, Amy Yates, Haijiao Zhang, Christopher R. Cogle, Robert H. Collins, Denise C. Connolly, Michael W. Deininger, Leylah Drusbosky, Christopher S. Hourigan, Craig T. Jordan, Patricia Kropf, Tara L. Lin, Micaela E. Martinez, Bruno C. Medeiros, Rachel R. Pallapati, Daniel A. Pollyea, Ronan T. Swords, Justin M. Watts, Scott J. Weir, David L. Wiest, Ryan M. Winters, Shannon K. McWeeney, and Brian J. Druker. 2018. “Functional Genomic Landscape of Acute Myeloid Leukaemia.” *Nature* 562(7728):526–31. doi: 10.1038/s41586-018-0623-z.

Uebbing, Lukas, Antje Ziller, Christian Siewert, Martin A. Schroer, Clement E. Blanchet, Dmitri I. Svergun, Srinivas Ramishetti, Dan Peer, Ugur Sahin, Heinrich Haas, and Peter Langguth. 2020. “Investigation of PH-Responsiveness inside Lipid Nanoparticles for Parenteral MRNA Application Using Small-Angle X-Ray Scattering.” *Langmuir* 36(44):13331–41. doi: 10.1021/acs.langmuir.0c02446.

Uekama, Kaneto, Fumitoshi Hirayama, and Tetsumi Irie. 1998. “Cyclodextrin Drug Carrier Systems.” *Chemical Reviews* 98(5):2045–76. doi: 10.1021/cr970025p.

Vader, Pieter, Leonardus J. Van Der Aa, Johan F. J. Engbersen, Gert Storm, and Raymond M. Schiffelers. 2012. “Physicochemical and Biological Evaluation of SiRNA Polyplexes Based on PEGylated Poly(Amido Amine)S.” *Pharmaceutical Research* 29(2):352–61. doi: 10.1007/s11095-011-0545-z.

Vermeulen, Lotte M. P., Stefaan C. De Smedt, Katrien Remaut, and Kevin Braeckmans. 2018. “The Proton Sponge Hypothesis: Fable or Fact?” *European Journal of Pharmaceutics and Biopharmaceutics* 129(May):184–90. doi: 10.1016/j.ejpb.2018.05.034.

Villari, Valentina, Antonino Mazzaglia, Raphael Darcy, Caitriona M. O'Driscoll, and Norberto Micali. 2013. "Nanostructures of Cationic Amphiphilic Cyclodextrin Complexes with DNA." *Biomacromolecules* 14(3):811–17. doi: 10.1021/bm3018609.

Wang, Lu, Nicolas Hartel, Kaixuan Ren, Nicholas Alexander Graham, and Noah Malmstadt. 2020. "Effect of Protein Corona on Nanoparticle-Plasma Membrane and Nanoparticle-Biomimetic Membrane Interactions." *Environmental Science: Nano* 7(3):963–74. doi: 10.1039/d0en00035c.

Wei, Dan, Kai Pang, Qingxiang Song, Yuanzhen Suo, Hao He, Xiaofu Weng, Xiaoling Gao, and Xunbin Wei. 2018. "Noninvasive Monitoring of Nanoparticle Clearance and Aggregation in Blood Circulation by in Vivo Flow Cytometry." *Journal of Controlled Release* 278(April):66–73. doi: 10.1016/j.jconrel.2018.03.024.

Whitehead, Kathryn A., Robert Langer, and Daniel G. Anderson. 2009. "Knocking down Barriers: Advances in SiRNA Delivery." *Nature Reviews Drug Discovery* 8(2):129–38. doi: 10.1038/nrd2742.

Whiteley, Andrew E., Trevor T. Price, Gaia Cantelli, and Dorothy A. Sipkins. 2021. "Leukaemia: A Model Metastatic Disease." *Nature Reviews Cancer* 21(7):461–75. doi: 10.1038/s41568-021-00355-z.

Witzigmann, Dominik, Jayesh A. Kulkarni, Jerry Leung, Sam Chen, Pieter R. Cullis, and Roy Van Der Meel. 2020. "Lipid Nanoparticle Technology for Therapeutic Gene Regulation in the Liver." *Advanced* (January).

Wong, Li Yen, Bingzhao Xia, Ernst Wolvetang, and Justin Cooper-White. 2018. "Targeted, Stimuli-Responsive Delivery of Plasmid DNA and MiRNAs Using a Facile Self-Assembled Supramolecular Nanoparticle System." *Biomacromolecules* 19(2):353–63. doi: 10.1021/acs.biomac.7b01462.

Wright, Kyle J., Vivek D. Badwaik, Shayak Samaddar, Seok Hee Hyun, Kristof Glauninger, Taeyoon Eom, and David H. Thompson. 2018. "Organocatalytic Synthesis and Evaluation of Polycarbonate Pendant Polymer:β-Cyclodextrin-Based Nucleic Acid Delivery Vectors." *Macromolecules* 51(3):670–78. doi: 10.1021/acs.macromol.7b02293.

Wu, Jun. 2021. "The Enhanced Permeability and Retention (Epr) Effect: The Significance of the Concept and Methods to Enhance Its Application." *Journal of Personalized Medicine* 11(8). doi: 10.3390/jpm11080771.

Xu, Fan, Huihai Zhong, Ya Chang, Dongdong Li, Hongyue Jin, Meng Zhang, Huiyuan Wang, Chen Jiang, Youqing Shen, and Yongzhuo Huang. 2018. "Targeting Death Receptors for Drug-Resistant Cancer Therapy: Codelivery of PTRAIL and Monensin Using Dual-Targeting and Stimuli-Responsive Self-Assembling Nanocomposites." *Biomaterials* 158:56–73. doi: 10.1016/j.biomaterials.2017.12.018.

Xu, Letao, Xing Wang, Yun Liu, Guangze Yang, Robert J. Falconer, and and Chun-Xia Zhao. 2022. "Lipid Nanoparticles for Drug Delivery." *Adv. NanoBiomed Res.* doi: https://doi.org/10.1002/anbr.202100109.

Xu, Wanjia, Xiumei Li, Liang Wang, Siyuan Li, Shengnan Chu, Jiachun Wang, Yijia

Li, Jinxing Hou, Quan Luo, and Junqiu Liu. 2021. “Design of Cyclodextrin-Based Functional Systems for Biomedical Applications.” *Frontiers in Chemistry* 9(February):1–13. doi: 10.3389/fchem.2021.635507.

Yamada, Yuma, Taku Nomura, Hideyoshi Harashima, Atsushi Yamashita, and Nobuhiko Yui. 2012. “Post-Nuclear Gene Delivery Events for Transgene Expression by Biocleavable Polyrotaxanes.” *Biomaterials* 33(15):3952–58. doi: 10.1016/j.biomaterials.2012.01.049.

Yang, Chuan, Xin Wang, Hongzhe Li, Suat Hong Goh, and Jun Li. 2007. “Synthesis and Characterization of Polyrotaxanes Consisting of Cationic α-Cyclodextrins Threaded on Poly[(Ethylene Oxide)-Ran-(Propylene Oxide)] as Gene Carriers.” *Biomacromolecules* 8(11):3365–74. doi: 10.1021/bm700472t.

Yokoyama, Nanako, Ji Hun Seo, Atsushi Tamura, Yoshihiro Sasaki, and Nobuhiko Yui. 2014. “Tailoring the Supramolecular Structure of Aminated Polyrotaxanes toward Enhanced Cellular Internalization.” *Macromolecular Bioscience* 14(3):359–68. doi: 10.1002/mabi.201300198.

Zalba, Sara, Timo L. M. ten Hagen, Carmen Burgui, and María J. Garrido. 2022. “Stealth Nanoparticles in Oncology: Facing the PEG Dilemma.” *Journal of Controlled Release* 351(May):22–36. doi: 10.1016/j.jconrel.2022.09.002.

Zhang, Mingming, Qingqing Xiong, Yinsong Wang, Zhibao Zhang, Wei Shen, Lingrong Liu, Quanyao Wang, and Qiqing Zhang. 2014. “A Well-Defined Coil-Comb Polycationic Brush with ‘Star Polymers’ as Side Chains for Gene Delivery.” *Polymer Chemistry* 5(16):4670–78. doi: 10.1039/c4py00311j.

Zheng, Yan, and Wanyi Tai. 2020. “Insight into the SiRNA Transmembrane Delivery—From Cholesterol Conjugating to Tagging.” *Wiley Interdisciplinary Reviews: Nanomedicine and Nanobiotechnology* 12(3):1–10. doi: 10.1002/wnan.1606.

Zhou, Libo, Lee E. Rubin, Chuanju Liu, and Yupeng Chen. 2021. “Short Interfering RNA (SiRNA)-Based Therapeutics for Cartilage Diseases.” *Regenerative Engineering and Translational Medicine* 7(3):283–90. doi: 10.1007/s40883-020-00149-z.

Zhou, Xiaoyan, Lanqin Xu, Jiake Xu, Jianping Wu, Thomas Brett Kirk, Dong Ma, and Wei Xue. 2018. “Construction of a High-Efficiency Drug and Gene Co-Delivery System for Cancer Therapy from a PH-Sensitive Supramolecular Inclusion between Oligoethylenimine- Graft-β-Cyclodextrin and Hyperbranched Polyglycerol Derivative.” *ACS Applied Materials and Interfaces* 10(42):35812–29. doi: 10.1021/acsami.8b14517.

Zhou, Yi, He Wang, Chengxi Wang, Yueshan Li, Wenfeng Lu, Shuifang Chen, Jiandong Luo, Yongnan Jiang, and Jianhai Chen. 2012. “Receptor-Mediated, Tumor-Targeted Gene Delivery Using Folate- Terminated Polyrotaxanes.” *Molecular Pharmaceutics*.

Zou, Yifang, Fang Xiao, Liu Song, Bingxue Sun, Dandan Sun, Di Chu, Limei Wang, Shulan Han, Zhuo Yu, Caitriona M. O’Driscoll, and Jianfeng Guo. 2021. “A Folate-Targeted PEGylated Cyclodextrin-Based Nanoformulation Achieves Co-Delivery of Docetaxel and SiRNA for Colorectal Cancer.” *International Journal*

of Pharmaceutics 606(July):120888. doi: 10.1016/j.ijpharm.2021.120888.

Zuckerman, Jonathan E., Ismael Gritli, Anthony Tolcher, Jeremy D. Heidel, Dean Lim, Robert Morgan, Bartosz Chmielowski, Antoni Ribas, Mark E. Davis, and Yun Yen. 2014. "Correlating Animal and Human Phase Ia/Ib Clinical Data with CALAA-01, a Targeted, Polymer-Based Nanoparticle Containing SiRNA." *Proceedings of the National Academy of Sciences of the United States of America* 111(31):11449–54. doi: 10.1073/pnas.1411393111.

7. Appendix

7.1. Supplementary information 2. Chapter

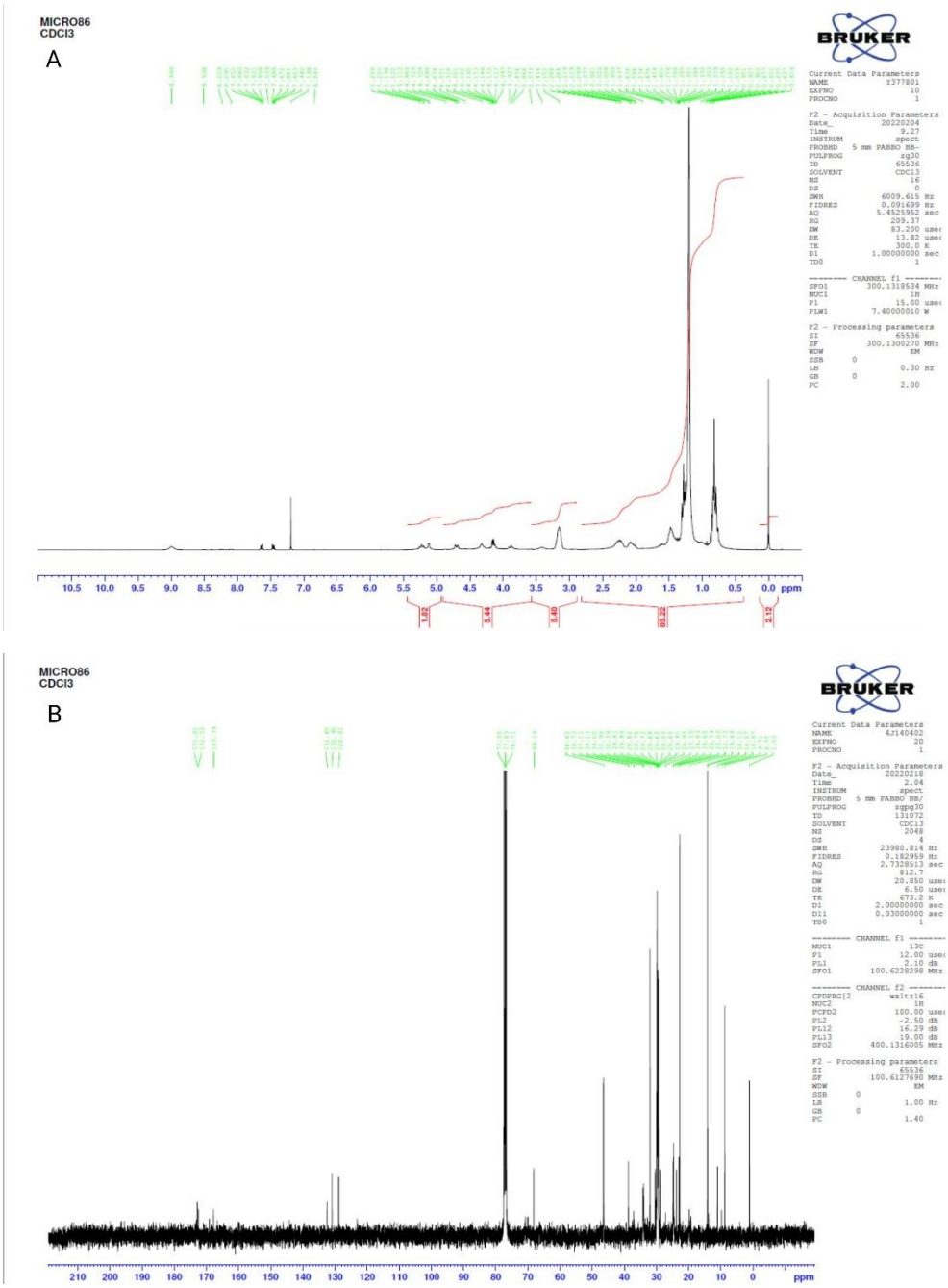

Figure 7-1 ^{1}H-NMR (A) and ^{13}C-NMR (B) spectra of the amphiphilic anionic CD.

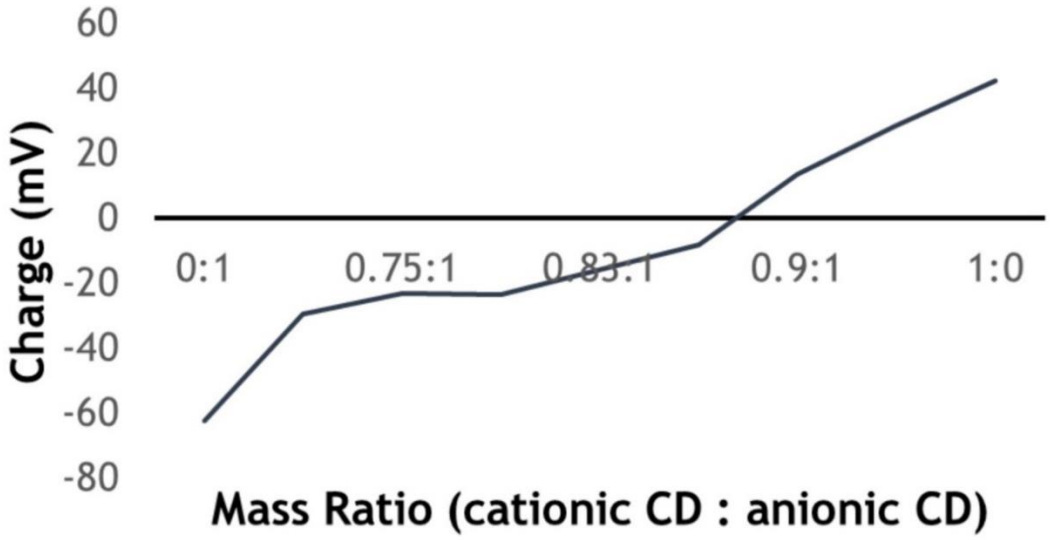

Figure 7-2 Behaviour of charged CDs in the absence of siRNA. Interaction between anionic and cationic amphiphilic CDs resulted in neutralisation at mass ratio 0.85:1 (cationic CD:anionic CD).

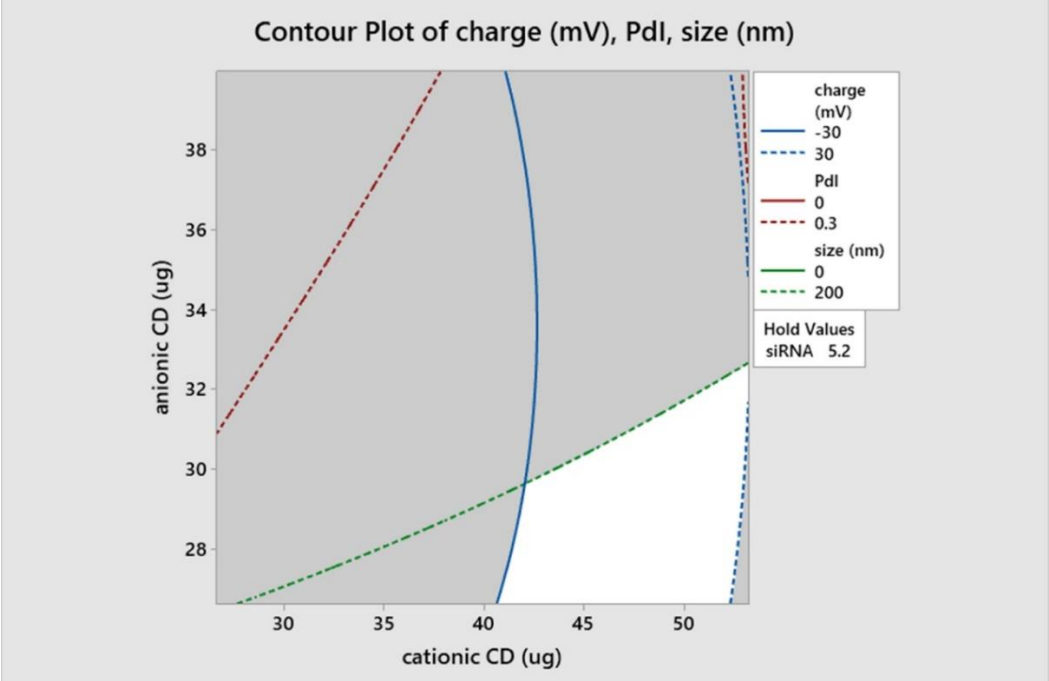

Figure 7-3 DoE assisted optimisation of mass ratio using Minitab Statistical Software. A 3-factor, 3-level Box Behnken design [49] (Minitab 17) was used. A contour plot with a hold value for siRNA at 5.2 µg (aiming 100 nM siRNA/well) and boundaries for charge between -30 mV to 30 mV, size up to 200 nm and PdI between 0-0.3 were used to determine the optimum mass ratio.

A 3-factor, 3-level Box Behnken design [49, 50] (Minitab 17) was utilised to optimize the MR of the siRNA and both CDs. Physicochemical characteristics including size, polydispersity index (PDI) and surface charge (dependent variables), were measured using dynamic light scattering (DLS) to investigate how independent variables (siRNA, amphiphilic cationic CD, and amphiphilic anionic CD quantity) affect the formulation development. Contour plots were used to indicate the optimal MR for the NPs for the in vitro cell culture studies. In vitro tests were conducted with the two formulations before and after adding the anionic CD.

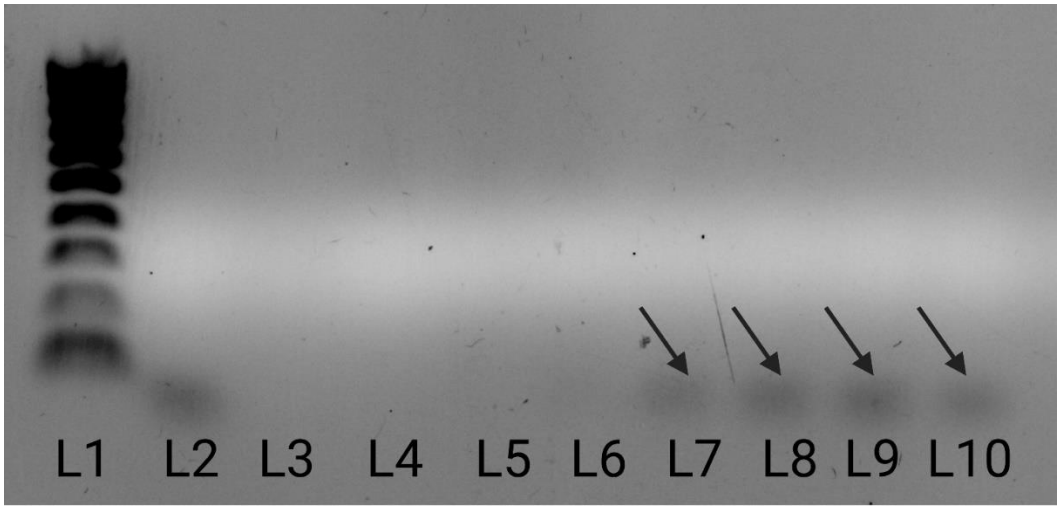

Figure 7-4 Assessment of higher amphiphilic anionic CD mass ratio (cationic CD:siRNA:anionic CD). A 1 %-Agarose gel was run at 90 V for 60 mins and imaged under UV. It could be seen that at a mass ratio of cationic CD to anionic CD higher than 1.67, the anionic CD displaces the siRNA (circled). L1 100 bp – 1000 bp DNA ladder; L2 siRNA control; L3 NP 10:1 (cationicCD:siRNA); L4 10:1:5; L5 10:1:6; L6 10:1:7.5; L7 10:1:10; L8 10:1:12.5; L9 10:1:15; L10 10:1:17.5.

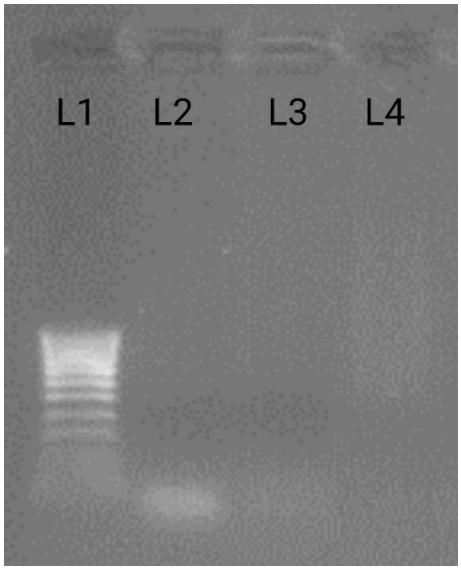

Figure 7-5 Complexation efficiency using 1%-Agarose gel. L1: 100 bp – 1000 bp DNA ladder, L2: siRNA control, L3: Formulation, L4: Co-formulation

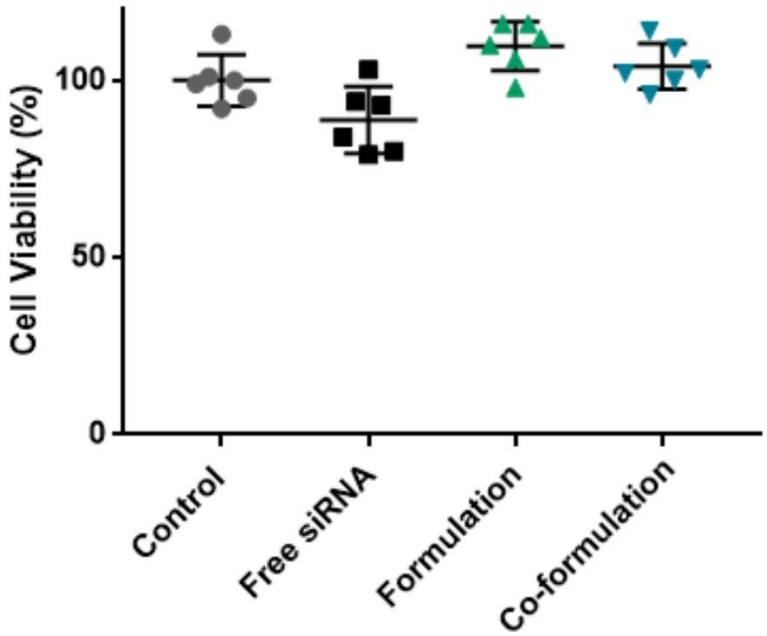

*Figure 7-6 Cytotoxicity assessment. Cell viability (as percentage relative to the control) in HL-60 cells (2.5 x10^5/ml) measured 72 h post-transfection using Cell Counting kit 8 (CCK8). Cells were treated with cyclodextrin-nanoparticles at a concentration of 100 nM/ well. Both formulations were safe to be used. Mean ± S.E.M of 3 technical replicates performed in triplicate. One-way ANOVA followed by Dunnett's post hoc test was used. *p <0.05 compared to untreated group. Formulation mass ratio 8.5:1 (cationic CD: siRNA); Co-formulation mass ratio 8.5:1:5.3 (cationic CD: siRNA: anionic CD).*

7.2. Supplementary information 3. Chapter

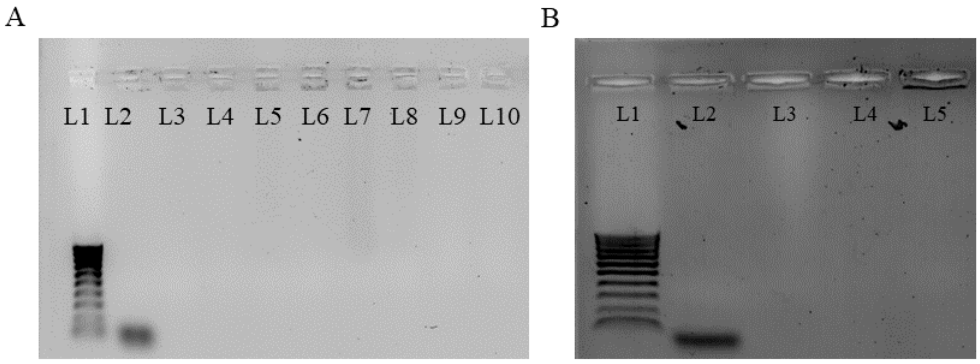

Figure 7-7 The complexation efficiency was investigated using a 1%Agarose gel. (A) L1 ladder, L2 positive control free siRNA, L3 CD B1 MR 7.5:1, L4 CD B1 MR 10:1, L5 CD B2 MR 7.5:1, L6 CD B2 MR 10:1, L7 CD G1 MR 7.5:1, L8 CD G1 MR 10:1, L9 CD G2 MR 7.5:1, L10 CD G1 MR 10:1; (B) L1 Ladder, L2 positive control free siRNA, L3 CD G3 MR 10:1, L4 CD G4 MR 10:1, L5 CD G5 MR 10:1.

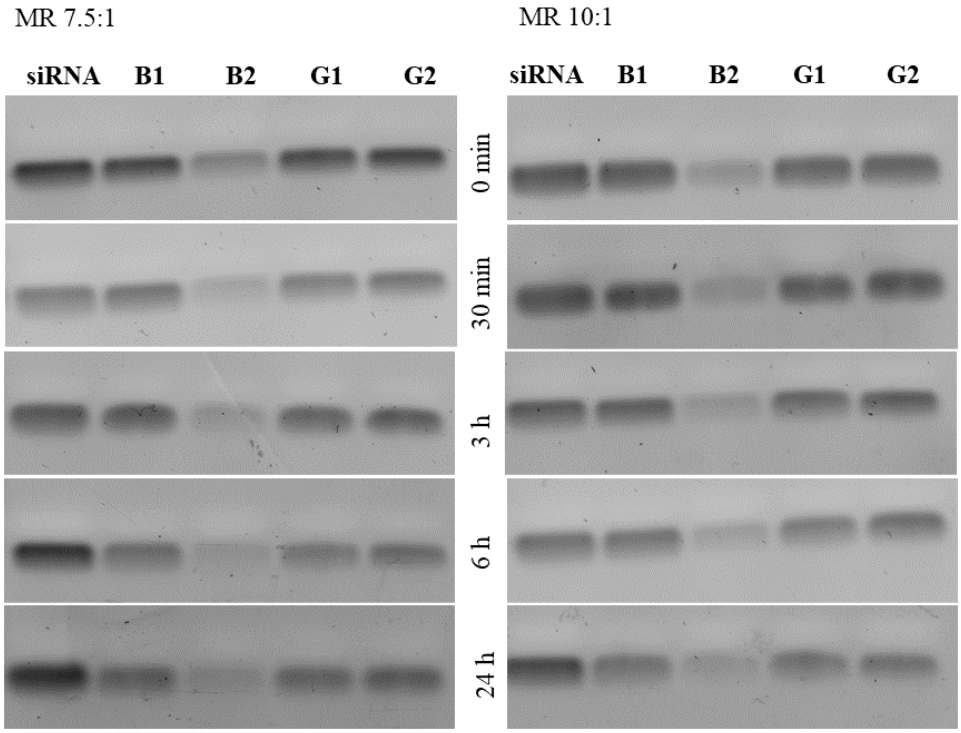

Figure 7-8 Heparin release of amphiphilic cationic CD-siRNA-NP after exposure to 20% heparin at different time points and subsequent analysis on agarose gel.

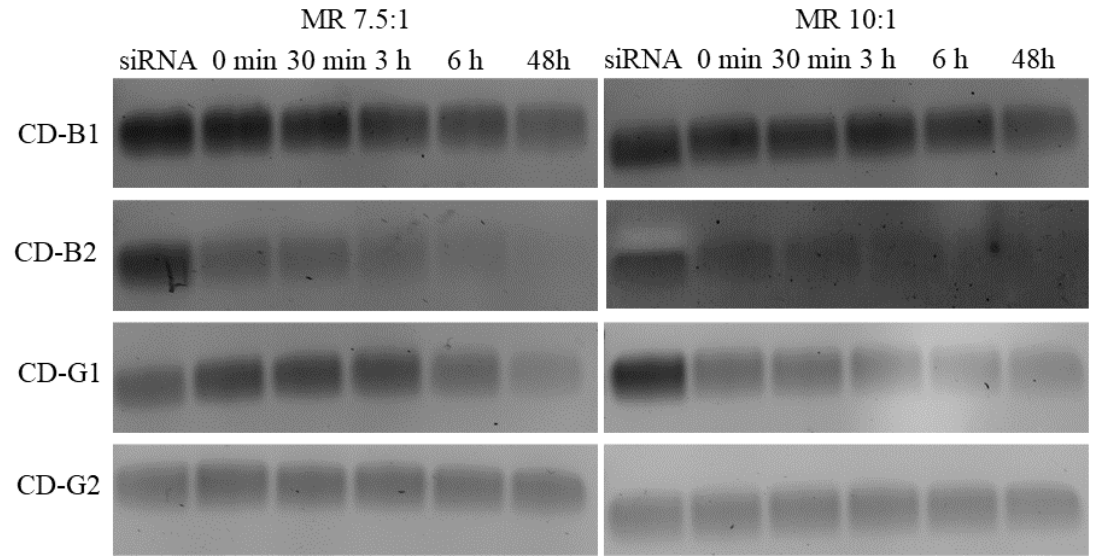

Figure 7-9 Stability of amphiphilic cationic CDs-siRNA-NP after exposure to 50% serum at different time points and subsequent analysis on agarose gel.

Table 7-1 Encapsulation efficiency measured with Quant-iT RiboGreen™ RNA Assay kit.

Formulation	Encapsulation efficiency (%)	
	MR 7.5:1	MR 10:1
CD-B1	99	98
CD-B2	88	94
CD-G1	99	97
CD-G2	100	100
CD-G3	N/A	100
CD-G4	N/A	99
CD-G5	N/A	98

7.2.1. Synthesis Details

Experimental

Material and Methods

BOC-protected 2-amino-ethyl-(3-azido-propyl) sulfide is a product of Wuxi. Gamma cyclodextrin is a product of Wacker Chemie. Triphenylphosphine (99%), iodine (99.8%), sodium methoxide in methanol (25 wt%), sodium azide (99.5%), anhydrous dichloromethane (DCM, >99.8%), anhydrous *N*,*N*-dimethylformamide (DMF, >99.8%), anhydrous dimethylsulfoxide (DMSO, >99.9%), 1-dodecanethiol (>98%), NaH (60% dispersion in mineral oil), allyl-bromide (ReagentPlus®, 99%,), propargyl bromide (80 wt. % in toluene), acetic acid (≥99.5%, FCC, FG), cysteamine hydrochloride (≥98%), 2,2'-Azobis(2-methylpropionitrile) (AIBN, 98%), *N*,*N*-dimethylaminoethanethiol hydrochloride (95%), triethylamine (TEA, for synthesis), trifluoroacetic acid (TFA, for synthesis) are product of Merck.

1,4-Dioxane (puriss.), 25% ammonia solution (analytical grade), 1-propanol (lab. grade), methanol (lab. grade), *n*-hexane (lab. grade), ethyl acetate (lab. grade), toluene (lab. grade) were from Molar KFT.

All the reagents were used without further purification. Solvents were dried by conventional methods and distilled immediately prior to use.

Dialysis tube cellulose membrane molecular weight cut-off= 2.000 was from Sigma.

Silica gel coated aluminum sheets were from Merck (Art. No.: 1.05554). Visualization was achieved under UV light at 254/366 nm by charring with a solution of EtOH (96%):H_2SO_4 (96%) = 9:1 charred by heating at 105-110 °C.

^{1}H-,^{13}C- NMR spectra and HSQC-DEPT spectra were recorded on a Varian VXR-600 at 400 or 600 MHz.

MALDI-TOF mass spectra were recorded on a Bruker Microflex LRF system. The microflex LRF operated in positive ion mode using the linear detector. Ion generation was achieved using a 60 Hz N_2-Cartridge-Laser including variable power attenuator and UV optics. The laser operated at 337 nm, 2,5-dihydroxybenzoic acid (DHB) was used as the matrix.

Octakis(6-deoxy-6-iodo)-gamma-cyclodextrin (I)

Triphenylphosphine (178 g, 0.68 mol) was added to DMF (mL) under inert atmosphere obtaining a colorless solution after a fast dissolution (endothermic process). The mixture was cooled down to 15 °C, iodine (170 g, 0.67mmol) was added portion-wise in 30 minutes by keeping the T_{in} below 40 °C, resulting in a dark orange suspension. Subsequently, the dry γ-cyclodextrin (50 g, 38.5 mmol) was added in two portions, cooling was removed and the reaction mixture was heated at 75 °C (T_{in}) for

10 hours. The reaction was monitored by TLC (1,4-dioxane:25% NH_3:1-propanol = 10:7:3). The DMF was concentrated at 60 °C under reduced pressure, MeOH (500 mL) was added and a yellow suspension was obtained. The pH was set to 9-10 with NaOMe/MeOH (25% w/w), to destroy the formate esters, getting a yellow precipitate, which was filtered through a sintered glass filter (porosity G3). The solid was washed extensively with MeOH (2x200 mL), H_2O (2x200 mL) and once more with MeOH (2x100 mL). The solid was collected and dried under vacuum yielding (I) as a yellowish solid (67 g, 30.8 mmol, 80% yield).

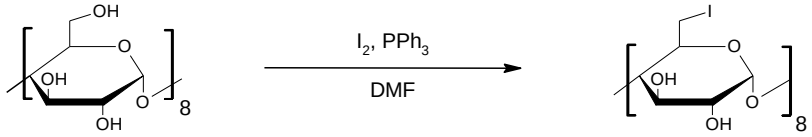

Octakis(6-deoxy-6-dodecylthio)-gamma-cyclodextrin (II)

1-Dodecanethiol (79.25 mL, 330.88 mmol) was added to DMF (400 mL) under inert atmosphere resulting in a colorless solution. The mixture was cooled down to 20 °C (T_{in}) and NaOMe/MeOH solution (68 mL, 1.2 mol, 25 wt%) was gradually added over 1 minute obtaining a purple solution. Preceding this step, a DMF solution (200 mL) of (I) (45 g, 20.68 mmol) was prepared under inert atmosphere in a Schott-Duran (note that in order to obtain the final orangish solution, several minutes of sonication should be applied). The cyclodextrin solution was rapidly added to the vessel and formation of a pinkish precipitate was observed. The cooling bath was removed and the reaction mixture was heated for 12 hours at 80 °C (T_{in}). Reaction was monitored by TLC (1,4-dioxane:25% NH_3:1-propanol = 10:7:3). The reaction crude was filtered through a sintered glass filter (porosity G3) and extensively washed with MeOH (3x200 mL). The solid was collected and dried under vacuum yielding compound (II) as a beige solid (55 g, 19.8 mmol, 96% yield).

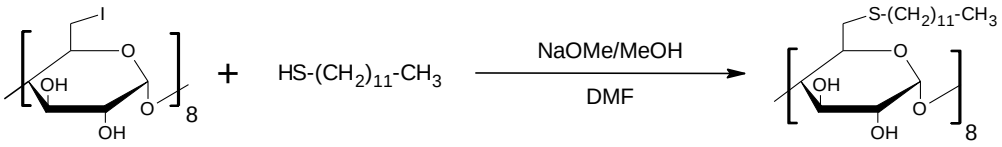

Octakis(6-deoxy-6-dodecylthio-2,3-di-*O*-allyl)-gamma-cyclodextrin (III)

Under nitrogen atmosphere, compound (II) (10 g, 3.60 mmol) was dissolved in DMSO (500 mL) resulting in a slightly yellow solution. The reaction was cooled to 5 °C (T_{in}), excess of NaH was added portion-wise (6.9 g, 173 mmol, 60% dispersion in mineral oil) into the reaction mixture (pH shifted to 9-10) and a yellow suspension was obtained. The reaction mixture was stirred under inert atmosphere for 24 h. The vessel was cooled-down to 5 °C (T_{in}), allyl-bromide (15.0 mL, 173 mmol) was added and the mixture was stirred for 2 days under inter atmosphere. The reaction was quenched with MeOH (50 mL), neutralized with acetic acid and concentrated under reduced pressure (~250 g). The mixture was extracted once with *n*-hexane:H_2O (500 mL:250 mL), the organic phase was extracted with H_2O (2x500 mL) and finally evaporated until dryness under reduced pressure (40 °C). The residue oil was then purified by chromatography (SiO_2, 20:80 EtOAc:*n*-hexane). Fractions were collected based on

TLC analysis and evaporated until dryness yielding compound (III) as colorless oil (8 g, 2.34 mmol, 65% yield).

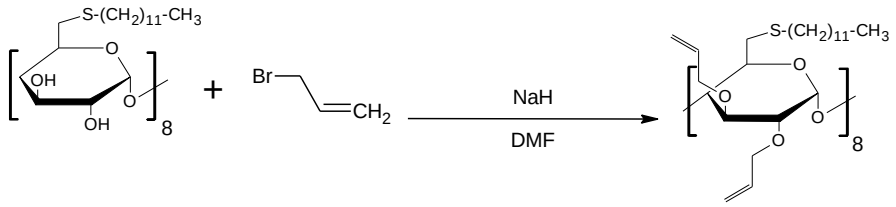

Octakis(6-deoxy-6-dodecylthio-2,3-di-*O*-(3-((2-aminoethyl)thio)propyl))-gamma-cyclodextrin * HCl (IV) (CD-G4)

Compound (III) (2 g, 0.59 mmol) was dissolved in dry DMF (100 mL) under constant nitrogen atmosphere obtaining a light-yellow solution. After complete solubilization, cysteamine hydrochloride (3.2 g, 28.32 mmol) was added. 2,2'-Azobis(2-methylpropionitrile) (AIBN) (465 mg, 2.83 mmol) was utilized as initiator and added portion-wise to the reaction mixture. Subsequently, the reaction was heated for 20 hours at 70 °C (T_{in}). Afterwards, the crude was precipitated with toluene (400 mL) and filtered through a sintered glass filter (G3), in order to remove the traces of AIBN. The solid was resolubilized in water and purified by dialysis (MWCO: 2000 Da). The solvent was changed once each day for 2 days. The cyclodextrin sample solution was evaporated until dryness at 40 °C obtaining (IV) as a yellow solid (1.7 g, 0.32 mmol, 55% yield).

Octakis(6-deoxy-6-dodecylthio-2,3-di-*O*-(3-((2-(dimethylamino)ethyl)thio)propyl))-gamma-cyclodextrin * HCl (V) (CD-G5)

Compound (IV) (2 g, 0.59 mmol) was dissolved in dry DMF (100 mL) under constant nitrogen atmosphere obtaining a light-yellow solution. After complete solubilization, *N*,*N*-dimethylaminoethanethiol hydrochloride (4.0 g, 28.32 mmol) was added. 2,2'-Azobis(2-methylpropionitrile) (AIBN) (465 mg, 2.83 mmol) was utilized as initiator and added portion-wise to the reaction mixture. Subsequently, the reaction was heated for 20 hours at 70 °C (T_{in}). Afterwards, the crude was precipitated with toluene (400 mL) and filtered through a sintered glass filter (G3), in order to remove the traces of AIBN. The solid was resolubilized in water and purified by dialysis (MWCO: 2000 Da). The solvent was changed once each day for 2 days. The cyclodextrin sample solution was evaporated until dryness at 40 °C obtaining (V) as a yellow solid (1.8 g, 0.32 mmol, 55% yield).

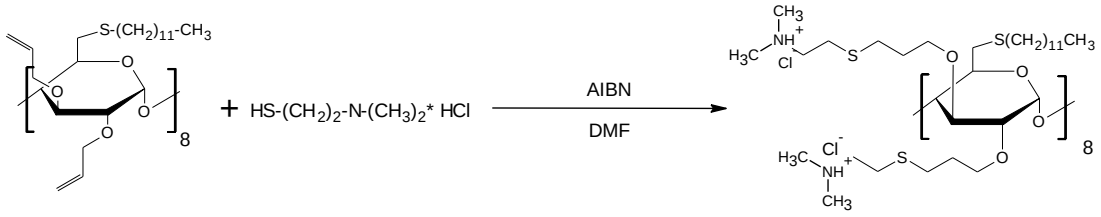

Octakis(6-deoxy-6-(2-aminoethylthio))-gamma-cyclodextrin (VI) (CD-G3)

Compound I (5 g, 2.3 mmol) was solubilized in DMF (15 mL) into a Schott-Duran under inert atmosphere. Cysteamine hydrochloride (4.2 g, 36.8 mmol) was solubilized in DMF (60 mL) into a 3-neck flask under inert atmosphere and TEA (10.2 mL, 73.6 mmol) was added to the vessel under vigorous stirring (pH shifted from 5-6 to 10-11). The cyclodextrin solution was added dropwise to the slightly yellow solution and the reaction mixture was stirred overnight. The slightly brownish suspension was filtered on a sintered glass filter (porosity 4), the crude was washed with MeOH (2x30 mL) and the resulting white solid was dried until constant weight into a vacuum drying box (KOH and P_2O_5 as drying agents). (3.8 g, 80.8%).

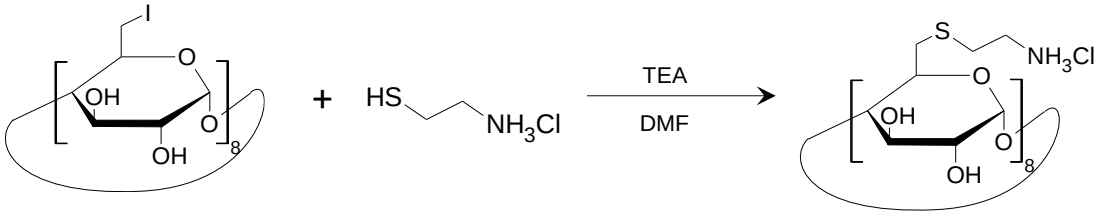

Octakis(6-deoxy-6-dodecylthio-2-*O*-propargyl)-gamma-cyclodextrin (VII)

Under nitrogen atmosphere, compound (II) (10 g, 3.60 mmol) was dissolved in DMSO (500 mL) resulting in a yellow solution. The reaction was cooled to 5 °C (T_{in}), excess of NaH was added portion-wise (3.5 g, 86 mmol, 60% dispersion in mineral oil) into the reaction mixture (pH shifted to 9-10) and a yellow suspension was obtained. The reaction mixture was stirred under inert atmosphere for 24 h. The vessel was cooled-down to 5 °C (T_{in}), propargyl-bromide (9.1 mL, 85 mmol) was added and the mixture was stirred for 2 days under inter atmosphere. The reaction was quenched with MeOH (50 mL), neutralized with acetic acid and concentrated under reduced pressure (~250 g). The mixture was extracted once with *n*-hexane:H_2O (500 mL: 250 mL), the organic phase was extracted with H_2O (2x500 mL) and finally evaporated until dryness under reduced pressure (40 °C). The residue oil was then purified by chromatography (SiO_2, 20:80 EtOAc:*n*-hexane). Fractions were collected based on TLC analysis and evaporated until dryness yielding compound (VII) as yellowish solid (5 g, 1.62 mmol, 45% yield).

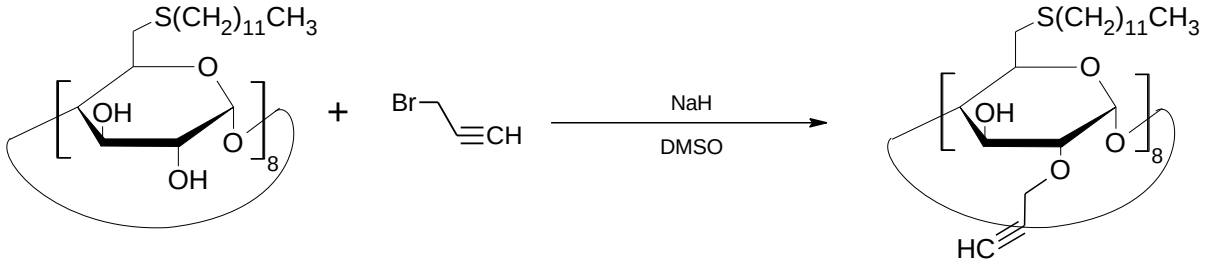

Octakis(6-deoxy-6-dodecylthio-2,3-di-*O*-propargyl)-gamma-cyclodextrin (VIII)

Under nitrogen atmosphere, compound (II) (10 g, 3.60 mmol) was dissolved in DMSO (500 mL) resulting in a yellow solution. The reaction was cooled to 5 °C (T_{in}), excess of NaH was added portion-wise (6.9 g, 173 mmol, 60% dispersion in mineral oil) into the reaction mixture (pH shifted to 9-10) and a yellow suspension was obtained. The reaction mixture was stirred under inert atmosphere for 24 h. The vessel was cooled-down to 5 °C (T_{in}), propargyl-bromide (18 mL, 173 mmol) was added and the mixture was stirred for 2 days under inter atmosphere. The reaction was quenched with MeOH (50 mL), neutralized with acetic acid and concentrated under reduced pressure (~250 g). The mixture was extracted once with *n*-hexane:H_2O (500 mL: 250 mL), the organic phase was extracted with H_2O (2x500 mL) and finally evaporated until dryness under reduced pressure (40 °C). The residue oil was then purified by chromatography (SiO_2, 10:90 EtOAc:*n*-Hexane). Fractions were collected based on TLC analysis and evaporated until dryness yielding a compound (VIII) as orangish solid (7.9 g, 2.34 mmol, 65% yield).

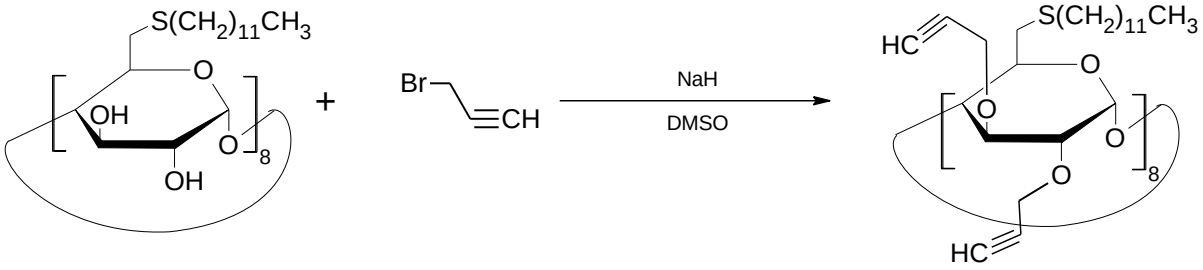

BOC-protected octakis(6-deoxy-6-dodecylthio-2-*O*-(4'-(3-((2-aminoethyl)thio)propyl)-1'-methyl-triazolyl)-gamma-cyclodextrin (IX)

Compound (VII) (3.1 g, 1 mmol) was solubilized in H_2O:DMF (1:1) mixture (100 mL) and BOC-protected 2-amino-ethyl-(3-azido-propyl) sulfide (1.2 equivalent per propargyl group, 2.5 g, 9.6 mmol) was added to the yellowish solution. CuBr (0.31 g, 2.2 mmol) was added to the mixture and the solution turned first into a greenish solution and then massive, dark precipitate formed (approximately after 15 min stirring). The suspension was stirred overnight. The reaction was monitored with TLC (toluene:ACN=3:1). The reaction crude was filtered on a sintered glass filter (porosity 4) and the mother liquor was evaporated to dryness under reduced pressure (60 °C). The residue solid was purified by gradient chromatography (toluene for removing side-products – toluene:ACN=3:1 for eluting the target compound). Fractions were combined based on TLC and evaporated to dryness under reduced pressure. Compound (IX) was isolated as yellowish solid (3.6 g, 0.7 mmol, 70% yield).

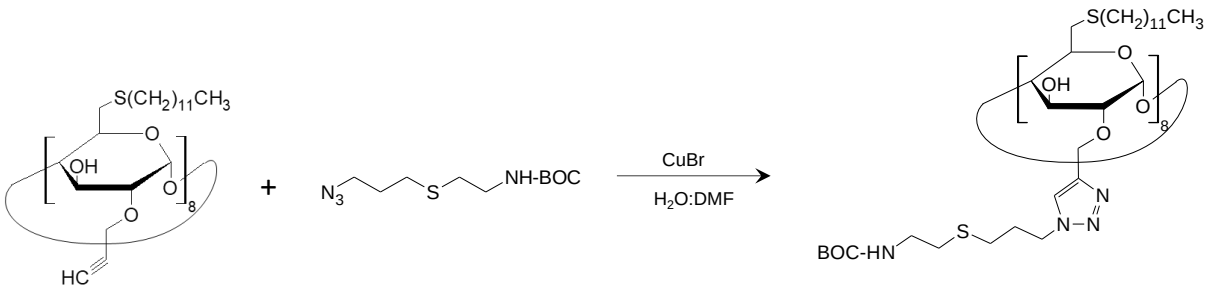

BOC-protected octakis(6-deoxy-6-dodecylthio-2-*O*-(4'-(3-((2-aminoethyl)thio)propyl)-1'-methyl-triazolyl)-gamma-cyclodextrin (X)

Compound (VIII) (3.4 g, 1 mmol) was solubilized in H_2O:DMF (1:1) mixture (120 mL) and BOC-protected 2-amino-ethyl-(3-azido-propyl) sulfide (1.2 equivalent per propargyl group, 5 g, 19.2 mmol) was added to the yellowish solution. CuBr (0.62 g, 4.4 mmol) was added to the mixture and the solution turned first into a greenish solution and then massive, dark precipitate formed (approximately after 15 min stirring). The suspension was stirred overnight. The reaction was monitored with TLC (DCM:MeOH:H_2O=10:1:0.1). The reaction crude was filtered on a sintered glass filter (porosity 4) and the mother liquor was evaporated to dryness under reduced pressure (60 °C). The residue solid was purified by gradient chromatography (DCM:MeOH=10:0.2 for removing side-products – DCM:MeOH:H2O=10:1:0.1 for eluting the target compound). Fractions were combined based on TLC and evaporated to dryness under reduced pressure. Compound (X) was isolated as yellowish solid (4.5 g, 0.6 mmol, 60% yield).

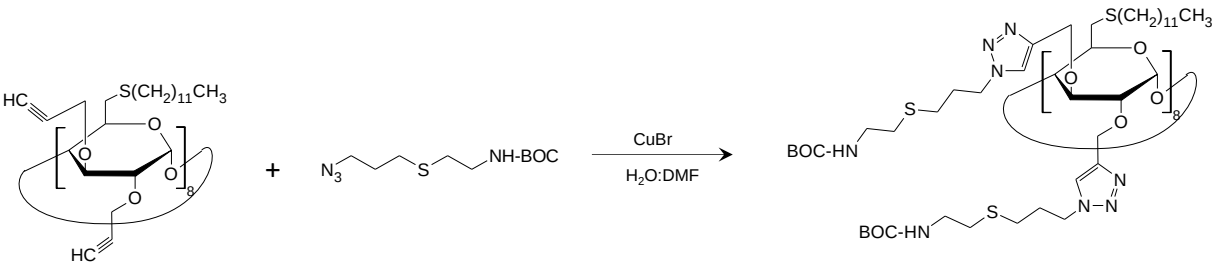

Octakis(6-deoxy-6-dodecylthio-2-*O*-(4'-(3-((2-aminoethyl)thio)propyl)-1'-methyl-triazolyl)-gamma-cyclodextrin * TFA salt (XI) (CD-G1)

Compound (IX) (2 g, 0.4 mmol) was solubilized under inert atmosphere in anhydrous DCM (20 mL) and TFA (5 mL) was added to the vessel. The reaction mixture was stirred for 24 h at room temperature. Volatiles were evaporated under reduced pressure and compound (XI) was isolated as yellowish solid (1.9 g, 0.36 mmol, 90% yield).

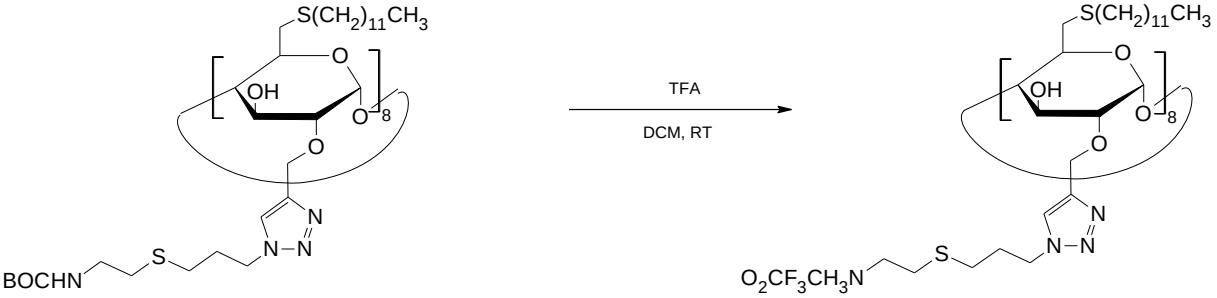

Octakis(6-deoxy-6-dodecylthio-2,3-di-*O*-(4'-(3-((2-aminoethyl)thio)propyl)-1'-methyl-triazolyl)-gamma-cyclodextrin * TFA salt (XII) (CD-G2)

Compound (X) (3 g, 0.4 mmol) was solubilized under inert atmosphere in anhydrous DCM (20 mL) and TFA (5 mL) was added to the vessel. The reaction mixture was stirred for 24 h at room temperature. Volatiles were evaporated under reduced pressure and compound (XII) was isolated as yellowish solid (2.8 g, 0.36 mmol, 90% Yield).

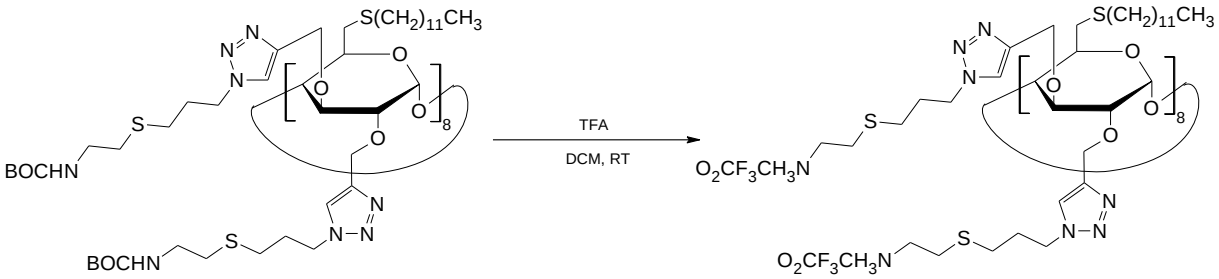

MALDI and NMR spectra

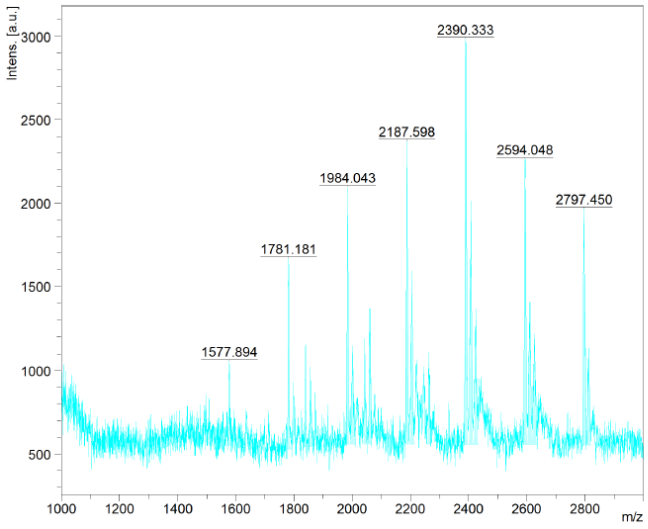

m/z	S/N	Quality Fac.	Res.	Intens.	Area
1577.894	3		494	1057	2221
1781.181	7		487	1668	5463
1839.503	4		750	1160	2098
1856.696	3		570	1023	1981
1984.043	9		495	2095	7458
2001.314	4		270	1150	4424
2043.377	4		535	1187	3845
2061.223	5		436	1367	4653
2187.598	10		453	2372	9335
2205.064	6		375	1592	6474
2264.130	3		538	1113	3245
2390.333	14		476	2986	13996
2408.505	8		456	2014	9582
2425.031	5		403	1367	6099
2594.048	10		481	2263	10786
2610.858	5		376	1406	6580
2626.582	4		363	1182	5505
2797.450	8		538	1966	7952
2812.721	3		491	1137	3672

Target	
Position	F8
Laser	
Laser beam attenuation	27.963
Laser repetition rate	60 Hz
Number of shots	40
Spectrometer	
positive voltage polarity	POS
PIE delay	140 ns
Ion source voltage 1	20 kV
Ion source voltage 2	16.5 kV
Lens voltage	8 kV
Linear detector voltage	2.842 kV
Deflection on	
Deflection mass	
SampleRate	2 ns
Reflector voltage 1	0 kV
Reflector detector voltage	0 kV
MSMS parent mass	
Instrument	
Instrument type	microflex
Serial instrument number	254472.00154
Name of computer	MALDI
Operator ID or name	admin
flexControl version	flexControl 3.4.204.10
flexAnalysis version	

Figure 1: MALDI spectrum of compound II.

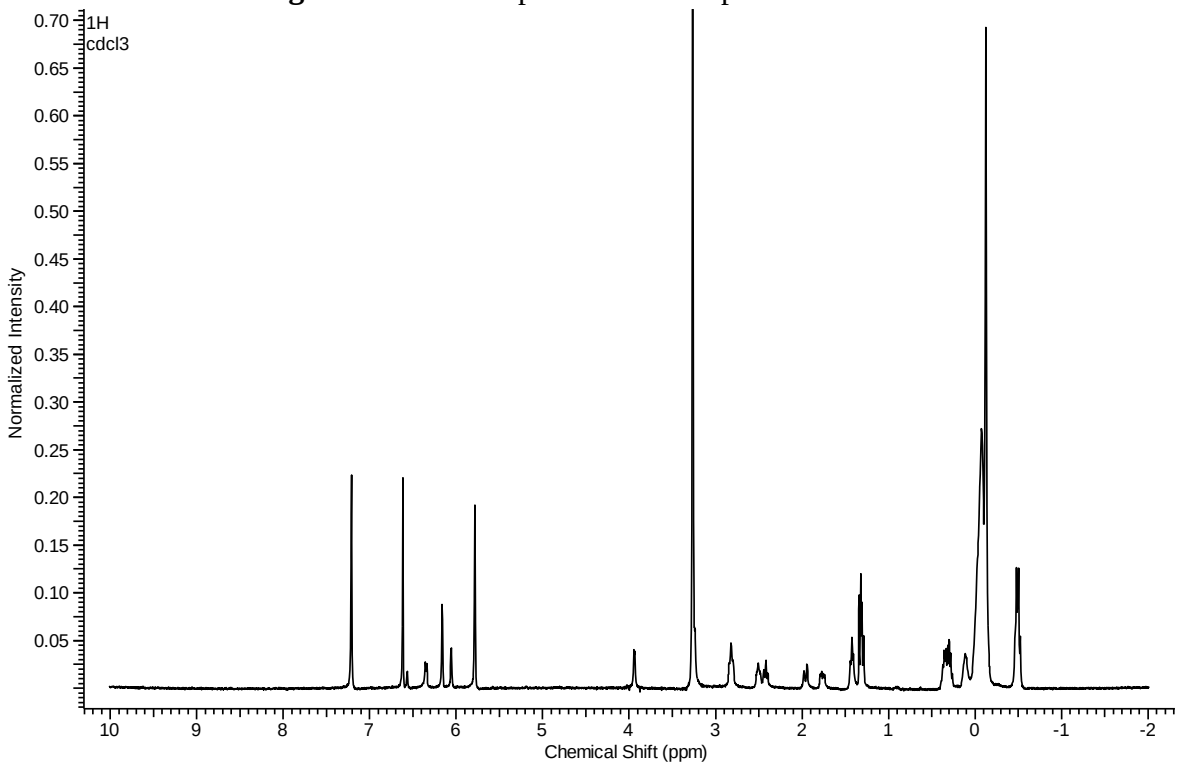

Figure 2: ^{1}H-NMR spectrum of compound II (Pyridine-d_5, 400 MHz).

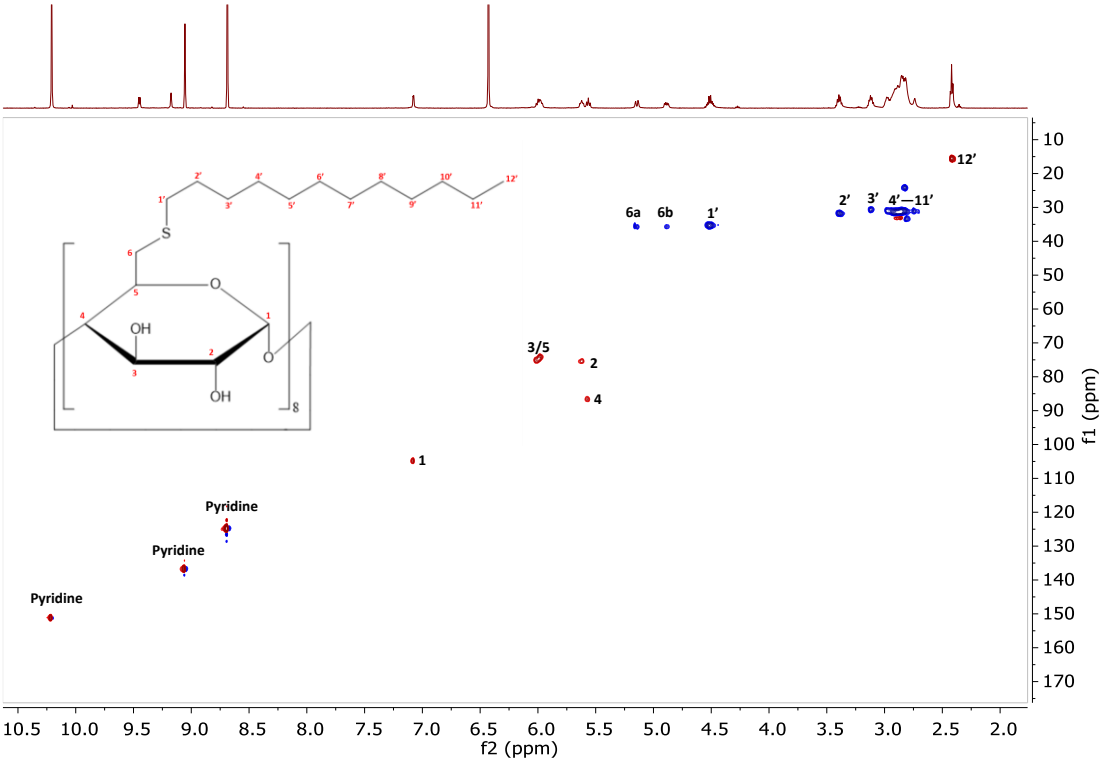

Figure 3: DEPT-edited HSQC spectrum of compound II (Pyridine-d_5, 400 MHz).

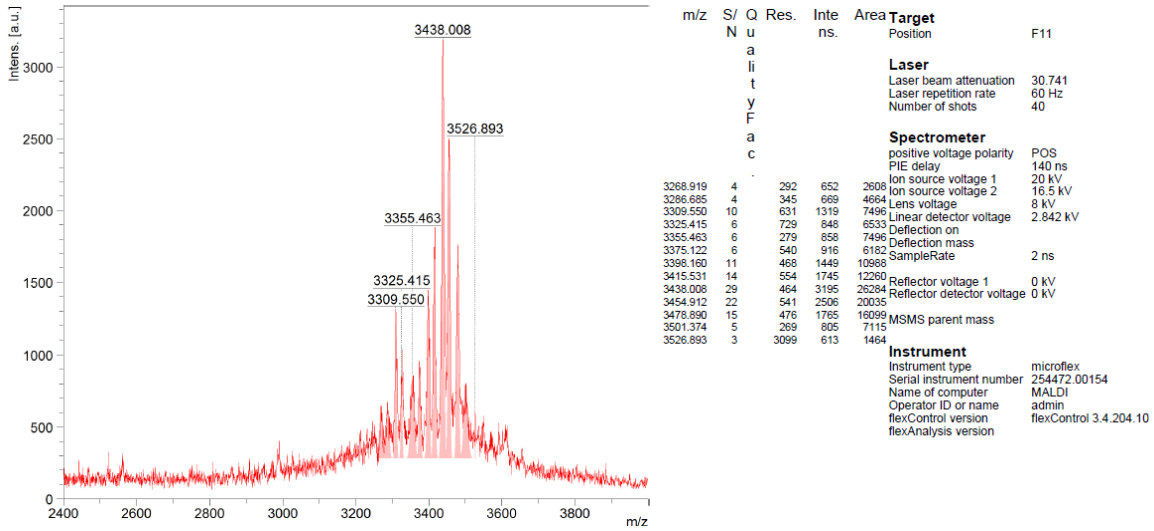

m/z	S/N	Quality Fac.	Res.	Intens.	Area
3268.919	4		292	652	2608
3286.685	4		345	669	4664
3309.550	10		631	1319	7496
3325.415	6		729	848	6533
3355.463	6		279	858	7496
3375.122	6		540	916	6182
3398.160	11		468	1449	10988
3415.531	14		554	1745	12260
3438.008	29		464	3195	26284
3454.912	22		541	2506	20035
3478.890	15		476	1765	16099
3501.374	5		269	805	7115
3526.893	3		3099	613	1464

Target
Position F11

Laser
Laser beam attenuation 30.741
Laser repetition rate 60 Hz
Number of shots 40

Spectrometer
positive voltage polarity POS
PIE delay 140 ns
Ion source voltage 1 20 kV
Ion source voltage 2 16.5 kV
Lens voltage 8 kV
Linear detector voltage 2.842 kV
Deflection on
Deflection mass
SampleRate 2 ns
Reflector voltage 1 0 kV
Reflector detector voltage 0 kV
MSMS parent mass

Instrument
Instrument type microflex
Serial instrument number 254472.00154
Name of computer MALDI
Operator ID or name admin
flexControl version flexControl 3.4.204.10
flexAnalysis version

Figure 4: MALDI spectrum of compound III.

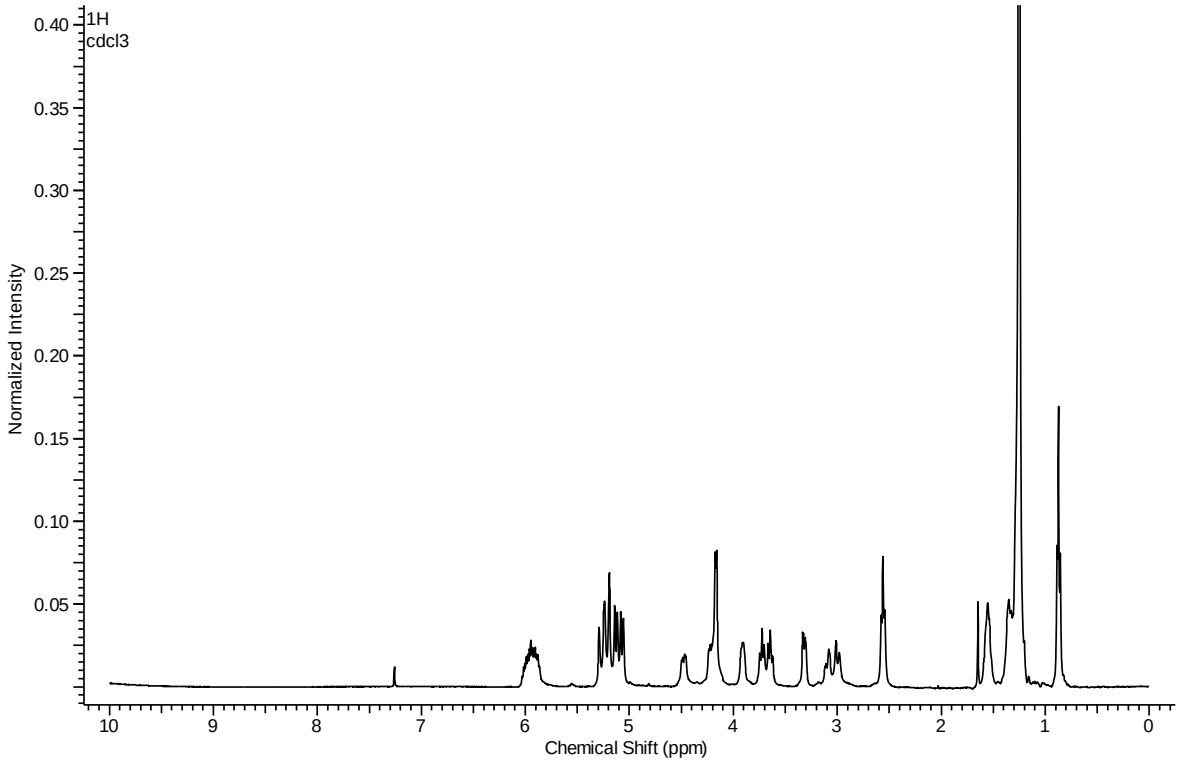

Figure 5: ^{1}H-NMR spectrum of compound III (Chloroform-d, 400 MHz).

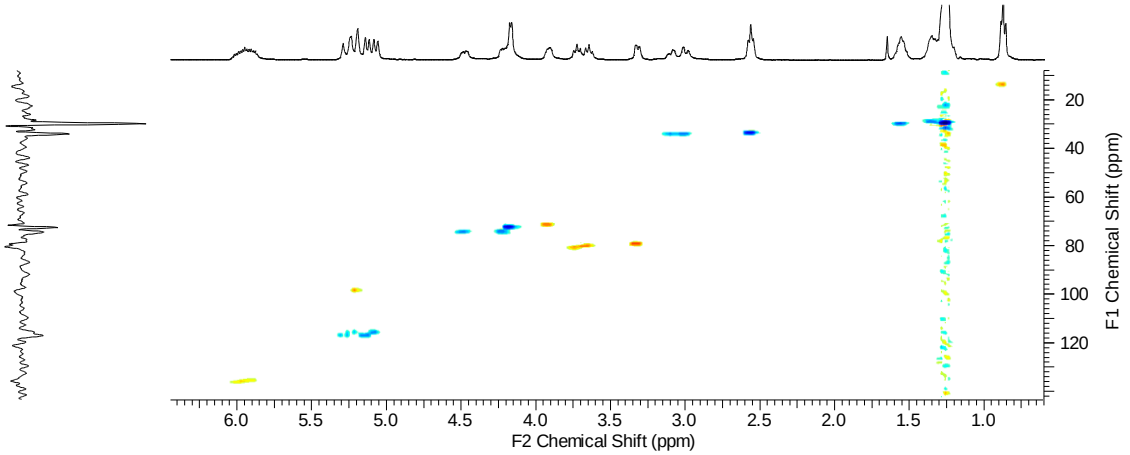

Figure 6: DEPT-edited HSQC spectrum of compound III (Chloroform-d, 400 MHz).

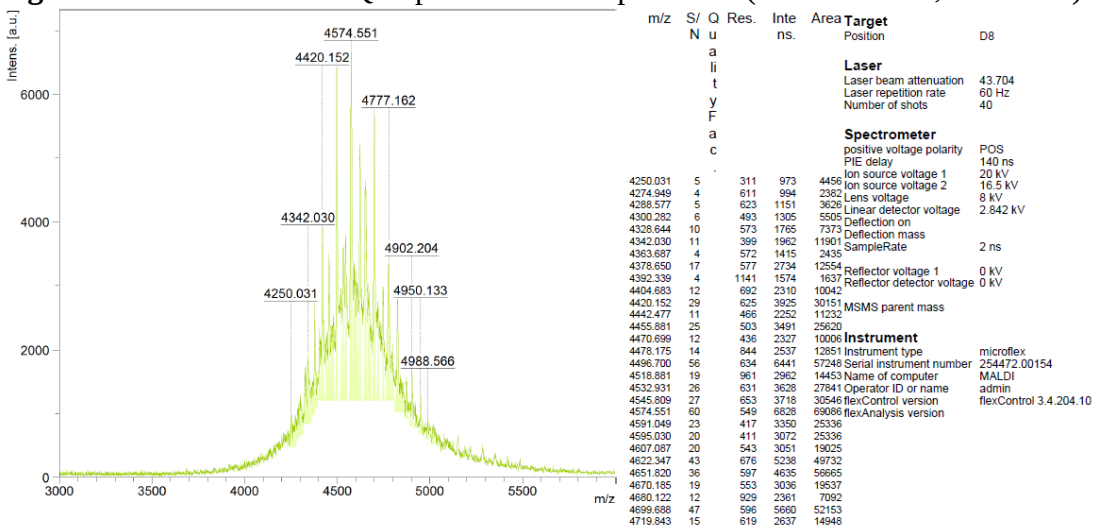

m/z	S/N	Quality Fac.	Res.	Intens.	Area
4250.031	5		311	973	4456
4274.949	4		611	994	2382
4288.577	5		623	1151	3626
4300.282	6		493	1305	5505
4328.644	10		573	1765	7373
4342.030	11		399	1962	11901
4363.687	4		572	1415	2435
4378.650	17		577	2734	12554
4392.339	4		1141	1574	1637
4404.683	12		692	2310	10042
4420.152	29		625	3925	30151
4442.477	11		466	2252	11232
4455.881	25		503	3491	25620
4470.699	12		436	2327	10006
4478.175	14		844	2537	12851
4496.700	56		634	6441	57248
4518.881	19		961	2962	14453
4532.931	26		631	3628	27841
4545.809	27		653	3718	30546
4574.551	60		549	6828	69086
4591.049	23		417	3350	25336
4595.030	20		411	3072	25336
4607.087	20		543	3051	19025
4622.347	43		676	5238	49732
4651.820	36		597	4635	56665
4670.185	19		553	3036	19537
4680.122	12		929	2361	7092
4699.688	47		596	5660	52153
4719.843	15		619	2637	14948

Target	
Position	D8
Laser	
Laser beam attenuation	43.704
Laser repetition rate	60 Hz
Number of shots	40
Spectrometer	
positive voltage polarity	POS
PIE delay	140 ns
Ion source voltage 1	20 kV
Ion source voltage 2	16.5 kV
Lens voltage	8 kV
Linear detector voltage	2.842 kV
Deflection on	
Deflection mass	
SampleRate	2 ns
Reflector voltage 1	0 kV
Reflector detector voltage	0 kV
MSMS parent mass	
Instrument	
Instrument type	microflex
Serial instrument number	254472.00154
Name of computer	MALDI
Operator ID or name	admin
flexControl version	flexControl 3.4.204.10
flexAnalysis version	

Figure 7: MALDI spectrum of compound IV (CD-G4).

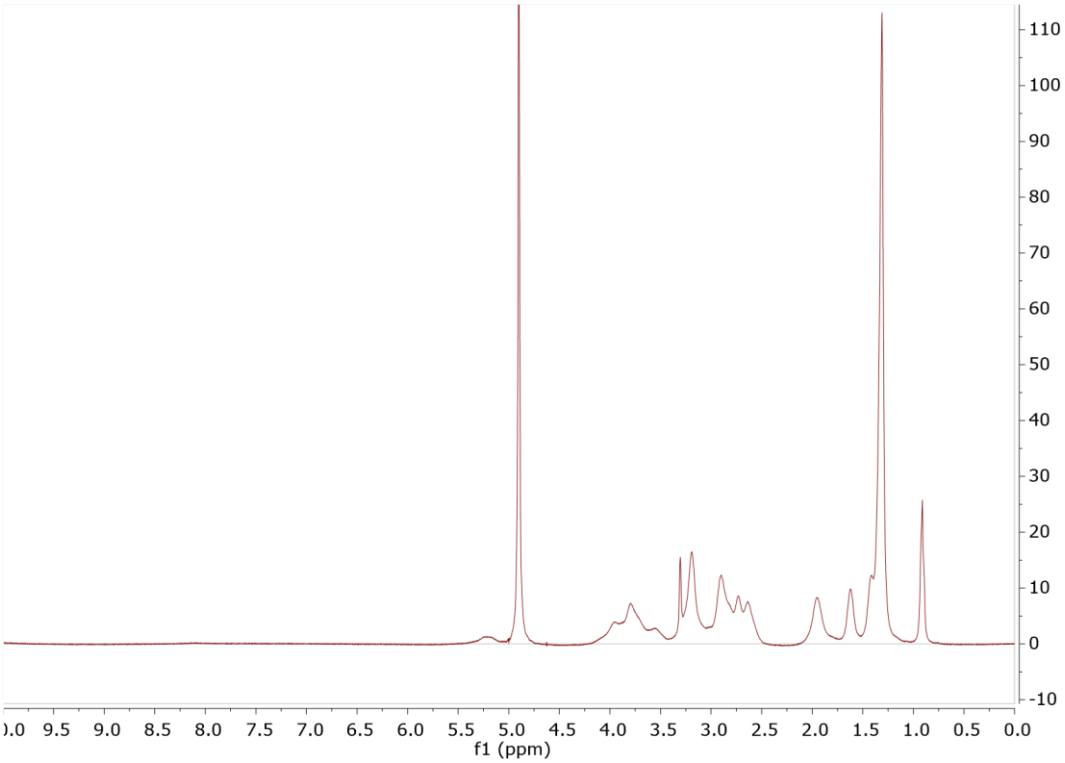

Figure 8: ^{1}H-NMR spectrum of compound IV (CD-G4) (Water-d_2, 400 MHz).

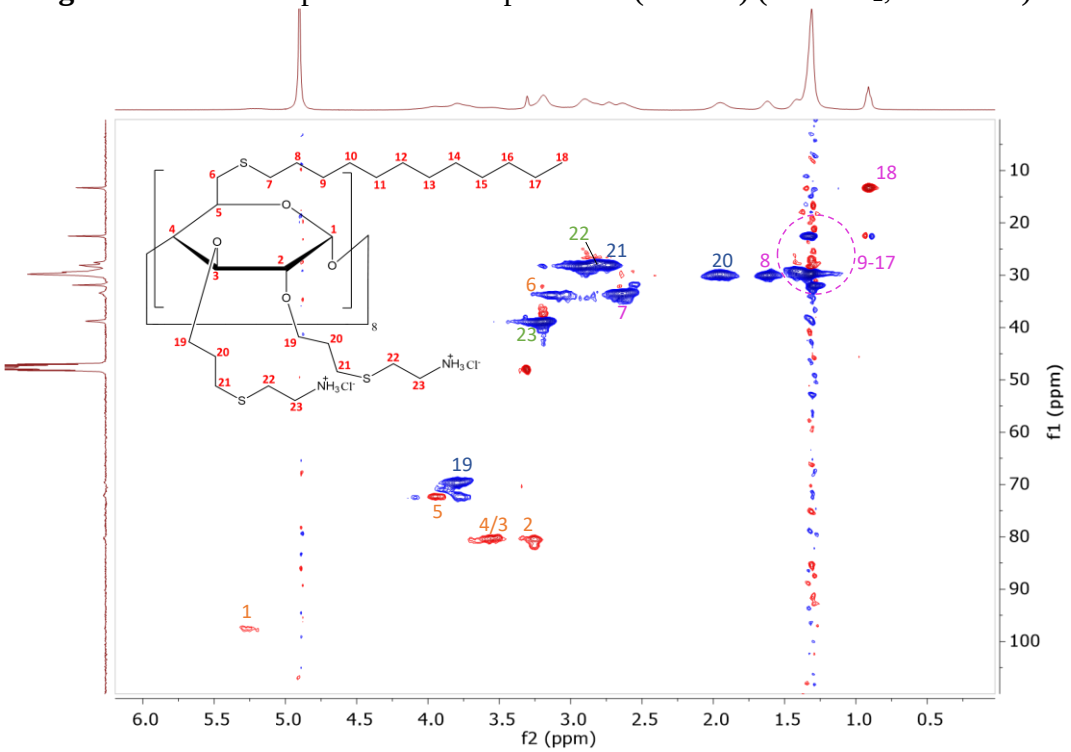

Figure 9: DEPT-edited HSQC spectrum of compound IV (CD-G4) (Water-d_2, 400 MHz).

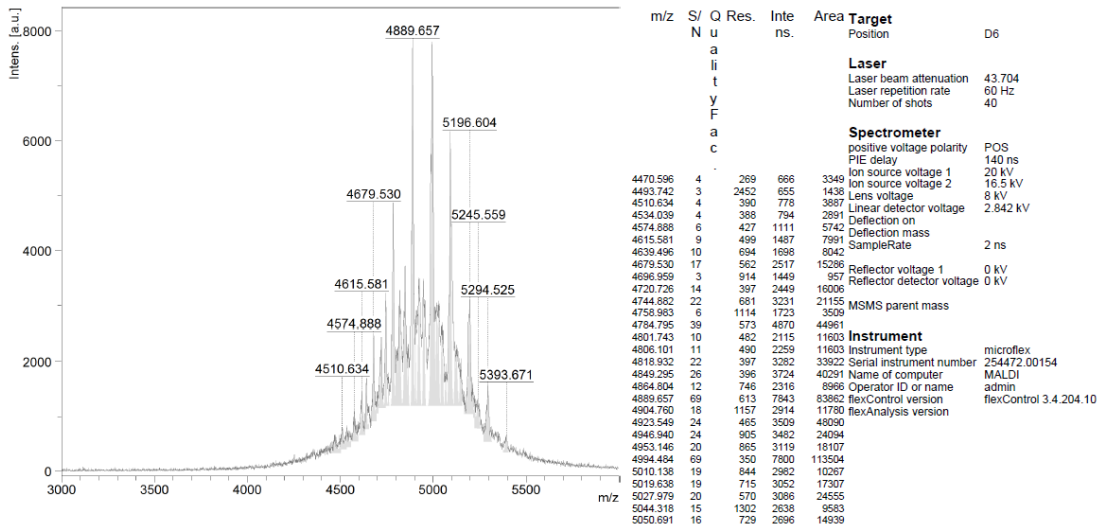

Figure 10: MALDI spectrum of compound V (CD-G5).

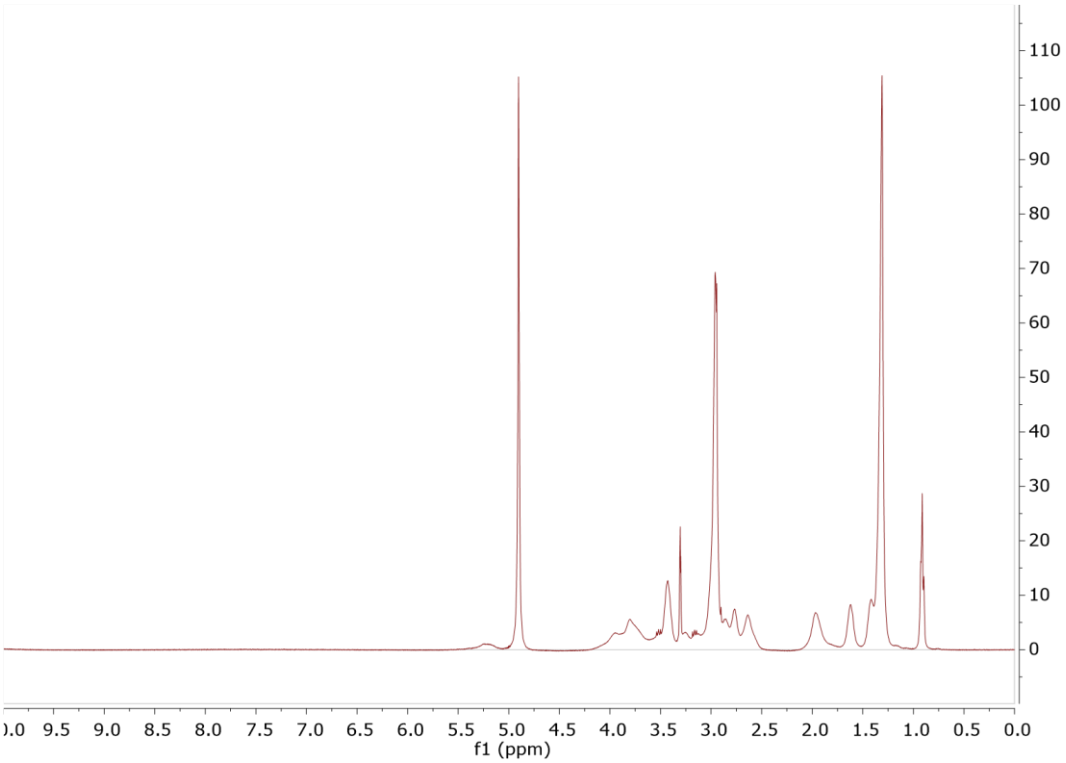

Figure 11: ^{1}H-NMR spectrum of compound V (CD-G5) (Water-d_2, 400 MHz).

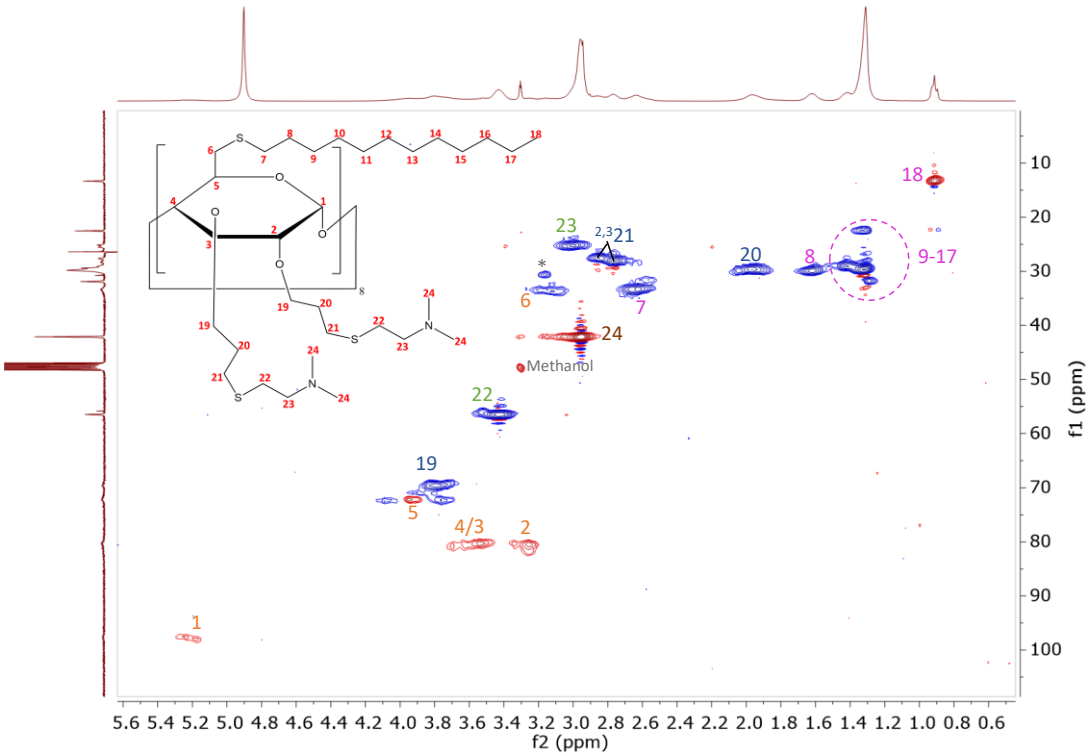

Figure 12: DEPT-edited HSQC spectrum of compound V (CD-G5) (Water-d_2, 400 MHz).

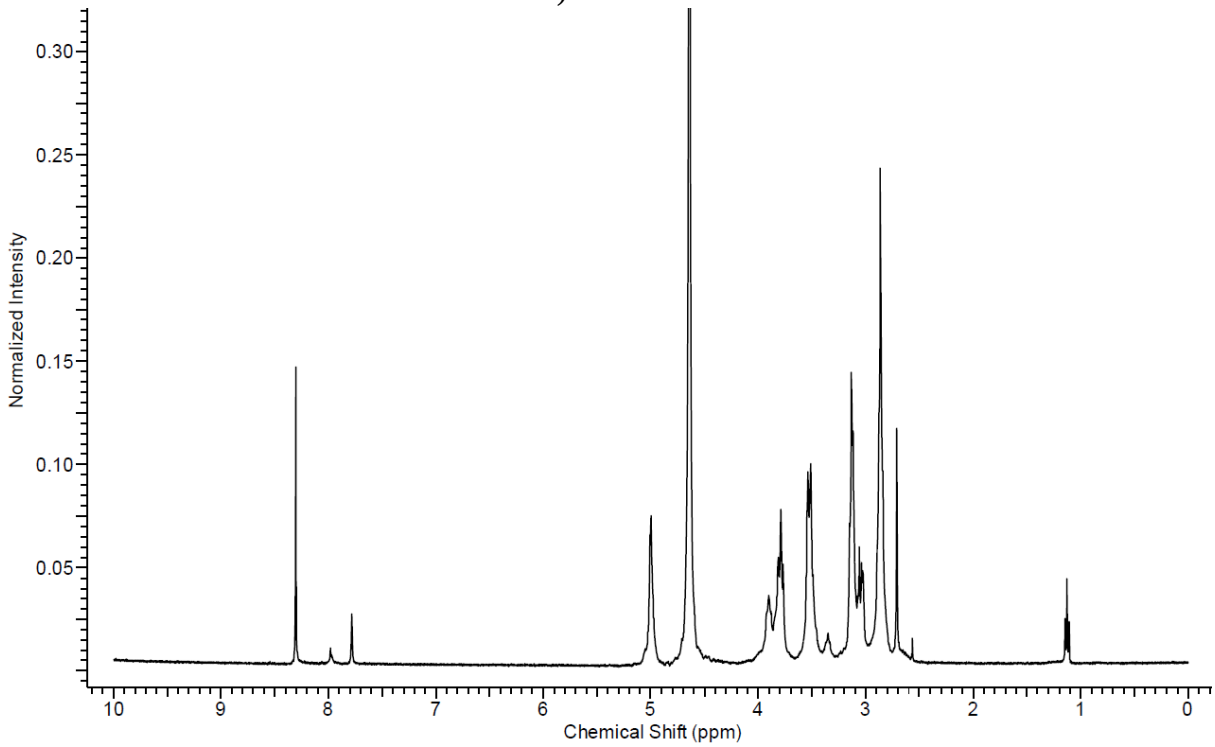

Figure 13: ^{1}H-NMR spectrum of compound VI (CD-G3) (Water-d_2, 400 MHz).

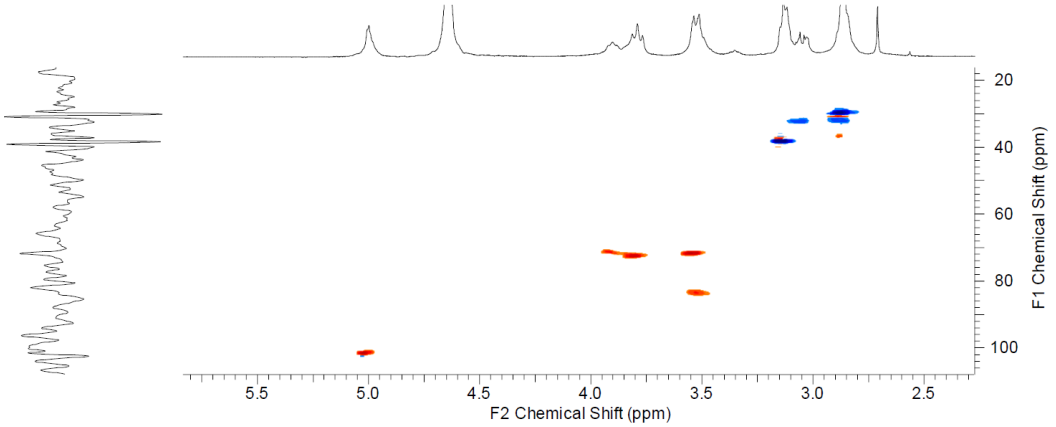

Figure 14: DEPT-edited HSQC spectrum of compound VI (CD-G3) (Water-d_2, 400 MHz).

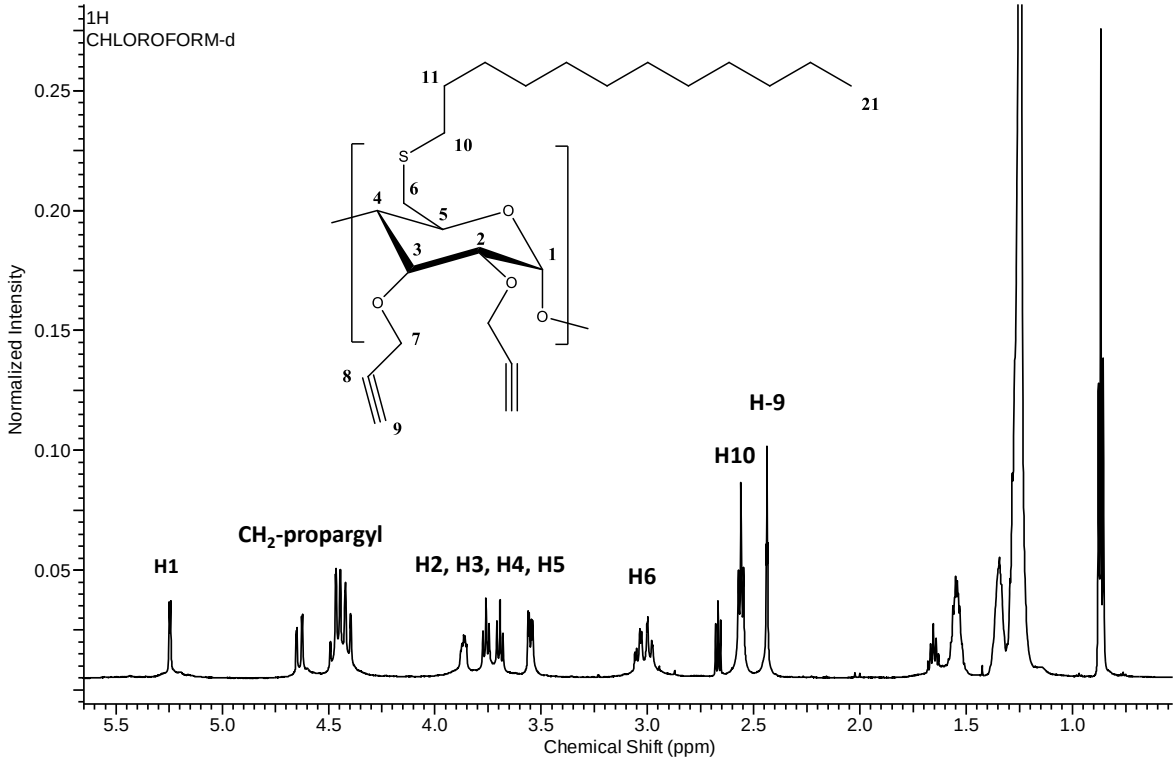

Figure 15: ^{1}H-NMR spectrum of compound VIII with partial assignment (Chloroform-d, 600 MHz).

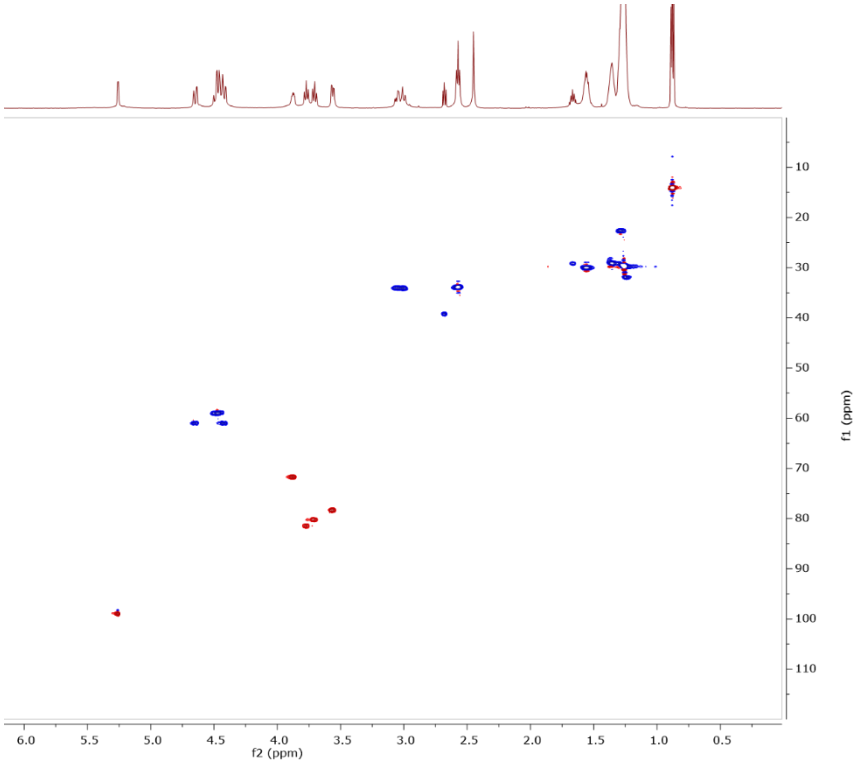

Figure 16: DEPT-edited HSQC spectrum of compound VIII (Chloroform-d, 600 MHz).

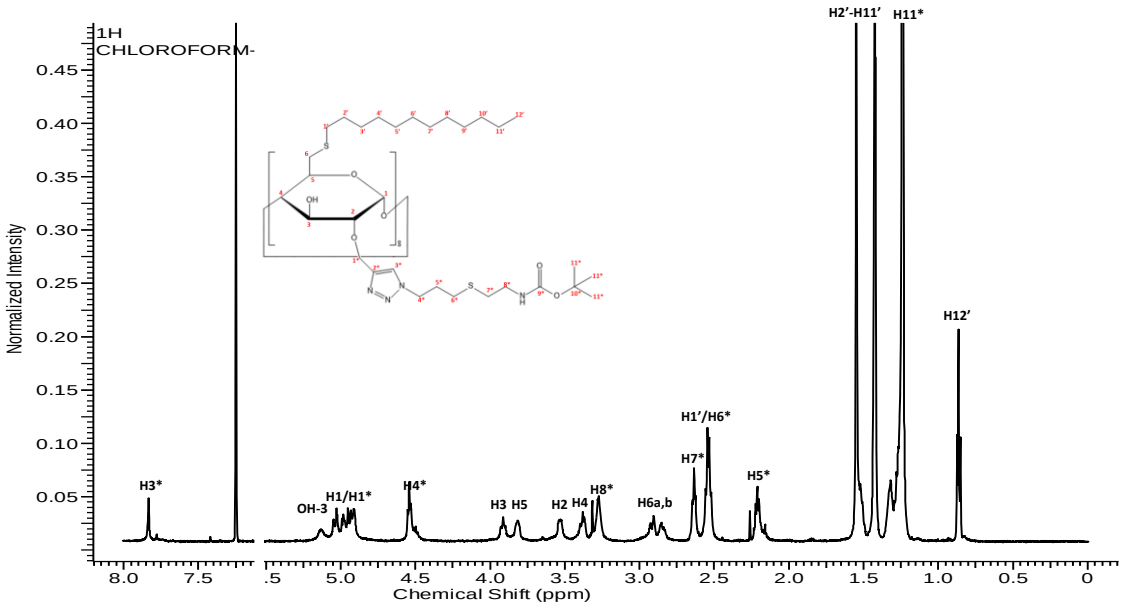

Figure 17: ^{1}H-NMR spectrum of compound IX with full assignment (Chloroform-d, 600 MHz).

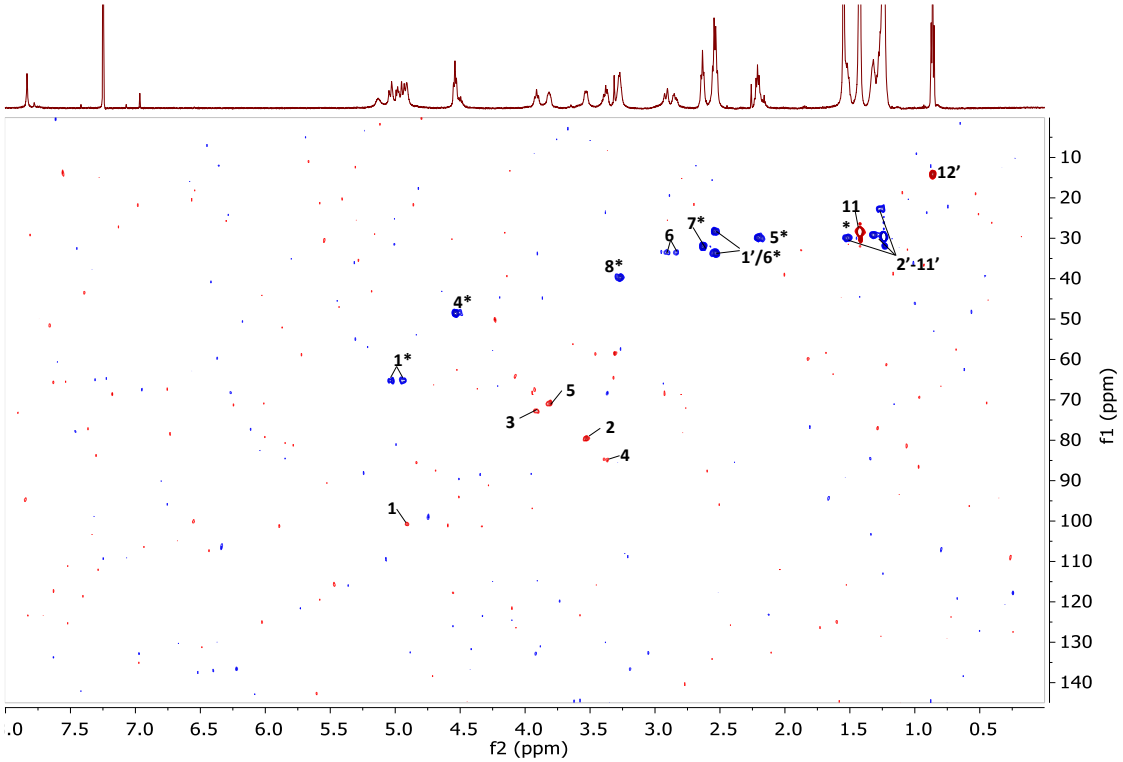

Figure 18: DEPT-edited HSQC spectrum of compound IX with full assignment (Chloroform-d, 600 MHz).

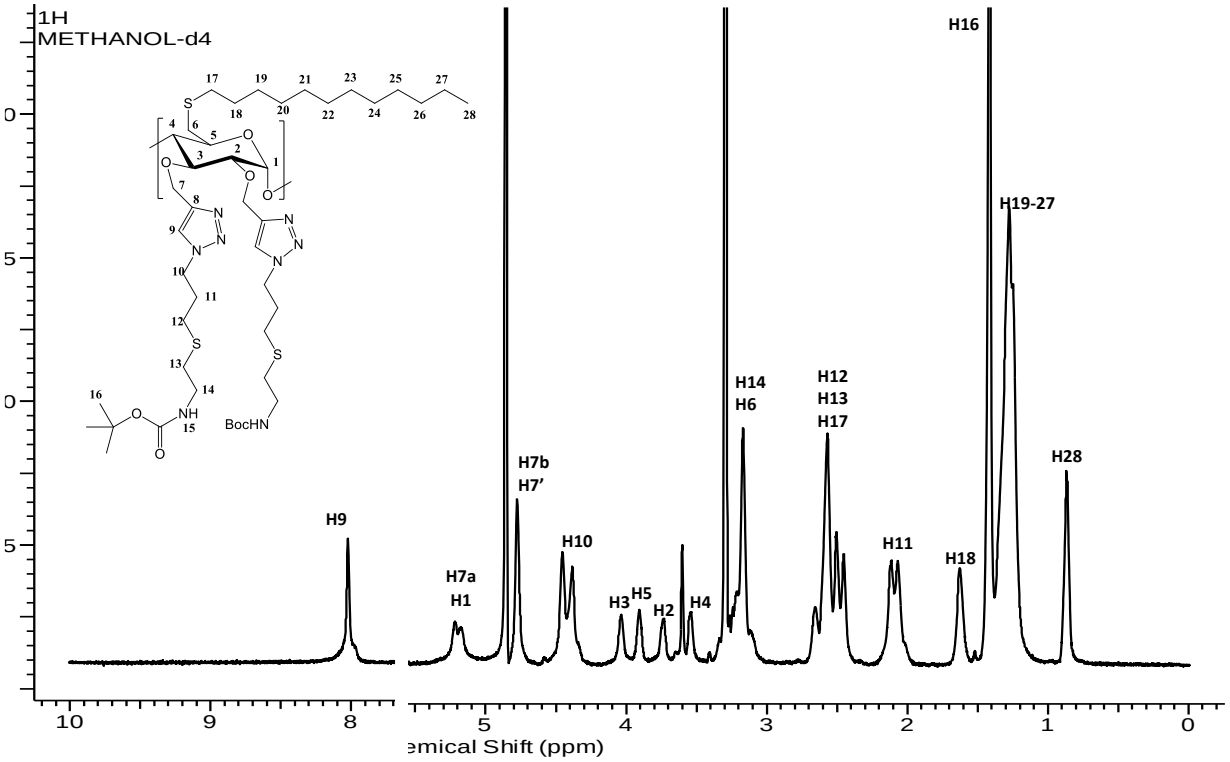

Figure 19: ^{1}H-NMR spectrum of compound X with full assignment (Methanol-d_4, 600 MHz).

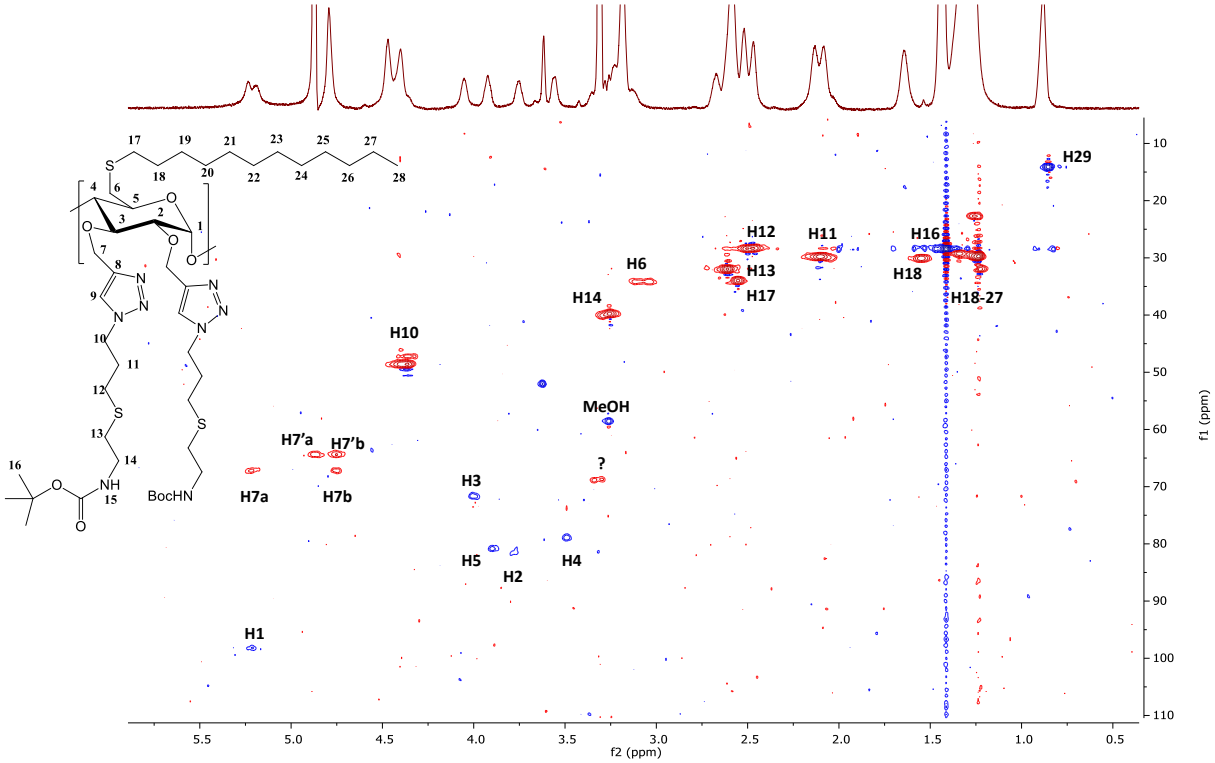

Figure 20: DEPT-edited HSQC spectrum of compound X with full assignment (Methanol-d_4, 600 MHz).

7.3. Supplementary information 4. Chapter

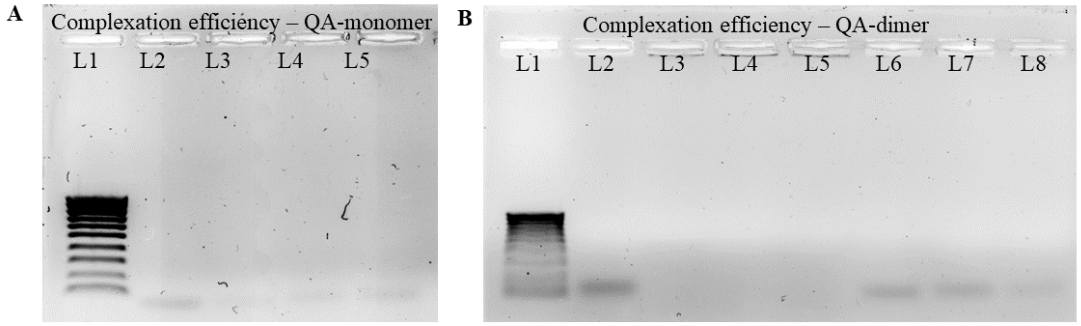

L1 Ladder
L2 positive control
L3 QA-monomer MR 5:1
L4 QA-monomer MR 7.5:1
L5 QA-monomer MR 10:1

L1 Ladder
L2 positive control
L6 QA-dimer MR 5:1
L7 QA-dimer MR 7.5:1
L8 QA-dimer MR 10:1

Figure 7-10 Complexation efficiency in 1%-Agarose gel. (A) QA-monomer (B) QA-dimer.

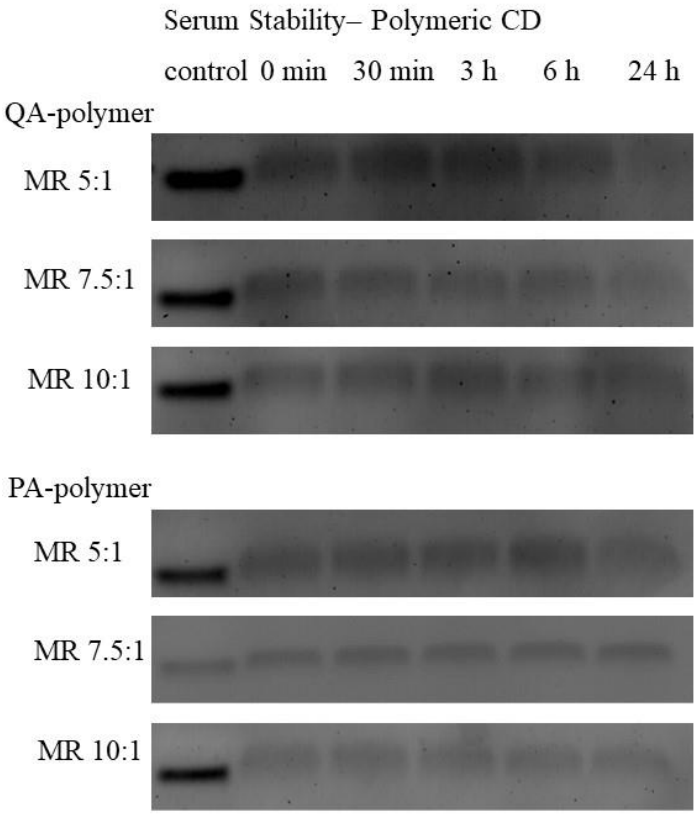

Figure 7-11 Stability of polymer-based NP after exposure to 50% serum at different time points and subsequent analysis on agarose gel. QA-polymer = quaternary ammonium-β-CD-polymer, PA-polymer = primary amine- β-CD-polymer.

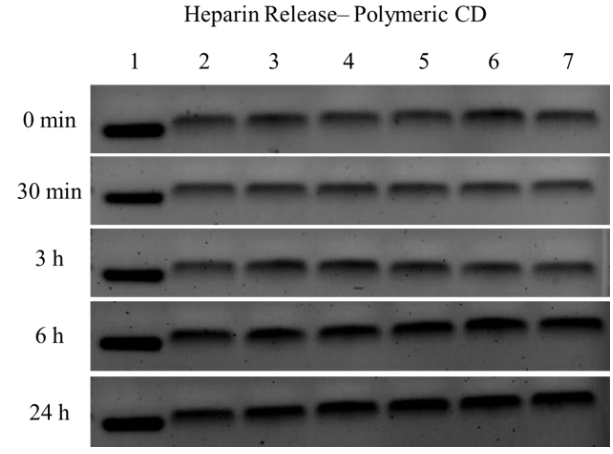

Figure 7-12 Heparin release of polymer-based NP after exposure to 20% heparin at different time points and subsequent analysis on agarose gel. 1 positive control free siRNA, 2 QA-NP MR5:1, 3 QA-NP MR7.5:1, 4 QA-NP MR10:1, 5 PA-NP MR5:1, 6 PA-NP MR7.5:1, 7 PA-NP MR10:1.

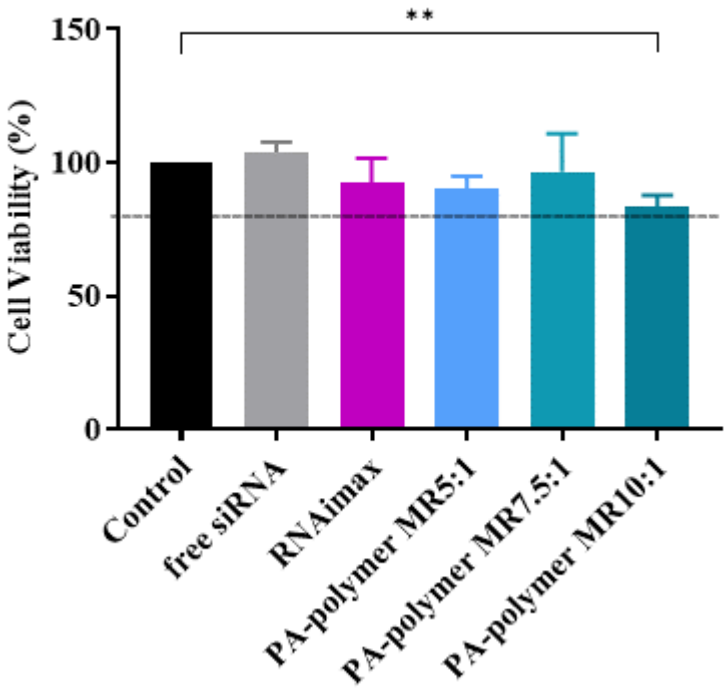

Figure 7-13 Cell viability of all MRs of PA-polymer.

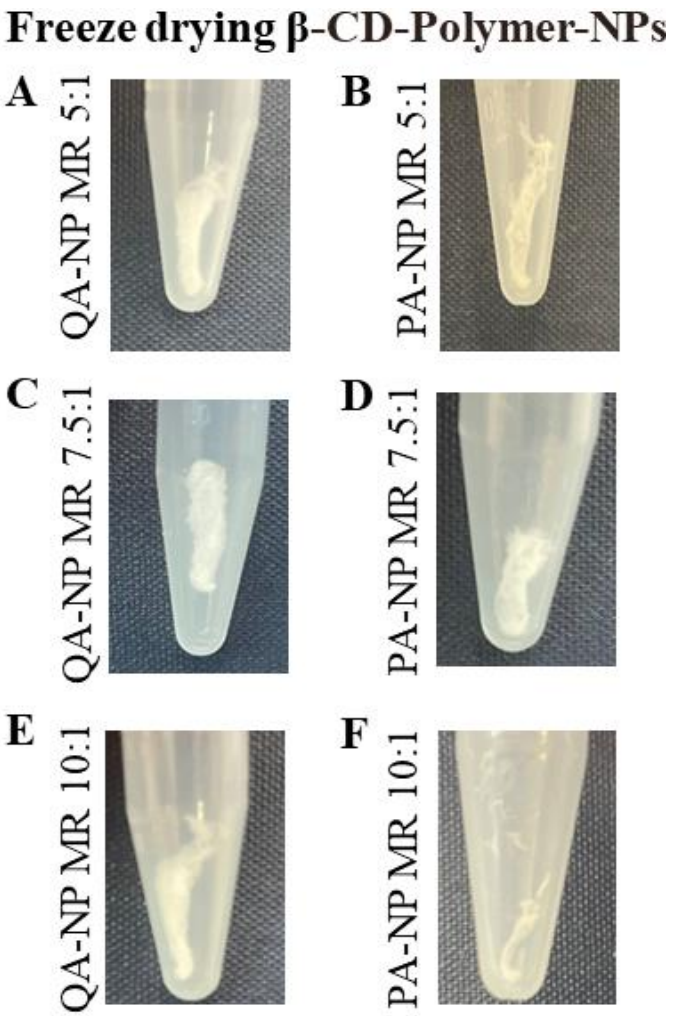

Figure 7-14 Lyophilisates of β-CD-polymer-based NPs.

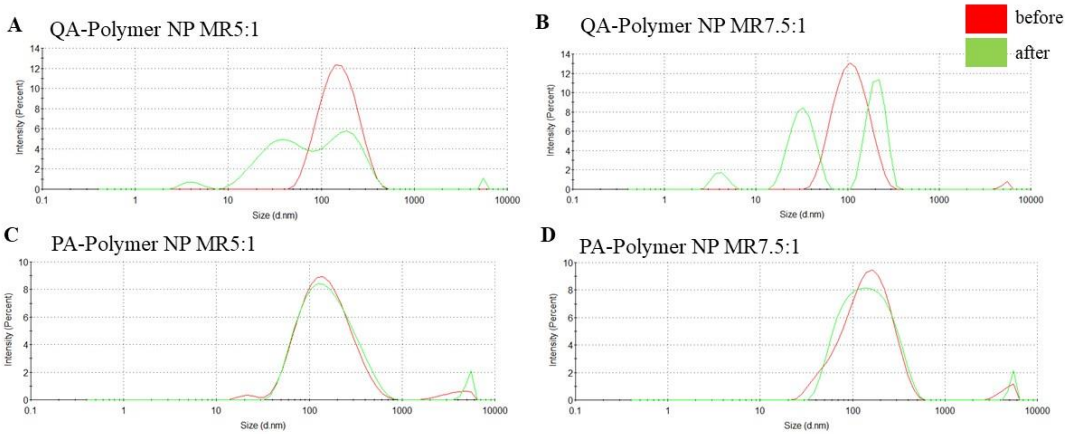

Figure 7-15 DLS measurements of QA-and PA-polymer-based NPs prior and post lyophilisation for MR5:1 and 7.5:1.

7.4. Other Publications

molecular pharmaceutics

pubs.acs.org/molecularpharmaceutics

Review

Advances in the Design of (Nano)Formulations for Delivery of Antisense Oligonucleotides and Small Interfering RNA: Focus on the Central Nervous System

Monique C. P. Mendonça, Ayse Kont, Maria Rodriguez Aburto, John F. Cryan, and Caitriona M. O'Driscoll*

Cite This: *Mol. Pharmaceutics* 2021, 18, 1491−1506

Read Online

ACCESS | Metrics & More | Article Recommendations

ABSTRACT: RNA-based therapeutics have emerged as one of the most powerful therapeutic options used for the modulation of gene/protein expression and gene editing with the potential to treat neurodegenerative diseases. However, the delivery of nucleic acids to the central nervous system (CNS), in particular by the systemic route, remains a major hurdle. This review will focus on the strategies for systemic delivery of therapeutic nucleic acids designed to overcome these barriers. Pathways and mechanisms of transport across the blood−brain barrier which could be exploited for delivery are described, focusing in particular on smaller nucleic acids including antisense oligonucleotides (ASOs) and small interfering RNA (siRNA). Approaches used to enhance delivery including chemical modifications, nanocarrier systems, and target selection (cell-specific delivery) are critically analyzed. Learnings achieved from a comparison of the successes and failures reported for CNS delivery of ASOs versus siRNA will help identify opportunities for a wider range of nucleic acids and accelerate the clinical translation of these innovative therapies.

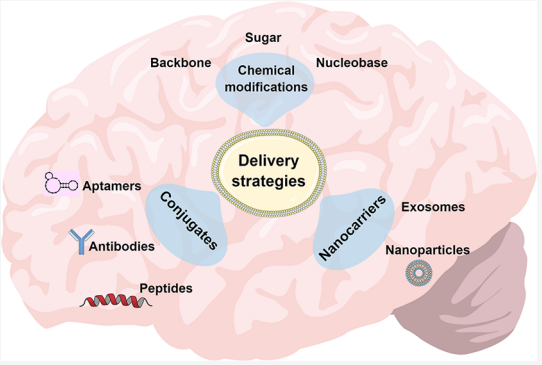

KEYWORDS: *antisense oligonucleotide, small interfering RNA, blood−brain barrier, systemic delivery, neurological diseases*

1. INTRODUCTION

Neurological disorders are the leading cause of disability and the second leading cause of death worldwide.[1] The incidence of neurological disorders is increasing in tandem with the aging of the population, representing a serious economic burden to society. Therefore, research is urgently needed to develop novel treatments in response to this clinical need.[2]

Gene therapy has emerged as a powerful therapeutic approach for the treatment of neurological diseases. Three different approaches can be used: (i) overexpression of genes, (ii) silencing of the disease-causing gene by RNA interference (RNAi), and (iii) gene editing by the insertion, removal, or replacement of genes in the genome using zinc finger nucleases (ZFNs), transcription activator-like effector nucleases (TALENs), and the recently developed clustered regularly interspaced short palindromic repeats (CRISPR)/associated protein 9 (Cas9) tools.[3,4]

For decades, overexpression of a missing gene product by an exogenous DNA sequence was the only approach for gene therapy. This approach typically utilizes viral vectors as delivery systems, which have been associated with insertional mutagenesis, innate and adaptive immune responses, and toxic effects.[5] Since the development of RNAi almost two decades ago, this technology has been intensively exploited and many clinical trials have been performed.[6,7] Antisense oligonucleotides (ASOs) and small interfering RNA (siRNA) are the two most widely studied approaches for silencing gene expression, particularly with respect to the central nervous system (CNS). The main advantages associated with RNA therapeutics are the high specificity to target pathogenic targets, decreasing toxicity associated with off-target effects, and relatively low dose requirement for therapeutic effect.[8−10] In comparison to RNAi, gene-editing tools exhibit more complex physicochemical and biopharmaceutical properties and are consequently more challenging to deliver especially to the brain.[11] Thus, this review will focus solely on the gene silencing approach.

Therapeutic targeting of RNA is currently based on two main approaches: single-stranded ASOs and double-stranded RNAi. RNAi process can be mediated by siRNAs, endogenous

Received: December 21, 2020
Revised: March 8, 2021
Accepted: March 8, 2021
Published: March 18, 2021

https://doi.org/10.1021/acs.molpharmaceut.0c01238
Mol. Pharmaceutics 2021, 18, 1491−1506

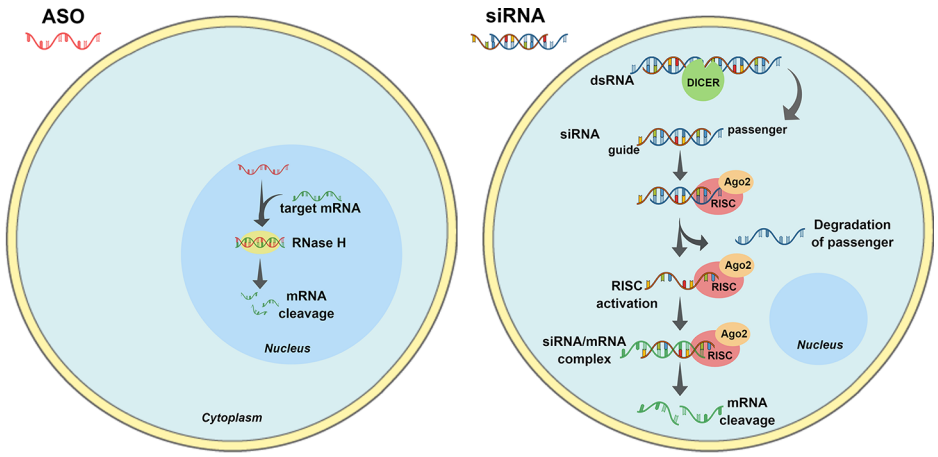

Structure	single-stranded	double-stranded
Lenght	12-30 bp	19-25 bp
Molecular weight	4-10 kDa	~14 kDa
Site of action	Cytoplasm/nucleus	Cytoplasm
mRNA cleavage	RNase H	RISC
Effective concentration	50-400 nM	5-100 nM

Figure 1. RNAi-based therapeutic main approaches: single-stranded antisense oligonucleotides (ASOs) and double-stranded small interfering RNA (siRNA). ASOs: Once bound to the target mRNA, ASOs can form an RNA−DNA hybrid that becomes a substrate for RNase H, which results in mRNA degradation. siRNA: Double-stranded RNA (dsRNA) is processed by Dicer into siRNA. The guide RNA strand is incorporated into the RNA-induced silencing complex (RISC) and Argonaute 2 (Ago2). Ago2 cleaves the passenger strand, and siRNA/RISC complex then binds the complementary sequence of the target mRNA resulting in the degradation of the target transcript.

microRNAs (miRNA), and short hairpin RNA (shRNA). In contrast to siRNA that acts in the cytosol, miRNA and shRNA require transport into the nucleus, an additional barrier to RNAi delivery.[12] Regarding drug development, siRNA is more suitable for drug use because it does not require genome integration and can be easily synthesized.[13]

ASOs are synthetic single-stranded nucleic acids generally containing 12−30 nucleotides in length (4−10 kDa), designed to bind a target RNA (pre-mRNA, mRNA, noncoding RNA) in a sequence-specific manner via Watson−Crick base-pairing rules. The single-stranded nature of ASOs may result in lower costs and simplify the delivery process when compared to siRNAs.[14] ASOs regulate RNA modulation either by mRNA cleavage through enzymatic degradation (RNase H) or by an occupancy-only mechanism, sometimes referred to as steric blocking. Furthermore, they can also modulate pre-mRNA splicing, reducing or restoring protein expression.[15−17]

RNase H triggering represents the most predominant knockdown mechanism. As illustrated in Figure 1, upon the introduction into cells, ASOs can enter the nucleus and engage with complementary sequences in pre-mRNAs. The formation of a DNA/RNA hybrid results in the recruitment of RNase H1, a ribonuclease that recognizes the DNA/RNA heteroduplex and catalyzes the cleavage of RNA, resulting in reduced mRNA levels.[18,19]

siRNAs are short double-stranded RNA molecules usually containing 19−25 base pairs (~14 kDa) that regulate gene expression and control a diverse array of biological processes. They consist of two strands: (i) the guide strand (antisense), containing the information for target-gene recognition, and (ii) the passenger strand (sense) required for loading into the RISC (RNA-induced silencing complex). Once in the cytoplasm, the RNAi process starts with the cleavage of long double-stranded RNA into siRNA by the Dicer enzyme (initiation phase). As shown in Figure 1, these small RNAs are then incorporated into the RISC (effector phase). The RISC nuclease Argonaute 2 (Ago2) cleaves siRNA strands and releases the guide strand, resulting in RISC activation. The guide strand anneals with its complementary mRNA leading to its degradation and the silencing of the targeted gene. The activated RISC complex (with antisense strand included) can move on to degrade additional targeted mRNA, allowing transient (3−7 days) gene silencing in rapidly dividing cells and, extending for several weeks, in slowly dividing cells.[19−21]

Although there has been a great progress, the treatment of neurological disorders using nucleic acids remains a challenging issue due to rapid degradation in the circulation, poor cellular uptake, lack of specificity for particular brain cell/tissues, and the complex structure of the brain and physiological barriers, especially the blood−brain barrier (BBB),[8] which restricts access to the CNS.[22,23]

The BBB is one of the most selective physiological barriers, regulating the transport of molecules, ions, and cells into and out of the brain and protecting the CNS from potentially harmful substances that enter the bloodstream. At the same time, the BBB controls CNS nutrition and homeostasis and maintains the chemical composition of the neuronal milieu required for proper neuronal functioning. The BBB is formed by a monolayer of nonfenestrated endothelial cells sealed by tight junctions (TJ) and adherens junctions (AJ), which

https://doi.org/10.1021/acs.molpharmaceut.0c01238
Mol. Pharmaceutics 2021, 18, 1491−1506

together with astrocytes, pericytes, neurons, and the basement membrane constitute the neurovascular unit.[23−25] The complexity of the BBB restricts CNS drug delivery, thus limiting the treatment of several neurological diseases.

This review will focus on the strategies for the systemic delivery of therapeutic nucleic acids targeting the CNS. Pathways and mechanisms of transport across the BBB which could be exploited for delivery are described, focusing in particular on smaller nucleic acids including ASOs and siRNA. Approaches used to enhance delivery including chemical modifications, nanocarrier systems, and cell-specific delivery are critically analyzed. A comparison of the successes and failures reported for CNS delivery of ASOs versus siRNA highlights learnings, which will help identify future translational opportunities for a wider range of therapeutic nucleic acids.

2. CHALLENGES FOR SYSTEMIC DELIVERY

The initial challenges faced by nucleic acids after systemic administration lie in the circulatory system. From the drug delivery point of view, RNA molecules have unfavorable physicochemical properties including a negative charge, high molecular weight and size, and serum instability. Naked RNA molecules are rapidly degraded by nucleases in biological fluids, which results in renal clearance and short circulation time in the blood (<10 min).[12] Degradation can stimulate the innate immune system, triggering inflammatory and other immune responses and serum protein interaction. This phenomenon, known as opsonisation, causes rapid uptake by the reticuloendothelial system (RES) (Figure 2). After

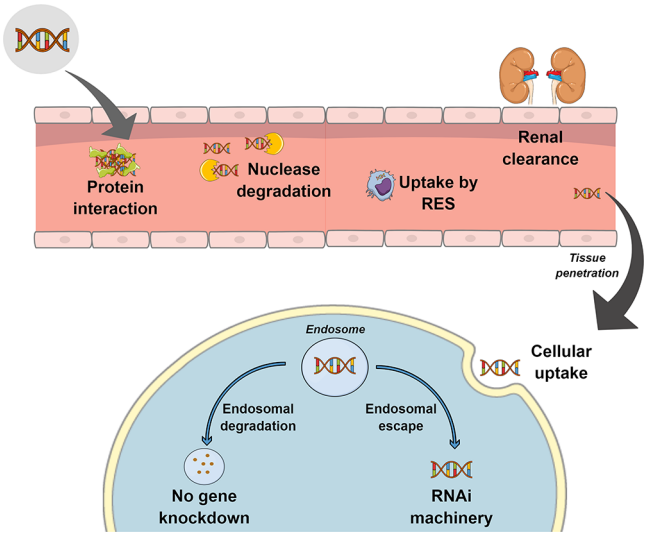

Figure 2. Physiological barriers to systemic delivery of RNA-based therapeutics. After systemic administration, the therapeutic nucleic acid must avoid interaction with bloodstream components, renal excretion, and uptake by phagocytes of the reticuloendothelial system (RES). Once at the targeted tissue, it must be internalized into the cell and escape from the endosome before degradation.

systemic administration, phagocytic cells of RES, specifically the Kupffer cells in the liver and the splenic macrophages, can easily endocytose RNA oligonucleotides, resulting in higher concentrations in these organs following intravenous administration.[13,26]

In addition, the circulating nucleic acids must cross the vascular endothelial barrier to accumulate in the target tissue. The structure and permeability of the capillary endothelia vary across different organs and tissue types, making some tissues more accessible to therapeutics than others. For example, the liver and spleen are composed of fenestrated capillaries and discontinuous basement membranes exhibiting large inter- and intracellular gaps, which allow the easy diffusion of nucleic acids into the tissue interstitium. The CNS capillaries, due to the BBB, exhibit nonfenestrated capillaries with dense intercellular junctional proteins (TJ and AJ) and a continuous basement membrane making extravasation of large molecules into the brain very difficult.[27]

After reaching the target cell, the next challenge is cellular uptake of the nucleic acid therapeutics. The cellular membrane is made of negatively charged phospholipids, and this charge is a barrier for nucleic acid uptake. Moreover, the high molecular weight, large size, and hydrophilic nature of RNA molecules impede membrane permeability. As a result, the major mode of internalization is via endocytosis, whereby the molecules are internalized together with a component of the cell membrane.[12] Finally, endosomal escape and release into the cytoplasm is a key problem that must be solved to ensure a safe delivery of RNA-based therapeutics and effective gene knockdown.[11]

In light of the challenges described above, generally, only small lipophilic molecules (<400 Da) freely diffuse across the brain endothelium (Figure 3 (1)). Other small water-soluble molecules can simply cross BBB through the TJ and AJ; however, paracellular transport is generally limited (Figure 3 (2)). Almost all other substances require certain endogenous transport systems to cross the BBB, such as transport proteins (carrier-mediated transport), absorptive-mediated transcytosis, or receptor-mediated transcytosis.[28]

Transport proteins (Figure 3 (3)) enable essential molecules such as glucose, amino acids, monocarboxylic acids, hormones, fatty acids, carbohydrates, nucleotides, inorganic ions, amines, choline, and vitamins to cross the BBB via substrate-specific transporters, e.g., GLUT1 for glucose and LAT1 for some amino acids.[23] Adsorptive-mediated transcytosis (Figure 3 (4)) is triggered by electrostatic interaction between a positively charged substance and the negatively charged membrane surface of the endothelial cells. Receptor-mediated transcytosis (Figure 3 (5)) enables the transport of small and large molecules including hormones, growth factors, enzymes, and plasma proteins. Endothelial cells have a limited number of receptors on their surface; thus, this route is normally a saturable process.[29,30]

Via receptor-mediated transcytosis, a specific receptor binds to its ligand on the luminal side of the endothelium and carries it to the abluminal side via the formation of endocytic vesicles. These vesicles can be either clathrin- or caveolae-dependent.[31] Importantly, the different nature of the endocytic vesicles will dictate the intracellular routes followed by the cargo prior to its delivery to the abluminal side (brain). Contrarily to the clathrin-dependent pathway, the caveolae-dependent pathway can bypass lysosomal storage.[32]

The above-described different transport systems across the BBB have been exploited to deliver therapeutic drugs to the brain. Generally, targeting transporters or receptors to access the brain involves creating complexes between the drug of interest and a receptor-targeting item. Such items can be the endogenous receptor/transporter ligands, mimetic ligands, or

https://doi.org/10.1021/acs.molpharmaceut.0c01238
Mol. Pharmaceutics 2021, 18, 1491−1506

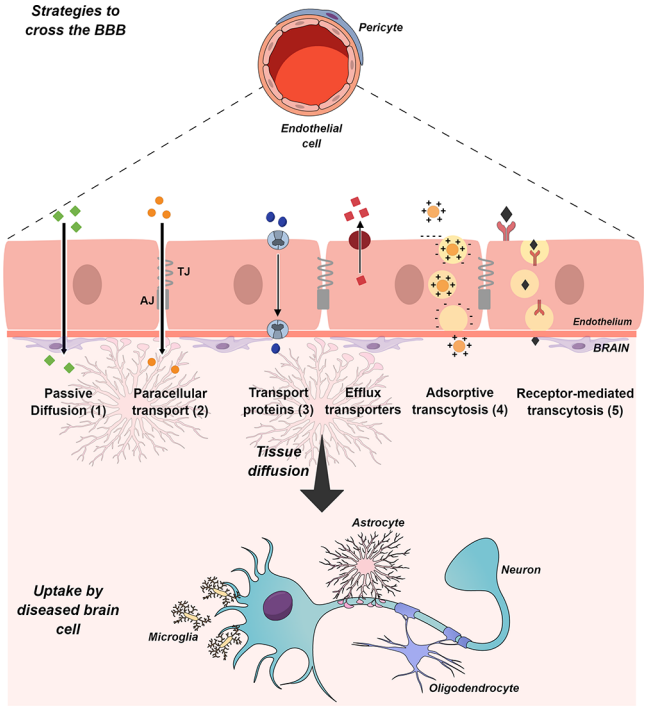

Figure 3. Schematic representation of the blood−brain barrier and the main transport routes for permeation and transport across the endothelium. (1) Small lipid-soluble agents can passively diffuse through the lipid bilayer. (2) Only small water-soluble molecules can diffuse through the intercellular spaces between endothelial cells. (3) The endothelium contains carriers for glucose, amino acids, nucleosides, purine bases, choline, and other substances. (4) Cationic molecules such as albumin and other plasma proteins are taken up by adsorptive-mediated transcytosis, which is consecutive of the endocytosis/exocytosis event. (5) Ligands such as insulin, transferrin, cholesterol-containing particles, and most other protein hormones are taken up by specific receptor-mediated transcytosis. Once across the BBB, the compounds must diffuse toward the disease site and be taken up by the diseased cells. TJ, tight junction; AJ, adherens junction.

an antibody targeting the receptor.[32] Accordingly, transport proteins present in the brain endothelium can be targeted to deliver the drug of interest into the brain. An example for this would be the use of glycosylated nanocarriers that can cross via the GLUT1 receptor.[33] One clear drawback is that many of these receptors, such as the GLUT receptors, are not exclusively expressed in the brain endothelium, which can lead to nonspecific targeting. Clathrin-dependend transport has also been used for drug delivery into the brain, especially the transferrin receptor. Despite being highly expressed in the brain endothelium, it is also expressed in other tissues throughout the body. Moreover, it is inefficient in delivering the cargo into the brain from the endothelial cytoplasm.[34,35] Caveolae-dependent transport has an important advantage in terms of intracellular trafficking of the cargo, as it does not involve the lysosomal pathway.[32,36] In this context low-density lipoprotein receptor is a good candidate to target for drug delivery purposes. To do so, the two main strategies include protein corona-mediated targeting and ligand-based targeting.[35] Both of these strategies are further detailed below.

Finally, endothelial cells express several ATP-driven drug efflux pumps, such as P-glycoprotein (P-gp), multidrug related protein (MRP), and breast cancer resistance protein (BCRP) transporters, which provide an additional layer of regulation by actively excluding many hydrophobic molecules from the CNS.[29,30] These efflux transporters constitute an important challenge for drug delivery into brain tissue, as they are known to greatly restrict brain permeability to a wide array of structurally diverse xenobiotics.[37] Therefore, it is essential that these transporters are considered while assessing drug transport properties in preclinical studies.

In summary, different approaches are being explored in order to overcome the limitations of each of these routes of transport across the BBB. Further investigation will allow optimization of drug delivery into the brain. In the past years, researchers have designed carriers (e.g., nanoparticles (NPs)) to target diseased cells in the brain with high specificity by overcoming the BBB and with reduced toxic side effects.[38] The main ligands targeting specific receptors on the BBB, as well as cell-specific markers on the diseased brain, are discussed below.

3. DESIGN AND DEVELOPMENT OF RNA-BASED THERAPEUTICS FOR SYSTEMIC DELIVERY

Despite the promising potential of RNA-based therapeutics, delivery strategies are required for the successful translation of ASOs and siRNA into the clinic. There are two broad strategies to improve the systemic delivery of RNA-based therapeutics. One is the chemical modification of the ASOs/siRNA structure itself while preserving the molecular nature and activity of the nucleic acid. The other is the incorporation of the nucleic acids into a delivery system. Both strategies aim to enhance the safety and potency of the nucleic acid, resulting in selective and stable systems.[39]

The main approaches for the delivery of ASOs and siRNA therapeutics are summarized in Figure 4. To date, unformulated/naked and chemical modifications predominate for ASOs, while conjugates and nanocarrier systems have been more widely studied for siRNA.

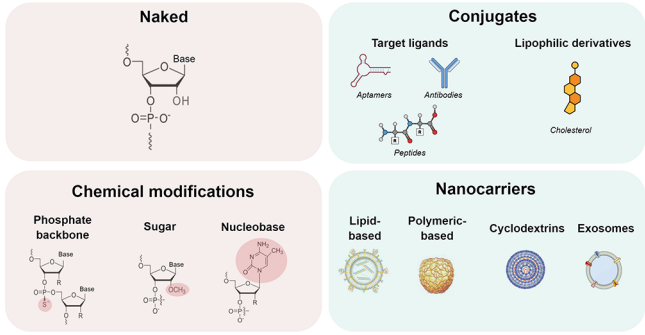

Figure 4. Main strategies for central nervous system delivery of antisense oligonucleotides (ASOs) and small interfering RNA (siRNA). Unformulated/naked and chemical modifications predominate for ASOs, while conjugates and nanocarrier systems have been more widely studied for siRNA.

3.1. Chemical Modifications. A variety of chemical modifications have been developed to improve the physical and pharmacological characteristics of RNA-based therapeutics (Table 1), such as ASOs and siRNA. Alterations in the chemical structure of the nucleic acids are focused on either the backbone, the sugar group (ribose), or the nucleobases.[39]

Nucleic acids consist of nucleotides all with a common structure. Nucleotides incorporate ribose linked at the 1′ position to a nucleobase and the 5′ position to a phosphate

https://doi.org/10.1021/acs.molpharmaceut.0c01238
Mol. Pharmaceutics 2021, 18, 1491−1506

Table 1. Common Chemical Modifications Used in RNA-Based Therapeutics[a]

strategy	content	goal
Backbone modifications	Phosphorothioate	Enhance nuclease stability
	Sugar-phosphate	Improve pharmacokinetics
Sugar modifications	2′-Ribose modifications (2′-OMe, 2′-F, 2′-OME, cEt, LNA)	Increase binding affinity to RNA
		Enhance stability against nucleases
		Decrease immune activation
Nucleobase modifications	5-Methylcytosine	Enhance RNA affinity
		Decrease proinflammatory properties
Conjugations	Biomolecules (antibodies, aptamers, peptides)	Modulate protein binding
	Hydrophobic derivatives	Modulate tissue distribution

[a]Abbreviations: 2′-OMe, 2′-*O*-methyl; 2′-F, 2′-fluoro; 2′-MOE, 2′-*O*-methoxyethyl; cET, 2′,4′-constrained 2′-*O*-ethyl; LNA, locked nucleic acid.

group. These structures are connected via phosphodiester bonds formed at 3′ and 5′ carbon of the ribose and make up the strands of the nucleic acids. The phosphate linkage and ribose are easy targets for metabolic degradation. Therefore, chemical modifications are preferentially performed at these sites.[40,41] Regarding their composition, siRNA and ASOs differ in their strand characteristics. siRNA consists of a double-strand and therefore leads to some restriction in the application of modifications due to duplex stability and interaction between siRNA and RISC complex.[42]

3.1.1. Backbone Modifications. The chemistry of the backbone has the largest impact on the pharmacokinetics and pharmacodynamics properties of nucleic acids.[41] Therefore, the replacement of the natural phosphodiester backbone by the inclusion of a more hydrophobic phosphorothioate (PS) was the first chemical modification implemented on nucleic acids. The PS modification replaces a nonbridging phosphate oxygen atom with a sulfur atom and has been extensively used to improve nuclease stability[43] of both ASOs[44,45] and siRNAs.[46]

The PS-modified backbones increase resistance against nucleases in serum and tissues and consequently prolonged circulation time. It promotes protein binding and thus supports interactions with albumin and other blood proteins, thereby retarding renal clearance and ensuring that PS-oligonucleotide can reach the tissues. The PS-modification is fully consistent with the RNase H activity.[41,47−49] Following intravenous administration of single-stranded PS-modified oligonucleotides, the distribution phase from plasma to tissues ranges from a few minutes to a few hours followed by a prolonged elimination phase that can last for several weeks. In contrast, unmodified oligonucleotides do not bind extensively to plasma proteins and are quickly cleared by the kidneys, accumulating at lower levels in tissues.[15,50]

Similar backbone modifications include the replacement of nonbridging oxygen with boron (boranophosphate), nitrogen (phosphoramidate), or methyl (methylphosphonate).[42,43] Phosphoramidate and methylphosphonate are preferentially used in ASOs and were not intensively studied in siRNA, whereas boranophosphate is applicable for both nucleic acids.[43]

The replacement of the sugar-phosphate by the introduction of a peptide or morpholino structure leads to the elimination of the charge of the nucleic acid backbone; this modification is mostly used for ASOs. The phosphodiester linkages are replaced with either phosphorodiamidate (morpholino) or polyamide (peptide) linkages.[39,47]

As a result of neutralization, the nucleic acids lose the ability to mobilize RNase H.[47,51,52] They gain protection against nuclease degradation but operate by translation inhibition through steric interference[52] and splice modification.[47,51,52] On the contrary, the neutral character of morpholino- and peptide-modified ASOs impairs cellular uptake due to the decreased probability of interaction with negatively charged cell membranes. To compensate for this drawback, two strategies have been investigated: the formulation into a lipid nanoparticle or the conjugation with a peptide which functions as a targeting ligand, leading to receptor-mediated uptake.[52]

3.1.2. Sugar Modifications. An approach to reduce the immune activation of nucleic acids while further enhancing the nuclease resistance includes substituting the 2′-hydroxy group at the ribose. This approach includes modification with 2′-*O*-methyl (2′-OMe), 2′-fluoro (2′-F), 2′-*O*-methoxyethyl (2′-MOE) groups, and bridged rings (2′,4′-constrained 2′-*O*-ethyl (cET), locked nucleic acid (LNA).[40,41]

All 2′-OH modifications, which can be applied to ASOs, can also be applied to siRNA, though with some restriction due to the mechanism of action of the siRNA. Modifications in siRNA can lead to impaired loading into the RISC complex, which decreases siRNA efficacy. 2′-OMe and 2′-F are the most commonly used modifications in siRNA.[50] The naturally occurring[40,48] and therefore nontoxic 2′-OMe modification is only used in alternate bases in siRNA to maintain efficacy and simultaneously gain resistance against recognition by the immune system and also enhanced nuclease resistance.[48]

The 2′-MOE modification is comparatively larger and therefore can only be applied at specific positions in the guide strand of the siRNA because of its negative impact on the silencing activity. Even in ASOs, 2′-MOE is mostly used in the so-called “gapmer” design (see section below).[48]

The bridged 2′,4′-ring of ribose is one of the most complicated 2′-ribose modification involved in ASOs chemistry, especially in the design of gapmer ASOs,[42] which comprises the binding of cET and LNA.[48] This modification provides an increased binding affinity to target-mRNA[53] but is unable to recruit RNase H.[47] Instead, it operates via alternative splicing or translational inhibition. A new type of oligonucleotide composition was investigated to regain the RNase H recruitment;[52] this provides the basis for the development of gapmers.[54] Gapmers contain a central unmodified region of nucleotides, flanked with 2′ modified nucleotides on each side.[47,48] The unmodified region features RNase H activity,[50] whereby the flanked regions only improve the binding affinity to target mRNA.[41] This approach represents high nuclease resistance, low toxicity, and increased hybridization affinities to mRNA.[42,48]

3.1.3. Nucleobase Modifications. Compared to modifications of the backbone and sugar moieties, nucleobase

https://doi.org/10.1021/acs.molpharmaceut.0c01238
Mol. Pharmaceutics 2021, 18, 1491−1506

Table 2. Selected Examples of Nanoparticle-Based RNA Formulations for *in Vivo* Brain Delivery via Systemic Administration[a]

formulation	nucleic acid	animal model	target	ref
		Lipid-Based NPs		
Angiopep-2- targeted liposomes	GOLPH3siRNA	U87-GFP-Luciferase-bearing BALB/c mouse	LRP-1	72
RVG-9r-targeted liposomes	Ataxin3 siRNAs	C57 BL/6 ataxin-3 [Q69]-transgenic	nACh	73
Calcium phosphate lipid NPs	SOD1 ASO	Transgenic zebrafish		74
		Polymeric NPs		
GLUT-1 targeted polymeric NPs	MALAT1-ASO	BALB/c mice	Glucose transporter	75
PBAE NPs	siRNA	Orthotopic GBM1A mouse model		76
		Hybrid NPs		
Angiopep-2 lipid-PLGA NPs	GOLPH3 siRNA	Nude U87 xenograft mice	LRP-1	77
		Cyclodextrin		
Transferrin targeted CD	RRM2 siRNA	Monkeys	Transferrin receptor	78
		Exosomes		
RVG-targeted exosomes	BACE1 siRNA	C57BL/6	nACh	79
T7-peptide targeted exosomes	microRNA-21 ASO	Glioblastoma rat model	Transferrin receptor	80

[a]Abbreviations: CD, cyclodextrin; GOLPH3, Golgi phosphoprotein 3; LRP-1, low density lipoprotein receptor-related protein 1; nACh, nicotinic acetylcholine receptor; NPs, nanoparticles; PBAE, poly(β-aminoester); RRM2, ribonucleotide reductase subunit M2; RVG, rabies virus glycoprotein; SOD, superoxide dismutase I.

modifications have not been used extensively for the stabilization of RNA-based therapeutics. Modifications to the nucleobases could create modified nucleosides metabolites that may be incorporated into native nucleic acids and interfere with the correct expression and maintenance of genetic material. There is, however, a notable exception: the C-5 methyl substitution on pyrimidine nucleobases (5-methylcytosine, 5-methylcytidine, and 5-methyluridine/ribothymidine).[42,55] The pyrimidine methylation has the effect of increasing the oligonucleotide melting temperature by ∼0.5 °C per modification and has been commonly incorporated into ASOs (e.g, those under development by Ionis Pharmaceuticals).[56,57]

The nucleobase modification can impact the nucleic acid activity in various ways: nuclease resistance, enhanced sequence selectivity to target mRNA, reduced off-target effects by preventing immune stimulation resulting in decreased proinflammatory characteristics[15,57] and more efficient gene activity.[58,59] Interestingly, 5-methyl substitution decreases the activity of siRNA and is therefore not beneficial in this regard.[57]

In summary, as described above, chemical modification is a promising approach to make nucleic acids a successful therapeutic modality to treat diseases including neurological disorders. However, despite the impressive preclinical potential of siRNA for treating brain diseases, most of the candidates, whether approved or in clinical trials, are ASOs. Currently, there are two FDA-approved ASOs: nusinersen (also known as Spinraza, ISIS 396443, ISIS-SMNRx, and ASO-10-27) and eteplirsen (Exondys 51). Nusinersen is indicated to treat spinal muscular atrophy, a hereditary disorder linked to deletion or mutation of the survival motor neuron 1 gene located on chromosome 5q13. It has two chemical modifications, one on its backbone (PS) and another at its sugar units (2′-MOE).[60] Eteplirsen is an ASO with phosphoroimidate morpholino modification at the backbone against Duchenne muscular dystrophy, a debilitating genetic disease characterized by the lack of functional dystrophin protein, which results in progressive lethal skeletal muscle degeneration.[61] There are also other candidates in phase 3 clinical trial; Trabedersen is an ASO from Isarna therapeutics design with a simple PS-modification tested against glioblastoma,[61] and tominersen is a gapmer-RNA modified with 2′-MOE PS developed for the treatment of Huntington disease.[62,63] Imetelstat, a second glioblastoma product, contains N3′-PS thiophosphorimidate with a covalently linked C16 lipid moiety at the 5′ end.[64]

3.2. Nanocarrier Systems. Parallel to the development of chemically modified nucleic acids, researchers have also been working on nucleic acid carrier systems. NPs have a proven track record as efficient carriers for systemic nucleic acid delivery including brain delivery (Table 2). Formulations include lipid-based NPs (LNPs), polymeric NPs, lipid−polymer hybrid NPs, and modified cyclodextrins (CDs). These NPs have demonstrated remarkable properties such as the ability to cross multiple biological barriers and protect target genes against nuclease degradation, improved pharmacokinetic profile by preventing renal excretion and RES clearance, enhanced stability in physiological solutions, and delivery to target specific tissues or cells.[65−68] Recently, exosomes have also emerged as a new delivery vehicle for siRNA, ASOs, and small molecules to the brain.[69−71] The characteristics of nanocarrier systems and examples of their formulation and use are reviewed below.

3.2.1. Lipid-Based NPs. Over the past decades, the delivery approach that is both most extensively used and most clinically advanced is to complex oligonucleotides with cationic lipids, thus forming LNPs, also called lipoplexes.[16,50,81] In 2018, the first-ever RNAi therapeutic, Onpattro (Patisiran), was approved by FDA and launched by Alnylam. Onpattro is formulated as a LNPs to delivery siRNA targeting transthyretin (TTR) into hepatocytes for the treatment of hereditary TTR-mediated amyloidosis in adults.[82] This drug represents the dawn of the RNA nanomedicine era, and it further accelerated the development of nucleic acid-loaded LNPs for various therapies. Recently, BioNTech/Pfizer and Moderna encapsulated their mRNA vaccines against COVID-19 using LNPs.[83]

https://doi.org/10.1021/acs.molpharmaceut.0c01238
Mol. Pharmaceutics 2021, 18, 1491−1506

Table 3. Cationic Lipids That Have Been Used in Lipid-Based NPs[a]

amino lipid	optimized ionizable lipid	lipidoid
Monovalent cationic: DOTAP; DOTMA; DMRIE	Dlin-DMA	C12-200
Monovalent ionizable: DODAP; DODMA	Dlin-KC2-DMA	98N12-5
Multivalent ionizable: DOGS	Dlin-MC3-DMA	
Cholesterol derivatives: DC-Chol; GL67		

[a]Abbreviations: DC-Chol, 3β-(*N*-(*N*′,*N*′-dimethylaminoethane)carbamoyl)cholesterol; DLinDMA, 1,2-dilinoleyloxy-3-dimethylaminopropane; DMRIE, *N*-(2-hydroxyethyl)-*N*,*N*-dimethyl-2,3-bis(tetradecyloxy)-1-propanaminium bromide; DODAP, 1,2-dioleoyl-3-dimethylammonium-propane; DODMA, 1,2-dioleyloxy-3-dimethylaminopropane; DOGS, *N*,*N*-dioctadecylamidoglycylspermine; DOTAP, *N*-[1-(2,3-dioleoyloxy)-propyl]-*N*,*N*,*N*-trimethylammonium methyl sulfate; DOTMA, *N*-[1-(2,3-dioleyloxy)propyl])-*N*,*N*,*N*-trimethylammonium chloride; GL-67, N4-spermine cholesterylcarbamate

Lipid-based NPs include liposomes, solid lipid NPs, and nanostructured lipid carriers. These nanocarrier systems are composed of cationic (ionizable) lipids that bind DNA or RNA molecules, neutral helper lipids that increase transfection efficiency, and a nucleic acid vector encoding for the target gene.[84] Sometimes an additional targeting ligand is also incorporated to enable selective delivery to targeted cells after systemic administration. Generally, the basic structure of the cationic lipid employed for gene delivery consists of three domains: a hydrophilic headgroup (monocation or polycation, linear or heterocyclic) attached, via a linker bond, to a hydrophobic tail group (cholesterol or aliphatic).[85] The positively charged headgroup not only is responsible for the nucleic acid complexation but also affects NPs characteristics such as the surface charge. A large number of cationic headgroup structures have been investigated for application in gene delivery; selected examples are shown in Table 3.[84]

Although permanently charged cationic lipids have proven useful for *in vitro* transfection purposes, their utility *in vivo* is limited due to reduced transfection efficiency and cellular toxicity. The toxicity is normally associated with higher charge ratios between the cationic lipids and the nucleic acids as well as the dose administered.[86] To overcome this issue, ionizable cationic lipids such as DODAP were developed with apparent pK_a values between 6 and 7.[87] This pK_a ensures an efficient encapsulation of nucleic acid polymers at acid pH, a near neutral or mildly charged surface in the circulation at physiological pH, and a high positive surface charge at the acid environment of the endosome, which destabilized the NPs to release their RNA cargo.[88]

The rational design of the linker and the tail group is another strategy to enhance the efficacy of the formulation. The linker affects not only the global pK_a of ionizable lipids but also the size, flexibility for charge presentation, and biodegradability of the delivery system. The lipid properties of the tail group such as the degree of saturation, chain length, and substitution also affect the transfection efficiency.[84]

Several groups have encapsulated nucleic acids into LNPs for brain targeted gene delivery using the aforementioned ionizable cationic lipids.[73,89−91] Cohen et al. developed LNPs composed of the ionizable cationic lipid DLin-MC3-DMA, helper lipids distearoylphosphatidylcholine (DSPC), and cholesterol, using dimyristoyl glycerol (DMG), PEG (DMG-PEG), and distearoylphosphatidylethanolamine (DSPE)-PEG amine as linkers. The formulation was further functionalized with hyaluronan to deliver PLK1-siRNA to glioma cells. The authors observed a robust silencing of 80% in PLK-1 expression and prolonged survival (+60%) of a U87 xenograft mouse model.[89] Conceição and coauthors use DODAP, cholesterol, and DSPC to formulate liposomes. The liposomes were further functionalized with the brain-targeting rabies virus glycoprotein (RVG)29−nona-arginine, and conjugated to DSPE-PEG-maleimide. Promising results were observed in two transgenic mouse models of Machado−Joseph disease (MJD), also called spinocerebellar ataxia type 3 (SCA3), upon intravenous administration of siRNA targeting mutant ataxin-3 mRNA. The efficient silence of mutant ataxin-3 reduced the neuropathology and motor behavior deficits of both mice strains.[73]

A further liposome-mediated delivery has been developed (DCL64) composed of dipalmitoylphosphatidylcholine, cholesterol, and poloxamer L64. Intravenous administration of DCL64 formulation resulted in the interaction with low-density lipoprotein receptors (LDLr and LRP-1) and subsequent accumulation of the oligonucleotides in Purkinje cells of mouse cerebellum.[92] In another study, cationic liposomes with angiopep-2, a specific ligand of LRP-1, were used to deliver Golgi phosphoprotein 3 (GOLPH3)-siRNA for glioma treatment. Using an U87-GFP-luciferase-bearing BALB/c mouse model, the authors demonstrated that the liposomes delivered GOLPH3-siRNA specifically to glioma and effectively inhibited glioma growth.[72]

3.2.2. Polymeric Nanoparticles. Polymeric NPs provide another widely used strategy for nucleic acid delivery. Although they have not progressed clinically to the same degree as LNPs, polymeric NPs have shown desirable features such as biological safety (low immunogenicity, absence of mutagenesis), chemical versatility, facile synthesis, and low production costs.[50,93,94]

At an early stage, natural polymers such as polysaccharides (chitosan, CDs, alginate) and proteins (gelatin, albumin) were investigated as sustained gene delivery vectors; however, they exhibited low transfection efficiency. Therefore, in an effort to increase transfection efficacy many synthetic polymers have been developed including poly(ethylenimine) (PEI), poly-(lactic acid) (PLA), poly(L-glutamic acid) (PLGA), poly(L-lysine) (PLL), poly-ε-caprolactone (PCL), poly(β-aminoester) (PBAE), poly(2-(dimethylamino)ethyl methacrylate) (PDMAEMA), and the dendrimer poly(amidoamine) (PAMAM). Synthetic polymers have been used alone or in combination with natural polymers in the preparation of NPs or incorporated into sustained-release systems such as hydrogels, nanospheres, microspheres, and scaffolds.[94−96] Regardless, PEGylation, functionalization with targeting ligands, or modification by introducing histidine residues in their backbones is still necessary to improve the transfection efficiency and circulation times of polymeric NPs.[97]

The most commonly explored compounds for brain gene delivery include the polymers PEI, PBAE, and PLGA and the dendrimer PAMAM.[96,98,99] However, without surface mod-

https://doi.org/10.1021/acs.molpharmaceut.0c01238
Mol. Pharmaceutics 2021, 18, 1491−1506

ification with target ligands, polymeric NPs have a limited capacity to cross the BBB in sufficient amounts for therapeutic application. In a recent study, GLUT-1 targeted polymeric NPs (glycosyl-PEG-PLL modified with 3-mercaptopropyl amidine and 2-thiolaneimine) were designed for the delivery of ASOs across the BBB. The nanocarrier demonstrated efficient brain accumulation 1 h after intravenous administration and exhibits significant knockdown of a target long noncoding RNA in various mouse brain regions, including the cerebral cortex and hippocampus.[75]

3.2.3. Lipid–Polymer Hybrid Nanoparticles. Lipid–polymer hybrid NPs for gene delivery (lipopolyplexes) combine the desirable features of both lipids and polymeric NPs with high *in vivo* transfection efficiencies, improved colloidal stability, and reduced cytotoxicity.[97] As shown in Figure 5,

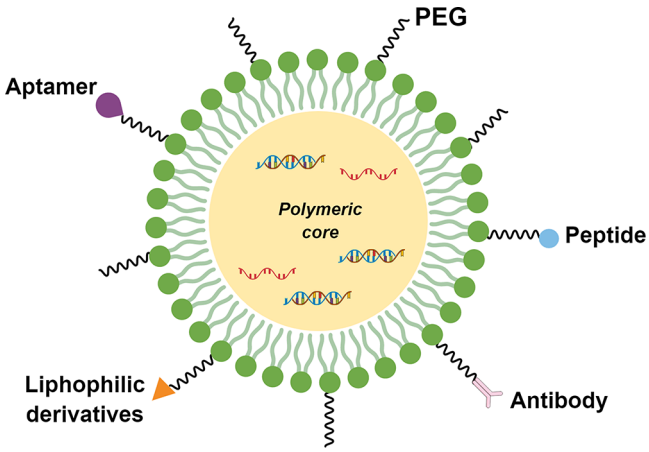

Figure 5. Schematic representation of a lipid–polymer hybrid nanoparticles (NPs). The NPs comprise a polymeric core containing a payload (siRNA or ASOs) surrounded by a lipid shell. Note that an additional outer PEG layer can be added and conjugated with targeting moieties such as aptamers, peptides, antibodies, and lipophilic derivatives (e.g., cholesterol). PEG, polyethylene glycol.

this type of nanostructure generally has a polymeric core containing the therapeutic agents to be delivered and a lipid shell that may either be a monolayer or bilayer. In some cases, an additional outer PEG layer and target ligands are further coated onto the lipid surface.[100]

An efficient delivery system based on DOTAP, PLGA, DSPE-PEG_{2000}, and Angiopep-2 was developed to co-deliver gefitinib and GOLPH3-siRNA across the BBB. The authors demonstrated that Angiopep-2 improved siRNA delivery to the brain tumor, downregulated GOLPH3 and EGFR expression after intravenous administration, and increased the median survival of the animals by 30% compared to nontreated controls.[77]

3.2.4. Cyclodextrins. CDs are a family of naturally occurring cyclic oligosaccharides obtained through bacterial digestion of starch, which are composed of glucose units linked by α-1,4-glycosidic bonds. The most common forms are α, β-, and γ-CDs, which consist of six, seven, and eight D-glucopyranose units (n = 6, 7 or 8), respectively.[101] CDs have a truncated cone-shaped appearance with upper (narrow, primary) and lower (wide, secondary) rims. The core is relatively hydrophobic due to the presence of CH groups and glycosidic oxygens, whereas the hydrophilicity at the cavity entrances (rims) is attributed to primary and secondary hydroxyl functional groups (−OH) (Figure 6).[102] Such unique structure results in an "inner–outer" amphiphilic characteristic enabling

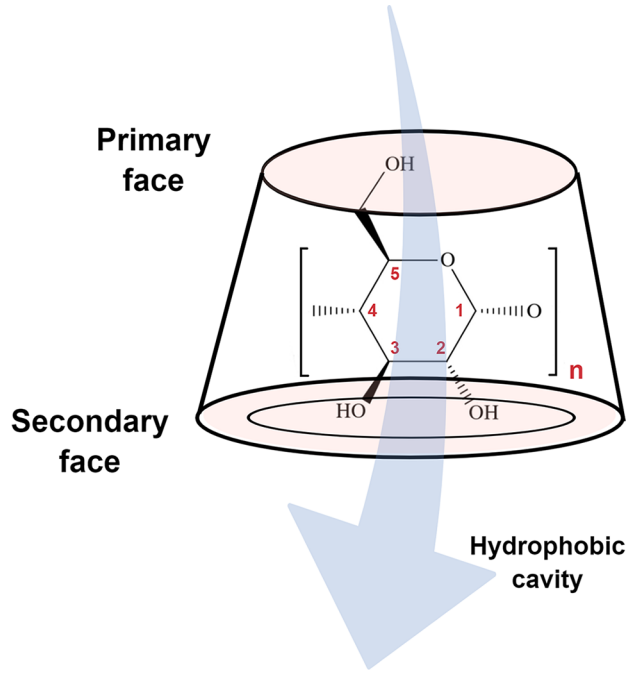

Figure 6. Schematic illustration of the 3D structure of cyclodextrin (CD). The CD comprises glucose units linked by α-1,4-glycosidic bonds and has a hydrophobic central cavity and a hydrophilic outer surface.

the CDs to encapsulate organic and inorganic molecules via host–guest interaction.[101] Due to these features and excellent biocompatibility and low toxicity, CDs have been profusely exploited by the pharmaceutical industry to improve the solubility of hydrophobic compounds and/or to improve stability, bioavailability, and delivery of hydrophilic as well as lipophilic drugs through biological membranes[101,103,104]

In the past decade, attention has been focused on the potential application of modified CD as gene delivery systems,[105−107] especially for treating brain diseases.[108−111] Modified amphiphilic β-cyclodextrins were used to deliver Huntingtin (HTT) targeted siRNAs to *in vitro* and *in vivo* models of Huntington disease. The formulation was stable in cerebrospinal fluid with limited toxicity. Sustained knockdown effects were observed associated with the alleviation of motor deficits.[108]

Besides its potential as a carrier, CDs can also act as therapeutic agents to treat neurodegenerative disorders exhibiting impaired cholesterol metabolism (e.g., Niemann–Pick type C (NPC), Alzheimer's, Huntington's, and Parkinson's diseases). CDs can directly interact with the BBB endothelial cells and modify cell membrane composition due to their ability of lipid extraction that directly influences cholesterol trafficking and homeostasis.[104] Two clinical trials are currently underway to evaluate the safety and pharmacokinetic and pharmacodynamic assessments of systemic iv administration of hydroxypropyl-β-cyclodextrin to NPC patients.[112]

3.2.5. Exosomes. Exosomes have recently emerged as a novel delivery system for biological therapeutics including siRNAs, ASOs, antibodies, and small molecules, especially those targeted to the brain tissue that require passage through

https://doi.org/10.1021/acs.molpharmaceut.0c01238
Mol. Pharmaceutics 2021, 18, 1491−1506

the BBB.[69−71] Exosomes are extracellular nanovesicles (40−120 nm) produced by almost every cell type, including B cells, T cells, dendritic cells, macrophages, neurons, glial cells, astrocytes, stem cells, and most tumor cell lines. They are generated mainly when multivesicular bodies fuse with the plasma membrane and release their content (exosomes) to the extracellular milieu. After exocytosis, exosomes are taken up by the recipient cells and release their cargo (e.g., nucleic acids, enzymes, peptides, lipids), which can mediate many physiological and pathological processes.[113,114]

Owing to desirable properties such as size, lipid membrane bilayer structure, and functional properties, exosome-based delivery has multiple advantages over other delivery systems. For instance, exosomes are stable in the bloodstream, enabling prolonged circulation. They are capable of carrying soluble drugs due to their hydrophilic core. Because exosomes are nanosized and are isolated from specific cells, they have a high capacity for overcoming various biological barriers, possess a natural targeting capacity, and thus have fewer off-target effects[71,113]

Pioneering work on exosome-mediated systemic CNS delivery of siRNA was initiated by Alvarez-Erviti and co-workers in 2011. Murine self-derived dendritic exosomes targeted with the neuron-specific RVG peptide and the exosomal membrane protein Lamp2b delivered GAPDH siRNA and BACE1 siRNA to neurons, microglia, oligodendrocytes in the mouse brain after intravenous administration. The exposure to RVG-decorated exosomes resulted in strong mRNA and protein knockdown of BACE-1 (∼60%), a therapeutic target in Alzheimer's disease.[79] Similarly, a T7 peptide-decorated exosome (T7-exo) was produced by incorporation T7, a transferrin receptor-binding peptide, into the exosome membrane as a fusion protein of T7 and Lamp2b. The T7-exo was evaluated as a carrier for brain-targeted delivery of antisense miRNA oligonucleotides against miR-21 (AMO-21), using RVG exosomes/AMO-21 as a control. Both brain-targeting ligands RVG and T7 increased the targeted trafficking of exosomes to the brain and reduced miR-21 levels in the glioblastoma by ∼80% and ∼60%, respectively, compared to the control group.[80]

3.3. Nucleic Acid Conjugates. Although significant progress has been made with chemical modifications and nanocarriers systems, brain-specific targeting is essential for an improved therapeutic effect of RNA-based therapeutics. To overcome the hurdles of selective CNS delivery of RNA-based technologies, reliable transport ligands have been linked to nucleic acids whether presented in naked form, as a chemical conjugate, or in association with a nanocarrier. Covalent conjugation of specific molecules to nucleic acids is a promising therapeutic approach to improve cellular uptake as well as pharmacokinetic properties.[40,115] However, conjugates can be applied to relatively small nucleic acid molecules such as ASOs and siRNA, but it is difficult to apply to large macromolecules such as mRNA, plasmid DNA, and CRISPR/Cas9. This method includes forming conjugates with (1) biomolecules capable of specifically binding receptors to the cell membrane such as folate, antibodies, aptamers, some peptides, and carbohydrates; (2) molecules capable of cell penetration by natural transport mechanisms (e.g., cholesterol and vitamins), or (3) molecules capable of interacting nonspecifically with the cell membrane such as positively charged compounds.[116]

These ligands target specific receptors on the BBB, as well as cell-specific markers on the diseased brain. The most widely studied ligands are transferrin, insulin, and low-density lipoprotein (LDL) receptors. Additional ligands that may have enhanced BBB specificity include aptamers, antibodies, peptides, and lipophilic derivatives.[116−118] The conjugation of siRNA (naked form) or NPs containing siRNA with ligands for targeted brain delivery will be discussed in detail below

3.3.1. Aptamers. Nucleic acid aptamers are short, single-stranded DNA or RNA oligonucleotides that assume unique tridimensional structures capable of specific molecular recognition of their cognate target. Generated through a process named systematic evolution of ligands by exponential enrichment (SELEX), aptamers demonstrate high affinity and specificity similar to the way that monoclonal antibodies bind to antigens.[119] Since aptamers can be synthetized against any target, they can potentially be used for the specific delivery to any organ, tissue, or cell where the desired target would be expressed.[120] Moreover, they have some crucial advantages, such as low immunogenicity and toxicity, prolonged stability, and low production variability.[121]

Aptamers have been identified as highly promising agents for brain-targeted therapy due to the ability of some aptamer conjugates to cross the BBB.[122−124] A bifunctional aptamer targeting the transferrin receptor (TfR) and the epithelial cell adhesion molecule (EpCAM), a cell surface marker overexpressed on several solid tumors has been developed. Since transferrin receptors are highly expressed on the surface of the BBB, TfR-EpCAM aptamer can bind to transferrin receptors on the surface of endothelial cells to be transported across the BBB and therefore deliver the payload to EpCAM-positive cells. In this study, the resulting bispecific TfR-EpCAM aptamer showed enhanced binding affinity and was able to effectively transcytose through an *in vitro* BBB model and also in healthy NOD/SCID mice following a single intravenous injection (40 nmol/kg).[123]

In recent years, aptamers have been transformed into multifunctional agents for the selective delivery of siRNAs, microRNA, small hairpin RNAs, and ASOs,[121] the so-called aptamer-chimeras. Aptamer-siRNA chimeras may offer dual functions in which the aptamer inhibits a receptor function while the RNAi internalizes into the cell to target a specific mRNA. Using a coculture model of human endothelial cells, astrocytes, and pericytes, it has been shown that both GL21.T and Gint4.T aptamers, either as single molecules or conjugated to microRNA-137 or anti-microRNA-10b, can cross the BBB. The RNA aptamers, GL21.T and Gint4.T, were able to bind with high affinity and inhibit the intracellular signaling of tyrosine kinase receptors (RTKs) Axl and the platelet-derived growth factor receptor β (PDGFRβ), respectively. These receptors are frequently highly expressed in glioblastoma stem-like cells and are associated with neovascularization.[124] A Gint4.T aptamer has successfully delivered STAT3 siRNA (Gint4.T-STAT3) to glioblastoma cells resulting in the silencing of STAT3 in PDGFRβ^+ glioblastoma cells, thereby reducing cell viability and migration. Importantly, Gint4.T-STAT3 reduced tumor growth and angiogenesis *in vivo* in a subcutaneous xenograft mouse model after repeated systemic injections.[125]

3.3.2. Antibodies. Monoclonal antibodies (mAbs), which act as a molecular "Trojan horse", have been adopted to deliver large molecules across the BBB. The receptor specific mAb penetrates the BBB via transcytosis mediated by specific

https://doi.org/10.1021/acs.molpharmaceut.0c01238
Mol. Pharmaceutics 2021, 18, 1491−1506

receptors on endothelial cells, commonly the insulin and transferrin receptors.[126] For example, OX26 (anti-rat TfR monoclonal antibody), R17-217 and 8D3 (both anti-mouse TfR monoclonal antibody), and 83-14 (anti-human insulin receptor) have all been investigated.[127,128]

The ability of a mAb against the human insulin receptor (HIRMab) combined with avidin−biotin technology successfully delivered siRNA across the BBB in an *in vivo* brain cancer model. Intravenous administration of the antibody-siRNA conjugate led to an efficient (69−81%) suppression in luciferase gene expression.[129] Following the same principle, antibodies against antigens expressed on glioblastoma stem cells (CD44 and EphA2) were conjugated to chemically modified ASOs against renal cell carcinoma (DRR), also called FAM107A, a genetic driver of glioblastoma invasion. The therapeutic conjugate was successfully internalized and reduced DRR/FAM107A expression in patient-derived glioblastoma stem cells.[130]

Despite decades of development, the use of antibodies remains limited due to the need for sophisticated production and purification equipment leading to high costs. A new generation of optimized antibodies including antibody fragments or diabodies are now emerging to tackle this limitation, but complex manufacturing processes remain a challenge.[120]

3.3.3. Cell-Penetrating Peptides. Cell-penetrating peptides (CPPs) are short peptidic sequences, generally with 5−30 amino acids, which facilitate drug or CPPs/cargo complexes to translocate across the cellular membrane. CPPs are classified into two categories: (1) based on the origin of peptides (synthetic, chimeric, protein-derived peptides) and (2) based on the physicochemical properties (cationic, amphipathic, and hydrophobic).[131,132] These short peptides are ligands for specific receptors that facilitate cell internalization by endocytosis and destabilization of endosomal compartments.[133]

Several BBB shuttle peptides with increasing efficiency and versatility have been reported including Angiopep-2, apolipoprotein (Apo) B, ApoE, peptide-22, THR, Leptin30, MiniAp-4, RVG29, RVG-9R, GSH, G23, TAT (47−57), and octaarginine (R8).[134,135] The short peptide RVG, which is known to specifically bind to acetylcholine receptors in neuronal cells, was the first CPP used in the transport of oligonucleotides into healthy mouse brains. Intravenous administration of RVG-9R siRNA complexes to wild-type Balb/C mice induced a significant reduction in both mRNA and protein levels of Cu−Zn superoxide dismutase (SOD1) in the brain.[136] Examples of other studies designed to deliver nucleic acids into the brain using RVG constructs have been discussed in detail above.[73,79,80]

As a further demonstration of CPPs delivery potential, Angiopep-2 modified PLGA NPs have successfully co-delivered doxorubicin and epidermal growth factor receptor (EGFR) siRNA for glioma therapy. This delivery system was capable of penetrating the BBB *in vivo*, resulting in extended survival of the glioma-bearing mice and cell apoptosis in the glioma tissue.[137]

3.3.4. Lipophilic Derivatives. Lipophilic molecules are often conjugated to oligonucleotides for delivery purposes. To date, lipophilic conjugates have been used for the delivery of both single- and double-stranded RNAs.[138] The concept behind conjugation with these molecules involves naturally occurring cell membrane transport mechanisms. More specifically, oligonucleotides modified with cholesterol are recognized by high- and low-density lipoproteins (HDL and LDL, respectively) and internalized via cholesterol binding receptors.[133] Additionally, the addition of these lipid moieties to oligonucleotides increases the lipophilicity of the nucleic acids and enhances their permeability across the cell membrane.[116]

Conjugation of siRNA with cholesterol, fatty acids, and vitamins (with or without a phosphocholine polar headgroup) has been shown to modulate siRNA tissue distribution and silencing activity *in vivo*.[139,140] In general, lipid-conjugated siRNAs primarily accumulate in clearance tissues (liver, kidney, and spleen). Higher lipophilic siRNAs preferentially bind LDL and distribute to the liver, whereas less lipophilic compounds bind to HDL in serum and accumulate in kidneys. No perfect correlation between compound accumulation and efficacy has been observed.[139,140]

Regarding the brain, the degree of distribution is strongly and inversely correlated with the hydrophobicity.[141] Although highly hydrophobic cholesterol-conjugated modified siRNAs (Chol-hsiRNAs) presented limited spread from the site of injection after intrastriatal injection, both docosahexaenoic acid (DHA)-conjugated, hydrophobic siRNA (DHA-hsiRNA) and phosphocholine-containing DHA-hsiRNA conjugate (PC-DHA-hsiRNA) diffused to other brain regions further away from the striatum and induced 70−80% silencing at both mRNA and protein levels.[142,143]

3.3.5. Protein Corona (Endogenous Ligands). Upon systemic administration, NPs encounter serum components, such as proteins, in the biological fluids resulting in the formation of a protein corona on the surface. Although protein corona formation has been associated with undesirable effects, recent studies suggest that corona-mediated targeting by controlling the function of target plasma proteins on nanosurface may provide a more specific drug delivery.[32,144−146]

With regard to the brain targeting, apolipoproteins play a key role. They are involved in the intercellular transport of insoluble lipids to various cell types, which are taken up via specific apolipoprotein-recognizing receptors (e.g., LDL receptor and scavenger receptor class B type I (SR-B1)) expressed in several tissues and in the brain.[147] For instance, Zhang et al. obtained a successful corona-mediated brain-targeting using a liposomal system loaded with doxorubicin and functionalized with a peptide derived from the amyloid β-protein ($A\beta_{1-42}$). When exposed to biological milieu, this peptide specifically interacts with the lipid-binding domain of the brain targeting apolipoproteins (i.e, ApoA1, ApoE, and ApoJ), resulting in the exposure of their receptor-binding domain. The reengineered liposomes demonstrated high brain-targeting capacity and improved anticancer effects compared to nontarget plain liposomes.[145] By use of a different approach, lipid NPs have been prefunctionalized with ApoE4 before systemic administration. This strategy increased NPs translocation into brain parenchyma and exhibited a 3-fold improvement in brain accumulation compared to undecorated NPs.[146]

Despite these promising results, there is no available data concerning the exploitation of corona proteins for systemic delivery of nucleic acid. However, lessons learned from these studies could offer further insights into formulations designed for targeted delivery of nucleic acids to the brain.

https://doi.org/10.1021/acs.molpharmaceut.0c01238
Mol. Pharmaceutics 2021, 18, 1491−1506

Table 4. ASO-Based Therapeutics for the Treatment of Brain Disease That Are FDA-Approved or Currently in Clinical Trials[a]

drug	disease	route	status	sponsor	NCT number
ASOs					
IONIS MAPTRx	Alzheimer disease	Intrathecal	Phase 1	Ionis Pharmaceuticals	NCT03186989
BIIB094	Parkinson disease	Intrathecal	Phase 1	Ionis Pharmaceuticals	NCT03976349
WVE-120101	Huntington disease	Intrathecal	Phase 1/2	Wave Life Sciences	NCT03225833
WVE-120102	Huntington disease	Intrathecal	Phase 1/2	Wave Life Sciences	NCT03225846
Imetelstat	Glioblastoma brainstem tumors	Intravenous	Phase 2, terminated	Geron	NCT01836549
Tominersen[b]	Huntington disease	Intrathecal	Phase 3, recruiting	Roche	NCT03842969
					NCT03761849
Trabedersen	Glioblastoma	Intratumoral	Phase 3, terminated	Isarna therapeutics	NCT00761280
Eteplirsen (Exondys 51)	DMD	Intravenous	FDA approved	Sarepta Therapeutics	
Nusinersen (Spinraza)	Spinal muscular atrophy	Intrathecal	FDA approved	Biogen	

[a]Abbreviations: ASOs, antisense oligonucleotides; DMD, Duchenne muscular dystrophy. NCT: ClinicalTrials.gov identifier number. Data were collected from ClinicalTrials.gov and ref 153. [b]Tominersen (previously known as IONIS-HTTRx and RG6042).

4. CLINICAL PROGRESS

Currently, there are a large number of preclinical studies focusing on the delivery of siRNA-based therapeutics into the brain. Although these drugs have not yet reached clinical trials, the successful delivery of siRNA to non-CNS tumor tissue using nanoparticle-based delivery systems following systemic administration has been demonstrated in multiple trials, providing proof-of-concept for RNAi-based therapeutics in humans.[148] Two nonviral siRNA drugs, namely, Onpattro (patisiran) and Givlaari (Ggivosiran), discussed in section 3.2.1, have already reached the market, and there are some other siRNA-based drugs in the pipeline for approval in the coming years.[149]

Almost two decades after the discovery of RNAi therapeutics, several challenges have limited the usefulness of siRNA in clinical trials for brain delivery.[8] To date, the main obstacles are delivery, limited diffusion/distribution, and durability (Figures 2 and 3). After injection directly into the brain, siRNA shows effective silencing for only a short period and remains regionally restricted to cells near the injection site. Similarly, after injection into the spinal cord, siRNA does not penetrate broadly into the brain parenchyma and requires several weeklong continuous perfusions to achieve efficacy. On the other hand, ASOs is effective for several weeks after a single intrathecal dose.[150] These and other challenges, such as clinical trial design and commercial considerations, have limited the usefulness of siRNA therapeutics and will require further optimization to produce successful drugs for brain disease therapy. With the increase in research addressing these challenges and with the recent emergence of siRNA-based drugs in the market, the hope is that the application of siRNA-based therapeutics for the treatment of neurological diseases will also be exploited in clinical settings in the near future.

Although systemic administration is more acceptable for patients compared to direct brain injection, this is not a common route of administration since nucleic acids do not cross the BBB after systemic administration. To simplify the delivery problem, drugs have been designed for administration directly into the brain and/or spinal cord. However, there are concerns regarding technical complications and the risks from highly invasive neurosurgery for patients. The complications are associated with the inaccurate insertion of the catheter, management of the device (including refills of the drugs), the possibility of an allergic reaction or rejection, infections, side effects, and tissue damage with each local administration.[151] Thus, safe and systemic delivery is the key focus in the development of novel nucleic acid delivery systems targeting the CNS.

The recent approval by the U.S. Food and Drug Administration (FDA) of two ASO-mediated therapies for the treatment of Duchenne muscular dystrophy (eteplirsen, Exondys 51) and spinal muscular atrophy (nusinersen, Spinraza) has opened a new era in nucleic acid-based therapeutics for neurodegenerative diseases.[10,152] To date, more than 100 ASOs are in preclinical development.[153] Table 4 summarizes some ASO-based therapeutics that have advanced from the bench to the clinical stages. The application of siRNA to neurodegenerative diseases is not as advanced as ASO technology.

5. FUTURE DIRECTIONS

Targeted gene modification via gene-editing tools (ZFNs, TALENs, and CRISPR/Cas9) has been emerging as a new therapeutic option for the treatment of neurodegenerative diseases.[154,155] However, there are still relevant drawbacks that need to be overcome before their clinical implementation. The major challenge is increasing the specificity and efficiency by decreasing the off-targets side effects. Furthermore, these components are more challenging to deliver, especially to the brain, due to the complexity and high molecular weight.[11,156] It is anticipated that research in gene editing will continue and advance significantly in the coming years.

A lesson learned from the research performed to date is that delivery tools do not necessarily adapt to all applications. The gene therapy approaches developed thus far have their own advantages and limitations, and therefore, choosing the best tool largely depends on the situation and clinical need.

6. CONCLUSIONS

This review highlighted the chemical modifications and nanocarriers systems that are currently under investigation for ASOs and siRNA delivery to the brain. There are many opportunities to optimize the formulation design to allow for systemic delivery. A combination strategy for delivery including chemical modification in tandem with a smart delivery system designed to achieve stability in the circulation, permeability across the BBB, diffusion to the diseased site, and specific uptake by the diseased cells may help the translation of these therapeutics for neurodegenerative diseases.

In summary, the past two decades have seen an exponential increase in RNA-based therapies. Several clinical trials have been approved, are ongoing, or completed, with successful

https://doi.org/10.1021/acs.molpharmaceut.0c01238
Mol. Pharmaceutics 2021, 18, 1491−1506

launches worldwide; however, RNAi has not yet achieved its full therapeutic potential. It is expected that new RNA-based medicines capaable of reaching nonliver or nontumor tissues following systemic administration will be produced in the coming years.

AUTHOR INFORMATION

Corresponding Author

Caitriona M. O'Driscoll − *Pharmacodelivery Group, School of Pharmacy, University College Cork, T12 YT20 Cork, Ireland*; Email: caitriona.odriscoll@ucc.ie

Authors

Monique C. P. Mendonça − *Pharmacodelivery Group, School of Pharmacy, University College Cork, T12 YT20 Cork, Ireland*; orcid.org/0000-0002-8129-2150

Ayse Kont − *Pharmacodelivery Group, School of Pharmacy, University College Cork, T12 YT20 Cork, Ireland*

Maria Rodriguez Aburto − *APC Microbiome Ireland, University College Cork, T12 YT20 Cork, Ireland; Department of Anatomy and Neuroscience, University College Cork, T12 XF62 Cork, Ireland*

John F. Cryan − *APC Microbiome Ireland, University College Cork, T12 YT20 Cork, Ireland; Department of Anatomy and Neuroscience, University College Cork, T12 XF62 Cork, Ireland*

Complete contact information is available at: https://pubs.acs.org/10.1021/acs.molpharmaceut.0c01238

Notes

The authors declare no competing financial interest.

ACKNOWLEDGMENTS

This publication has emanated from research supported in part by a grant from Science Foundation Ireland (SFI) and the European Regional Development Fund (ERDF) under Grant 13/RC/2073_2 (Centre for Research in Medical Devices, CÚRAM). A.K. acknowledges funding from SFI under Grant 17/RC-PhD/3477 and Grant 12/RC/2278_P2 (Advanced Materials and BioEngineering Research, AMBER).

REFERENCES

(1) Carroll, W. M. The Global Burden of Neurological Disorders. *Lancet Neurol.* **2019**, *18* (5), 418−419.

(2) DiLuca, M.; Olesen, J. The Cost of Brain Diseases: A Burden or a Challenge? *Neuron* **2014**, *82* (6), 1205−1208.

(3) Li, M.; Snider, B. J. Gene Therapy Methods and Their Applications in Neurological Disorders. In *Gene Therapy in Neurological Disorders*; Li, M., Snider, B. J., Eds.; Elsevier Inc., 2018; pp 3−39, DOI: 10.1016/B978-0-12-809813-4.00001-6.

(4) Duarte, F.; Déglon, N. Genome Editing for CNS Disorders. *Front. Neurosci.* **2020**, *14*, 579062.

(5) Han, Z. Gene Therapy Using Genomic DNA: Advances and Challenges. In *Gene Therapy in Neurological Disorders*; Li, M., Snider, B. J., Eds.; Elsevier Inc., 2018; pp 63−80, DOI: 10.1016/B978-0-12-809813-4.00003-X.

(6) Roovers, J.; de Jonghe, P.; Weckhuysen, S. The Therapeutic Potential of RNA Regulation in Neurological Disorders. *Expert Opin. Ther. Targets* **2018**, *22*, 1017−1028.

(7) Sheridan, C. Billion-Dollar Deal Propels RNAi to CNS Frontier. *Nat. Biotechnol.* **2019**, *37*, 699−706.

(8) Zheng, M.; Tao, W.; Zou, Y.; Farokhzad, O. C.; Shi, B. Nanotechnology-Based Strategies for SiRNA Brain Delivery for Disease Therapy. *Trends Biotechnol.* **2018**, *36* (5), 562−575.

(9) Chery, J. RNA Therapeutics: RNAi and Antisense Mechanisms and Clinical Applications. *Postdoc J.* **2016**, *4* (7), 35−50.

(10) Watts, J. K.; Brown, R. H.; Khvorova, A. Nucleic Acid Therapeutics for Neurological Diseases. *Neurotherapeutics* **2019**, *16*, 245−247.

(11) Dowdy, S. F. Overcoming Cellular Barriers for RNA Therapeutics. *Nat. Biotechnol.* **2017**, *35* (3), 222−229.

(12) Wang, J.; Lu, Z.; Wientjes, M. G.; Au, J. L. Delivery of SiRNA Therapeutics: Barriers and Carriers Delivery of SiRNA Therapeutics: Barriers and Carriers. *AAPS J.* **2010**, *12* (4), 492−503.

(13) Xu, C.; Wang, J. Delivery Systems for SiRNA Drug Development in Cancer Therapy. *Asian J. Pharm. Sci.* **2015**, *10* (1), 1−12.

(14) Watts, J. K.; Corey, D. R. Silencing Disease Genes in the Laboratory and the Clinic. *J. Pathol.* **2012**, *226* (2), 365−379.

(15) Bennett, C. F. Therapeutic Antisense Oligonucleotides Are Coming of Age. *Annu. Rev. Med.* **2019**, *70* (1), 307−321.

(16) Aartsma-Rus, A.; Jackson, A. L.; Levin, A. A. Mechanisms of Oligonucleotide Actions. In *Oligonucleotide-Based Drugs and Therapeutics*; Ferrari, N., Seguin, R., Eds.; John Wiley & Sons, Ltd., 2018; pp 1−37.

(17) Laina, A.; Gatsiou, A.; Georgiopoulos, G.; Stamatelopoulos, K.; Stellos, K. RNA Therapeutics in Cardiovascular Precision Medicine. *Front. Physiol.* **2018**, *9*, 953.

(18) Kitson, J. D. A.; Kamola, P. J.; Kane, L. Hybridization-Dependent Effects: The Prediction, Evaluation, and Consequences of Unintended Target Hybridization. In *Oligonucleotide-Based Drugs and Therapeutics*; Seguin, R., Ferrari, N., Eds.; John Wiley & Sons, Ltd., 2018; pp 191−226.

(19) Macchi, C.; Sirtori, C. R.; Corsini, A.; Santos, R. D.; Watts, G. F.; Ruscica, M. A New Dawn for Managing Dyslipidemias: The Era of Rna-Based Therapies. *Pharmacol. Res.* **2019**, *150*, 104413.

(20) Caillaud, M.; El Madani, M.; Massaad-Massade, L. Small Interfering RNA from the Lab Discovery to Patients' Recovery. *J. Controlled Release* **2020**, *321*, 616−628.

(21) Nikam, R. R.; Gore, K. R. Journey of SiRNA: Clinical Developments and Targeted Delivery. *Nucleic Acid Ther.* **2018**, *28* (4), 209−224.

(22) Niu, X.; Chen, J.; Gao, J. Nanocarriers as a Powerful Vehicle to Overcome Blood-Brain Barrier in Treating Neurodegenerative Diseases: Focus on Recent Advances. *Asian J. Pharm. Sci.* **2019**, *14* (5), 480−496.

(23) Sweeney, M. D.; Zhao, Z.; Montagne, A.; Nelson, A. R.; Zlokovic, B. V. Blood-Brain Barrier: From Physiology to Disease and Back. *Physiol. Rev.* **2019**, *99*, 21−78.

(24) Hawkins, B. T.; Davis, T. P. The Blood-Brain Barrier/Neurovascular Unit in Health and Disease. *Phamacol. Rev.* **2005**, *57* (2), 173−185.

(25) Pandit, R.; Chen, L.; Götz, J. The Blood-Brain Barrier: Physiology and Strategies for Drug Delivery. *Adv. Drug Delivery Rev.* **2020**, *165*−*166*, 1−14.

(26) Weng, Y.; Huang, Q.; Li, C.; Yang, Y.; Wang, X.; Yu, J.; Huang, Y.; Liang, X.-J. Improved Nucleic Acid Therapy with Advanced Nanoscale Biotechnology. *Mol. Ther.–Nucleic Acids* **2020**, *19* (March), 581−601.

(27) Kuebler, A. R.; Pries, W. M. Normal Endothelium. In *The Vascular Endothelium I. Handbook of Experimental Pharmacology*; Moncada, S., Higgs, A., Eds.; Springer: Berlin, 2006; pp 1−40.

(28) Bellettato, C. M.; Scarpa, M. Possible Strategies to Cross the Blood - Brain Barrier. *Ital. J. Pediatr.* **2018**, *44* (Suppl.2), 131.

(29) Patel, M.; Patel, B. Crossing the Blood-Brain Barrier: Recent Advances in Drug Delivery to the Brain. *CNS Drugs* **2017**, *31* (2), 109−133.

(30) Chen, Y.; Liu, L. Modern Methods for Delivery of Drugs across the Blood - Brain Barrier. *Adv. Drug Delivery Rev.* **2012**, *64* (7), 640−665.

(31) Ayloo, S.; Gu, C. Transcytosis at the Blood-Brain Barrier. *Curr. Opin. Neurobiol.* **2019**, *57*, 32−38.

(32) Kimura, S.; Harashima, H. Current Status and Challenges Associated with CNS-Targeted Gene Delivery across the BBB. *Pharmaceutics* **2020**, *12* (12), 1216.
(33) Patching, S. G. Glucose Transporters at the Blood-Brain Barrier: Function, Regulation and Gateways for Drug Delivery. *Mol. Neurobiol.* **2017**, *54*, 1046−1077.
(34) Li, H.; Qian, Z. M. Transferrin/Transferrin Receptor- Mediated Drug Delivery. *Med. Res. Rev.* **2002**, *22* (3), 225−250.
(35) Preston, J. E.; Abbott, N. J.; Begley, D. J. Transcytosis of Macromolecules at the Blood-Brain Barrier. In *Pharmacology of the Blood Brain Barrier: Targeting CNS Disorders*; Davis, T., Ed.; Elsevier Inc., 2014; Vol. *71*, pp 147−163, DOI: 10.1016/bs.apha.2014.06.001.
(36) Kiss, A. L.; Botos, E. Endocytosis via Caveolae: Alternative Pathway with Distinct Cellular Compartments to Avoid Lysosomal Degradation ? *J. Cell. Mol. Med.* **2009**, *13* (7), 1228−1237.
(37) Schinkel, A. H.; Jonker, J. W. Mammalian Drug Efflux Transporters of the ATP Binding Cassette (ABC) Family: An Overview. *Adv. Drug Delivery Rev.* **2003**, *55*, 3−29.
(38) Zhang, F.; Lin, Y.; Kannan, S.; Kannan, R. M. Targeting Specific Cells in the Brain with Nanomedicines For. *J. Controlled Release* **2016**, *240*, 212−226.
(39) Setten, R. L.; Rossi, J. J.; Han, S.-P. The Current State and Future Directions of RNAi-Based Therapeutics. *Nat. Rev. Drug Discovery* **2019**, *18* (6), 421−446.
(40) Yu, A. M.; Jian, C.; Yu, A. H.; Tu, M. J. RNA Therapy: Are We Using the Right Molecules? *Pharmacol. Ther.* **2019**, *196*, 91−104.
(41) Geary, R. S.; Norris, D.; Yu, R.; Bennett, C. F. Pharmacokinetics, Biodistribution and Cell Uptake of Antisense Oligonucleotides. *Adv. Drug Delivery Rev.* **2015**, *87*, 46−51.
(42) Deleavey, G. F.; Damha, M. J. Designing Chemically Modified Oligonucleotides for Targeted Gene Silencing. *Chem. Biol.* **2012**, *19* (8), 937−954.
(43) Behlke, M. A. Chemical Modification of SiRNAs for in Vivo Use. *Oligonucleotides* **2008**, *18* (4), 305−319.
(44) Papargyri, N.; Pontoppidan, M.; Andersen, M. R.; Koch, T.; Hagedorn, P. H. Chemical Diversity of Locked Nucleic Acid-Modified Antisense Oligonucleotides Allows Optimization of Pharmaceutical Properties. *Mol. Ther.–Nucleic Acids* **2020**, *19* (March), 706−717.
(45) Min, H. S.; Kim, H. J.; Naito, M.; Ogura, S.; Toh, K.; Hayashi, K.; Kim, B. S.; Fukushima, S.; Anraku, Y.; Miyata, K.; Kataoka, K. Systemic Brain Delivery of Antisense Oligonucleotides across the Blood-Brain Barrier with a Glucose-Coated Polymeric Nanocarrier. *Angew. Chem.* **2020**, *132* (21), 8250−8257.
(46) Alterman, J. F.; Godinho, B. M. D. C.; Hassler, M. R.; Ferguson, C. M.; Echeverria, D.; Sapp, E.; Haraszti, R. A.; Coles, A. H.; Conroy, F.; Miller, R.; Roux, L.; Yan, P.; Knox, E. G.; Turanov, A. A.; King, R. M.; Gernoux, G.; Mueller, C.; Gray-Edwards, H. L.; Moser, R. P.; Bishop, N. C.; Jaber, S. M.; Gounis, M. J.; Sena-Esteves, M.; Pai, A. A.; DiFiglia, M.; Aronin, N.; Khvorova, A. A Divalent SiRNA Chemical Scaffold for Potent and Sustained Modulation of Gene Expression throughout the Central Nervous System. *Nat. Biotechnol.* **2019**, *37* (8), 884−894.
(47) Schoch, K. M.; Miller, T. M. Antisense Oligonucleotides: Translation from Mouse Models to Human Neurodegenerative Diseases. *Neuron* **2017**, *94* (6), 1056−1070.
(48) Chi, X.; Gatti, P.; Papoian, T. Safety of Antisense Oligonucleotide and SiRNA-Based Therapeutics. *Drug Discovery Today* **2017**, *22* (5), 823−833.
(49) Selvam, C.; Mutisya, D.; Prakash, S.; Ranganna, K.; Thilagavathi, R. Therapeutic Potential of Chemically Modified SiRNA: Recent Trends. *Chem. Biol. Drug Des.* **2017**, *90* (5), 665−678.
(50) Juliano, R. L. The Delivery of Therapeutic Oligonucleotides. *Nucleic Acids Res.* **2016**, *44* (14), 6518−6548.
(51) Amantana, A.; Iversen, P. L. Pharmacokinetics and Biodistribution of Phosphorodiamidate Morpholino Antisense Oligomers. *Curr. Opin. Pharmacol.* **2005**, *5* (5), 550−555.
(52) Karaki, S.; Paris, C.; Rocchi, P. Antisense Oligonucleotides, A Novel Developing Targeting Therapy. In *Antisense Therapy*; IntechOpen, 2019; DOI: 10.5772/intechopen.82105.
(53) Rigo, F.; Chun, S. J.; Norris, D. A.; Hung, G.; Lee, S.; Matson, J.; Fey, R. A.; Gaus, H.; Hua, Y.; Grundy, J. S.; Krainer, A. R.; Henry, S. P.; Bennett, C. F. Pharmacology of a Central Nervous System Delivered 2′-O-Methoxyethyl- Modified Survival of Motor Neuron Splicing Oligonucleotide in Mice and Nonhuman Primates. *J. Pharmacol. Exp. Ther.* **2014**, *350* (1), 46−55.
(54) Scoles, D. R.; Minikel, E. V.; Pulst, S. M. Antisense Oligonucleotides: A Primer. *Neurol. Genet.* **2019**, *5* (2), e323.
(55) Rozners, E. RNA Metabolism and Drug Design. In *Translational Medicine: Molecular Pharmacology and Drug Discovery*; Meyers, R. A., Ed.; Wiley, 2018; pp 827−869.
(56) Roberts, T. C.; Langer, R.; Wood, M. J. A. Advances in Oligonucleotide Drug Delivery. *Nat. Rev. Drug Discovery* **2020**, *19*, 673−694.
(57) Wan, W. B.; Seth, P. P. The Medicinal Chemistry of Therapeutic Oligonucleotides. *J. Med. Chem.* **2016**, *59*, 9645−9667.
(58) Peacock, H.; Kannan, A.; Beal, P. A.; Burrows, C. J. Chemical Modification of SiRNA Bases to Probe and Enhance RNA Interference. *J. Org. Chem.* **2011**, *76* (18), 7295−7300.
(59) Yamakawa, K.; Nakano-Narusawa, Y.; Hashimoto, N.; Yokohira, M.; Matsuda, Y. Development and Clinical Trials of Nucleic Acid Medicines for Pancreatic Cancer Treatment. *Int. J. Mol. Sci.* **2019**, *20* (17), 4224.
(60) Sheng, L.; Rigo, F.; Bennett, C. F.; Krainer, A. R.; Hua, Y. Comparison of the Efficacy of MOE and PMO Modifications of Systemic Antisense Oligonucleotides in a Severe SMA Mouse Model. *Nucleic Acids Res.* **2020**, *48* (6), 2853−2865.
(61) Dirin, M.; Winkler, J. Influence of Diverse Chemical Modifications on the ADME Characteristics and Toxicology of Antisense Oligonucleotides. *Expert Opin. Biol. Ther.* **2013**, *13* (6), 875−888.
(62) Shen, X.; Corey, D. R. Chemistry, Mechanism and Clinical Status of Antisense Oligonucleotides and Duplex RNAs. *Nucleic Acids Res.* **2018**, *46* (4), 1584−1600.
(63) Rodrigues, F. B.; Ferreira, J. J.; Wild, E. J. Huntington's Disease Clinical Trials Corner: June 2019. *J. Huntington's Dis.* **2019**, *8* (3), 363−371.
(64) Kazmi, F.; Sensenhauser, C.; Greway, T. Characterization of the in Vitro Inhibitory Potential of the Oligonucleotide Imetelstat on Human Cytochrome P450 Enzymes with Predictions of in Vivo Drug-Drug Interactions. *Drug Metab. Dispos.* **2019**, *47* (1), 9−14.
(65) Singh, B. N.; Prateeksha; Gupta, V. K.; Chen, J.; Atanasov, A. G. Organic Nanoparticle-Based Combinatory Approaches for Gene Therapy. *Trends Biotechnol.* **2017**, *35* (12), 1121−1124.
(66) Costantino, L.; Boraschi, D. Is There a Clinical Future for Polymeric Nanoparticles as Brain-Targeting Drug Delivery Agents ? *Drug Discovery Today* **2012**, *17* (7−8), 367−378.
(67) Yang, L.; Ma, F.; Liu, F.; Chen, J.; Zhao, X.; Xu, Q. Efficient Delivery of Antisense Oligonucleotides Using Bioreducible Lipid Nanoparticles In Vitro and In Vivo. *Mol. Ther.–Nucleic Acids* **2020**, *19* (March), 1357−1367.
(68) Riley, M. K., II; Vermerris, W. Recent Advances in Nanomaterials for Gene Delivery — A Review. *Nanomaterials* **2017**, *7*, 94.
(69) Das, C. K.; Jena, B. C.; Banerjee, I.; Das, S.; Parekh, A.; Bhutia, S. K.; Mandal, M. Exosome as a Novel Shuttle for Delivery of Therapeutics across Biological Barriers. *Mol. Pharmaceutics* **2019**, *16*, 24−40.
(70) Zipkin, M. Exosome Redux. *Nat. Biotechnol.* **2019**, *37*, 1395−1400.
(71) Seyfizadeh, N.; Seyfizadeh, N.; Borzouisileh, S.; Elahimanesh, F.; Hosseini, V.; Nouri, M. Exosome-Mediated Therapeutic Delivery: A New Horizon for Human Neurodegenerative Disorders' Treatment (with a Focus on SiRNA Delivery Improvement). *Process Biochem.* **2019**, *85*, 164−174.
(72) Yuan, Z.; Zhao, L.; Zhang, Y.; Li, S.; Pan, B.; Hua, L.; Wang, Z.; Ye, C.; Lu, J.; Yu, R.; Liu, H. Inhibition of Glioma Growth by a GOLPH3 SiRNA-Loaded Cationic Liposomes. *J. Neuro-Oncol.* **2018**, *140* (2), 249−260.

(73) Conceição, M.; Mendonça, L.; Nóbrega, C.; Gomes, C.; Costa, P.; Hirai, H.; Moreira, J. N.; Lima, M. C.; Manjunath, N.; Pereira de Almeida, L. Intravenous Administration of Brain-Targeted Stable Nucleic Acid Lipid Particles Alleviates Machado-Joseph Disease Neurological Phenotype. *Biomaterials* **2016**, *82*, 124−137.
(74) Chen, L.; Watson, C.; Morsch, M.; Cole, N. J.; Chung, R. S.; Saunders, D. N.; Yerbury, J. J.; Vine, K. L. Improving the Delivery of SOD1 Antisense Oligonucleotides to Motor Neurons Using Calcium Phosphate-Lipid Nanoparticle. *Front. Neurosci.* **2017**, *11*, 476.
(75) Min, H. S.; Kim, H. J.; Naito, M.; Ogura, S.; Toh, K.; Hayashi, K.; Kim, B. S.; Fukushima, S.; Anraku, Y.; Miyata, K.; Kataoka, K. Systemic Brain Delivery of Antisense Oligonucleotides across the Blood-Brain Barrier with a Glucose-Coated Polymeric Nanocarrier. *Angew. Chem., Int. Ed.* **2020**, *59*, 8173−8180.
(76) Karlsson, J.; Rui, Y.; Kozielski, K. L.; Placone, A. L.; Choi, O.; Tzeng, S. Y.; Kim, J.; Keyes, J. J.; Bogorad, M. I.; Gabrielson, K.; Guerrero-CAzares, H.; Quiñones-Hinojosa, A.; Searson, P. C.; Green, J. J. Engineered Nanoparticles for Systemic SiRNA Delivery to Malignant Brain Tumours. *Nanoscale* **2019**, *11*, 20045−20057.
(77) Ye, C.; Pan, B.; Xu, H.; Zhao, Z.; Shen, J.; Lu, J.; Yu, R.; Liu, H. Co-Delivery of GOLPH3 SiRNA and Gefitinib by Cationic Lipid-PLGA Nanoparticles Improves EGFR-Targeted Therapy for Glioma. *J. Mol. Med.* **2019**, *97*, 1575−1588.
(78) Heidel, J. D.; Yu, Z.; Liu, J. Y.; Rele, S. M.; Liang, Y.; Zeidan, R. K.; Kornbrust, D. J.; Davis, M. E. Administration in Non-Human Primates of Escalating Intravenous Doses of Targeted Nanoparticles Containing Ribonucleotide Reductase Subunit M2 SiRNA. *Proc. Natl. Acad. Sci. U. S. A.* **2007**, *104* (14), 5715−5721.
(79) Alvarez-Erviti, L.; Seow, Y.; Yin, H.; Betts, C.; Lakhal, S.; Wood, M. J. A. Delivery of SiRNA to the Mouse Brain by Systemic Injection of Targeted Exosomes. *Nat. Biotechnol.* **2011**, *29* (4), 341−347.
(80) Kim, G.; Kim, M.; Lee, Y.; Byun, J. W.; Hwang, D. W.; Lee, M. Systemic Delivery of MicroRNA-21 Antisense Oligonucleotides to the Brain Using T7-Peptide Decorated Exosomes. *J. Controlled Release* **2020**, *317*, 273−281.
(81) Parashar, D.; Rajendran, V.; Shukla, R.; Sistla, R. Lipid-Based Nanocarriers for Delivery of Small Interfering RNA for Therapeutic Use. *Eur. J. Pharm. Sci.* **2020**, *142*, 105159.
(82) Hoy, S. M. Patisiran: First Global Approval. *Drugs* **2018**, *78* (15), 1625−1631.
(83) Chung, Y. H.; Beiss, V.; Fiering, S. N.; Steinmetz, N. F. COVID-19 Vaccine Frontrunners and Their Nanotechnology Design. *ACS Nano* **2020**, *14*, 12522.
(84) Buck, J.; Grossen, P.; Cullis, P. R.; Huwyler, J.; Witzigmann, D. Lipid-Based DNA Therapeutics: Hallmarks of Non-Viral Gene Delivery. *ACS Nano* **2019**, *13* (4), 3754−3782.
(85) Moss, K. H.; Popova, P.; Hadrup, S. R.; Astakhova, K.; Taskova, M. Lipid Nanoparticles for Delivery of Therapeutic RNA Oligonucleotides. *Mol. Pharmaceutics* **2019**, *16*, 2265−2277.
(86) Lv, H.; Zhang, S.; Wang, B.; Cui, S.; Yan, J. Toxicity of Cationic Lipids and Cationic Polymers in Gene Delivery. *J. Controlled Release* **2006**, *114* (1), 100−109.
(87) Cullis, P. R.; Hope, M. J. Lipid Nanoparticle Systems for Enabling Gene Therapies. *Mol. Ther.* **2017**, *25* (7), 1467−1475.
(88) Rietwyk, S.; Peer, D. Next-Generation Lipids in RNA Interference Therapeutics. *ACS Nano* **2017**, *11* (8), 7572−7586.
(89) Cohen, Z. R.; Ramishetti, S.; Peshes-Yaloz, N.; Goldsmith, M.; Wohl, A.; Zibly, Z.; Peer, D. Localized RNAi Therapeutics of Chemoresistant Grade IV Glioma Using Hyaluronan-Grafted Lipid-Based Nanoparticles. *ACS Nano* **2015**, *9* (2), 1581−1591.
(90) Rungta, R. L.; Choi, H. B.; Lin, P. J. C.; Ko, R. W. Y.; Ashby, D.; Nair, J.; Manoharan, M.; Cullis, P. R.; MacVicar, B. A. Lipid Nanoparticle Delivery of Sirna to Silence Neuronal Gene Expression in the Brain. *Mol. Ther. - Nucleic Acids* **2013**, *2*, e136.
(91) Cardoso, A. M.; Guedes, J. R.; Cardoso, A. L.; Morais, C.; Cunha, P.; Viegas, A. T.; Costa, R.; Jurado, A.; Pedroso de Lima, M. C. Recent Trends in Nanotechnology Toward CNS Diseases: Lipid-Based Nanoparticles and Exosomes for Targeted Therapeutic Delivery. *Int. Rev. Neurobiol.* **2016**, *130*, 1−40.
(92) Ashizawa, A. T.; Holt, J.; Faust, K.; Liu, W.; Tiwari, A.; Zhang, N.; Ashizawa, T. Intravenously Administered Novel Liposomes, DCL64, Deliver Oligonucleotides to Cerebellar Purkinje Cells. *Cerebellum* **2019**, *18* (1), 99−108.
(93) Rai, R.; Alwani, S.; Badea, I. Polymeric Nanoparticles in Gene Therapy: New Avenues of Design and Optimization for Delivery Applications. *Polymers (Basel)* **2019**, *11* (4), 745.
(94) Xiang, Y.; Oo, N. N. L.; Lee, J. P.; Li, Z.; Loh, X. J. Recent Development of Synthetic Nonviral Systems for Sustained Gene Delivery. *Drug Discovery Today* **2017**, *22* (9), 1318−1335.
(95) Wang, Y.; Ye, M.; Xie, R.; Gong, S. Enhancing the in Vitro and in Vivo Stabilities of Polymeric Nucleic Acid Delivery Nanosystems. *Bioconjugate Chem.* **2019**, *30* (2), 325−337.
(96) Mc Carthy, D. J.; Malhotra, M.; O'Mahony, A. M.; Cryan, J. F.; O'Driscoll, C. M. Nanoparticles and the Blood-Brain Barrier: Advancing from in-Vitro Models towards Therapeutic Significance. *Pharm. Res.* **2015**, *32* (4), 1161−1185.
(97) Rafael, D.; Andrade, F.; Arranja, A.; Luís, S.; Videira, M. Lipoplexes and Polyplexes: Gene Therapy. In *Encyclopedia of Biomedical Polymers and Polymeric Biomaterials*; Taylor & Francis, 2015; pp 4335−4347, DOI: 10.1081/e-ebpp-120050058.
(98) Lu, Y.; Jiang, C. Brain-Targeted Polymers for Gene Delivery in the Treatment of Brain Diseases. *Top. Curr. Chem.* **2017**, *375* (2), 48.
(99) Gomes, M. J.; Fernandes, C.; Martins, S.; Borges, F.; Sarmento, B. Tailoring Lipid and Polymeric Nanoparticles as SiRNA Carriers towards the Blood-Brain Barrier - from Targeting to Safe Administration. *J. Neuroimmune Pharmacol.* **2017**, *12*, 107−119.
(100) Mukherjee, A.; Waters, A. K; Kalyan, P.; Achrol, A. S.; Kesari, S.; Yenugonda, V. M. Lipid - Polymer Hybrid Nanoparticles as a next-Generation Drug Delivery Platform: State of the Art, Emerging Technologies, and Perspectives. *Int. J. Nanomed.* **2019**, *14*, 1937−1952.
(101) Jambhekar, S. S.; Breen, P. Cyclodextrins in Pharmaceutical Formulations I: Structure and Physicochemical Properties, Formation of Complexes, and Types of Complex. *Drug Discovery Today* **2016**, *21* (2), 356−362.
(102) Jacob, S.; Nair, A. B. Cyclodextrin Complexes: Perspective from Drug Delivery and Formulation. *Drug Dev. Res.* **2018**, *79*, 201−217.
(103) Mellet, C. O.; Fernandez, J. M. G.; Benito, J. M. Cyclodextrin-Based Gene Delivery Systems. *Chem. Soc. Rev.* **2011**, *40*, 1586−1608.
(104) Coisne, C.; Tilloy, S.; Monflier, E.; Wils, D.; Fenart, L.; Gosselet, F. Cyclodextrins as Emerging Therapeutic Tools in the Treatment of Cholesterol-Associated Vascular and Neurodegenerative Diseases. *Molecules* **2016**, *21*, 1748.
(105) Zhang, J.; Ma, P. X. Cyclodextrin-Based Supramolecular Systems for Drug Delivery: Recent Progress and Future Perspective. *Adv. Drug Delivery Rev.* **2013**, *65* (9), 1215−1233.
(106) O'Mahony, A. M.; Godinho, B. M. D. C.; Cryan, J. F.; O'Driscoll, C. M. Non-Viral Nanosystems for Gene and Small Interfering RNA Delivery to the Central Nervous System: Formulating the Solution. *J. Pharm. Sci.* **2013**, *102*, 3469−3484.
(107) Mohammed, A. F. A.; Motoyama, K.; Higashi, T.; Arima, H. Promising Use of Cyclodextrin-Based Non-Viral Vectors for Gene and Oligonucleotide Drugs. In *Cyclodextrin—A Versatile Ingredient*; Arora, P., Dhingra, N., Eds.; IntechOpen, 2018; pp 239−261, DOI: 10.5772/intechopen.74614.
(108) Godinho, B. M. D. C.; Ogier, J. R.; Darcy, R.; O'Driscoll, C. M.; Cryan, J. F. Self-Assembling Modi Fi Ed β - Cyclodextrin Nanoparticles as Neuronal SiRNA Delivery Vectors: Focus on Huntington' '' s Disease. *Mol. Pharmaceutics* **2013**, *10* (2), 640−649.
(109) O'Mahony, A. M.; Godinho, B. M. D. C.; Ogier, J.; Devocelle, M.; Darcy, R.; Cryan, J. F.; O'Driscoll, C. M. Click-Modified Cyclodextrins as Nonviral Vectors for Neuronal SiRNA Delivery. *ACS Chem. Neurosci.* **2012**, *3*, 744−752.
(110) Gooding, M.; Malhotra, M.; Mccarthy, D. J.; Godinho, B. M. D. C.; Cryan, J. F.; Darcy, R.; O'Driscoll, C. M. Synthesis and

Characterization of Rabies Virus Glycoprotein-Tagged Amphiphilic Cyclodextrins for SiRNA Delivery in Human Glioblastoma Cells: In Vitro Analysis. *Eur. J. Pharm. Sci.* **2015**, *71*, 80−92.
(111) Godinho, B. M. D. C.; Ogier, J. R.; Quinlan, A.; Darcy, R.; Griffin, B. T.; Cryan, J. F.; O'Driscoll, C. M. PEGylated Cyclodextrins as Novel SiRNA Nanosystems: Correlations between Polyethylene Glycol Length and Nanoparticle Stability. *Int. J. Pharm.* **2014**, *473*, 105−112.
(112) Hastings, C.; Vieira, C.; Liu, B.; Bascon, C.; Gao, C.; Wang, R. Y.; Casey, A.; Hrynkow, S. Expanded Access with Intravenous Hydroxypropyl- β-Cyclodextrin to Treat Children and Young Adults with Niemann-Pick Disease Type C1: A Case Report Analysis. *Orphanet J. Rare Dis.* **2019**, *14*, 228.
(113) Osier, N.; Motamedi, V.; Edwards, K.; Puccio, A.; Diaz-Arrastia, R.; Kenney, K.; Gill, J. Exosomes in Acquired Neurological Disorders: New Insights into Pathophysiology and Treatment. *Mol. Neurobiol.* **2018**, *55*, 9280−9293.
(114) Jiang, X.; Gao, J. Exosomes as Novel Bio-Carriers for Gene and Drug Delivery. *Int. J. Pharm.* **2017**, *521* (1−2), 167−175.
(115) Gooding, M.; Malhotra, M.; Evans, J. C.; Darcy, R.; O'Driscoll, C. M. Oligonucleotide Conjugates - Candidates for Gene Silencing Therapeutics. *Eur. J. Pharm. Biopharm.* **2016**, *107*, 321−340.
(116) Chernikov, I. V.; Vlassov, V. V.; Chernolovskaya, E. L. Current Development of SiRNA Bioconjugates: From Research to the Clinic. *Front. Pharmacol.* **2019**, *10*, 444.
(117) Zhang, R.; Qin, X.; Kong, F.; Chen, P.; Pan, G. Improving Cellular Uptake of Therapeutic Entities through Interaction with Components of Cell Membrane. *Drug Delivery* **2019**, *26* (1), 328−342.
(118) Mathupala, S. P. Delivery of Small-Interfering RNA (SiRNA) to the Brain. *Expert Opin. Ther. Pat.* **2009**, *19* (2), 137−140.
(119) Zhou, J.; Rossi, J. Aptamers as Targeted Therapeutics: Current Potential and Challenges. *Nat. Rev. Drug Discovery* **2017**, *16*, 181−202.
(120) Catuogno, S.; Esposito, C. L.; Condorelli, G.; de Franciscis, V. Nucleic Acids Delivering Nucleic Acids. *Adv. Drug Delivery Rev.* **2018**, *134*, 79−93.
(121) Nuzzo, S.; Roscigno, G.; Affinito, A.; Ingenito, F.; Quintavalle, C.; Condorelli, G. Potential and Challenges of Aptamers as Specific Carriers of Therapeutic Oligonucleotides for Precision Medicine in Cancer. *Cancers* **2019**, *11*, 1521.
(122) Cheng, C.; Chen, Y. H.; Lennox, K. A.; Behlke, M. A.; Davidson, B. L. In Vivo SELEX for Identification of Brain-Penetrating Aptamers. *Mol. Ther.–Nucleic Acids* **2013**, *2*, No. e67.
(123) Macdonald, J.; Henri, J.; Goodman, L.; Xiang, D.; Duan, W.; Shigdar, S. Development of a Bifunctional Aptamer Targeting the Transferrin Receptor and Epithelial Cell Adhesion Molecule (EpCAM) for the Treatment of Brain Cancer Metastases. *ACS Chem. Neurosci.* **2017**, *8* (4), 777−784.
(124) Esposito, C. L.; Nuzzo, S.; Kumar, S. A.; Rienzo, A.; Lawrence, C. L.; Pallini, R.; Shaw, L.; Alder, J. E.; Ricci-Vitiani, L.; Catuogno, S.; De Franciscis, V. A Combined MicroRNA-Based Targeted Therapeutic Approach to Eradicate Glioblastoma Stem-like Cells. *J. Controlled Release* **2016**, *238*, 43−57.
(125) Esposito, C. L.; Nuzzo, S.; Catuogno, S.; Romano, S.; de Nigris, F.; De Franciscis, V. De STAT3 Gene Silencing by Aptamer-SiRNA Chimera as Selective Therapeutic for Glioblastoma. *Mol. Ther.–Nucleic Acids* **2018**, *10* (March), 398−411.
(126) Pardridge, W. M. Delivery of Biologics Across the Blood-Brain Barrier with Molecular Trojan Horse Technology. *BioDrugs* **2017**, *31* (6), 503−519.
(127) Jones, A. R.; Shusta, E. V. Blood-Brain Barrier Transport of Therapeutics via Receptor-Mediation. *Pharm. Res.* **2007**, *24* (9), 1759−1771.
(128) Johnsen, K. B.; Burkhart, A.; Thomsen, L. B.; Andresen, T. L.; Moos, T. Targeting the Transferrin Receptor for Brain Drug Delivery. *Prog. Neurobiol.* **2019**, *181* (May), 101665.
(129) Xia, C. F.; Zhang, Y.; Zhang, Y.; Boado, R. J.; Pardridge, W. M. Intravenous SiRNA of Brain Cancer with Receptor Targeting and Avidin-Biotin Technology. *Pharm. Res.* **2007**, *24* (12), 2309−2316.
(130) Arnold, A. E.; Malek-Adamian, E.; Le, P. U.; Meng, A.; Martínez-Montero, S.; Petrecca, K.; Damha, M. J.; Shoichet, M. S. Antibody-Antisense Oligonucleotide Conjugate Downregulates a Key Gene in Glioblastoma Stem Cells. *Mol. Ther.–Nucleic Acids* **2018**, *11* (June), 518−527.
(131) Xie, J.; Bi, Y.; Zhang, H.; Dong, S.; Teng, L.; Lee, R. J.; Yang, Z. Cell-Penetrating Peptides in Diagnosis and Treatment of Human Diseases: From Preclinical Research to Clinical Application. *Front. Pharmacol.* **2020**, *11*, 697.
(132) Derakhshankhah, H.; Jafari, S. Cell Penetrating Peptides: A Concise Review with Emphasis on Biomedical Applications. *Biomed. Pharmacother.* **2018**, *108*, 1090−1096.
(133) Benizri, S.; Gissot, A.; Martin, A.; Vialet, B.; Grinstaff, M. W.; Barthelemy, P. Bioconjugated Oligonucleotides: Recent Developments and Therapeutic Applications. *Bioconjugate Chem.* **2019**, *30*, 366−383.
(134) Oller-Salvia, B.; Sánchez-Navarro, M.; Giralt, E.; Teixidó, M. Blood-Brain Barrier Shuttle Peptides: An Emerging Paradigm for Brain Delivery. *Chem. Soc. Rev.* **2016**, *45*, 4690−4707.
(135) Mcclorey, G.; Banerjee, S. Cell-Penetrating Peptides to Enhance Delivery of Oligonucleotide-Based Therapeutics. *Biomedicines* **2018**, *6*, 51.
(136) Kumar, P.; Wu, H.; Mcbride, J. L.; Jung, K.; Kim, M. H.; Davidson, B. L.; Lee, S. K.; Shankar, P.; Manjunath, N. Transvascular Delivery of Small Interfering RNA to the Central Nervous System. *Nature* **2007**, *448* (July), 39−45.
(137) Wang, L.; Hao, Y.; Li, H.; Zhao, Y.; Meng, D.; Li, D.; Shi, J.; Zhang, H. Co-Delivery of Doxorubicin and SiRNA for Glioma Therapy by a Brain Targeting System: Angiopep-2-Modified Poly (Lactic-Co-Glycolic Acid) Nanoparticles. *J. Drug Targeting* **2015**, *23*, 832−846.
(138) Osborn, M. F.; Khvorova, A. Improving SiRNA Delivery In Vivo Through Lipid Conjugation. *Nucleic Acid Ther.* **2018**, *28* (3), 128−136.
(139) Biscans, A.; Coles, A.; Echeverria, D.; Khvorova, A. The Valency of Fatty Acid Conjugates Impacts SiRNA Pharmacokinetics, Distribution, and Efficacy in Vivo. *J. Colloid Interface Sci.* **2019**, *28*, 116−125.
(140) Biscans, A.; Coles, A.; Haraszti, R.; Echeverria, D.; Hassler, M.; Osborn, M.; Khvorova, A. Diverse Lipid Conjugates for Functional Extra-Hepatic SiRNA Delivery in Vivo. *Nucleic Acids Res.* **2019**, *47* (3), 1082−1096.
(141) Godinho, B. M. D. C.; Gilbert, J. W.; Haraszti, R. A.; Coles, A. H.; Biscans, A.; Roux, L.; Nikan, M.; Echeverria, D.; Hassler, M.; Khvorova, A. Pharmacokinetic Profiling of Conjugated Therapeutic Oligonucleotides: A High-Throughput Method Based Upon Serial Blood Microsampling Coupled to Peptide Nucleic Acid Hybridization Assay. *Nucleic Acid Ther.* **2017**, *27* (6), 323−334.
(142) Nikan, M.; Osborn, M. F.; Coles, A. H.; Godinho, B. M. D. C.; Hall, L. M.; Haraszti, R. A.; Hassler, M. R.; Echeverria, D.; Aronin, N.; Khvorova, A. Docosahexaenoic Acid Conjugation Enhances Distribution and Safety of SiRNA upon Local Administration in Mouse Brain. *Mol. Ther.–Nucleic Acids* **2016**, *5*, No. e344.
(143) Nikan, M.; Osborn, M. F.; Coles, A. H.; Biscans, A.; Godinho, B. M. D. C.; Haraszti, R. A.; Sapp, E.; Echeverria, D.; DiFiglia, M.; Aronin, N.; Khvorova, A. Synthesis and Evaluation of Parenchymal Retention and Efficacy of a Metabolically Stable, O-Phosphocholine-N-Docosahexaenoyl-L-Serine SiRNA Conjugate in Mouse Brain. *Bioconjugate Chem.* **2017**, *28* (6), 1758−1766.
(144) Chen, D.; Ganesh, S.; Wang, W.; Amiji, M. Protein Corona-Enabled Systemic Delivery and Targeting of Nanoparticles. *AAPS J.* **2020**, *22*, 83.
(145) Zhang, Z.; Guan, J.; Jiang, Z.; Yang, Y.; Liu, J.; Hua, W.; Mao, Y.; Li, C.; Lu, W.; Qian, J.; Zhan, C. Brain-Targeted Drug Delivery by Manipulating Protein Corona Functions. *Nat. Commun.* **2019**, *10*, 3561.

https://doi.org/10.1021/acs.molpharmaceut.0c01238
Mol. Pharmaceutics 2021, 18, 1491−1506

(146) Dal Magro, R.; Albertini, B.; Beretta, S.; Rigolio, R.; Donzelli, E.; Chiorazzi, A.; Ricci, M.; Blasi, P.; Sancini, G. Artificial Apolipoprotein Corona Enables Nanoparticle Brain Targeting. *Nanomedicine* **2018**, *14* (2), 429−438.
(147) Wang, H.; Eckel, R. H. What Are Lipoproteins Doing in the Brain ? *Trends Endocrinol. Metab.* **2014**, *25* (1), 8−14.
(148) Zuckerman, J. E.; Davis, M. E. Clinical Experiences with Systemically Therapeutics in Cancer. *Nat. Rev. Drug Discovery* **2015**, *14*, 843−856.
(149) Subhan, A.; Torchilin, V. P. SiRNA Based Drug Design, Quality, Delivery and Clinical Translation. *Nanomedicine* **2020**, *29*, 102239.
(150) Davidson, B. L. Doubling down on SiRNAs in the Brain. *Nat. Biotechnol.* **2019**, *37*, 865−868.
(151) Di Napoli, R.; Esposito, G.; Cascella, M. Intrathecal Catheter. StatPearls [Internet], StatPearls Publishing: Treasure Island, FL, 2020.
(152) Rinaldi, C.; Wood, M. J. A. Antisense Oligonucleotides: The next Frontier for Treatment of Neurological Disorders. *Nat. Rev. Neurol.* **2018**, *14* (1), 9−22.
(153) Weng, Y.; Huang, Y. The Advances of Biomacromolecule-Based Nanomedicine in Brain Disease. In *Nanomedicine in Brain Diseases*; Xue, X., Ed.; Springer Singapore, 2019; pp 181−208, DOI: 10.1007/978-981-13-8731-9_7.
(154) Conniot, J.; Talebian, S.; Simões, S.; Ferreira, L.; Conde, J. Revisiting Gene Delivery to the Brain: Silencing and Editing. *Biomater. Sci.* **2021**, *9*, 1065−1087.
(155) Liu, X. S.; Jaenisch, R. Editing the Epigenome to Tackle Brain Disorders Trends in Neurosciences. *Trends Neurosci.* **2019**, *42* (12), 861−870.
(156) Khan, S. H. Genome-Editing Technologies: Concept, Pros, and Cons of Various Genome-Editing Techniques and Bioethical Concerns for Clinical Application. *Mol. Ther.–Nucleic Acids* **2019**, *16* (June), 326−334.

https://doi.org/10.1021/acs.molpharmaceut.0c01238
Mol. Pharmaceutics 2021, 18, 1491−1506

Design of lipid-based nanoparticles for delivery of therapeutic nucleic acids

Monique C.P. Mendonça [1], Ayse Kont [1], Piotr S. Kowalski, Caitriona M. O'Driscoll *

School of Pharmacy, University College Cork, T12 YT20 Cork, Ireland

The successful development of nonviral delivery systems for nucleic acids has been reported extensively over the past number of years. Among them, lipid-based nanoparticles (LNPs) represent the most advanced platform. This review provides an overview of the state-of-the-art in LNP technology, focusing on the delivery of a range of nucleic acids. Recent advances in the development of an efficient and safe lipid-based system are critically analyzed with a particular emphasis on the rationale behind the design of LNPs and on attempts to elucidate the resulting molecular assembly and structure, their interactions with cellular proteins and biodistribution. In addition, manufacturing methods including microfluidics and their potential to influence stability and scale-up are summarized.

Keywords: Gene therapy; non-viral delivery; siRNA; mRNA; lipid excipients

Monique CP Mendonca is a postdoctoral researcher at University College Cork. Originally a pharmacist, she obtained a PhD in Pharmacology at the University of Campinas in 2016, where she studied the effects of nanomaterials on the blood-brain barrier. Her focus is on developing new nanotechnology-based nucleic acid delivery systems capable of crossing the blood-brain barrier and could be applied for the treatment of neurodegenerative diseases triggered or affected by genetic mechanisms.

Ayse Kont is a PhD candidate at University College Cork, graduated with a pharmacy degree from Goethe University in Frankfurt am Main, Germany, in 2016. Her research aims to develop nonviral nanocarrier systems for systemic nucleic acid delivery in the treatment of leukemia.

Piotr S. Kowalski is an Associate Professor in advanced therapies at the School of Pharmacy, University College Cork, Ireland. He is a biochemist by training, he earned his PhD from Groningen University in 2014 and received his postdoctoral training at the Koch Institute for Integrative Cancer Research at Massachusetts Institute of Technology, Cambridge, USA. His research is centered on engineering novel therapeutic RNA modalities and developing clinically relevant biomaterials and drug delivery technologies to facilitate effective RNA-based therapies, aimed at high medical need diseases that lack effective treatment.

* *Corresponding author: O'Driscoll, C.M. (caitriona.odriscoll@ucc.ie)*

[1] These authors contributed equally to this work.

Caitriona M. O'Driscoll is Professor and Chair of Pharmaceutics in the School of Pharmacy, University College Cork, Ireland. Originally a pharmacist, she completed her PhD in pharmaceutical sciences at Trinity College Dublin and was Senior Lecturer there until 2003. Her research interests are translational in nature and include oral and systemic delivery of nanotherapeutics incorporating nucleic acids formulated using novel biomaterials. Manufacturing hurdles and new tools to efficiently assess and facilitate licencing of these innovative therapies are also of interest.

Introduction

Gene therapy is a promising treatment option for a wide range of diseases including genetic disorders, cancer, cardiovascular and autoimmune diseases. It is based on the introduction of specific genetic material into cells of the patients to: (i) increase the expression of the transferred gene; (ii) silence the expression of the disease-causing gene; or (iii) modify a target gene by inserting, removing or replacing the gene with its functioning version [1–2]. Currently, therapeutic nucleic acids primarily include complementary Watson-Crick base-pairing, such as ribozymes, deoxyribozymes, antisense oligonucleotides (ASOs), plasmid DNA (pDNA), small interfering RNAs (siRNAs), microRNA (miRNA), clustered regularly interspaced short palindromic repeat (CRISPR)-associated protein (Cas) and other gene-editing technologies; as well as nucleic acids that are not complementary to the target sequence, such as aptamers, and decoy nucleic acids [3].

Despite considerable progress in the field, safe and effective delivery to diseased sites including biodistribution beyond the liver remains a major challenge (Fig. 1). Nuclease degradation, following intravenous administration, leads to a short half-life (<10 min). Physicochemical properties of nucleic acids including the high molecular weight, the hydrophilic nature, and the negative charge impede uptake across biological membranes. Additional barriers include nonspecific tissue distribution, poor intracellular trafficking, high renal clearance and off-target effects. At the cellular level, endosomal escape is essential for activity and remains one of the main challenges [4–5]. To overcome these barriers to the clinical translation of gene therapeutics, extensive research into the design and evaluation of smart, effective and safe delivery systems has been performed [6].

Currently, there are two clinically relevant approaches to delivery: viral and nonviral. Viral-based strategies are very effective; however, drawbacks including manufacturing challenges and immunogenicity issues of viral vectors [7] have promoted the development of nonviral approaches [8–10]. In general, nonviral delivery vectors are easy to scale up and have the capacity to address many of the limitations of viral vectors, mainly concerning safety [8,11]. A range of biocompatible materials has been designed to complex, encapsulate and deliver therapeutic nucleic acids with varying degrees of effectiveness [12–14]. Among the diversity of formulations based on nanocomplexes, lipid-based nanoparticles (LNPs) represent the most advanced platform for systemic delivery [15].

This review provides an overview of the state-of-the-art in LNP technology, focusing on the delivery of nucleic acids. Recent advances in the development of an efficient and safe lipid-based delivery system are critically analyzed with a particular emphasis on the rationale behind the design of LNPs and on attempts to elucidate the resulting molecular assembly and structure, their interactions with cellular proteins and biodistribution. In addition, manufacturing issues including scale-up and stability and the role of production methods including microfluidics are summarized.

Design rationale of lipid-based nanoparticles: Composition and molecular assembly

Over the past decades, several lipid-based systems have been examined for gene delivery including liposomes, lipid nanoemulsions, LNPs, solid-lipid nanoparticles and nanostructured lipid carriers. Previous studies have shown that LNPs are suitable carriers for different types of nucleic acids including siRNA, mRNA and pDNA [16–18]. Generally, LNPs are composed of ionizable cationic lipids, phospholipids, cholesterol and polyethyleneglycol (PEG)-lipids. As such, iterative screening processes were combined with rational design approaches to determine the optimal combination of amino headgroups, linkers and alkyl chains [19,17,20–22]. Selected examples of lipids used for the therapeutic delivery of nucleic acids are shown in Fig. 2.

Here, a description of the technical basis of LNP composition is provided. The latter topic is a major focus on ongoing efforts for LNP optimization with a particular emphasis on the rationale behind the design of LNPs for specific nucleic acids.

Ionizable cationic lipids

Ionizable cationic lipids (ICLs) are amphiphilic structures constructed with a positively charged hydrophilic head linked to a long lipophilic body (Figs. 2 and 3) [23]. After systemic administration, ICLs should be able to modulate their charge based on the pH of the environment, such as blood (pH 7.4) and endocytic

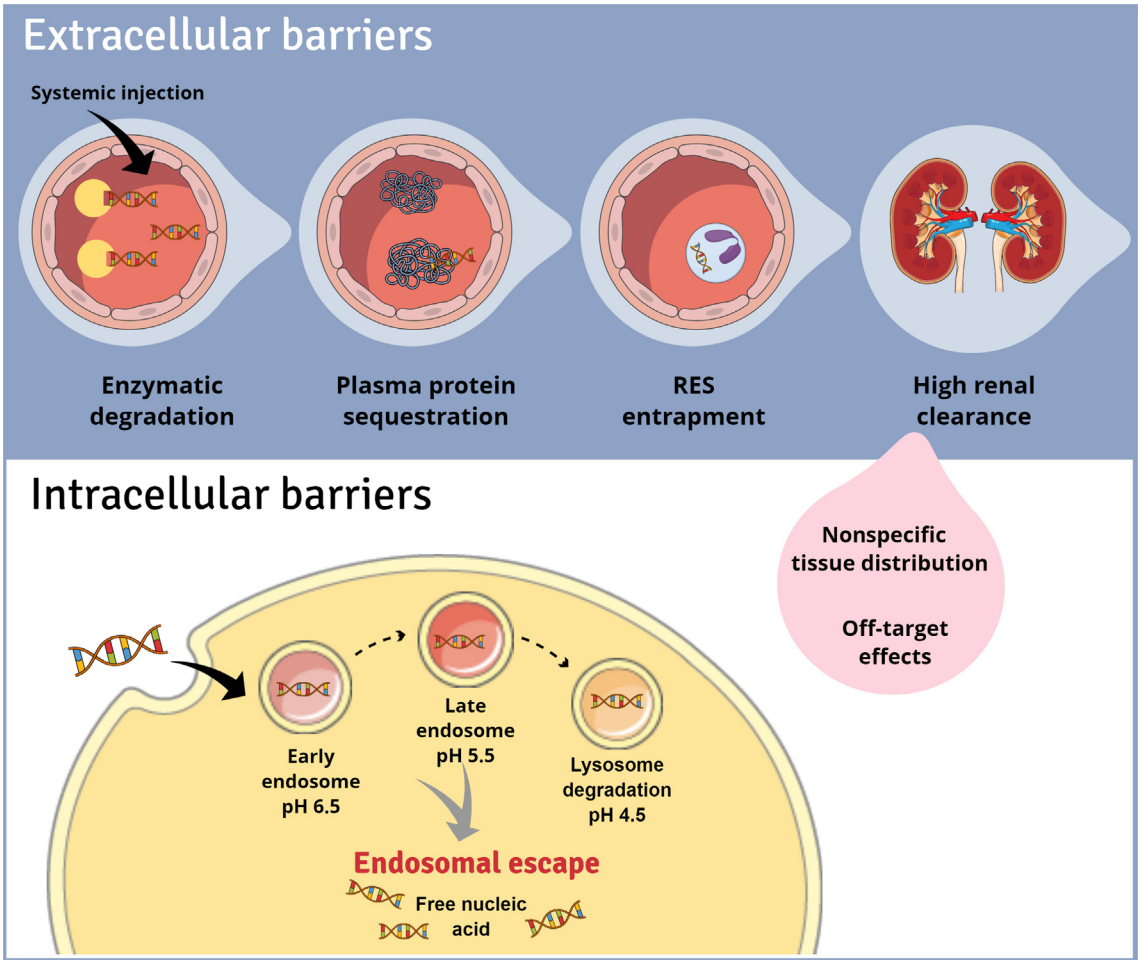

FIG. 1

Barriers encountered by nucleic acids following systemic administration. Extracellular barriers: enzymatic degradation in the bloodstream, phagocytosis and renal excretion. Cellular barriers: cell-specific uptake, endosomal uptake and release.

organelles (pH 5.5–6.5), to ensure appropriate vector formation, optimal blood circulation and effective nucleic acid release into the cytosol [24]. This flexibility is dependent on the ionization character of the incorporated lipid [16]. For example, ionizable lipids should be positively charged (protonated) at low pH during the preparation of LNPs to maximize the electrostatic interactions with the negatively charged nucleic acid. Then, a neutral surface charge at pH 7.4 is essential to ensure prolonged circulation time in the bloodstream by preventing rapid sequestration by reticuloendothelial system (RES) cells (e.g., splenic macrophages and Kupfer cells). Ideally, at acidic pH (i.e., endosomal environment), the heads of the ICLs should be positively charged again to promote binding to the negatively charged lipids exposed on the endosomal membrane. As a result of this interaction, the original endosomal membrane organization is disrupted, leading to the formation of a hexagonal H_{II} lipid phase structure (Fig. 3) with consequent delivery of the nucleic acid payload into the cytoplasm and unrestricted interaction with the cell machinery (Fig. 1) [24–25]. The endosomal release is often the rate-limiting step for successful delivery and *in vivo* activity of the nucleic acid [26,23,27].

Amine headgroups

The ICL headgroup is not only responsible for interacting with negatively charged nucleic acids but also has an impact on nanoparticle properties such as the surface charge/pK_a [28]. Previous studies demonstrated a strong correlation between pK_a and *in vivo* activity [29–30]. Ideally, ICLs should have a pK_a in the range of 6.2–6.5, being largely neutral at neutral pH (7.4) and positively charged at acidic pH (<6.0). ICLs with a pK_a lower or higher than 6.2–6.5 display a rapid decline in hepatic gene silencing activity, emphasizing the importance of the ionization behavior [31–32].

Modifications of the amine group have included substitution with piperazino, morpholino, trimethylamine or *bis*-dimethylamino groups. Initially, DLin-K-DMA, which contains a dimethylamino as the headgroup, was identified as a lead compound. Subsequently, the distance between the dimethylamino headgroup and the dioxolane linker in DLin-K-DMA was modified, because this distance affects the dissociation constant [23]. Then, DLin-KC2-DMA was created by adding additional methylene groups in DLin-K-DMA, which enabled an increase in potency. A headgroup length greater than di-

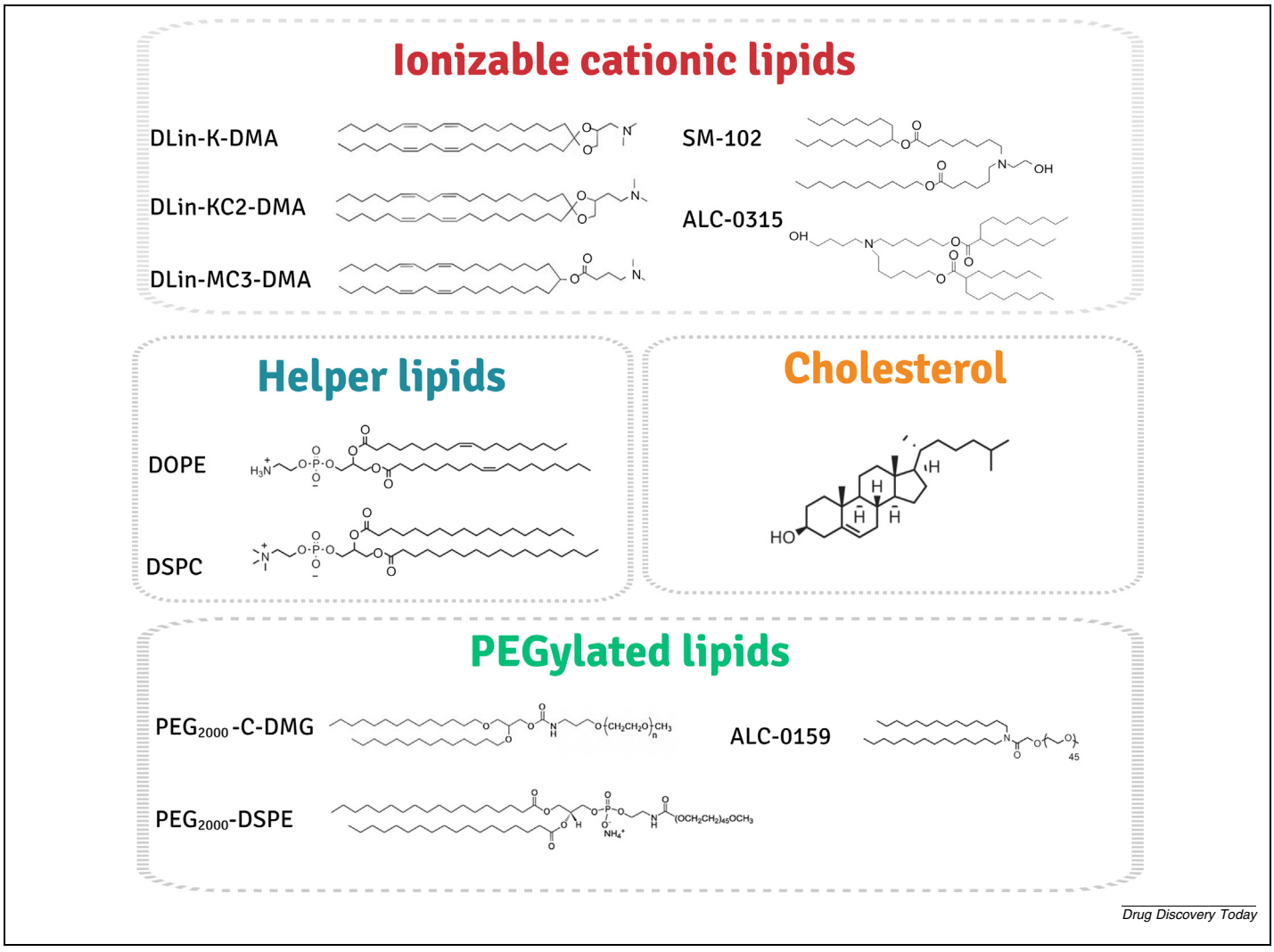

FIG. 2

Chemical structure of representative lipids used for delivery of therapeutic nucleic acids. Abbreviations: DLin-K-DMA, 1,2-dilinoleyloxy-keto-N,N-dimethyl-3-aminopropane; DLin-KC2-DMA, 2,2-dilinoleyl-4-(2-dimethylaminoethyl)-[1,3]-dioxolane; DLin-MC3-DMA, heptatriaconta-6,9,28,31-tetraen-19-yl 4(dimethylamino)butanoate; DOPE, dioleoylphosphatidylethanolamine; DSPC, sistearoylphosphatidylcholine; mPEG$_{2000}$-DSPE, 1,2-distearoyl-*ras*-glycerol-3-phosphoethanol amine-*N*-polyethyleneglycol-2000; PEG$_{2000}$-C-DMG,1,2-dimyristoyl-rac-glycero-3methoxypolyethylene glycol-2000; ALC-0159, 2-[(polyethyleneglycol)-2000]-*N*,*N*-ditetradecylacetamide.

methylaminopropane showed decreased activity. DLin-KC2-DMA has been used frequently for the delivery of nucleic acid into liver cells [20,27,31]. Further optimization distance of the dimethylamine headgroup from the linker led to DLin-MC3-DMA, which was the 'gold standard' cationic lipid for LNP formulations containing nucleic acids for several years [16,31].

DLin-MC3-DMA was employed in the first ever RNAi therapeutic product that was clinically approved by the FDA and launched by Alnylam in 2018: Onpattro® (patisiran) [33]. DLin-MC3-DMA-based LNPs have also been used in inclisiran (Leqvio®, ALN-PCS) a first-in-class siRNA developed by Novartis for the treatment of hypercholesterolemia. It was approved by the European Commission in 2020 and is currently under review by the FDA [34]. However, because siRNA products require repeated dosing for chronic diseases, biodegradable derivatives of DLin-MC3-DMA have been developed to increase biocompatibility while preserving high transfection efficiency. Representative examples of this new class of biodegradable lipids include L319, Lipid 5, SM-102 and ALC-0315. Compared with DLin-MC3-DMA, biodegradable L319 was developed by replacing one double bond with an ester linker, assuming this compound could be metabolized through β-oxidation and hydrolysis. SM-102 and ALC09315 have ester linkages in the lipid tail (Fig. 2). The distribution of esters in two tails keeps the pK_a in the optimal range (6.2–6.5), whereas the side-chain consisting of secondary ester can facilitate the formation of a 'cone shape' structure (Fig. 3) [35]. It is worth mentioning that SM-102 and ALC-0315 are the ionizable delivery components in the Moderna Spikevax, also referred to as mRNA-1273, and BioNTech-Pfizer Comirnaty (BNT162b2) COVID-19 vaccines, respectively [36–37].

Linker

The linker is the next important functional moiety, which connects the amine headgroup with the lipid tail. The linker oxygen

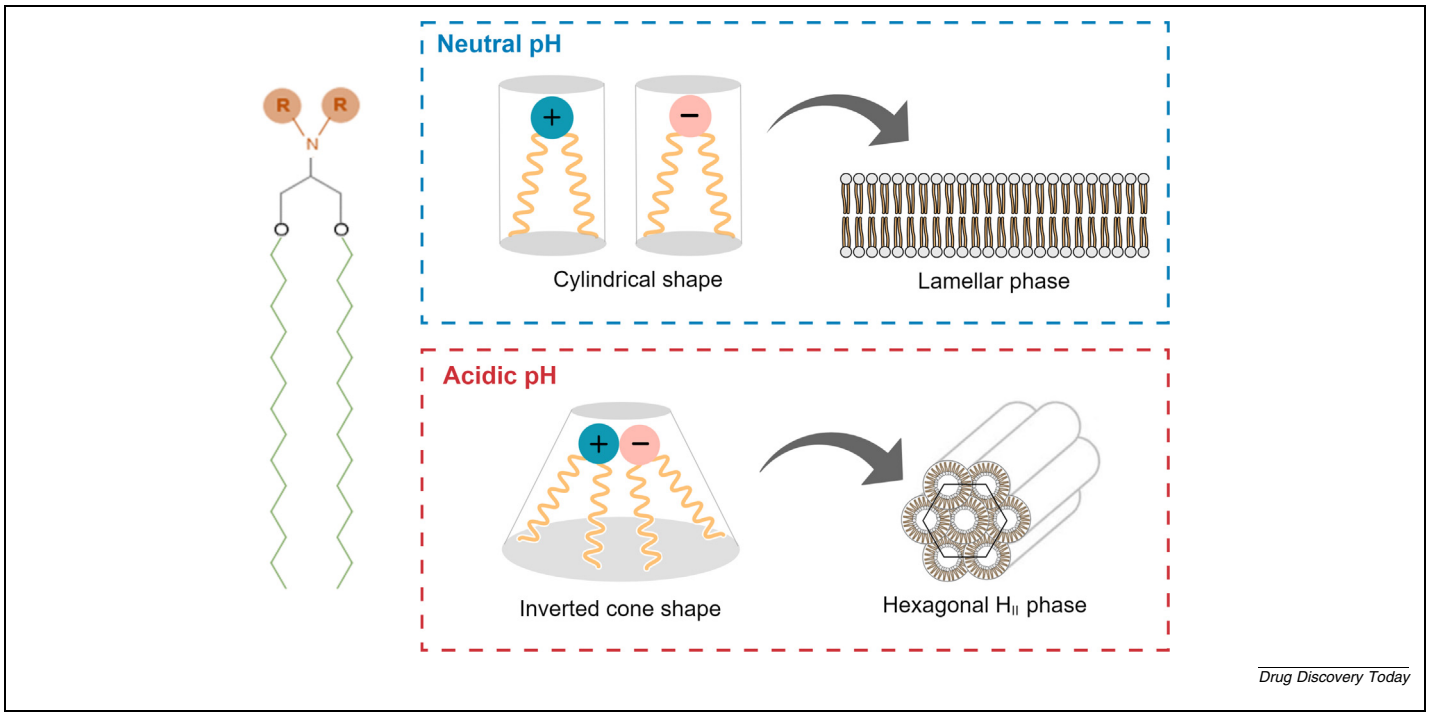

FIG. 3

Schematic representation of the mechanism of action proposed for membrane disruptive effects of cationic lipids. Left: cationic lipids are divided into amino headgroup (orange), linker (grey) and tail chain domains (green). Right top: in isolation, cationic and anionic lipids adopt a cylindrical structure, which causes them to assemble into a bilayer configuration (lamellar phase). Right bottom: when cationic lipids are mixed with anionic lipids they combine to form ion pairs that adopt an inverted conical structure, which assembles into the hexagonal H_{II} phase.

plays a key part in transfection efficacy by affecting the pK_a of the ICL and controlling the chemical and enzymatic stability of the lipid. Depending on the structure, linkers are grouped into ethers, esters, amides, carbamates and disulfide groups (Table 1). Besides the functional group, the spacing between the headgroup and the linker, the length and steric hindrance also impact transfection efficiency [38,28].

Lipid tail

Lipid tail saturation/unsaturation (double bond content), length, level of substitution and the tail structure (branched vs linear) can affect the ICL transfection efficiency [28]. Given the importance of the lipid tail saturation for transfection efficacy, a series of analogs to 1,2-dioleoyl-3-dimethylammonium propane (DODAP) with different degrees of unsaturation, lengths and linker groups were synthesized. DODAP was the first ICL that contains two alkyl chains bound through ester bonds and has a pK_a value of 6.6–7.0. This milestone served as a benchmark for the next generations of lipids with even greater transfection efficacies. The introduction of double bonds led to a decrease in the pK_a of the LNP surface, from 7.0 down to 6.7, owing to the altered arrangement of the lipids within the LNP.[36]DLin-DMA, an ether analog of DODAP containing linoleic acyl chains and with a pK_a of 6.7, was the first type of rationally designed ionizable lipid. It was used to develop the first therapeutically relevant RNAi-mediated approach for gene silencing in non-human primates [39] and, further, the RNAi therapeutics designed to treat solid tumors: TKM-080301 (TKM-PLK1) from Tekmira Pharmaceuticals, ALN-VSP and ALN-TTR01 from Alnylam Pharmaceuticals, currently being investigated in clinical trials [40].

DLin-DMA was further modified to produce DLin-KC2-DMA and DLin-MC3- DMA. DLin-KC2-DMA having a pK_a of 6.7 is 100-fold more powerful than DLin-DMA for silencing liver targets. DLin-MC3-DMA, which has a pK_a of 6.44, has a 1000-fold higher potency than DLin-DMA [41,30]. Besides the liver, DLin-KC2-DMA and DLin-MC3-DMA were both also effective in the delivery of siRNA to dendritic cells derived from human monocytes; however, particularly in these cells, DLin-KC2-DMA was more effective at silencing programmed cell death ligand-1 (PD-L1) gene than DLin-MC3-DMA [42].

TABLE 1

Representative chemical structures of linker groups.

Linker bond	Chemical structure	Examples
Ether		DOTMA (cationic lipid)
Ester		DLin-MC3-DMA (ionizable cationic lipid)
Amide		TT3 (ionizable cationic lipid)
Urethane (or carbamate)	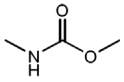	PEG_{2000}-C-DMG (PEG-lipid)
Disulfide		BAME-O16B (ionizable cationic lipid)

Helper lipids

Helper lipids, such as 1,2-dioleoyl-*sn*-glycero-3-phosphoethanolamine (DOPE) and 1,2-distearoyl-*sn*-glycero-3-phosphocholine (DSPC), are important components of LNP formulations included to provide fusion with cell and endosomal membranes, facilitating cellular uptake and endosomal release [43].

DOPE was one of the first helper lipids successfully used for the delivery of nucleic acids using cationic liposomes [44]. DOPE has a very similar structure to DSPC; however, it also exhibits important differences (Fig. 2). DOPE is a phosphoethanolamine with two unsaturated chains (C18). As a consequence of the unsaturation, DOPE has fusogenic characteristics and, therefore, facilitates improved fusion of LNPs with the endosomal membrane via promoting the non-bilayer inverted hexagonal H_{II} phase [45]. By contrast, DSPC is a saturated amphiphilic lipid. It has a neutral overall charge, consisting of a quaternary amine and a negatively charged phosphate group, connected to two saturated chains (C18). As a consequence of the saturated hydrocarbon chains, DPSC has a cylindrical shape and therefore, does not show membrane destabilizing characteristics, rather it tends toward the formation of the stable bilayer phase [16,45]. Noteworthy, both mRNA-based COVID-19 vaccines contain DPSC as the helper lipid. Interestingly, LoPresti *et al.* investigated helper lipids with varying characteristics (neutral, cationic and anionic) and could show that altering the chemistry and concentration of helper lipids affects nanoparticle surface charge and, therefore, impacts the distribution and effectiveness of nanoparticles in specific tissue. Neutral helper lipids, such as 1,2-dioleoyl-*sn*-glycero-3-phosphocholine (DOPC), sphingomyelin and ceramide, preserved liver targeting, whereas anionic helper lipids (phosphatidylserine, phosphatidylglycerol and phosphatidic acid) increased the distribution to the spleen. The pioneer for cationic lipids, 1,2-dioleoyl-3-trimethylammonium propane (DOTAP), now used as a cationic helper lipid, shifted the protein expression to the lung [46].

Cholesterol

Cholesterol belongs to a class of steroid compounds and shows a unique structure compared to the other LNP components (Fig. 2). The tetracyclic core bestows a planar and rigid structure that enables cholesterol to intercalate into bilayer structures and stabilize them, hence it protects the particle in the presence of serum proteins [45,47]. By contrast, cholesterol, depending on its percentage in the composition, can promote the fusion of the LNP with the membrane of endosomes in the presence of unsaturated lipids, which improves intracellular delivery [47]. Cheng *et al.* reported that high concentrations of cholesterol enhance the activity of cationic lipids which supports the aforementioned fusogenicity. These characteristics give cholesterol the ability to be evenly distributed within the LNP [45].

PEG-lipid

The incorporation of PEG-lipids into LNPs has been widely used to improve the pharmacokinetics of therapeutic LNPs. It helps prevent the interaction with serum proteins, reduce opsonization and, therefore, recognition by the cells of the RES, resulting in longer circulation times [48]. Besides, PEGylation decreases the particle size and prevents LNP aggregation during storage and extends the shelf-life [49]. However, PEGylation also has limitations. The addition of PEG on the surface of the NPs can reduce the cellular uptake and endosome escape efficiency by limiting the interaction between the ionizable cationic lipid and the lipids into the cellular membrane owing to steric hindrance [50]. Although PEG is considered safe, repetitive administration of PEGylated NPs can induce the production of anti-PEG antibodies (IgG and IgM), which causes accelerated blood clearance phenomenon, hypersensitivity reactions and, in some rare cases, fatal anaphylaxis [51]. For example, PEG has been associated with some cases of anaphylaxis to BioNTech-Pfizer Comirnaty and Moderna Spikevax COVID-19 vaccines in individuals with a known allergy to PEG [52–54].

By optimizing the PEGylation chemistry and the density of PEG on the LNP surface, it is possible to alter the pharmacokinetics and pharmacodynamics of the NPs [48].

For example, very short PEG (<1 kDa) did not prevent interaction with serum proteins and hence cannot extend the circulation time efficiently whereas very long PEG (>5 kDa) or a high mole fraction of PEG (>15 mol%) led to a decrease in the membrane permeability, which severely reduces the cellular uptake [48,55–56]. Thus, generally, PEG molecules with moderate molecular weight (~2 kDa) are used for LNP modification in a ratio <5% [57,50,58–59]. Currently, the Moderna COVID-19 vaccine uses 1.5% of PEG_{2000}-DMG, whereas the BioNTech-Pfizer vaccine uses 1.6% of ALC-0159 in their respective formulations [36]. Regarding the chain length, much faster dissociation was observed for PEG-lipids with a chain length of 14 carbons (e.g., PEG-DMPE and PEG-DMG) compared with those with a chain length of 18 carbons [e.g., PEG-DSPE and PEG-1,2-distearoyl-rac-glycero-3-methoxypolyethylene (DSG)], which could facilitate cellular uptake and endosomal escape of LNPs [37,60].

There are multiple approaches under investigation to reduce PEG-associated immunity. Promising alternatives for the replacement of PEG include synthetic polypeptides or polypeptoids - analogs of polypeptides such as Polysarcosine (PSar) [61–62]. In a recent study, the incorporation of PSar lipids into LNPs resulted in higher RNA transfection potency with a reduced immunostimulatory response compared with the PEGylated counterpart (PEG-DMG) after intravenous injection. Similar to PEGylated lipids, the molar fraction and the number of PSar repeat units also influence the physicochemical characteristics of the resulting delivery system [63].

Structural and physicochemical properties of LNPs

To elucidate the structure of nanosystems, it is important to carry out detailed systematic investigations. Cryogenic transmission electron microscopy (Cryo-TEM) and scattering techniques [X-ray diffraction (XRD), small angle X-ray scattering (SAXS) and small angle neutron scattering (SANS)] give information about shape, inner structure and dimensions of nano pharmaceutical forms that could not be identified otherwise [64–65]. However, characterization of mRNA delivery vehicles with cryo-TEM is more common because it facilitates quantitative and qualitative analysis of the nanomaterial structure [66].

The structure of LNP is highly dependent on the lipid compositions and proportions as well as the type of nucleic acid encapsulated. Based on Cryo-TEM analysis it has been proposed that LNPs containing a high ICL content (≥40 mol%), cholesterol and possibly a small amount of DSPC form inverted micelles around the siRNA (Fig. 4a). The excess of these compounds form 'empty' inverted micelles. By contrast, LNPs containing a lower ICL content (~20 mol%) and a higher amount of DSPC (~30 mol%) results in the formation of some inverted micelles mainly consisting of ICL and cholesterol, whereas DSPC accumulates in the bilayer area (Fig. 4b) [20].

The design rationale for using DSPC and cholesterol on siRNA LNP formulations relies on the fact that DSPC interacts with the ICL via its phosphate group on one side and complexes with the negatively charged nucleic acid via its choline group on the other side. This is vital for a stable encapsulation of siRNA and, consequently, LNP-siRNA function [67]. Cholesterol serves as a filler in the curvature formed by the ICL and siRNA interaction. In the presence of high DSPC and low ICL cholesterol also helps in the formation of the bilayers [68,38]. The PEG-lipid is located on the outer layer owing to its relatively high hydrophilicity and its steric size [50].

Owing to electrostatic interaction, the more pronounced the electronegativity of the nucleic acid the more effective the formation of the inverted micellar structure. This assembly pattern will subsequently affect the loading capacity of the LNPs, the biodistribution and *in vivo* efficacy [49]. Although important, these parameters alone fail to give a full insight and understanding of the performance of LNPs. The performance of LNPs is strongly impacted by the chemical structure of each component, the interactions between them and the physicochemical properties of the final formulation. Another factor that influences the structure of LNPs is the preparation technique used, discussed in detail below.

Physicochemical characteristics

Physicochemical characteristics of the LNPs, including size, surface charge (zeta potential) and surface modifications, have a direct influence on the efficacy, pharmacokinetics and biodistribution of LNPs [45]. Nanoparticles with sizes <10 nm are more likely to undergo renal filtration, whereas NPs > 200 nm can activate the Complement system and be quickly removed from the bloodstream [69]. For this reason, NPs in the range 20–200 nm are preferential, with NPs of ~100 nm considered optimal for cellular uptake [70–71].

The charge of the formulated LNP is also a crucial factor for sufficient exposure in the circulation and uptake into tissue. High surface charge, either positive (+30 mV) or negative (−30 mV), usually results in faster blood clearance and quick RES capture whereas neutrally charged LNPs (from −10 to +10 mV) promote prolonged blood circulation and reduced RES uptake. In addition, positively charged NPs exhibited higher internalization than neutral or negatively charged NPs owing to the interaction with the cell membrane which is negatively charged, resulting in increased toxicity [72–73]. For this reason,

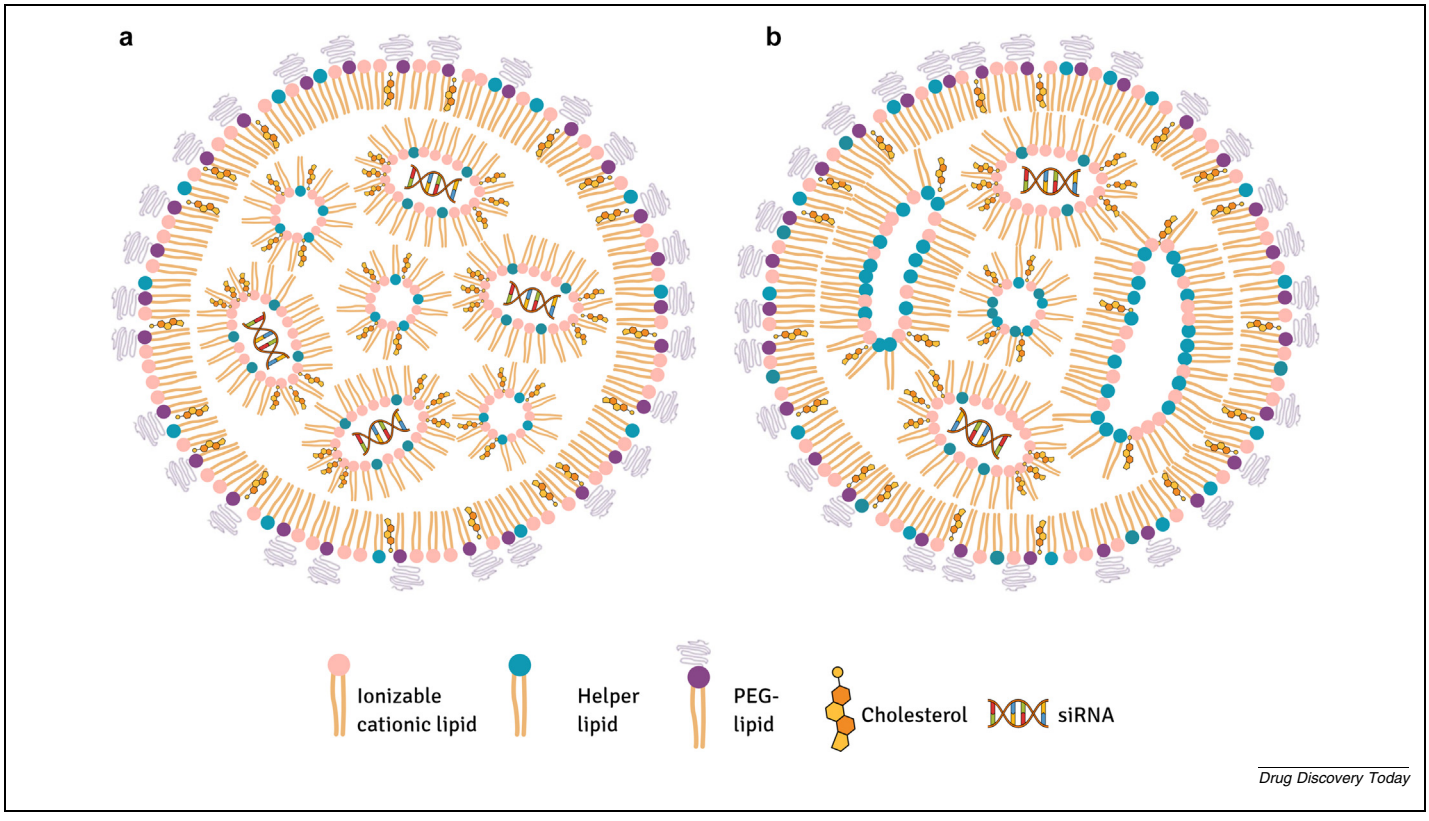

FIG. 4

Schematic representation of the proposed structure of LNPs containing siRNA. (a) Nanostructure dense core. LNPs displayed a nanostructured, electron dense core, where the siRNA is complexed with the cationic lipids into inverted micelles, surrounded by cholesterol and DSPC stabilizing the micelles. (b) Multilamellar structure presents an outer bilayer and solid interior core. Adapted, with permission, from [20].

LNPs with near-neutral zeta potential have been predominantly used in the clinic.

Lipid composition and molar ratio

LNP composition is reported in molar ratios between each lipid component, varying between certain ranges depending on the incorporated nucleic acid: 40–50 mol% for the ICL, 10–12 mol % for the phospholipid, 38–45 mol% for cholesterol and 1–2 mol% for the PEGylated lipid. Table 2 lists the lipid components and molar ratio employed in LNPs. The ratio between the lipid components and the nucleic acid is reported as N:P ratio, referring to the ratio of nitrogen atoms from the cationic lipid to the number of phosphate atoms from the nucleic acid, or as weight ratio, referring to the ratio of cationic lipid mass per nuclei acid [28].

Following the successful development of the first RNAi Onpattro®, Moderna applied a similar rational design in the development of Spikevax. As shown in Table 2, Onpattro® and Spikevax exhibited the same molar lipid ratio and similar composition, except for the replacement of DLin-MC3-DMA by the degradable lipid SM-102, identified as optimal for intramuscular administration [74]. ALC-0315 combined with DSPC, cholesterol and the PEGylated lipid ALC-0159 is the delivery system in the BioNTech-Pfizer vaccine. To achieve satisfactory results the molar ratios were adjusted: a decrease of ~3.7 in the cationic lipid and 0.6% in DSPC, with an increase of 4.7% in cholesterol and 0.1% in the PEGylated lipid in comparison to Onpattro® and Spikevax (Table 2).

The main goal of this review is to better understand how LNP composition influences the morphology and effectiveness of the final formulation. For this reason, the modification (nature and quantity) of the following parameters: N:P molar ratio, helper lipids, PEGylated lipid as well as the type of nucleic acid, will be discussed in more detail.

The formulation DLin-KC2-DMA, DSPC or DOPE, cholesterol, and PEG_{2000}-c-DMA have been investigated by Leung *et al.* [20] for the encapsulation of siRNA, pDNA and mRNA. Cryo-TEM and molecular simulation studies indicated that LNPs formed from DLin-KC2-DMA/DSPC/cholesterol/PEG_{2000}-c-DMG (40/11.5/47.5/1 mol%) exhibit the characteristic electron-dense interior as described above (Fig. 4a). When the amount of cationic lipid is decreased by 20 mol% and the amount of DSPC increased by 20 mol% [DLin-KC2-DMA/DSPC/cholesterol/PEG$_{2000}$-c-DMG (20/31.5/47.5/1 mol%)], lamellar structures start to comprise the outer layer of the LNP, whereas the interior remains solid (Fig. 4b), probably as a consequence of the decrease in unsaturation. This electron-dense core was also detected in mRNA-LNPs at 50/10/38.3/1.5 mol% (Dlin-MC3-DMA/DSPC/cholesterol/PEG_{2000}-DMPE) [75].

Alterations in the ICL content not only influence the morphology of the LNP but the encapsulation efficacy as well. A 30% rise in the ICL molar ratio followed by a proportional reduction of cholesterol content (Table 2) resulted in a reduction of

TABLE 2

Formulation composition of LNPs.

	Components	Molar ratio (%) Condition 1	Condition 2	Payload
Onpattro® (patisiran)	DLin-MC3-DMA	50		siRNA
	DSPC	10		
	Cholesterol	38		
	PEG_{2000}-c-DMG	1.5		
Spikevax (mRNA-1273)	SM-102	50		mRNA
	DSPC	10		
	Cholesterol	38		
	PEG_{2000}-DMG	1.5		
Comirnaty (BNT162b2)	ALC-0315	46.3		mRNA
	DSPC	9.4		
	Cholesterol	42.7		
	ALC-0159	1.6		
Leung et al. (2015)	DLin-KC2-DMA	40	20	siRNA
	DSPC	11.5	31.5	
	Cholesterol	47.5	47.5	
	PEG_{2000}-c-DMA	1	1	
Leung et al. (2015)	DLin-KC2-DMA	50	80	pDNA/mRNA
	DSPC or DOPE	11.5	11.5	
	Cholesterol	37.5	7.5	
	PEG_{2000}-c-DMA	1	1	
Arteta et al. (2018)	DLin-MC3-DMA	50		mRNA
	DSPC	10		
	Cholesterol	40		
	PEG_{2000}-DMPE	0.25–3.00[a]		
Kulkarni et al. (2019)	DLin-KC2-DMA	50	19–94	siRNA
	DSPC	10	2.5–40.0	
	Cholesterol	38.5	2.5–40.0	
	PEG_{2000}-DSPE	0.5–2.5	1	

[a] Content decreased by cholesterol content.

encapsulation efficiency of siRNA, although the same solid core structure was maintained. Neutral cyclic lipids, such as cholesterol, enhance the ability of ICLs to interact with nucleic acids, hence using an inadequate molar ratio leads to a decreased encapsulation [38,67,32]. If the formulation contained higher percentages of PEG lipid (2.5 or 5 mol%), the encapsulation efficiency reduction was even more pronounced [20]. As expected, the LNP becomes smaller as the PEG-lipid content is increased [67]. However, LNPs with low PEG-lipid content (0.5 mol%) exhibited the best gene silencing activity, owing to superior endosomal release [75].

Of note, the size of LNPs increased from 50 nm to 100 nm as the ICL content was increased from 50% to 80 mol% and cholesterol decreased from 37.5 to 7.5 mol% [20]. A comparable decrease in particle size was observed by increasing cholesterol content (10–60 mol%) and decreasing the ratio of the cationic lipid DDAB (78 to 28 mol%) while maintaining the structural lipid DSPC and the PEG-lipid at fixed molar ratios (10 and 2 mol%, respectively) (DDAB/DSPC/cholesterol/PEG_{2000}-DMG) [76]. This phenomenon highlights the importance of cholesterol in the formulation for improving the size of LNPs.

Using a different approach, Kulkarni and collaborators maintained the cholesterol:DSPC ratio at 1:1 (mol:mol) and evaluated the morphology and encapsulation of the LNP as the amount of DSPC:cholesterol was increased (5–80 mol%) in relation to the amount of ICL (94–19 mol%). The PEG_{2000}-DSPE was maintained at 1 mol%. As visualized by cryo-TEM, LNP exhibited a conventional solid core that decreased in size as the DSPC-cholesterol level was increased from 5 to 60 mol%; and then showed a remarkable hybrid solid core within a lipid bilayer morphology for LNP containing 80 mol% DSPC-cholesterol. Regarding the encapsulation efficiency, at low DSPC-cholesterol levels (<40 mol% DSPC-cholesterol) the efficiency of siRNA encapsulation is gradually reduced whereas, for systems containing >40 mol%, DSPC-cholesterol encapsulation efficiencies ~80% were achieved [67].

Nowadays, DSPC is frequently used as the helper lipid in LNP-nucleic-acid commercial formulations (Table 2), although several groups reported that DOPE, instead of DSPC, resulted in a higher release of mRNA and pDNA as a result of the fusogenic character of the phosphoethanolamine [45,77–78]. Using molecular dynamics (MD) simulations, the strong associations between the DOPE headgroups, the lipid tails and the oxygens of the ester linker of DLin-MC3-DMA were confirmed. This association resulted in the positioning of DLin-MC3-DMA at the membrane surface, which slows down the lateral diffusion of all simulated bilayers. This could explain why lipid bilayers with phosphatidylethanolamines have low water penetration and why

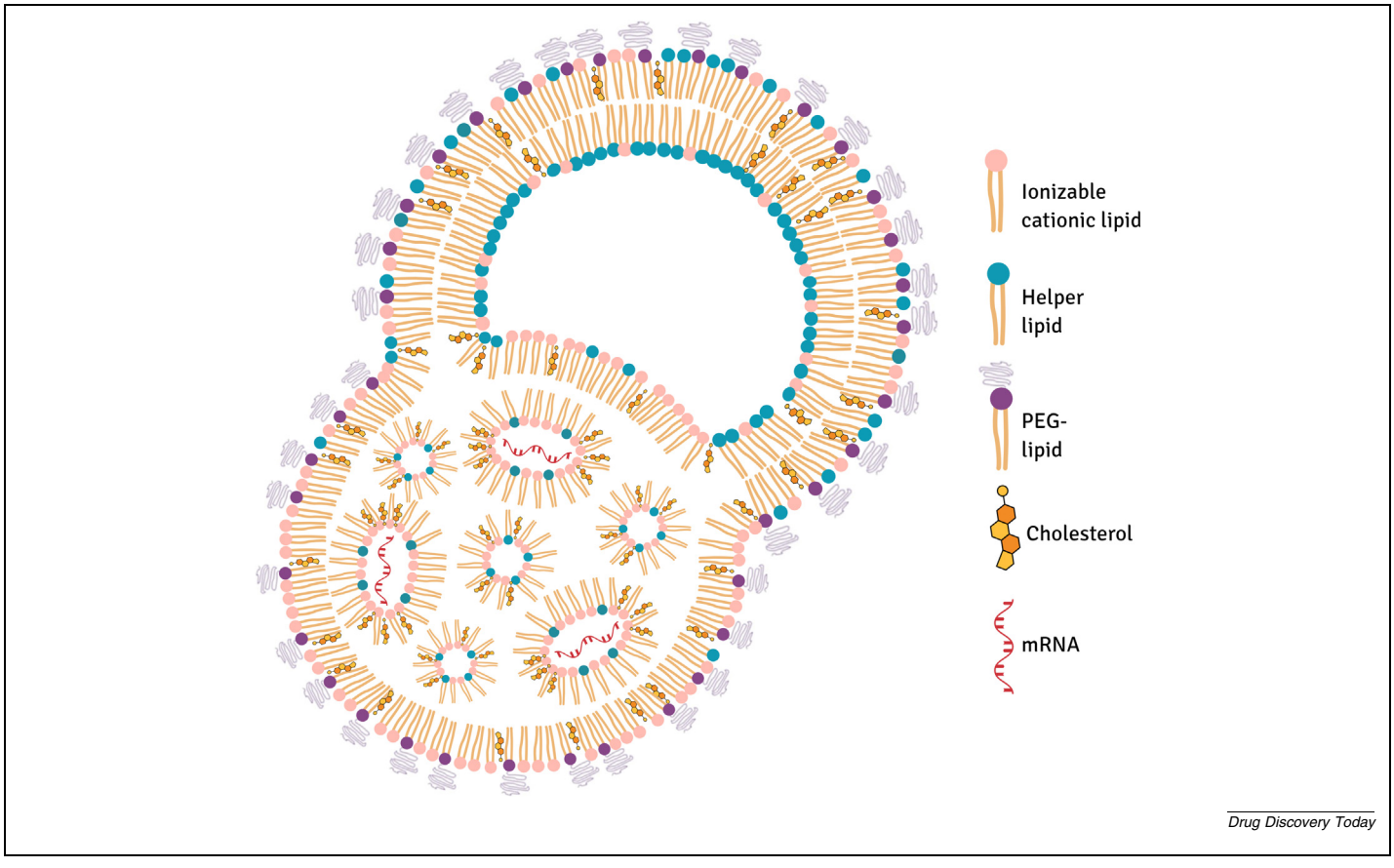

FIG. 5
Schematic representation of the 'bleb' structure. Cationic lipid (rose) is primarily associated with the mRNA to form a solid core structure whereas DSPC is largely segregated into bilayer bleb structure. Adapted, with permission, from [20].

LNPs containing a mix of DOPE and DLin-MC3-DMA in the formulation are most likely to exhibit poor transfection capabilities [79].

Type of nucleic acid

The impact of the nucleic acid type was investigated by comparing siRNA, mRNA and pDNA loaded into LNPs formulated using the same lipid composition (50/11.5/37.5/1 DLin-KC2-DMA/DSPC/cholesterol/PEG-lipid) [20]. As visualized by Cryo-TEM, the loading of larger nucleic acids, such as mRNA and pDNA, leads to the formation of a 'bleb' structure (Fig. 5). Owing to the smaller size of siRNA, it exposes a larger surface area per base to interact with the helper lipids. The comparably larger nucleic acids cannot accommodate as much helper lipids as siRNA, which leads to the segregation of DSPC in bleb structures on the surface, which are protrusions where DSPC forms a separate bilayer with an aqueous interior.

This alteration in the morphology is followed by differences in the encapsulation efficacy. The encapsulation efficiencies for mRNA and pDNA were >70% compared with full encapsulation (100%) of siRNA [20]. This difference is a result of the different size of the nucleic acids. The larger the nucleic acid is the lower is the amount that can be encapsulated. This indicates that the lipid composition needs to be adjusted accordingly. The adjustments can include the replacement of components and changes in the molar ratio [77–78]. For example, using DOPE instead of DSPC led to the loss of the bleb structure, supporting the hypothesis that unsaturation of the lipids highly impacts the formation of an electron-dense core, consisting of inverted micellar structures [20,38,75]. In summary, different nucleic acids require

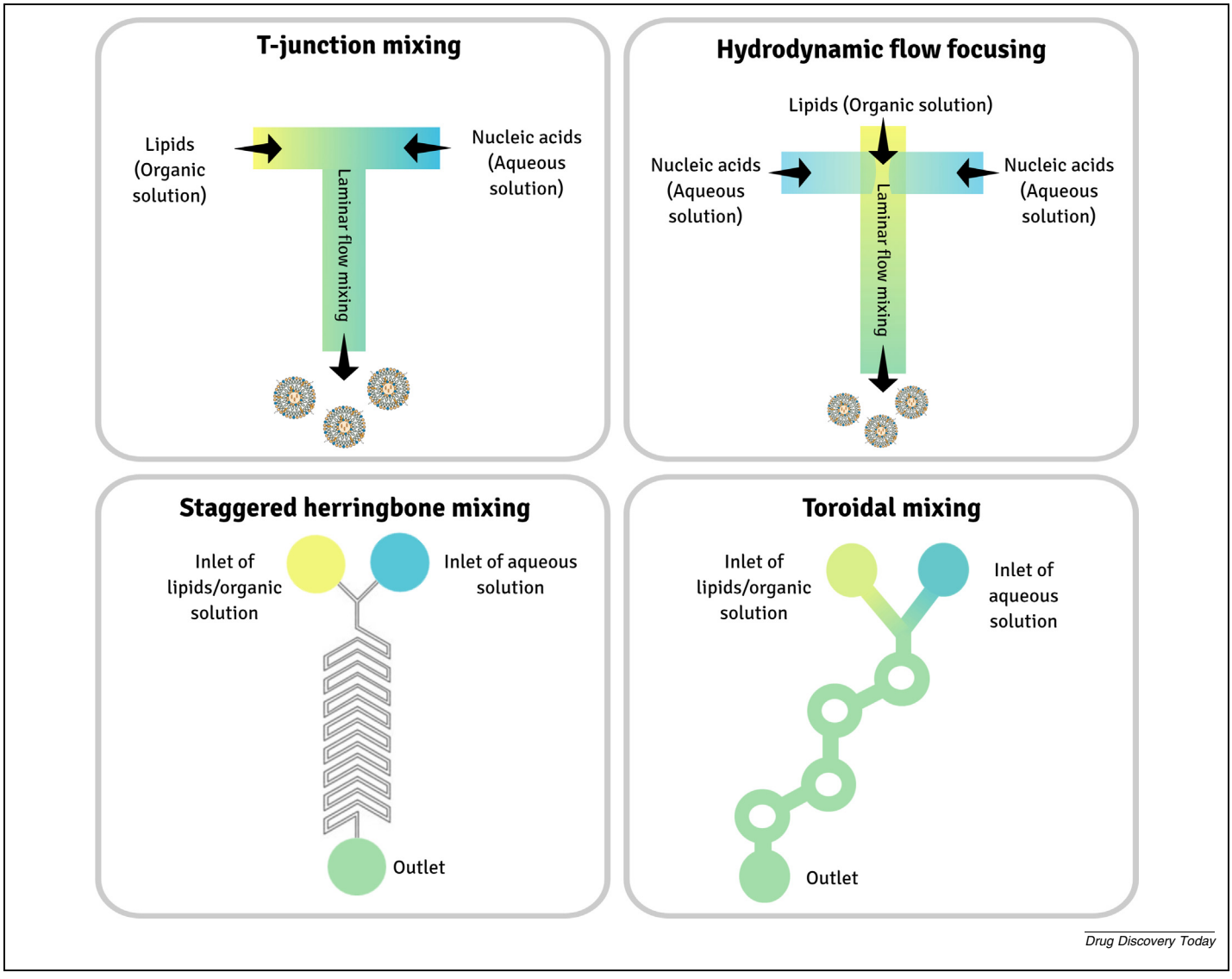

FIG. 6

Schematic illustration of microfluidic mixing methods: T-junction mixing, hydrodynamic flow focusing, staggered herringbone and toroidal mixer. The aqueous phase is illustrated in blue and the organic phase in yellow, the resulting mixture containing nanoparticles in green.

slightly different lipid compositions to achieve the same LNP structure and efficacy.

Formulation and manufacturing

Microfluidic technologies

Microfluidic platforms have been gaining popularity over the past years owing to four important aspects: (i) high controllability of the flow rate and mixing conditions, which resulted in uniform (monodispersed) NPs and reduced batch-to-batch variation; (ii) ability to scale up to an industrial level and enhance production rate; (iii) real-time monitoring of the production occurring inside the microchannels; and (iv) microfluidic devices with customized microchannel geometries and architecture for enhancing drug loading and colloidal stability of NPs [80–81].

T-junction mixing

The T-junction is one of the earliest and most basic geometric designs of a microfluidic device. In the T-junction mixing (in-line) method the aqueous medium containing the nucleic acid is combined with the lipid-organic solvent (typically an ethanol solution) in a T-connector using a dual pump system (Fig. 6). Owing to this fast mixing, the lipid molecules became supersaturated, allowing LNPs to self-assemble into the desired structure without the application of size-reduction methods. The last step consists of filtration to further stabilize the particles. Although this method exhibits many benefits compared with conventional methods, some reproducibility challenges remain. For this reason, optimized methods applying other microchannel designs were developed [44,82–83].

Hydrodynamic flow focusing

One of the most widely used approaches for continuous production of different types of LNPs is hydrodynamic flow focusing mixing. In this approach, an organic solution containing the lipids is passed through the central inlet channel, whereas an aqueous solution is injected from two side-inlet channels. The mixture of these two streams occurs in a small area, which allows droplet generation under controlled laminar flow conditions. Fig. 6 shows a typical T-shaped microfluidic channel; however, the shape of the microchannels can be further modified for a Y-shape or as a serpentine microchannel. The diameter of the central channel and the microchannel design can also be modified to adjust the mixing time [84,81].

Staggered herringbone and toroidal mixer

It was possible to further improve this preparation process by utilizing a staggered herringbone structure connected to a microfluidic device. This approach was developed to improve control over the mixing process and reduce the mixing time. The lipids in the organic solution and the nucleic acid in the aqueous solution are pumped into two separate inlets. Then, the staggered herringbone structure induces chaotic advection of the laminar stream causing a rapid and efficient mixing of the two solutions owing to the exponential increase of the interface between the fluids (Fig. 6) [44]. However, for commercial scale purposes, the herringbone design has limitations because it is difficult to achieve the high-throughput speeds (flow rate capacity) required for good manufacturing practice (GMP). To overcome these issues, the toroidal mixer architecture was developed by Precision NanoSystems (Fig. 6). The toroidal design allows improved mixing by chaotic advection by increasing the number of vortices and centrifugal forces. Currently, the classic NanoAssemblr Benchtop® was replaced by NanoAssemblr NexGen Ignite® and NanoAssemblr NexGen Blaze® [85]. A drawback of all above-mentioned microfluidic techniques is the restricted solubility of some lipids in organic solvents, which can result in lower concentrations of LNPs in the mixed solutions and the need to concentrate the LNPs post formulation [44].

Stability profile

To translate LNP-nucleic-acid formulations from bench to bedside and enable distribution, stability studies are essential to help establish the shelf-life and the optimum storage conditions for the final product. The stability of LNP-nucleic-acid formulations depends on processing parameters such as temperature, humidity and light; and also on the properties of the nucleic acids and the lipid excipients [36,86].

Methods to improve LNP-RNA stability include formulation strategies such as addition of buffers, surfactants and other excipients, use of effective process controls, and by freezing or lyophilization using appropriate cryoprotectants (sucrose, trehalose or mannitol) [87–88]. Moderna and BioNTech-Pfizer, for example, use sucrose as a cryoprotectant. Both mRNA COVID-19 vaccines are concentrated buffered dispersions in water for injection (WFI). Moderna uses tromethamine (Tris)-HCl buffer to regulate the pH of the final formula to 7–8, whereas BioNTech-Pfizer uses phosphate (potassium dihydrogen phosphate and disodium hydrogen phosphate dihydrate). Because the pH can change upon freezing and the COVID-19 vaccines must be stored at ultra(low) temperatures, the selection of the buffering system and osmolyte is crucial [36,89]. Moderna Spikevax is stored at −25 °C to −15 °C and is stable up to 19 h at 2 °C to 25 °C after initial puncture [90], whereas BioNTech-Pfizer Comirnaty is stored at −90 °C to −60 °C and is stable up to 6 h at 2–30 °C after thawing and dilution by saline [91]. At refrigerated temperatures (2–8 °C), the Moderna and BioNTech-Pfizer vaccines are stable for 30 and 5 days, respectively [36].

Several studies described the stability of LNP-nucleic-acid formulations under different storage (aqueous, frozen or lyophilized) temperatures and using different types of cryoprotectants [36–37,87–89,92]. Ball et al. showed that a LNP-siRNA formulation (lipidoid $306O_{13}$, cholesterol, DSPC, PEG_{2000}-DMG) was stable at 2 °C for up to 160 days when stored at a pH of 3, 7.4 or 9. If freezing or lyophilization was necessary, the addition of 20% (w/v) sucrose or trehalose was essential to prevent aggregation and loss of drug efficacy [87]. Using LNP-mRNA, Zhao *et al.* further confirmed that the addition of 5% (w/v) sucrose or trehalose in freezing conditions was a suitable method for long-term storage [88].

In summary, given the complexity of the LNP composition and assembly, as well as the possibility of nonlinear degradation kinetics, stability tests should be conducted on several lots and as early as possible during preclinical development [93]. According to the International Council for Harmonization of Technical Requirements for Pharmaceuticals for Human Use (ICH) guidelines, the stability can be investigated by evaluating the mean particle size, size distribution, encapsulation efficiency and drug-release kinetics over storage periods at various temperatures [94].

Quality by design

Quality by design (QbD) brings a systematic approach to drug development that aims to optimize the quality, efficacy and safety of the final product by understanding the product, the manufacturing process and risk assessment of variables [95]. As shown in Fig. 7, QbD starts by establishing the quality target product profile (QTTP). Based on the QTPP, the critical quality attributes (CQAs) of the product and their ranges are determined. Then, based on the CQAs, critical material attributes (CMAs) and critical process parameter (CPPs) ranges are defined using a risk assessment scoring. From these ranges, the design of experiments (DoE) can be created obtaining a mathematical model of the production process. Further, the control strategy dictates each step of the manufacturing process including characteristics and attributes related to the drug substances, drug product materials, excipients and final product specifications, as well as controls for each step of the manufacturing process (facility and equipment operating conditions, in-process controls and the associated methods and frequency of monitoring and control) [96–97].

Recently, QbD has been used to assist the development and optimization of new nanoformulations. For example, optimization of LNP formulations for mRNA delivery were developed using design of experiment (DoE) principles including definitive screening and fractional factorial designs. By simultaneously varying the C12-200:mRNA weight ratio, the phospholipid identity (DSPC, DSPE, DOPC or DOPE) and the molar composition of the LNP formulation (40–60 mol% for ICL, 4–16 mol% for helper lipids, 21.55–55.50 mol% for cholesterol and 0.5–2.5 mol% for PEG_{2000}-DSPE) the authors created a library to identify a lead optimized formulation for mRNA delivery. The optimized formulation (10:1 C12-200:mRNA weight ratio with 35% C12-200, 16% DOPE, 46.5% cholesterol and 2.5% C14-PEG_{2000} molar composition) increased EPO mRNA delivery *in vivo* by over sevenfold [98]. Similarly, Billingsley and collaborators applied an orthogonal DOE methodology to screen a library of LNP formulations with varied excipient molar ratios for improved mRNA delivery to T cells. Ionizable lipid C14-4, DOPE, cholesterol and PEG were used as a standard formulation and the molar ratio of 40 C14-4: 30 DOPE: 20 cholesterol: 2.5 PEG exhibited a three-

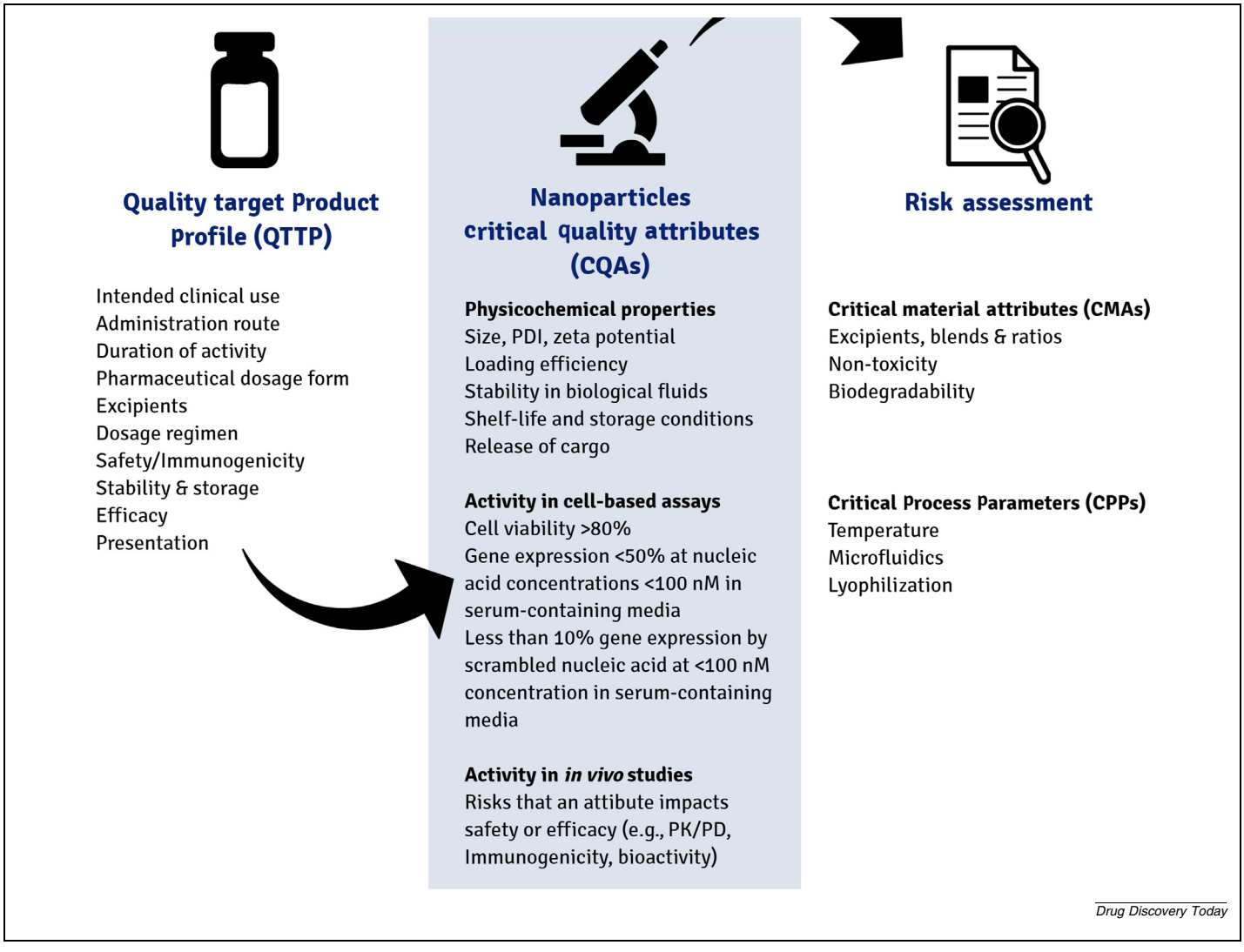

FIG. 7

Framework for production of lipid-based nanosystems for nucleic acid delivery by applying a quality by design (QbD) approach. Adapted, with permission, from [97].

fold increase in mRNA delivery in Jurkat cells [99]. Blakney and collaborators applied a DoE approach to optimize LNP formulations for self-amplifying RNA (saRNA) delivery in human skin explants. The authors concluded that between all factors [i.e., cationic (DDA, DOTAP), ionizable (C12-200) and zwitterionic (cephalin) lipids, the ratio of total lipid to RNA, the lipid and particle concentrations and the ratio of cationic to zwitterionic lipids], only the lipid identity and lipid concentration had a significant impact on luciferase saRNA expression in human skin explants. Compared with the original formulation, the optimized formulation exhibited a sevenfold increase in the expression of luciferase [100].

Delivery to the liver and beyond the liver: Biodistribution and pharmacokinetics

Biodistribution, pharmacokinetics and therapeutic outcomes of LNP-nucleic-acid formulations can be greatly influenced by the administration route which is often determined by the properties of the nanocarrier system and the therapeutic applications [37]. Thereby, understanding these issues can lead to the improvement and development of more convenient noninvasive administration routes, optimized LNP-nucleic-acid formulations with fewer side-effects, improved biodistribution and extended duration of effect.

Intravenous administration

After intravenous administration, the majority of LNPs accumulate in all major liver cell types (i.e., hepatocytes, Kupffer cells and liver sinusoidal endothelial cells) [101]. LNPs are directed to the liver mainly because of their physicochemical properties (size, cationic and neutral charge, presence of lipophilic ligands) and owing to the anatomical and physiological features of the organ including high blood flow, discontinuous nature of the hepatic capillaries and lipid metabolism [102]. Within the liver, the use of a specific receptor-targeted ligand can be effective for distinguishing between the distinct hepatic cells preventing accumulation in any other cell type. For example, apolipoprotein E (ApoE)-binding receptors on hepatocytes was the strategy used by Alnylam on Onpattro®, which is an LNP formulation of siRNA for the treatment of polyneuropathies resulting from the hereditary ATTR amyloidosis. Initially, the LNP binds to circulation ApoE. Then, this complex binds to lipoprotein receptors on the hepatocyte surface, thereby promoting internalization by endocytosis [49].

Following the success of gene-editing therapy for the treatment of ATTR amyloidosis, a new CRISPR-Cas9-based candidate was developed by Intellia Therapeutics and Regeneron Pharmaceuticals, called NTLA-2001. NTLA-2001 comprises a LPN-encapsulating mRNA for Cas9 protein and a single guide RNA targeting *TTR*, which led to a decrease in the production of wild-type and mutant TTR after a single intravenous administration [103].

To expand the use of LNP-nucleic-acids to treat a wider range of diseases, biodistribution to other organs, not just the liver, must be achieved. Modification of the LNP with targeting ligands has been suggested to overcome this challenge. Representative targeting moieties, with potential for nucleic acid delivery, include antibodies, proteins, peptides, aptamers and small molecules such as folate and vitamins (Table 3). These targeting moieties interact with molecules on the target cell surface, for example, ligand-receptor, enzyme-substrate or antibody-antigen, and, in this way, increase retention at the target site and NP uptake by the target cells [104–105]. Despite the benefits of surface targeting, the formulation of targeted NPs is complex because targeting efficiency varies with ligand density, receptor density, hydrophilicity and molecular weights of ligands [106–107]. Additionally, it is difficult to identify a receptor specifically expressed at the diseased site, disease markers can vary among diseased cells within a patient as well as between different patients [105]. Based on a fundamental understanding of these issues, there are now several groups designing high-throughput libraries of NPs to identify optimal formulations that selectively target specific tissues such as spleen, liver or lungs [108–111]. The Siegwart group reported a novel strategy termed selective organ targeting (SORT) wherein a supplemental SORT molecule is added to traditional LNPs (ionizable cationic lipids, DOPE, cholesterol and $PEG_{2000}DMG$) that direct them to particular locations in the body such as the liver, lungs and spleen as a function of the percentage and biophysical property of the SORT molecule [109]. This targeted delivery could be achieved owing to (i) desorption of PEG-lipids from the LNP surface exposing SORT molecules, (ii) recognition and binding of exposed SORT molecules by distinct serum proteins and (iii) interaction between surface-adsorbed proteins and cognate receptors expressed by cells in target organs [112]. Permanently cationic SORT lipids include DDAB, EPC and DOTAP whereas anionic SORT lipids include 14PA, 18BMP, 18PA. LNPs are compatible with multiple gene-editing techniques, including mRNA, Cas9 mRNA/single guide

TABLE 3

Targeted RNA-based therapeutics for systemic delivery to specific organs/cells.

Ligand	Target	Target organ	Cargo	Formulation	Refs
Anti-EGFR Ab	EGFR	Tumors	Vim and JAK3 siRNAs	Liposomes	[95]
ASSET (IgG mAbs)	Ly6C+	Leukocytes	IRF8 siRNA	LNPs	[96]
Folate	Folate receptor	Tumors	Doxorubicin/Bmi1 siRNA	Liposomes	[97]
Glu-urea-Lys PSMA	Androgen receptor	Prostate tumor	AR21 and AR25 siRNAs	LNPs	[98]
Peptide iRGD	α_v integrins	Glioma	EGFR and PD-L1 siRNAs	SLNs	[99]
RVG-9r	nAChR	Brain	Ataxin-3 siRNA	SNALPs	[100]
RVG	nAChR	Brain	HTT siRNA	Cyclodextrins	[101]
Tryptamine-derived lipidoids	Neurotransmitters	Brain	Tau ASO	LNPs	[102]

Abbreviations: EGFR, epidermal growth factor receptor; IRF8, interferon regulatory factor 8; nAChRs, nicotinic acetylcholine receptors; PSMA, prostate-specific membrane antigen; RVG, rabies virus glycoprotein; SLNs, solid lipid nanoparticles; SNALPs, stable nucleic acid lipid particles; HTT, Huntingtin.

RNA (sgRNA) and Cas9 ribonucleoprotein (RNP) complexes [109]. In a follow-up to this study, a novel class of multi-tailed ionizable phospholipids (iPhos) was developed. Optimized iPhos lipids contain a pH-switchable small zwitterionic head consisting of an amine, a phosphate group and three hydrophobic tails, facilitating endosomal escape and thus improving delivery of mRNA and/or sgRNA for *in vivo* gene editing. According to SAR studies, the chain lengths of iPhos are responsible for controlling *in vivo* mRNA delivery effectiveness and organ selectivity. The chain length at the amine side determined efficacy, and a 8–10 carbon chain length mediated high *in vivo* mRNA expression. By contrast, the alkyl length next to the phosphate group influenced organ selectivity, with shorter chains (9–12 carbons) showing mRNA translation in the liver, whereas longer chains (13–16 carbons) transfer protein expression to the spleen [113].

Dan Peer's group presented another strategy to overcome the challenges of selective targeted delivery. The researchers developed a modular targeting platform named ASSET (anchored secondary scFv enabling targeting), which is based on the incorporation of a lipoprotein into siRNA-loaded LNPs that interact with the antibody crystallizable fragment (Fc) domain of a selected targeting antibody. This approach allows the creation of a hypothetically infinite amount of targeted carriers, which enables a flexible switching between different targeting antibodies [114].

Subcutaneous, intradermal and intramuscular administration

Besides intravenous injection, local injection [i.e., intradermal (ID), subcutaneous (SC) and intramuscular (IM)] can also stimulate systemic responses; for example, ID, SC and IM routes are often employed for vaccination owing to the presence of active antigen-presenting cells (APCs) in the skin and muscles [37]. Thus, LNP-mRNA vaccine administration can induce a robust immune response by two distinct mechanisms: either LNP-mRNA locally transfects APCs in the muscle which then migrate to the lymphatics or the LNP-mRNAs are passively drained via the lymphatic system, delivering the mRNA payload directly near draining lymph-node-resident APCs and T cells [115].

The majority of the licensed vaccines are administered by IM injection including both LNP-mRNA vaccines for COVID-19. Following IM administration, myocytes effectively take up the LNPs before the cytoplasmic release of the mRNAs for encoding SARS-CoV-2 Spike protein. In comparison to the ID and SC routes, the IM route enables a considerably larger volume to be injected [116]. Even before the COVID-19 pandemic, several research groups were developing delivery technologies including LNPs for mRNA vaccines [117–120]. Now this is expanding for mRNA flu vaccines and other infectious diseases [22,121].

Oral administration

Compared with parenteral administration routes, oral administration is the most convenient for patients being noninvasive, painless, safe and cheap. In addition, one of the main advantages of oral administration is that it provides the opportunity to locally treat a number of diseases in the gut tissue, for example IBD and cancer, while avoiding the side effects associated with systemic delivery. However, oral delivery of LNP-nucleic-acid formulations comes with many challenges owing to the physiological barriers in the gastrointestinal tract. The barriers include the acidic milieu of the stomach (pH 1.5–1.9) and the presence of bile salts and digestive enzymes (i.e., pepsin in the stomach and amylase, trypsin or lipase in the intestine). In addition, the existence of the mucus layer at the membrane surface can restrict the diffusion of the LNP to the membrane surface. If systemic versus local delivery is required, membrane permeability can also be a significant barrier [122].

To help overcome these limitations to delivery a range of formulation strategies have been explored [123]. Several systematic mechanistic studies have investigated the application of LNPs for oral delivery of nucleic acids. Data from these studies have been key to quantifying the individual barriers to oral delivery, to elucidating how these LNPs behave in the GIT and to identifying how modifications in the formulation including the choice of the lipid excipients used can help to overcome these barriers. A total of 96 unique LNP formulations encapsulating DNA barcodes were synthetized and given orally to mice. Results showed that LNP retention in the gastrointestinal system is improved as the molar ratio of cholesterol to the PEGylated lipid is increased, and a balance of hydrophobic:hydrophilic components can confer stability and mucus-penetration abilities to LNPs [124]. Ball *et al.* investigated oral delivery of siRNA-LNPs using *in vitro* and *in vivo* models. LNP efficacies were unaffected by pH changes; however, the presence of pepsin, bile salts and mucin decreased efficacy. Mouse studies showed that, despite the barriers and the lack of gene silencing efficacy, LNPs were able to enter mouse intestine and colon cells. It was suggested that a coating with a pH-responsive polymer (e.g., Eudragit®) preventing pepsin digestion and bile salt interaction could help to increase efficacy in oral delivery [125].

To facilitate regular oral administration by tablets and/or capsules and to achieve long-term storage lyophilization might be an option. To this end, tablets containing a freeze-dried LNP-siRNA delivery system were prepared. Results indicated that, following exposure to the requisite compression forces, the structure of the siRNA and a degree of gene-silencing efficacy were maintained [126].

In summary, although LNPs have demonstrated successful delivery of siRNA to the liver after intravenous administration, and of mRNA as a vaccine after intramuscular injection, further development is necessary to enable this technology to reach other organs in the body to exploit the potential of nucleic acids to treat a wide spectrum of diseases. To achieve this goal, an urgent need exists to develop new lipid excipients to further enhance the delivery of RNA. The initiative to move beyond the 'tried and tested' GRAS (generally regarded as safe) listed excipients is already being pursued by the FDA [127]. Ongoing work on the synthesis of novel lipid excipients, including lipidoids [29], will help to progress this delivery technology.

Concluding remarks and future perspectives

Given the clinical success of mRNA-based vaccines for COVID-19, now is the right time to further push beyond the state-of-the-art in RNA-based therapies and focus on the urgent and unmet need for advanced therapies targeting noncommunicable

diseases affecting tissues other than the liver. Successful delivery systems for nucleic-acid-based drugs have been a bottleneck for clinical translation. Although delivery using viral approaches has traditionally been more well-established, recent studies have raised concerns related to integration into the genome, resulting in long-term life-threatening side effects. By contrast, nonviral delivery has recently gained attraction with the success of the siRNA product patisiran, for liver disease, marketed by Alnylam, and the Moderna and Pfizer COVID-19 mRNA vaccines, all of which deliver RNA using the nonviral approach of LNPs, indicating the potential of this delivery approach. The rapid development and regulatory approval of mRNA vaccines has promoted confidence across the industry, as well as with regulators and the public. The opportunity now exists to capitalize on this momentum and to expand this LNP technology to noncommunicable and non-liver-based diseases. The commercial potential for RNA therapeutics is growing rapidly, the market for mRNA non-vaccine-based therapeutics alone is predicted to be US$4–5 billion by 2035 [10]; however, long-term opportunities will depend on the availability of efficient delivery technologies including LNPs.

Conflicts of interest

The authors declare that they have no known competing financial interests or personal relationships that could have appeared to influence the work reported in this paper.

Data availability

No data was used for the research described in the article.

Acknowledgments

This publication has emanated from research supported in part by Science Foundation Ireland and the European Regional Development Fund, Grant 17/RC-PhD/3477 and 12/RC/2278_P2 (Advanced Materials and BioEngineering Research, AMBER); Jazz Pharmaceuticals, and, by an anonymous philanthropic donation for prostate cancer research. MCPM acknowledges funding from Irish Research Council under Grant GOIPD/2021/276. PSK acknowledges funding from the Health Research Board Emerging Investigator Award (Grant reference EIA-2019-006). The authors wish to thank Dr Michael F Cronin for advice on the chemistry.

References

[1] Xiao, Y. *et al*. (2019) Engineering Nanoparticles for Targeted Delivery of Nucleic Acid Therapeutics in Tumor. *Mol. Ther. Methods Clin. Dev.* 12, 1–18. DOI: 10.1016/j.omtm.2018.09.002.

[2] Tang, R. and Xu, Z. (2020) Gene therapy: a double–edged sword with great powers. *Mol. Cell. Biochem.* 474, 73–81. DOI: 10.1007/s11010-020-03834-3.

[3] Weng, Y. *et al*. (2020) Improved Nucleic Acid Therapy with Advanced Nanoscale Biotechnology. *Mol. Therapy: Nucleic Acid.* 19, 581–601. DOI: 10.1016/j.omtn.2019.12.004.

[4] Guo, J. *et al*. (2017) Antibody-Targeted Cyclodextrin-Based Nanoparticles for siRNA Delivery in the Treatment of Acute Myeloid Leukemia: Physicochemical Characteristics, in Vitro Mechanistic Studies, and ex Vivo Patient Derived Therapeutic Efficacy. *Mol. Pharm.* 14, 940–952. DOI: 10.1021/acs.molpharmaceut.6b01150.

[5] Guo, J. *et al*. (2014) Biomimetic nanoparticles for siRNA delivery in the treatment of leukaemia. *Biotechnol. Adv.* 32, 1396–1409. DOI: 10.1016/j.biotechadv.2014.08.007.

[6] Dowdy, S.F. (2017) Perspective Overcoming cellular barriers for RNA therapeutics. *Nat. Biotechnol.* 35, 222–229. DOI: 10.1038/nbt.3802.

[7] Van Der, L.J. and Wright, J.F. (2016) Progress and challenges in viral vector manufacturing. *Hum. Mol. Genet.* 25, 42–52. DOI: 10.1093/hmg/ddv451.

[8] Yin, H. *et al*. (2014) Non-viral vectors for gene-based therapy. *Nat. Rev. Genet.* 15, 541–555. DOI: 10.1038/nrg3763.

[9] Zu, H. and Gao, D. (2021) Non-viral Vectors in Gene Therapy : Recent Development, Challenges, and Prospects. *AAPS J.* 23, 78. DOI: 10.1208/s12248-021-00608-7.

[10] Xie, W. *et al*. (2021) Evolution of the market for mRNA technology. *Nat. Rev. Drug Discov.* 20, 735–736. DOI: 10.1038/d41573-021-00147-y.

[11] Guo, J. *et al*. (2010) Therapeutic targeting in the silent era =: advances in non-viral siRNA delivery. *Molecular Bio System System.* 6, 1143–1161. DOI: 10.1039/c001050m.

[12] Singh, R.P. *et al*. (2019) Self-Assembled Cationic β-Cyclodextrin Nanostructures for siRNA Delivery. *Mol. Pharm.* 16, 1358–1366. DOI: 10.1021/acs.molpharmaceut.8b01307.

[13] Zhuang, Y. and Cui, W. (2021) Biomaterial-based delivery of nucleic acids for tissue regeneration. *Adv. Drug Deliv. Rev.* 176. DOI: 10.1016/j.addr.2021.113885.

[14] Zhao, W. *et al*. (2019) RNA delivery biomaterials for the treatment of genetic and rare diseases. *Biomaterials* 217. DOI: 10.1016/j.biomaterials.2019.119291.

[15] Samaridou, E. *et al*. (2020) Lipid nanoparticles for nucleic acid delivery : Current perspectives. *Adv. Drug Deliv. Rev.* 154–155, 37–63. DOI: 10.1016/j.addr.2020.06.002.

[16] Cullis, P.R. and Hope, M.J. (2017) Lipid Nanoparticle Systems for Enabling Gene Therapies. *Mol. Ther.* 25, 1467–1475. DOI: 10.1016/j.ymthe.2017.03.013.

[17] Kulkarni, J.A. *et al*. (2017) Design of lipid nanoparticles for in vitro and in vivo delivery of plasmid DNA. *Nanomedicine* 13, 1377–1387. DOI: 10.1016/j.nano.2016.12.014.

[18] Yonezawa, S. *et al*. (2020) Recent advances in siRNAdeliverymediated by lipid-based nanoparticles. *Adv. Drug Deliv. Rev.* 154–155, 64–78.

[19] Weinstein, S. (2015) Harnessing RNAi-based nanomedicines for therapeutic gene silencing in B-cell malignancies. *PNAS* E16–E22. DOI: 10.1073/pnas.1519273113.

[20] Leung, A.K.K.K. *et al*. (2015) Microfluidic Mixing: A General Method for Encapsulating Macromolecules in Lipid Nanoparticle Systems. *J. Phys. Chem. B* 119, 8698–8706. DOI: 10.1021/acs.jpcb.5b02891.

[21] Kulkarni, J.A. *et al*. (2018) On the Formation and Morphology of Lipid Nanoparticles Containing Ionizable Cationic Lipids and siRNA. *ACS Nano* 12, 4787–4795. DOI: 10.1021/acsnano.8b01516.

[22] Chaudhary, N. *et al*. (2021) mRNA vaccines for infectious diseases: principles, delivery and clinical translation. *Nat. Rev. Drug Discov.* 20, 817–838. DOI: 10.1038/s41573-021-00283-5.

[23] Semple, S.C. *et al*. (2010) Rational design of cationic lipids for siRNA delivery. *Nat. Biotechnol.* 28, 172–176. DOI: 10.1038/nbt.1602.

[24] Schlich, M. *et al*. (2021) Cytosolic delivery of nucleic acids: The case of ionizable lipid nanoparticles. *Bioeng. Transl. Med.* 6, 1–16. DOI: 10.1002/btm2.10213.

[25] Eygeris, Y. *et al*. (2022) Chemistry of Lipid Nanoparticles for RNA Delivery. *Acc. Chem. Res.* 55, 2–12. DOI: 10.1021/acs.accounts.1c00544.

[26] Cullis, P.H.M. (2017) Lipid Nanoparticle Systems for Enabling Gene Therapies. *Mol. Ther.* 25, 1467–1475. DOI: 10.1016/j.ymthe.2017.03.013.

[27] Tam, Y.Y.C. *et al*. (2013) Advances in Lipid Nanoparticles for siRNA Delivery. *Pharmaceutics* 5, 498–507. DOI: 10.3390/pharmaceutics5030498.

[28] Buck, J. *et al*. (2019) Lipid-Based DNA therapeutics : Hallmarks of non-viral gene delivery. *ACS Chem. Nerosci.* 13, 3754–3782. DOI: 10.1021/acsnano.8b07858.

[29] Hajj, K.A. *et al*. (2019) Branched-Tail Lipid Nanoparticles Potently Deliver mRNA In Vivo due to Enhanced Ionization at Endosomal pH. *Small* 15, 1–7. DOI: 10.1002/smll.201805097.

[30] Patel, P. *et al*. (2021) The Importance of Apparent pKa in the Development of Nanoparticles Encapsulating siRNA and mRNA. *Trends Pharmacol. Sci.* 42, 448–460. DOI: 10.1016/j.tips.2021.03.002.

[31] Jayaraman, M. *et al*. (2012) Maximizing the Potency of siRNA Lipid Nanoparticles for Hepatic Gene Silencing In Vivo. *Angew. Chem.* Table 1, 8529–8533. DOI: 10.1002/anie.201203263.

[32] Sato, Y. *et al*. (2018) Understanding structure-activity relationships of pH-sensitive cationic lipids facilitates the rational identification of promising lipid nanoparticles for delivering siRNAs in vivo. *J. Control. Release* 2019, 140–152. DOI: 10.1016/j.jconrel.2019.01.001.

[33] Hoy, S.M. (2018) Patisiran: First Global Approval. *Drugs* 78, 1625–1631. DOI: 10.1007/s40265-018-0983-6.

[34] Lamb, Y.N. (2021) Inclisiran: First Approval. *Drugs* 81, 389–395. DOI: 10.1007/s40265-021-01473-6.

[35] Wang, W. *et al*. (2021) Prediction of lipid nanoparticles for mRNA vaccines by the machine learning algorithm. *Acta Pharm. Sin. B* DOI: 10.1016/j.apsb.2021.11.021.

[36] Schoenmaker, L. *et al*. (2021) mRNA-lipid nanoparticle COVID-19 vaccines: Structure and stability. *Int. J. Pharm*. 601. DOI: 10.1016/j.ijpharm.2021.120586 120586.

[37] Hou, X. *et al*. (2021) Lipid nanoparticles for mRNA delivery. *Nat. Rev. Mater*. 0123456789. DOI: 10.1038/s41578-021-00358-0.

[38] Ponti, F. *et al*. (2021) Cationic lipids for gene delivery : many players, one goal. *Chem. Phys. Lipids* 235. DOI: 10.1016/j.chemphyslip.2020.105032 105032.

[39] Zimmermann, T.S. *et al*. (2006) RNAi-mediated gene silencing in non-human primates. *Nature* 441, 111–114. DOI: 10.1038/nature04688.

[40] Hu, B. *et al*. (2020) Therapeutic siRNA: state of the art. *Signal Transduct. Target. Ther*. 5. DOI: 10.1038/s41392-020-0207-x.

[41] Ansari, A.S. *et al*. (2017) Biomaterials for polynucleotide delivery to anchorage-independent cells. *J. Mater. Chem. B* 5, 7238–7261. DOI: 10.1039/c7tb01833a.

[42] Hobo, W. *et al*. (2013) Improving dendritic cell vaccine immunogenicity by silencing PD-1 ligands using siRNA-lipid nanoparticles combined with antigen mRNA electroporation. *Cancer Immunol. Immunother*. 62, 285–297. DOI: 10.1007/s00262-012-1334-1.

[43] Hajj, K.A. and Whitehead, K.A. (2017) Tools for translation: Non-viral materials for therapeutic mRNA delivery. *Nat. Rev. Mater*. 2, 1–17. DOI: 10.1038/natrevmats.2017.56.

[44] Evers, M.J.W. *et al*. (2018) State-of-the-Art Design and Rapid-Mixing Production Techniques of Lipid Nanoparticles for Nucleic Acid Delivery. *Small Methods* 1700375, 1–20. DOI: 10.1002/smtd.201700375.

[45] Cheng, X. and Lee, R.J. (2016) The role of helper lipids in lipid nanoparticles (LNPs) designed for oligonucleotide delivery. *Adv. Drug Deliv. Rev*. 99, 129–137. DOI: 10.1016/j.addr.2016.01.022.

[46] LoPresti, S.T. *et al*. (2022) The replacement of helper lipids with charged alternatives in lipid nanoparticles facilitates targeted mRNA delivery to the spleen and lungs. *J. Control. Release* 345, 819–831. DOI: 10.1016/j.jconrel.2022.03.046.

[47] Tenchov, B.G. *et al*. (2006) Cubic Phases in Phosphatidylcholine-Cholesterol Mixtures : Cholesterol as Membrane "Fusogen". *Biophys. J* . 91, 2508–2516. DOI: 10.1529/biophysj.106.083766.

[48] Suk, J.S. *et al*. (2016) PEGylation as a strategy for improving nanoparticle-based drug and gene delivery. *Adv. Drug Deliv. Rev*. 99, 28–51. DOI: 10.1016/j.addr.2015.09.012.PEGylation.

[49] Akinc, A. *et al*. (2018) The Onpattro story and the clinical translation of nanomedicines containing nucleic acid-based drugs. *Nat. Nanotechnol*. 2019, 1084–1087. DOI: 10.1038/s41565-019-0591-y.

[50] Ge, X. *et al*. (2021) Rationale and Application of PEGylated Lipid-Based System for Advanced Target Delivery of siRNA. *Front. Pharmacol*. 11, 1–15. DOI: 10.3389/fphar.2020.598175.

[51] Kozma, G.T. *et al*. (2020) Anti-PEG antibodies: Properties, formation, testing and role in adverse immune reactions to PEGylated nano-biopharmaceuticals. *Adv. Drug Deliv. Rev*. 154–155, 163–175. DOI: 10.1016/j.addr.2020.07.024.

[52] McSweeney, M.D. *et al*. (2021) Anaphylaxis to Pfizer/BioNTech mRNA COVID-19 Vaccine in a Patient With Clinically Confirmed PEG Allergy. *Front. Allergy* 2, 1–5. DOI: 10.3389/falgy.2021.715844.

[53] Sellaturay, P. *et al*. (2021) Polyethylene glycol (PEG) is a cause of anaphylaxis to the Pfizer/BioNTech mRNA COVID-19 vaccine. *Clin. Exp. Allergy* 51, 861–863. DOI: 10.1111/cea.13874.

[54] Sampath, V. *et al*. (2021) Vaccines and allergic reactions: The past, the current COVID-19 pandemic, and future perspectives. *Allergy: Eur. J. Allergy Clin. Immunol*. 76, 1640–1660. DOI: 10.1111/all.14840.

[55] Shi, L. Zhang, J. and Zhao, M., *et al* (2021) Effects of polyethylene glycol on the surface of nanoparticles for targeted drug delivery. *Nanoscale* 13, 10748–10764. DOI: 10.1039/d1nr02065j.

[56] Xia, Y. Tian, J. and Chen, X. (2016) Effect of surface properties on liposomal siRNA delivery. *Biomaterials* 79, 56–68. DOI: 10.1016/j.biomaterials.2015.11.056.

[57] Nosova, A.S. Koloskova, O.O. and Nikonova, A.A., *et al* (2019) Diversity of PEGylation methods of liposomes and their influence on RNA delivery. *Medchemcomm*. 10, 369–377. DOI: 10.1039/c8md00515j.

[58] Chen, S. Tam, Y.Y.C. Lin, P.J.C. Leung, A.K.K. Tam, Y.K. and Cullis, P.R. (2014) Development of lipid nanoparticle formulations of siRNA for hepatocyte gene silencing following subcutaneous administration. *J. Control. Release* 196, 106–112. DOI: 10.1016/j.jconrel.2014.09.025.

[59] Ryals, R.C. *et al*. (2020) The effects of PEGylation on LNP based mRNA delivery to the eye. *PLoS One* 15, 1–17. DOI: 10.1371/journal.pone.0241006.

[60] Kumar, V. *et al*. (2014) Shielding of lipid nanoparticles for siRNA delivery: Impact on physicochemical properties, cytokine induction, and efficacy. *Mol. Ther. Nucleic Acids* 3, e210.

[61] Hou, Y. and Lu, H. (2019) Protein PEPylation: A New Paradigm of Protein-Polymer Conjugation. *Bioconjug. Chem*. 30, 1604–1616. DOI: 10.1021/acs.bioconjchem.9b00236.

[62] Hu, Y. *et al*. (2018) Polysarcosine as an Alternative to PEG for Therapeutic Protein Conjugation. *Bioconjug. Chem*. 29, 2232–2238. DOI: 10.1021/acs.bioconjchem.8b00237.

[63] Nogueira, S.S. *et al*. (2020) Polysarcosine-Functionalized Lipid Nanoparticles for Therapeutic mRNA Delivery. *ACS Appl. Nano Mater*. 3, 10634–10645. DOI: 10.1021/acsanm.0c01834.

[64] Hallan, S.S. *et al*. (2021) Challenges in the Physical Characterization of Lipid Nanoparticles. *Pharmaceutics* 13, 1–31.

[65] Esposito, E. *et al*. (2016) Structural Studies of Lipid-Based Nanosystems for Drug Delivery: X-ray Diffraction (XRD) and Cryogenic Transmission Electron Microscopy (Cryo-TEM). In *Handbook of Nanoparticles* Aliofkhazraei M., ed. pp. 861–889, Springer. DOI: 10.1007/978-3-319-15338-4.

[66] Kim, J. *et al*. (2021) Self-assembled mRNA vaccines. *Adv. Drug Deliv. Rev*. 170, 83–112. DOI: 10.1016/j.addr.2020.12.014.

[67] Kulkarni, J.A. *et al*. (2019) On the role of helper lipids in lipid nanoparticle formulations of siRNA. *Nanoscale* 11, 21733–21739. DOI: 10.1039/c9nr09347h.

[68] Leung, A.K.K. *et al*. (2012) Lipid Nanoparticles Containing siRNA Synthesized by Micro fl uidic Mixing Exhibit an Electron-Dense Nanostructured Core. *Phys. Chem*. 116, 18440–18450. DOI: 10.1021/jp303267y.

[69] Hoshyar, N. *et al*. (2016) The effect of nanoparticle size on in vivo pharmacokinetics and cellular interaction. *Nanomedicine (Lond.)* 11, 673–692.

[70] Huang, J. *et al*. (2010) Effects of Nanoparticle Size on Cellular Uptake and Liver MRI with Polyvinylpyrrolidone-Coated Iron Oxide Nanoparticles. *ASC Nano* 4, 7151–7160.

[71] Nimesh, S. (2012) Potential implications of nanoparticle characterization on in vitro and in vivo gene delivery. *Ther. Deliv*. 3, 1347–1356.

[72] Zhao, Z. *et al*. (2019) Effect of physicochemical and surface properties on in vivo fate of drug nanocarriers. *Adv. Drug Deliv. Rev*. 143, 3–21. DOI: 10.1016/j.addr.2019.01.002.

[73] Foroozandeh, P. and Aziz, A.A. (2018) Insight into Cellular Uptake and Intracellular Trafficking of Nanoparticles. *Nanoscale Res. Lett*. 13, 339. DOI: 10.1186/s11671-018-2728-6.

[74] Buschmann, M.D. *et al*. (2021) Nanomaterial delivery systems for mrna vaccines. *Vaccines (Basel)* 9, 1–30. DOI: 10.3390/vaccines9010065.

[75] Arteta, M. *et al*. (2018) Successful reprogramming of cellular protein production through mRNA delivered by functionalized lipid nanoparticles. *PNAS* 115, E3351–E3360. DOI: 10.1073/pnas.1720542115.

[76] Roces, C.B. *et al*. (2020) Manufacturing Considerations for the Development of Lipid Nanoparticles Using Microfluidics. 2.

[77] Lee, S.M. *et al*. (2021) A Systematic Study of Unsaturation in Lipid Nanoparticles Leads to Improved mRNA Transfection In Vivo. *Angew. Chem. – Int. Ed*. 60, 5848–5853. DOI: 10.1002/anie.202013927.

[78] Kulkarni, J.A. *et al*. (2018) Lipid Nanoparticles Enabling Gene Therapies: From Concepts to Clinical Utility. *Nucleic Acid Ther*. 28, 146–157. DOI: 10.1089/nat.2018.0721.

[79] Ermilova, I. and Swenson, J. (2020) DOPC versus DOPE as a helper lipid for gene-therapies: molecular dynamics simulations with DLin-MC3-DMA. *PCCP* 22, 28256–28268. DOI: 10.1039/d0cp05111j.

[80] Ilhan-ayisigi, E. *et al*. (2021) Advances in microfluidic synthesis and coupling with synchrotron SAXS for continuous production and real-time structural characterization of nano-self-assemblies. *Colloids Surf. B Biointerfaces* 201. DOI: 10.1016/j.colsurfb.2021.111633 111633.

[81] Tomeh, M.A. and Zhao, X. (2020) Recent Advances in Micro fl uidics for the Preparation of Drug and Gene Delivery Systems. *Mol. Pharm*. 17, 4421–4434. DOI: 10.1021/acs.molpharmaceut.0c00913.

[82] Jeffs, L.B. *et al*. (2005) A scalable, extrusion-free method for efficient liposomal encapsulation of plasmid DNA. *Pharm. Res*. 22, 362–372. DOI: 10.1007/s11095-004-1873-z.
[83] Kulkarni, J.A. *et al*. (2017) Rapid synthesis of lipid nanoparticles containing hydrophobic inorganic nanoparticles. *Nanoscale* 9, 13600–13609. DOI: 10.1039/c7nr03272b.
[84] Amreen, K. and Goel, S. (2021) Review — Miniaturized and Microfluidic Devices for Automated Nanoparticle Synthesis Review — Miniaturized and Micro fl uidic Devices for Automated Nanoparticle Synthesis. *ECS J. Solid State Sci. Technol*. 10. DOI: 10.1149/2162-8777/abdb19 017002.
[85] Webb, C. *et al*. (2020) Using microfluidics for scalable manufacturing of nanomedicines from bench to GMP: A case study using protein-loaded liposomes. *Int. J. Pharm*. 582. DOI: 10.1016/j.ijpharm.2020.119266 119266.
[86] Zhang, Y. *et al*. (2021) Lipids and Lipid Derivatives for RNA Delivery. *Chem. Rev*. DOI: 10.1021/acs.chemrev.1c00244.
[87] Ball, R.L. *et al*. (2017) Achieving long-term stability of lipid nanoparticles: examining the effect of pH, temperature, and lyophilization. *Int. J. Na* 12, 305–315.
[88] Zhao, P. *et al*. (2020) Long-term storage of lipid-like nanoparticles for mRNA delivery. *Bioact. Mater*. 5, 358–363. DOI: 10.1016/j.bioactmat.2020.03.001.
[89] Crommelin, D.J.A. *et al*. (2021) Addressing the Cold Reality of mRNA Vaccine Stability. *J. Pharm. Sci*. 110, 997–1001. DOI: 10.1016/j.xphs.2020.12.006.
[90] EMA (2021) Spikevax: Summary of Product Characteristics. Published 2021. https://www.ema.europa.eu/en/documents/product-information/spikevax-previously-covid-19-vaccine-moderna-epar-product-information_en.pdf.
[91] EMA (2022) Comirnaty: Summary of Product Characteristics. Published 2022. https://www.ema.europa.eu/en/documents/product-information/comirnaty-epar-product-information_en.pdf.
[92] Pozo-rodríguez, A. *et al*. (2009) Short- and long-term stability study of lyophilized solid lipid nanoparticles for gene therapy. *Eur. J. Pharm. Biopharm*. 71, 181–189. DOI: 10.1016/j.ejpb.2008.09.015.
[93] Gindy, M.E. *et al*. (2012) Challenges in the pharmaceutical development of lipid-based short interfering ribonucleic acid therapeutics. *Expert Opin. Drug Deliv*. 171–182. DOI: 10.1517/17425247.2012.642363.
[94] Dhiman, N. *et al*. (2021) Lipid Nanoparticles as Carriers for Bioactive Delivery. *Front. Chem*. 9. DOI: 10.3389/fchem.2021.580118 580118.
[95] Rawal, M. *et al*. (2019) Quality-by-Design Concepts to Improve Nanotechnology-Based Drug Development. *Pharm. Res*. 36, 153.
[96] Yu, L.X. *et al*. (2014) Understanding Pharmaceutical Quality by Design. *AAPS J*. 16, 771–783. DOI: 10.1208/s12248-014-9598-3.
[97] Cunha, S. *et al*. (2020) Using the quality by design (QbD) approach to optimize formulations of lipid nanoparticles and nanoemulsions: A review. *Nanomedicine* 28. DOI: 10.1016/j.nano.2020.102206 102206.
[98] Kauffman, K.J. *et al*. (2015) Optimization of Lipid Nanoparticle Formulations for mRNA Delivery in Vivo with Fractional Factorial and Definitive Screening Designs. *Nano Lett*. 15, 7300–7306. DOI: 10.1021/acs.nanolett.5b02497.
[99] Billingsley, M.M. *et al*. (2021) Orthogonal Design of Experiments for Optimization of Lipid Nanoparticles for mRNA Engineering of CAR T Cells. *Nano Lett*. 22, 533–542. DOI: 10.1021/acs.nanolett.1c02503.
[100] Blakney, A.K. *et al*. (2019) The Skin You Are In: Design-of-Experiments. *ACS Nano* 13, 5920–5930. DOI: 10.1021/acsnano.9b01774.
[101] Witzigmann, D. *et al*. (2020) Lipid nanoparticle technology for therapeutic gene regulation in the liver. *Adv. Drug Deliv. Rev*. 159, 344–363.
[102] Lorenzer, C. *et al*. (2015) Going beyond the liver: Progress and challenges of targeted delivery of siRNA therapeutics. *J. Control. Release* 203, 1–15. DOI: 10.1016/j.jconrel.2015.02.003.
[103] Gillmore, J.D. *et al*. (2021) CRISPR-Cas9 In Vivo Gene Editing for Transthyretin Amyloidosis. *N. Engl. J. Med*. 385, 493–502. DOI: 10.1056/NEJMoa2107454.
[104] Zhao, Z. *et al*. (2020) Targeting Strategies for Tissue-Specific Drug Delivery. *Cell* 181, 151–167. DOI: 10.1016/j.cell.2020.02.001.
[105] Mitchell, M.J. *et al*. (2020) Engineering precision nanoparticles for drug delivery. *Nat. Rev. Drug Discov*. 20, 101–124. DOI: 10.1038/s41573-020-0090-8.
[106] Li, J. *et al*. (2017) Insight into the interactions between nanoparticles and cells. *Biomater. Sci*. 5, 173–189. DOI: 10.1039/c6bm00714g.
[107] Elias, D.R. *et al*. (2013) Effect of ligand density, receptor density, and nanoparticle size on cell targeting. *Nanomedicine* 9, 194–201. DOI: 10.1016/j.nano.2012.05.015.
[108] Wei, T. *et al*. (2020) Systemic nanoparticle delivery of CRISPR-Cas9 ribonucleoproteins for effective tissue specific genome editing. *Nat. Commun*. 1–12. DOI: 10.1038/s41467-020-17029-3.
[109] Cheng, Q. *et al*. (2020) Selective organ targeting (SORT) nanoparticles for tissue-specific mRNA delivery and CRISPR-Cas gene editing. *Nat. Nanotechnol*. 15, 313–320. DOI: 10.1038/s41565-020-0669-6.
[110] Dahlman, J.E. *et al*. (2017) Barcoded nanoparticles for high throughput in vivo discovery of targeted therapeutics. *PNAS* 114, 2060–2065. DOI: 10.1073/pnas.1620874114.
[111] Liu, S. *et al*. (2021) Membrane-destabilizing ionizable phospholipids for organ-selective mRNA delivery and CRISPR–Cas gene editing. *Nat. Mater*. 20, 701–712. DOI: 10.1038/s41563-020-00886-0.
[112] Dilliard, S.A. *et al*. (2021) On the mechanism of tissue-specific mRNA delivery by selective organ targeting nanoparticles. *Proc. Natl. Acad. Sci*. 118. DOI: 10.1073/pnas.2109256118 e2109256118.
[113] Liu, S. *et al*. (2021) Membrane-destabilizing ionizable phospholipids for organ-selective mRNA delivery and CRISPR-Cas gene editing. *Nat. Mater*. 20, 701–712. DOI: 10.1038/s41563-020-00886-0.
[114] Kedmi, R. *et al*. (2018) A modular platform for targeted RNAi therapeutics. *Nat. Nanotechnol*. 13, 214–219. DOI: 10.1038/s41565-017-0043-5.
[115] Verbeke, R. *et al*. (2019) Three decades of messenger RNA vaccine development. *Nano Today* 28. DOI: 10.1016/j.nantod.2019.100766 100766.
[116] Wu, Z. and Li, T. (2021) Nanoparticle-Mediated Cytoplasmic Delivery of Messenger RNA Vaccines: Challenges and Future Perspectives. *Pharm. Res*. 38, 473–478.
[117] Hassett, K.J. *et al*. (2019) Optimization of Lipid Nanoparticles for Intramuscular Administration of mRNA Vaccines. *Mol. Ther. Nucleic Acids* 15, 1–11. DOI: 10.1016/j.omtn.2019.01.013.
[118] Zukancic, D. *et al*. (2020) The Importance of Poly (ethylene glycol) and Lipid Structure in Targeted Gene Delivery to Lymph Nodes by Lipid Nanoparticles. *Pharmaceutics* 12, 1068.
[119] Huang, H. *et al*. (2021) The investigation of mRNA vaccines formulated in liposomes administrated in multiple routes against SARS-CoV-2. *J. Control. Release* 335, 449–456. DOI: 10.1016/j.jconrel.2021.05.024.
[120] Carrasco, M.J. *et al*. (2021) Ionization and structural properties of mRNA lipid nanoparticles influence expression in intramuscular and intravascular administration. *Commun. Biol*. 4, 956. DOI: 10.1038/s42003-021-02441-2.
[121] Dolgin, E. (2021) mRNA flu shots move into trials. *Nat. Rev. Drug Discov*. 20, 801–803. DOI: 10.1038/d41573-021-00176-7.
[122] Busignies, V. Charrueau, C. Tchoreloff, P. and Escriou, V. (2017) Nanostructures for oral delivery of therapeutic nucleic acids*Nanostructures for Oral Medicine*, Elsevier Inc.pp. 147–172, Elsevier Inc.. DOI: 10.1016/B978-0-323-47720-8/00007-9.
[123] O'Driscoll, C.M. *et al*. (2019) Oral delivery of non-viral nucleic acid-based therapeutics - do we have the guts for this? *Eur. J. Pharm. Sci*. 133, 190–204. DOI: 10.1016/j.ejps.2019.03.027.
[124] El-Mayta, R. *et al*. (2020) A Nanoparticle Platform for Accelerated In Vivo Oral Delivery Screening of Nucleic Acids. *Adv. Ther. (Weinh.)* 2000111, 1–11. DOI: 10.1002/adtp.202000111.
[125] Ball, R.L. *et al*. (2018) Oral delivery of siRNA lipid nanoparticles: Fate in the GI tract. *Sci. Rep*. 8, 1–12. DOI: 10.1038/s41598-018-20632-6.
[126] Busignies, V. *et al*. (2020) Compression of Vectors for Small Interfering RNAs Delivery: Toward Oral Administration of siRNA Lipoplexes in Tablet Forms. *Mol. Pharm*. 17, 1159–1169. DOI: 10.1021/acs.molpharmaceut.9b01190.
[127] FDA (2021) Novel Excipient Review Pilot Program. Published 2021. https://www.fda.gov/drugs/development-approval-process-drugs/novel-excipient-review-pilot-program.